This is to certify that the

thesis entitled

THE EFFECTS OF FORCING ON A SINGLE
STREAM SHEAR LAYER AND ITS PARENT
BOUNDARY LAYER

presented by

Richard Courtney Haw Jr.

has been accepted towards fulfillment
of the requirements for

___M.S.___ degree in __Mechanical__ Engineering
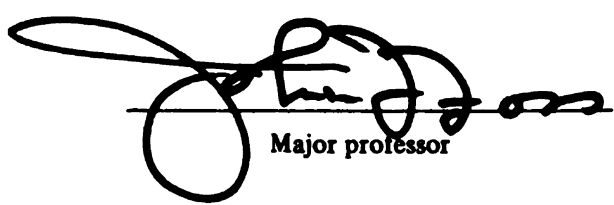
Major professor

Date___9 November___

1989

PLACE IN RETURN BOX to remove this checkout from your record.
TO AVOID FINES return on or before date due.

DATE DUE	DATE DUE	DATE DUE
_____	_____	_____
_____	_____	_____
_____	_____	_____
_____	_____	_____
_____	_____	_____
_____	_____	_____
_____	_____	_____

MSU Is An Affirmative Action/Equal Opportunity Institution

THE EFFECTS OF FORCING ON A SINGLE
STREAM SHEAR LAYER AND ITS PARENT
BOUNDARY LAYER

By

Richard Courtney Haw Jr.

A THESIS

Submitted to
Michigan State University
in partial fulfillment of the requirements
for the degree of

Master of Science

Department of Mechanical Engineering

1989

ABSTRACT

THE EFFECTS OF FORCING ON A SINGLE
STREAM SHEAR LAYER AND ITS PARENT
BOUNDARY LAYER

By

Richard Courtney Haw Jr.

The detailed response of a large $R_{\theta(0)}$ single stream shear layer to a sinusoidal forcing at x = 0 has been documented. The increased width and measures of the phase dependent response in the shear layer are characterized by velocity magnitude measurements. These observations are consistent with and complement those of Fiedler and Mensing[1].

[1] Fiedler, H.E. and Mensing, P. [1985] "The Plane Turbulent Shear Layer with Periodic Excitation", Journal of Fluid Mechanics, vol 15, pp281-309.

I dedicate this thesis to my wife, Valerie

ACKNOWLEDGMENTS

iv

TABLE OF CONTENTS

LIST OF TABLES

LIST OF FIGURES

Nomenclature

A,B,n	coefficients for Collis and Williams equation
A_e	piston amplitude
$C_0 .. C_n$	polynomial coefficients
c_f	local skin friction coefficient
f	frequency
E	hot wire voltage
Q	velocity at hot-wire
Q_3	velocity on wire 3
Q_4	velocity on wire 4
R_θ	Reynolds number based on θ
S_t	Strouhal number
u'	streamwise velocity fluctuation
$u'(\phi)$	u' at phase angle ϕ
U^+	streamwise velocity in wall units
U_τ	friction velocity
U_0	free Stream velocity
v'	lateral velocity fluctuation
$v'(\phi)$	v' at phase angle ϕ
V_e	entrainment velocity
w_p	piston width
x	streamwise coordinate
x_0	virtual shear layer origin

y	lateral coordinate
y^+	lateral coordinate in wall units
z	transverse coordinate

GREEK SYMBOLS

α	angular acceleration
γ	angle in the XY plane between velocity vector and axis or X array probe
$\delta u, \delta v$	velocity fluctuation see (13)
δ^*	boundary layer displacement thickness
ζ	hot-wire voltage ratio
η	offset hot-wire voltage ratio
θ	momentum deficit thickness or angular position
θ_0	momentum deficit thickness at separation
ν	kinematic viscosity
ξ	locally scaled perturbation level, see (14)
ϕ	phase angle
ω	angular acceleration
Δ	width measure of the forced shear layer, see (17)

SPECIAL SYMBOLS

$(\bar{\ })$	time average of the quantity ( )
$(\tilde{\ })$	rms of the fluctuating quantity ()
$(< >)$	phase average of the quantity ( )
$(\ )_f$	the quantity ( ) for the forced condition

1

INTRODUCTION

1.1 Overview

Forcing and its effect on fluid flows has become an accepted tool in the study and control of flow systems. It has been used both as a diagnostic tool, to explore the development and interaction of coherent structures, and as a method of controlling the behavior of the flow. A number of forcing methods have been used in order to provide a perturbation to the flow; among these are the use of an oscillating trailing edge, acoustically driven slots, external acoustic forcing, and mechanical piston methods.

There have been numerous studies into the effects of forcing on free shear layers. Substantial information can be found in the review articles (e.g. Fiedler [1988] and Hussain [1986]) and in the original publications which they cite.

The investigation presented here documents the effect of a planar mechanical piston forcing on a single stream shear layer; it can be noted that this is one of the lesser studied free shear layers. The single stream shear layer can be characterized by its primary flow velocity scale U_0 and the thickness of the separating boundary layer θ_0. The velocity scale U_0 is constant over the length of the flow field; $\theta(x)$ can be used as a width scale to characterize the unforced shear layer. In the case of the forced shear layer the velocity field is a function of phase time and definition of a width measure becomes somewhat problematic.

1.2 Similar prior work

The effects of sinusoidal forcing of the separating boundary layer in a single stream shear layer have been studied by Fiedler and Mensing [1985] and Disimile [1986]. An acoustic forcing mechanism was used in the Fiedler and Mensing study; the acoustic wave was applied to the separating boundary layer through a wave guide channel. Two separate trailing edge geometries were used in their study, see Figure 1. The separating boundary layer for their study had an R_θ value of 830. Experimental observations of the resulting large scale motions included both hot-wire measurements and smoke visualizations. Hot-wire measurements in the shear layer indicated maximum $\tilde{v}$ levels at $S_t = (x - x_0)f/U_0 \simeq 1$. This result, combined with the flow visualization data, suggests that the large scale coherent motion has its maximum organization at this location. A comprehensive evaluation of the

effect of forcing frequency and amplitude effects on the shear layer is provided by the Fiedler and Mensing study.

The Disimile investigation, which was executed on the same apparatus as the current study, used a mechanically driven piston to provide a low amplitude forcing of the separating boundary layer. Expressing the forcing piston amplitude as $A(t) = A_0 \cos \omega t$, the Disimile investigation was performed using $A_0 = 0.76$ mm, or $A_0/\theta_0 \simeq 0.12$. The Disimile study revealed the formation of a large scale coherent motion and documented its translation properties in phase time. A negligible influence by the forcing input on the separating boundary layer was indicated.

1.3 The current experiment

The study documented here, which was designed to build upon the previous investigations, was to examine the effect of large amplitude forcing at separation on the separating boundary layer. The effects of forcing on the developing shear layer constituted the second phase of the present study. A third phase of the work was to examine the behavior of the entrainment field for the shear layer, and its response to the strongly forced shear layer.

The experimental approach taken was to provide a large amplitude forcing to a large separating boundary layer. In particular, a forcing amplitude of $A_0/\theta_0 = 0.58$ was used with a separating boundary layer characterized by $R_{\theta(0)} = 5500.$ and $\theta_0 = 6.5$ mm. Phase averaged

measurements, using a single hot-wire anemometer, were performed throughout the development region of the shear layer and the upstream boundary layer. Planar velocity vector measurements in the entrainment region were provided through the use of a 4 wire probe. As a result of the large physical dimension of the separating boundary layer ($\theta_0 - 6.5$ mm) a 4 wire probe was able to be used to examine the planar velocity field just downstream of the separation lip.

EXPERIMENTAL EQUIPMENT AND PROCEDURES

2.1 Experimental Facility

2.1.1 Tunnel

The tunnel used for the present study was a single stream shear layer suction tunnel, a plan view of which is presented in Figure 2. The test section for the tunnel was subatmospheric, with the open volume of the laboratory between the fan exit and the inlet to the tunnel serving as a settling chamber for the return flow. The test section for the tunnel is shown in Figure 3, with a 0.5m x 0.8m core flow exiting into a 1.7 m x 0.8 m x 3.0 m test section. (The height for the entire area shown in Figure 3 was a constant 0.8 m.) The tunnel was equipped with a glass wall over the entire length of the test section which enabled optical positioning methods to be used to locate the probe. The test section, downstream of the separation step (at $x = 0.0$) was equipped with a movable floor traversing mechanism, as shown schematically in Figure 4.

The prime mover for the tunnel was a Chicago 30.5 SQA airfoil fan powered by a 15 Hp variable speed DC motor. The motor was equipped with a tachometer feedback control system which maintained the motor speed to within ± 0.5% of the set value.

Flow conditioning upstream of the test section was provided by three two-dimensional contractions with an overall contraction ratio of 22.6 to 1. Additional conditioning was provided by turbulence manipulators downstream of the first two contractions. These manipulators consisted of a 3.175 mm diameter honeycomb with an l/d ratio of 8, and a set of 30 mesh screens spaced 12.7 mm apart. A final asymmetric contraction, to the boundary layer development section, was placed downstream of the manipulators.

The boundary layer development section, as shown in Figure 5, conditions the boundary layer upstream of the separation lip. This conditioning takes the form of removing the upstream boundary layer formed during the last contraction through use of a separate bleed fan. This low momentum fluid was extracted using a splitter plate as shown in Figure 5. The plenum downstream of the splitter plate exhausted into the receiver through a Buffalo Forge 37v fan. This fan was driven by a 3 Hp A/C constant speed motor through an adjustable speed belt drive allowing the adjustment of the bleed flow.

A distributed roughness trip mechanism, consisting of 609. mm of 16 grit sandpaper, was employed. This trip method was based on the

work by Klebanoff and Diehl [1951]. The distributed roughness was followed by 1290. mm of smooth wall. The final 655. mm of wall consisted of white formica covered particle board providing a surface with the following desirable characteristics;

a) A low surface roughness; which minimized wall roughness effects on the developing boundary layer.

b) A non-conducting surface; which provided desirable heat transfer properties. When operated near a conducting surface the heat loss from a hot-wire anemometer will give rise to significant errors in measurement. Usage of a non-conducting surface such as formica covered particle board minimizes this effect.

c) A white smooth surface; which enabled an optical wire-shadow positioning method to be used to accurately determine the position of the hot-wire when near the wall.

In contrast with many single stream shear layer facilities, the facility used in this study had the attribute of being able to both condition and to have control over the fluid stream entrained by the shear layer. The entrained fluid was taken from the open laboratory volume through filter media and into a settling chamber. One wall of the settling chamber consisted of a series of throttle modules, which allowed for the control of the flow rate through the use of a sliding throttle plate as shown in Figure 6. The flow passed through the throttle modules, then through a coarse screen, a contraction to the

0.8 m test section height, and into a honeycomb and fine screen turbulence manipulators; see Figure 7.

2.1.2 Traverse system

The probes were positioned by means of a 3 axis traversing system, shown schematically in Figure 8. This traverse consisted of a rack and pinion drive in the X direction, a screw feed drive in the Y direction, and a worm gear drive in the θ direction. Each axis was driven through stepper motors under computer control. The resolution in the X, Y, and θ directions were .8 mm, .01 mm, and .02 degrees respectively.

2.1.3 Forcing System

Forcing of the separating shear layer was provided by a motor driven piston forcing mechanism. The basic mechanical system was employed in previous research of lower amplitude forcing effects; see Disimile [1984] and Figure 9. The piston was belt driven using a constant speed (1760 RPM) 1 Hp AC motor and variable pitch pulleys. The piston motion was obtained using an eccentric as shown in Figure 10. The time dependant position of the piston can be written as:

$$A = A_0 \times \cos(\phi) \tag{1}$$

Where ϕ is the angular position of the rotating shaft.

This study was performed using an amplitude $A_0 = 3.84$ mm and a frequency of 16.1 Hz. Phase information was obtained through use of an optical pickup on the forcing piston drive shaft as shown in Figure 11.

2.2 Measuring Equipment

2.2.1 Pressure measurements

Pressure measurements were made using an MKS baratron model 310 1 Torr pressure transducer and 170M 6-C amplifier. The overall uncertainty for all pressure measurements is ±.08% of indicated plus ±.00001 Torr.

2.2.2 Anemometry

All hot-wire measurements in this study used locally fabricated hot-wires and probes. A typical straight wire is shown in Figure 12. The wire itself is 5 micron tungsten with an overall length of 3 mm and an active length of 1 mm. The inactive portions of the wire are copper plated to a nominal diameter of 50 microns. The wires were mounted on the tips of jewelers broachs, the plating as well as the small diameter prongs lead to minimal interference effects. The measurements were all performed with the wires operated in the constant temperature mode at a nominal overheat of 0.7.

Two types of probes were used in this study, single wire probes and a compact vorticity probe. The single wire probes consisted of a

single wire as described above, operated with the wire parallel to the Z axis. A modified wire mounting was used for the wires involved in the boundary layer measurements. Specifically, the wire was mounted on the side of the tip of the broachs, rather than the end of the broachs; see Figure 13. This allowed the active portion of the wire to be brought closer to the wall.

The compact vorticity probe is a 4 wire probe allowing for the resolution of velocity components and gradients in a single plane. The probe is shown schematically in Figure 14 and consists of a single X array, with the addition of two straight wires. The individual wires are as described above.

As can be seen from Figure 14, the overall size of the measurement area is 1 mm^2 normal to the mean flow. Although no large scale model studies have been performed on this probe to determine possible prong interference effects, results up to the time of this writing indicate that such effects are minimal. Measurements at various orientations in the calibration stream return the correct values given the probe orientation. In addition measurements of the thermal interference between wires, obtained by running all possible on and off combinations of wires while the probe is in the calibration stream, show no thermal interference between wires.

Two types of anemometers were used in this work; these were the DISA model 55M01 and the TSI model 1755. In both instances the

nominal output was approximately 4.5 volts at the free stream speed of 13 mps. Electrical noise levels for both types of anemometers were approximately 1 millivolt rms. Frequency response for the anemometry was approximately 20 KHz at 13 mps.

2.3 Data Acquisition System

2.3.1 Computer system

The computer system used for both the data taking and all data processing was a DEC 11/73 microcomputer; this system is shown diagrammatically with the associated data acquisition and laboratory interface hardware in Figure 15. This computer consisted of the central processing unit, two RD-53 70 megabyte hard disk drives, a 90 megabyte Tk50 tape drive, an AXV11C A/D, a KWV11C programmable clock, a DRV11J digital interface, a DRV11W DMA interface, and miscellaneous other serial and networking interconnects.

The AXV11C A/D provided limited sampling capability which was used primarily for monitoring the tunnel speed and other experimental parameters prior to the actual data taking.

The DRV11J digital interface and KWV11C programmable clock, in conjunction with a custom built stepper motor translator and driver system provided computer control over the traversing system.

2.3.2 Primary A/D

The primary A/D used for the experimental work was a TSI IFA200 12 bit simultaneous sample 10 channel unit. This A/D was configured to provide an input signal range of 0 to +5 volts, giving a least significant bit level of 1.22 millivolts. The IFA200 is a self contained unit providing it's own internal clock and sampling circuitry. Interface to the 11/73 computer was through a DRV11W DMA interface, providing a maximum single channel sample rate of 50 KHz, and a total throughput of 250 thousand samples per second. The IFA200 used was a true simultaneous sample A/D, consisting of 10 independent A/Ds which were driven by a common sample signal. An analog delay adjust in the sample signal was provided, and for all data in this study the A/D was calibrated to provided a channel to channel sample uncertainty equivalent to a 0.0001 mm convection length at the typical free stream velocity of 13 mps.

2.3.3 Phase pickup

The phase trigger used to conditionally sample the forced data in this study was provided by means of a metal tab passing between the sensing elements of an optical pickup, see Figure 11. This arm was mounted at a radius of 100 mm giving a mechanical positional uncertainty of approximately 0.2 degrees.

An electrical schematic of the pickup and conditioning circuit is shown in Figure 16. The electrical output from the pickup is

amplified, fed into a one-shot multivibrator, buffered to standard TTL levels and fed to the IFA200 A/D. The one-shot multivibrator is used to provide a positive output duration of approximately 30% of the forcing period. The overall uncertainty caused by the electrical system is negligible for the forcing period used.

2.4 Data Processing

2.4.1 Single Wire

The hot wires were all calibrated in the low disturbance free stream flow of the tunnel. The physical location x - 150. mm and y - -250. mm was used for the calibrations. The calibration data were obtained as the mean of 2000 samples taken at 200 Hz. A single calibration data set consisted of measurements at 7 or more speeds ranging from 1.0 to 13.5 mps. A pitot static tube was used in conjunction with the MKS baratron pressure transducer to provide the reference velocity.

The calibration data were used to define the coefficients (A,B,n) in the modified Collis and Williams relation,

$$E^2 - A + B \times Q^n \tag{2}$$

where E is the measured wire voltage and Q is the tunnel speed.These A, B, and n were values determined by using an ordinary least squares method to determine A and B given n, and minimizing that relation as a

function of n.

All processing of the anemometry data was executed by first con-
verting the measured voltages to velocities using the calibration con-
stants on a data point by data point basis, and then performing
statistical processing on the resulting velocities.

2.4.2 Compact Vorticity Probe

2.4.2.1 Calibration

The calibration of the compact vorticity probe was also executed
in the low disturbance free stream flow of the tunnel at X — 150. mm
and Y — -250. mm using a pitot static tube and the Baratron pressure
transducer as a velocity reference. Sampling details for a single
calibration point were the same as those used for a straight wire;
however, as a result of the processing algorithm used, the calibration
data were required at a number of angles (θ) with respect to the flow.
These data were taken at angles from -36° to +36° in 6° steps.

Since small differences in the velocities measured by the wires
can translate into large gradients because of the compact size of the
probe, improved calibrations were obtained by using one of the
straight wires rather than the pressure transducer as a velocity
reference. This was accomplished by first fitting A,B,n values to the
two straight wires for all angles, then selecting the wire with the
minimum standard deviation (based on velocity) and using the resulting

coefficients for that wire along with the calibration data to generate the calibration velocities for the other three wires of the probe. Calibration constants were then determined for all wire and angle combinations using the new velocities.

The variation in the hot wire response with respect to flow angle was modeled by defining a voltage ratio ζ as follows:

$$\zeta = E(\gamma) \ / \ E(0) \tag{3}$$

where $E(\gamma)$ is the hot-wire voltage at the probe angle γ and $E(0)$ is the hot-wire voltage at the probe angle of 0. This function is non-linear and strongly speed dependant. At any given speed the function can be modeled as a polynomial. Since the function has an inflection around $\zeta = 1.0$, it is advantageous to redefine the voltage ratio as an offset value:

$$\eta = E(\gamma) \ / \ E(0) - 1.0 \tag{4}$$

which allows γ to be accurately modeled as a rational polynomial of the form:

$$\gamma = C_5\eta^5 + C_4\eta^4 + C_3\eta^3 + C_2\eta^2 + C_1\eta + C_0 \tag{5}$$

where $C_5, C_4, C_3, C_2, C_1, C_0$ are fitted coefficients. Typical rms values of this fit are 0.3°. Representative calibration data and fitted

curves are shown in Figure 17.

Since equation 5 is a strong function of velocity, see Figure 17, a separate set of coefficients were determined at 51 discrete speeds equally spaced over the range from the minimum to the maximum calibration speed. The η value at each speed and angle is computed from calculated voltages using the A,B,n values for the wire at that angle and the arbitrary speed.

2.4.2.2 Processing

2.4.2.2.1 Determination of the u,v components

The x and y velocity components of the flow (u and v) can be computed by knowing the velocity magnitude in the xy plane, and the indicated velocity from one of the slant wires. The velocity magnitude was taken as the average of the indicated velocities from the two straight wires, Q_3 and Q_4. Once this velocity had been determined, the flow angle γ could be computed from either of the slant wires. In practice the angle was computed using both of the slant wires, and this angle was compared to the calibrated angle range. If the indicated angles were both within the calibrated range, ($-36° < \gamma < +36°$), the average is used. If only one computed angle was outside of the calibration range the value which lay within the calibration range was used. If both angles lay outside the calibration range the $\gamma = f(\eta)$ polynomial for the wire most normal to the flow was extrapolated to yield the angle, and the point was marked as suspect.

Since the response of the vertical wires does, to a slight degree, depend on the flow angle, two calculations were made for each wire at each point in the data set. For the second calculation the angle information from the first calculation was used to determine the calibration constants $A(\gamma)$, $B(\gamma)$, and $n(\gamma)$ to be used in the determination of Q_3 and Q_4.

2.4.2.2.2 Accuracy

The accuracy of the processing algorithm was verified for each set of experimental data by processing time series data taken in the free stream during calibration. In all cases the computed flow angles were within 0.5° of the physical probe angle.

The validity of the extrapolations of the $\eta - f(\gamma)$ relation were verified by taking time series data in the calibration stream at probe angles with respect to the flow direction of ±6° beyond the normal calibration range. The extrapolated values, so computed, were accurate to within ±1.0°.

2.4.3 Phase Averaging

Phase averaged data acquisition was performed by sampling both the analog input channels of interest and the conditioned phase signal from the forcing mechanism optical pickup at a high data rate. The resulting time series was then divided into intervals based on the pickup signal. Each of these intervals, representing one forcing

period, was then divided into 16 equally spaced intervals and the phase average sample extracted from the time series at these points. As an example consider a block of data where the leading edge of the pickup signal occurred at data points 1 and 384. Dividing the forcing period into 16 intervals, only points 1, 25, 49... would be saved; corresponding to phase locations of 0., 22.5, 45.0... degrees.

For this study, data were taken at 5000 samples per second, and the mean forcing period was 62 milliseconds. This gives an uncertainty of ± 0.6 degrees in any specific phase value due to the sampling rate. Since the subdivision of the intervals over which the phase averaging was performed was based on one revolution of the arm, uncertainties due to long term, (time scales greater than one forcing period) variations in motor speed were eliminated. In addition this method allowed for accurate monitoring of the actual motor speed, since the length of each period sampled is also saved. For all of the data presented in this thesis, the variation in the periods was on the order of the sampling time of 0.2 milliseconds, or 0.3% of the mean period.

3

CHARACTERIZATION OF THE EXPERIMENTAL CONDITIONS

-

3.1 Boundary Layer

3.1.1 Bleed setting procedure

The boundary layer formed during the final contraction was
removed through a bleed slot as shown in Figure 5.   The initial at-
tempt at a setting for the bleed port flow rate was accomplished
visually by using tufts at the bleed port;   those observations proved
difficult to interpret with the desired precision.   In an attempt to
achieve a better bleed setting, velocity profiles were taken just
upstream of the bleed slot using a single hot-wire probe.   The bleed
flow was then adjusted to yield a locally symmetric velocity profile
about the leading edge of the splitter plate. Upon examination of the
boundary layer profiles at the separation lip, it was found that this
approach yielded too large a bleed flow, and a distorted downstream
velocity profile.

The final approach taken to set the bleed flow was to adjust the bleed flow rate such that the an optimum turbulent boundary layer profile was obtained at the separation lip.

3.1.2 Turbulent Characteristics

3.1.2.1 At separation

The boundary layer data were plotted in law of the wall coordinates, U^+ and Y^+;

$$U^+ = \frac{u}{U_\tau} \tag{6}$$

$$y^+ = \frac{yU_\tau}{\nu} \tag{7}$$

$$U_\tau = U_0 \left[\frac{C_f}{2}\right]^{1/2} \tag{8}$$

The local skin friction coefficient ($C_f = \tau_w/0.5\rho U_0^2$) was determined from a Clauser [Clauser 1951] plot. The momentum thickness, θ was determined from

$$\theta = \int_0^\infty \frac{\bar{u}}{U_0}\left[1-\frac{\bar{u}}{U_0}\right] dy \tag{9}$$

and the displacement thickness, δ^* was determined from

$$\delta^* = \int_0^\infty \left[1 - \frac{\bar{u}}{U_0} \right] dy \qquad (10)$$

Clauser plots for the separating boundary layer are presented for the unforced case in Figure 18 and for the forced case in Figure 19. The resulting C_f values were 2.95×10^{-3} for the unforced case and 3.03×10^{-3} for the forced case. The unforced boundary layer had a momentum thickness at separation (θ_0) of 6.72 mm, with a displacement thickness δ^* of 9.11 mm, yielding a shape factor of 1.36. For the forced condition θ_0 was equal to 6.02 mm and $\bar{\delta}^*$ was equal to 8.21 mm yielding a shape factor of 1.36. U_τ at separation was 0.485 for the unforced condition and 0.492 for the forced condition. In addition turbulent intensity measurements in the boundary layer yielded a maximum value for u'/U_τ equal to 2.65 in the unforced case.

Mean profiles for the separating boundary layer, for both the unforced and forced condition, were plotted in law of the wall coordinates (u^+, y^+) [Coles 1962] as shown in Figure 20. As indicated in the figure, the data show very good agreement with the law of the wall,

$$u^+ = 5.6 \log_{10} y^+ + 4.9 \qquad (11)$$

over the log law region. This agreement, along with a shape factor of approximately 1.4 and a u'/U_τ value of approximately 2.5 indicate an equilibrium turbulent boundary layer [Hussain 1983].

3.1.2.2 Prior to separation

The momentum thickness θ and friction velocity (U_τ) for the developing boundary layer are shown in Figure 21 and Figure 22. As indicated in Figure 21 the boundary layer follows the expected pattern of growth up to a streamwise location of $x/\theta_0 = -1.0$. A decrease in the momentum thickness is indicated at the separation lip; this effect is presumably due to acceleration at the separation lip.

The boundary layer growth rate, $(d\theta/dx)$, can be related to the wall friction coefficient for an equilibrium boundary layer as:

$$c_f = 2 \frac{d\theta}{dx} \tag{12}$$

This comparison was made with the experimental data over the range $-30 < x/\theta_0 < -1.0$ and found to be in poor agreement. Given the limited streamwise span of the data, accurate resolution of $d\theta/dx$ would have required a determination of θ to a precision not possible with the experimental configuration used. The uncertainty in the determined θ values is hypothesized to be the cause of the poor agreement of the data applied to (12).

3.2 Forcing system

3.2.1 Forcing frequency

The forcing frequency for this study was chosen based on the prior work of Mensing and Fiedler [1985]. Their studies showed a maximum intensity of $\tilde{v}$ at a saturation length X_s, defined as $X_s = f/U_0$, approximately equal to 1. The forcing frequency used in this study, 16.2 Hz, was chosen based on this criteria to give a saturation location of 0.8 m, or 30% of the test section length. The resulting Strouhal number based on the separating boundary layer thickness, $(f\theta_0/U_0)$, was 0.0081. The natural frequency of the shear layer, as exhibited by fluctuations in the entrainment field, was 3.5 Hz or $f\theta_0/U_0 = 0.0018$; see Foss et.al. [1987].

The data sampling and processing method provided data on every forcing period taken during this study. The rms fluctuations of the period were below the measurement uncertainty involved in the sampling (0.2 msec).

The frequency domain content of the forcing system was examined by placing piezo-electric accelerometers on the forcing piston at a variety of locations. Power spectra of the measurements taken at the piston center, and either extreme end are shown in Figure 23 through Figure 25. As indicated the piston motion has little harmonic content at the center of travel. A small amount of energy is found in

harmonics at either end; presumably these are a result of minor deflections of the forcing piston.

3.2.2 Effect of the forcing on the flow

An accurate determination of the forcing level, by a given forcing apparatus, is one of the major problems in experimental work on forced flows. For the present study, two approaches were taken to accurately quantify the effect of the forcing on the separating boundary layer. Measurements were made with no primary flow in order to isolate the effect of the piston forcing on the air mass in its neighborhood, and measurements were made in the separating boundary layer under nominal test conditions.

3.2.2.1 $U_0 = 0$ Data

Both velocity and pressure measurements were made in the neighborhood of the separation lip with no mean flow. Velocity measurements were made using a single wire hot-wire anemometer; pressure measurements were made utilizing a microphone and pinhole chamber arrangement.

For the hot-wire measurements, calibrations were performed using a drop-test calibration technique; see appendix Appendix B for more information on this technique. The wire was calibrated in the data taking orientation, (with respect to the gravitational field), in order to minimize the error introduced by the natural convection field

of the hot-wire. The results of the hot-wire measurements are presented in Figure 26 through Figure 29; the velocity data presented therein are in units of meters per second, and the coordinates are non-dimensionalized with respect to the piston width (w_p). As expected, there is a strong shadow effect of the separation lip. Results for $x>0$ suggest a strong jet pumping effect which generated a mean entrained velocity in the -y direction.

The technique used for the pressure measurements is documented in Appendix C, and tabular results are presented in Appendix D. The data showed no significant change in the amplitude of the rms pressure fluctuations over the measurement domain; the technique used apparently registered the acoustic wave generated by the piston.

3.2.2.2 Perturbations of the separating boundary layer

The forcing amplitude can be characterized by three non-dimensional velocity measures; the rms velocity of the piston, the magnitude of the imposed velocity in the direction of piston motion, or the velocity change at some point in the separating boundary layer. Specifically, all of these velocities can be non-dimensionalized with respect to the free stream velocity. The forcing levels for the current study were large with respect to the prior work of Disimile [1984], and corresponded to the larger amplitudes used by Fiedler and Mensing [1985]. Specific levels are shown in Table 1.

Table 1 - Forcing Amplitude Measures

Forcing Measure	Amplitude
$\tilde{v}_{piston}/U_0$	0.021
$\tilde{v}_f/U_0$	0.015
$(\tilde{v}_f^2+\tilde{u}_f^2)^{1/2}/U_0$	0.045

As would be expected, there is some attenuation from the piston face velocity to the induced v velocity (v_f) in the separating boundary layer. The large difference in the maximum velocity change in the flow ($(\tilde{v}_f^2+\tilde{u}_f^2)^{1/2}/U_0$) relative to the magnitude of the induced v velocity ($\tilde{v}_f/U_0$) should be noted.

If the physical size of separating boundary layer is relatively small, for example $\theta_0 = 1.14$ mm in the Fiedler and Mensing [1985] study, hot-wire velocity measurements are limited to those which can be made with a single wire probe. Since a single wire probe resolves a planar velocity magnitude, an important distinction should be made between the total induced velocity change and the induced velocity change in the transverse direction; the former being larger due to steerage of the sharp velocity gradient near the wall. As indicated in Table 1, for the present study the ratio of total to transverse induced velocity fluctuation was 3 to 1.

Due to the small physical size of the separating boundary layer in other studies magnitudes are often expressed using the former measure since only single hot-wire probes can be utilized. This

should be clearly delineated from the magnitude of the induced v velocity, the former being much larger in magnitude due to steering of the sharp velocity gradient near the wall.

3.3 Entrainment

The throttle plates were adjusted to give a "natural" shear layer, or $dU/dX \simeq 0.0$. The value of dU/dX was determined from measurements of $\bar{u}$ in the high speed nonvortical flow at two streamwise locations as indicated in Figure 30. The resulting value of dU/dX represented a velocity defect over the indicated range of less than 1% of the free stream velocity.

3.4 Probe Positioning

Determination of the probe position for the data taken in the boundary layer and near the separation point for the shear layer is critical due to the steep velocity gradients in the Y direction.

A preliminary attempt to verify the wire location by heat transfer to the wall was attempted. However, due to the minimal thermal effect provided by the wall it proved to be difficult to approach the wall close enough to get an accurate position and still not come in physical contact with the wall. A number of calibration tests showed that coming in contact with the wall, even slightly, altered the characteristics of the wire; see Appendix A.

The final positioning method used in the case of the straight wires for the boundary layer and near separation point data was an optical one. A point light source was used to illuminate the wire at an angle of approximately 14 degrees. When the wire was near the wall it then cast a shadow which could be measured through use of a sighting device viewing normal to the wall. This allowed the wire to be accurately positioned to 0.2 mm from the wall surface. In each case the wire was placed slightly closer to the wall than this, then the traverse was driven so as to move the wire away from the wall until any mechanical play in the traversing system had been taken up. The amount of play was nominally .2 mm.

For positioning of the compact vorticity probe the wall shadow approach could not be used due to the construction of the probe. For the runs using the compact vorticity probe, the probe was positioned by placing it directly behind the separation step at X = 5. mm and Y = 0. mm. The Y location was ascertained by means of a sighting device positioned directly downstream of the separation point.

4

RESULTS AND DISCUSSION

4.1 Response of the upstream boundary layer to the forcing input

Mean velocity distributions, $\bar{u}(y)$, were obtained in the boundary layer region for $-30 \leq x/\theta_0 \leq 0$. These data were evaluated using the Clauser chart technique (Clauser [1954]) to determine the wall shear stress; see Figure 22. As shown in Figure 20, the mean velocity profile at the separation point for the forced and unforced conditions were only slightly different. However, at $x/\theta_0 = -5$ the mean profiles for the forced and unforced conditions were essentially the same; see Figure 31. The effect of the forcing at $x/\theta_0 = -5$ was, however, still visible as a difference in the phase averaged values; see Figure 32. Farther upstream, at $x/\theta_0 = -10$, the effect of the forcing is minimal; see Figure 33.

4.2 The Velocity Field in the Neighborhood of the Separation Lip

4.2.1 Mean velocity profiles for the unforced condition

Velocity distributions for the forced and unforced conditions, $u(y)$ and $v(y)$, were obtained for the separating flow at $x/\theta_0 = 1$ and $x/\theta_0 = 3$; see Figure 34. The mean velocity profile of the transverse velocity component for the unforced condition, $\bar{v}(y)$, is presented in Figure 35. As indicated in the figure, the transverse velocity has a mean positive value near $y = 0$, and the magnitude is greater at $x/\theta_0 = 3$ than at $x/\theta_0 = 1$. This behavior is apparently the result of the cavity formed by the piston and bounding plate assembly, which creates a low pressure region on the downstream side of the separation lip.

4.2.2 Mean velocity profiles for forced condition

Mean velocity profiles of the transverse velocity component for the forced condition, $\langle\bar{v}\rangle(y)$, are presented in Figure 36 through Figure 39. Also shown for reference on these figures is the physical geometry of the forcing piston for the indicated phase condition. As indicated in Figure 36, at $\phi = 0°$ the piston is fully extended towards the flow, $\langle\bar{v}\rangle$ is larger than the unforced case, and the difference is more pronounced at $x/\theta_0 = 3$ than at $x/\theta_0 = 1$. As the piston retracts through $\phi = 90°$ to $\phi = 180°$, Figure 37 and Figure 38, the difference between $\langle\bar{v}\rangle$ and $\bar{v}$ is increased. At $\phi = 270°$, Figure 39, the piston is at its maximum velocity in the $-y$ direction and while $\langle\bar{v}\rangle \simeq \bar{v}$ at

$x/\theta_0 - 1$, there is still a significant increase of $<\bar{v}>$ over $\bar{v}$ at $x/\theta_0 - 3$.

In order to better identify the phase behavior of the forcing on the flow, a velocity difference δu can be defined as:

$$\delta u - <u(x,y,\phi)> - <u(x,y)> \tag{13}$$

where $<u(x,y)>$ is the average over all phase angles.

To clarify the response of the separating shear layer to the forcing input, δu and δv are plotted as a function of the phase angle ϕ; see Figure 40 through Figure 47. At $y/\theta_0 - 0$, Figure 40 and Figure 41, $\tilde{\delta u}$ is much larger than $\tilde{\delta v}$ as a result of the lateral displacement of the fluid with a large velocity gradient. At $y/\theta_0 - -1$ $\tilde{\delta u}$ has decreased with respect to $\tilde{\delta v}$ and the difference between $\tilde{\delta u}$ at $x/\theta_0 - 1$ and at $x/\theta_0 - 3$ has been reduced. At $y/\theta_0 - -3$ the magnitudes of $\tilde{\delta u}$ and $\tilde{\delta v}$ are approximately equal and show little change from $x/\theta_0 - 1$ to x/θ_0-3. In the outer edge of the forming shear layer, $y/\theta_0 - -9.5$, δu is nearly zero while δv indicates a strong influence of the forcing. These data suggest a lateral displacement of the separating boundary layer in the $\pm y$ direction by the action of the forcing. This hypothesis leads to the definition of the quantity ξ, defined as

$$\xi - \frac{\tilde{\delta u}}{\tilde{\delta v} \ \dfrac{d<u>}{dy}} \tag{14}$$

which was computed for both the $x/\theta_0 - 1$ and $x/\theta_0 - 3$ locations; see Figure 48. For an idealized condition of a lateral displacement of a velocity gradient ξ should be a constant. As indicated in Figure 48, ξ is approximately constant for $1 \leq x/\theta_0 \leq 8$.

4.2.3 Kinematic Reynolds stress in the separating shear layer

The kinematic Reynolds stress distribution for the separating flow, along with data for an equilibrium turbulent boundary layer (Klebanoff [1954]), are presented in Figure 49. As indicated in the figure there is little change in the high speed region, both the data at $x/\theta_0 - 1$ and $x/\theta_0 - 3$ are in good agreement with an equilibrium boundary layer. In the region $-4 \leq y/\theta_0 \leq -0.5$ the relaxation of $\overline{u'v'}$ as a result of the removal of the wall is indicated; the increase of $\overline{u'v'}$ in the region $-0.5 \leq y/\theta_0 \leq 1$ for the evolving shear layer can also be seen.

4.3 Evolution of the unforced and forced shear layers

4.3.1 Mean velocity profiles

Mean and phase averaged velocity data were obtained using single wire measurements for the region $1 \leq x/\theta_0 \leq 230$. Isotachs for the unforced conditions are presented in Figure 50 and Figure 51, along with similar amplitude results from the Fiedler and Mensing [1985] study. As can be seen from the figures, the strongly forced shear layer exhibits a stepped growth rate, with a plateau at $1.0 < (x-x_s)f/U_0 < 1.5$. It is pertinent to note the qualitative agreement between the current

study, (ie. Figure 51), and the prior work by Fiedler and Mensing [1985], (ie. Figure 52). In the latter case the strong levels of forcing led to a premature separation of the boundary layer which was not present in the current study.

Mean velocity profiles for the single wire data; average unforced, long term average forced, and minimum and maximum phase average forced, are presented in Figure 53 through Figure 65. The trends in these data are most easily seen in the large x/θ_0 data where the differences between the long term averaged forced data and the unforced data, along with the differences between the minimum and maximum phase averaged values of the forced data, are quite apparent. Little effect of the forcing is seen in the mean profiles at $x/\theta_0 - 1$; the gradual evolution between this location and that of $x/\theta_0 - 230$ can be easily traced from the figures.

The minimum and maximum values for the forced condition exhibit a dramatic acceleration and deceleration characteristic on the high speed side of the shear layer in the downstream region; see Figure 60. It is inferred that the accelerated state is similar to the "inviscid acceleration past an obstruction" since the phase averaged velocity values, $\langle \bar{u} \rangle$ are significantly larger than U_0. The data for the unforced condition (at the same streamwise location as Figure 60), indicate the lack of a similar effect; see Figure 66. The corresponding minimum values for the forced condition are are also inferred to represent pressure effects.

4.3.2 Phase averaged data

The evolution of characteristics in the forced flow field can be readily seen from phase averaged isotachs of the single wire data. Plots of δu (as defined in 13) versus the phase angle ϕ are presented in Figure 67 through Figure 79. The characteristics of these data can be plausibly related to the forcing effects as noted in the following:

a) For the region downstream of the separation lip, $1 \leq x/\theta_0 \leq 5$, Figure 67 to Figure 69, the positive ($\phi \simeq 120$) and negative ($\phi \simeq 270$) locations represent the effects of the piston motion in the +y and -y directions respectively. The primary effect of the forcing at this point is a steering of the large mean velocity gradient; as shown in the figure the influence region is quite limited in the y direction. At $x/\theta_0 = 5$, the appearance of isolated correlation contours in phase space can be noted. For the sake of brevity these will be referred to simply as correlation contours in the following discussion.

b) For $10 \leq x/\theta_0 \leq 25$, Figure 70 to Figure 72, the positive and negative correlation contours are better defined and the region of influence is wider. At $x/\theta_0 = 25$ the centroid of the correlation contour is located closer to the high speed side of the shear layer than it was at $x/\theta_0 = 10$.

c)   For $40 \leq x/\theta_0 \leq 77$ (Figure 73 to Figure 75), the magnitudes of the correlation contours reach a maximum and the formation of correlation contours of opposite sign on the low speed side of the shear layer is first noted. The correlation contours on the high speed side of the shear layer will be referred to as the primary correlation contours, while those on the low speed side will be referred to as the secondary correlation contours.

d)   For $115 \leq x/\theta_0 \leq 153$ (Figure 76 to Figure 77), the primary correlation contours have migrated farther in the direction of the high speed side; the intensity of the primary correlation contours has continued to decrease, while that of the secondary correlation contours has increased.

e)   For $192 \leq x/\theta_0 \leq 230$, Figure 78 to Figure 79, the intensity of the primary correlation contours has dropped below that of the secondary correlation contours; the secondary correlation contours dominate the field.

The distinctive feature of the correlation contours allow a convection velocity to be defined at a given downstream location. Specifically the phase shift between the correlation contour peaks at two x/θ_0 locations, see Figure 80, can be related to a time difference using the forcing period as follows:

$$t_2 - t_1 = \left[\frac{\phi_2 - \phi_1}{360} + 360\,n \right] \times \tau_f \qquad (15)$$

where n is an integer number of forcing periods. If the data locations are sufficiently close together, as is the case in the current study, n is 0. From this time difference and the spatial distance between the data sampling locations, a convection velocity for the disturbance can be defined as:

$$U_c = \frac{X_2 - X_1}{t_2 - t_1} \qquad (16)$$

Using these procedures, the convection speed was determined for the data locations $x/\theta_0 \geq 15$; see Figure 81. The increasing U_c values as function of x/θ_0 are rational considering the previously noted migration of the primary disturbance towards the high speed side of the shear layer.

The width of the disturbance region $\Delta(x)$ can be arbitrarily defined using the integral quantities

$$\Delta^2 = \frac{\int_0^{2\pi} \int_{-\infty}^{\infty} |\delta u| (y - y_c)^2 \, dy \, d\phi}{\int_0^{2\pi} \int_{-\infty}^{\infty} |\delta u| \, dy \, d\phi} \qquad (17)$$

where y_c is the centroid of the disturbance field, as defined in (18).

$$y_c = \frac{\displaystyle\int_0^{2\pi} \int_{-\infty}^{\infty} |\delta u|(y) \, dy \, d\phi}{\displaystyle\int_0^{2\pi} \int_{-\infty}^{\infty} |\delta u| \, dy \, d\phi} \tag{18}$$

The data for Δ/θ_0 as a function of x/θ_0 are presented in Figure 82 along with the growth rates of $\theta(x)$ for the forced and unforced conditions.

Empirically, the growth of the disturbance field can be described as a power law relationship:

$$\Delta/\theta_0 = 0.0063 \, (x/\theta_0)^{1.64} \tag{19}$$

for $0 \le x/\theta_0 \le 60.0$ and as a linear relationship:

$$\Delta/\theta_0 = 0.0784 \, x/\theta_0 - 0.319 \tag{20}$$

for $77 \le x/\theta_0 \le 192$.

The discontinuity of the growth rate at $x/\theta_0 \simeq 60$ is apparently related to the indicated saturation (ie. the peak δu value) at this x location. The indicated linear growth rate is nominally the same as the growth rate of $\theta(x)$ over the same domain.

Fiedler and Mensing [1985] also observed a saturation effect; theirs was defined in terms of the maximum of the transverse velocity components. Defining this streamwise location as x_s, their result showed that for a forcing level which was comparable to that used in the present study,

$$\frac{f(x_s - x_0)}{U_0} \simeq 0.75 \qquad (21)$$

where x_0 was defined as a virtual origin. This virtual origin was defined from their data of $x_s - x_s(f)$ at a given amplitude. It was observed that $(1/f)$ is a linearly increasing function of x_s. An extrapolation of this relationship to $(1/f) \rightarrow 0$ defined the x_0 value for the given forcing amplitude.

An apparent origin cannot be determined herein since a single frequency was used in the present study. In order to compare the two investigations, it can be assumed that only kinematic effects are represented in the f, x_s, and U_0 relationships and a comparison of the values (fx_s/U_0) can be made for "equivalent" forcing amplitudes.

The present observations permit the maximum value of

$$\left[\tilde{u}_f^2 + \tilde{v}_f^2 \right]^{1/2} / U_0 = 0.045 \qquad (22)$$

to be determined at $x/\theta_0 = 1$. Similarly, Fiedler and Mensing [1985] present data from a single hot-wire immediately downstream of the

slot.   Their   values   of   (0.065)   and   (0.0065)   bracket   those   of   the
present study.

Defining   a   saturation   length   for   the   current   study   based   on   the
maximum δu values results in a value of x_s − 0.5 m.   Hence,

$$\frac{fx_s}{U_0} = 0.62. \tag{23}$$

Using   the   Fiedler and Mensing [1985] $(1/f) \propto x_s$ results   and   in-
terpolation for the forcing amplitude parameter,   a frequency   of   13.2
Hz   is   estimated   for   the   saturation   length   of the current study:
0.5 m.   The corresponding fx_s/U_0 value is 0.60.

The   striking   agreement   between   these   two   results,   in   spite   of   the
significant differences in the forcing geometries and in the   Reynolds
numbers   of the separating boundary layers (5500 cf 830),   supports the
assumption that the forcing process is kinematic in character.

4.4   Response of the entrainment field to the forcing input

Velocity   vector   measurements   of   the   entrained   flow   were   performed
in the region $100 \leq x/\theta_0 \leq 200$ for both the unforced and forced condi-
tions.   The data for the unforced condition and the mean forced condi-
tion are presented in the form of a velocity vector plot in Figure 83.
As   indicated   in that figure,   there is a noticeable mean steering ef-
fect of the entrained fluid beyond the active,   (ie.   vortical),   shear
layer.   Prior investigations in the same facility,   Ali et.al.   [1985],

verified a uniform velocity at the exit of the entrainment condition-
ing section, $10 < x/\theta_0 < 420$, for the unforced condition. The ob-
served mean steering is consistent with other observed data for the
facility as discussed in the following.

An evident feature of the isotachs for the forced shear layer is
their greater width on the low speed side of the shear layer. This
clearly suggests that a greater mass flux exists at a given downstream
location. Other evidence, however, does not support this interpreta-
tion. Specifically, with the fan motor set to a fixed operating
speed, it was observed that the free stream velocity of the primary
flow (U_0) remained unchanged between the unforced and forced condi-
tions. Since the U_0 value is dictated by the pressure difference from
the atmosphere to the test section and since the constancy of the: i)
pressure rise from the receiver (ie., the domain that receives the
flow from the test section and delivers it to the fan) to the atmos-
phere and ii) the fan rpm, dictate a constant operating point on the
characteristic curve, it is inferred that the volume flow rate through
the fan is a constant. It is therefore concluded that the magnitude
of the entrainment flow rate into the test section is not affected by
the forcing.

These separate observations can only be compatible if there is a
significant steering effect of the entrainment streamlines as shown
schematically in Figure 84. Specifically, with forcing, the
entrainment fluid is added to the active shear layer and the flux of

vortical fluid at a given x/θ_0 value is larger than that of the un-forced case. Similarly, the streamline trajectories of the unforced case deliver a significant volume flow rate of non-vortical fluid past a given x/θ_0 plane, shown as $\beta\dot{m}$ in Figure 84

As a result of experimental difficulties, identified below, quantitative measures of the steering could not be obtained to verify the above hypothesis, However, the qualitative trends of the data are apparent, and they support the proposed flow model of Figure 84.

Previous flow visualization measurements in the entrainment region, Foss [1987], indicated a mean flow angle for the entrained fluid of approximately 60°. Based on this data, quantitative measurements were made in the entrainment region using a compact vorticity probe oriented at an angle of 60°. Additional surveys were made at probe orientations of 45° and 90°. The resulting data indicated a strong steering effect, causing the measured velocity to tend to be aligned with the probe body. This effect could be caused by aerodynamic influence of the probe body, momentum wake effects of the wire support prongs, thermal wake interference between the wires, or perhaps a combination of all three. The exact cause of this effect is not clear at the time of this writing.

5

CONCLUSIONS

A relatively small perturbation of the separating boundary layer evolves into a strong perturbation of the developing shear layer.

The effect of the forcing on the separating boundary layer for the geometry of the current study is twofold: i) A lateral displacement of the mean velocity profile for $y/\theta_0 > 1$ and ii) an unsymmetrical widening effect for $y/\theta_0 < 0$. For the region $0 < y/\theta_0 < 1$ a combination of these effects is inferred.

For equivalent forcing amplitudes, the qualitative evolution of the shear layer is consistent with the prior work of Fiedler and Mensing [1985]; specifically, quite similar values of (fx_s/U_0) were observed in spite of quite different values of the forcing methods and separation lip geometries.

Phase averaged variations (δu) about the mean values of forced flow ($\bar{\delta u}$) exhibit closed contours in phase space. A convection velocity of the closed contours can be computed from the phase shift between two axial locations (see Figure 81). A width measure of the disturbance field can be defined as a moment of δu in phase space (see Figure 82). The apparent motions of the closed contours are consistent with the trends observed for the computed convection velocity.

The entrainment region outside the active shear layer exhibits a mean steering of the flow field for the forced condition relative to the unforced condition. This mean steering is consistent with other observed data for the facility.

The well documented conditions at separation for this study, specifically the detailed measurements of u and v as a function of forcing phase angle, should provide a good test case for numerical simulations.

Trailing edge:
version 1

$$R_\theta = 830$$

Trailing edge:
version 2
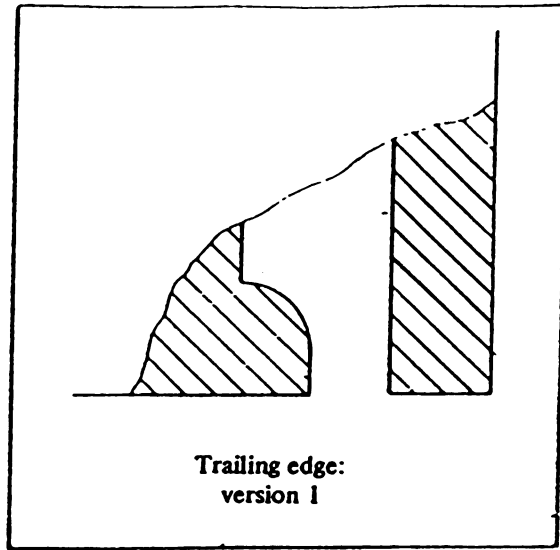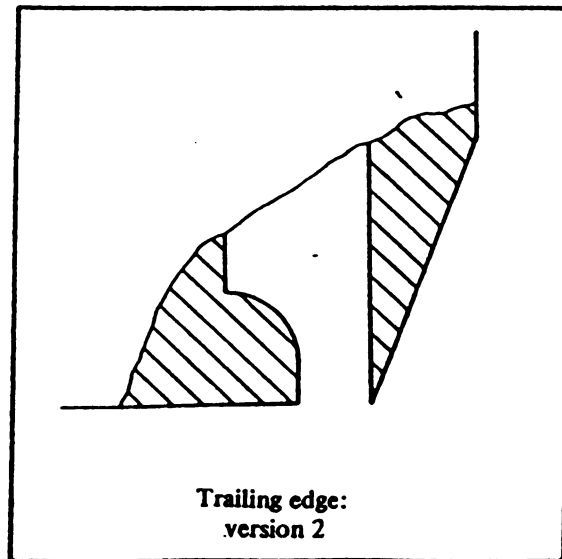
Adapted from Fiedler and Mensing [1985]

Figure 1 - Separation lip geometry for Fiedler and Mensing [1986]

Legend: AD   - ACCESS DOOR
        AF   - AIR FILTER (THREE FRONT SURFACES)
        ZC   - ZEROTH CONTRACTION
        FCE - FIRST CONTRACTION EXTENSION
        FC   - FIRST CONTRACTION
        TM   - TURBULENCE MANIPULATORS
        SC   - SECOND CONTRACTION
        BLT - BOUNDARY LAYER TRANSITION MODULE
        VP   - VIEWING PLATFORM
        TS   - TEST SECTION
        EM   - ENTRAINMENT AIR INLET
        TSE - TEST SECTION EXTENSION
        BP   - BLEED FLOW PLENUM
        BF   - BLEED FAN
        M   - BLEED FAN MOTOR
        PF   - PRIMARY FAN
        FB/SC - FEED BACK/SPEED CONTROL FOR PRIMARY FAN
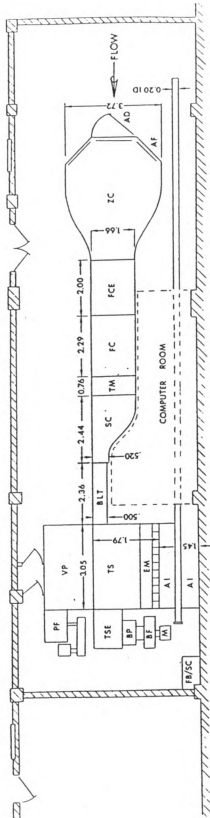
ALL DIMENSIONS ARE IN METERS
DO NOT SCALE

Figure 2 - Plan view of experimental facility

Test Section for the
Single Stream Shear Layer

Turbulence Manipulators:
Entrainment

x=3.0m

x

ū

yl/2

Distributed
Roughness
(16 Grit
Sandpaper)

1.21 m

0.5 m

U₀

y
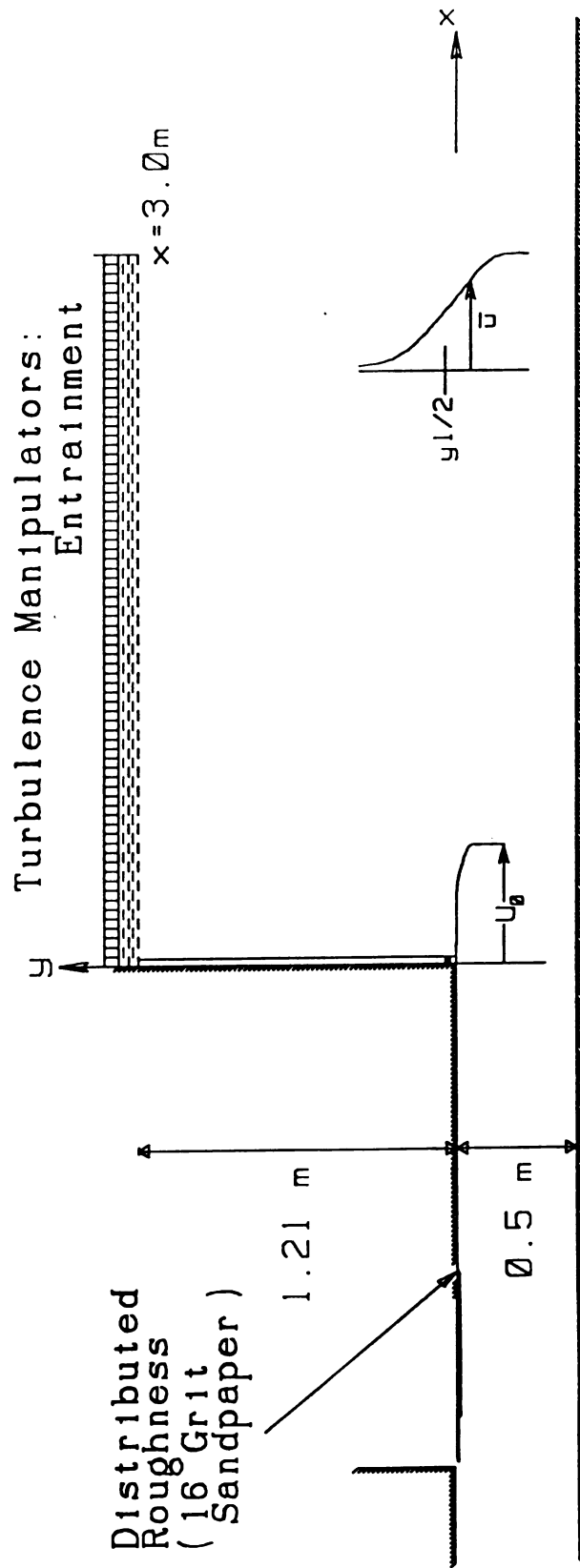
Figure 3 - Test section
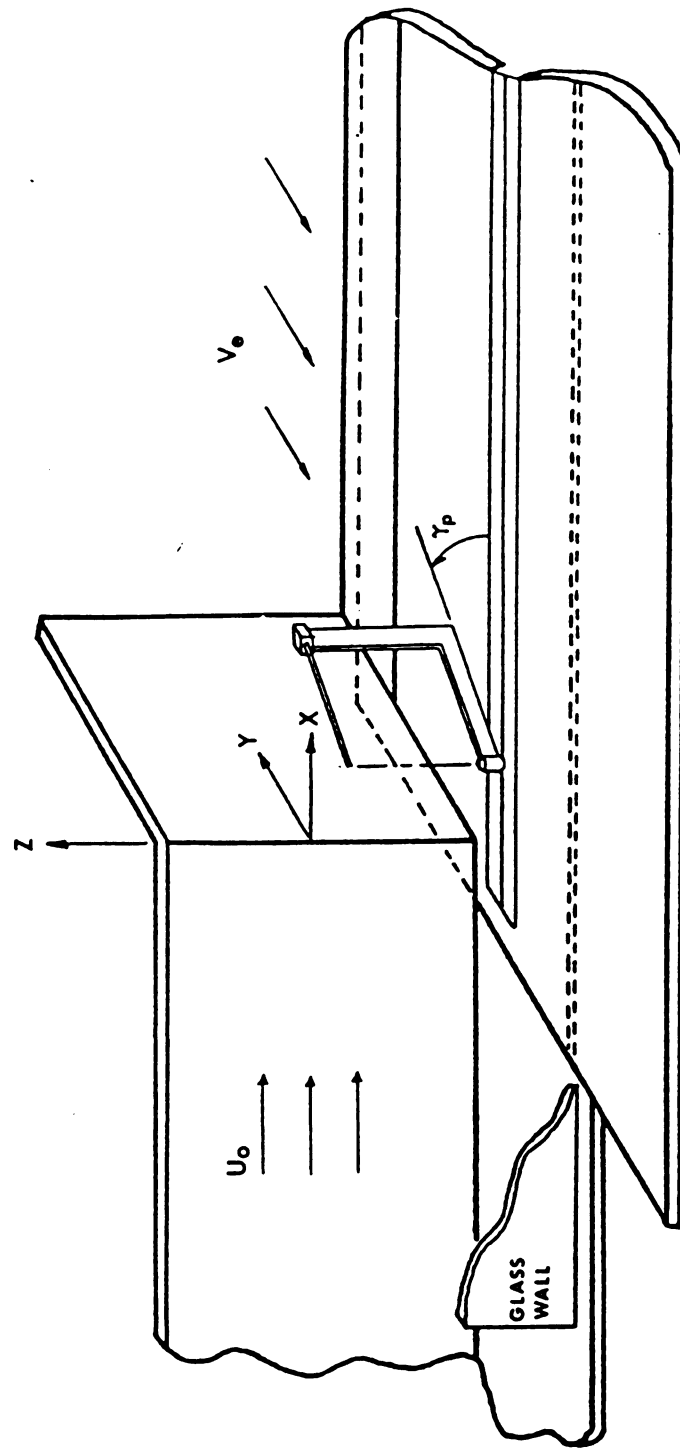
Figure 4 - Schematic Representation of the Traverse System
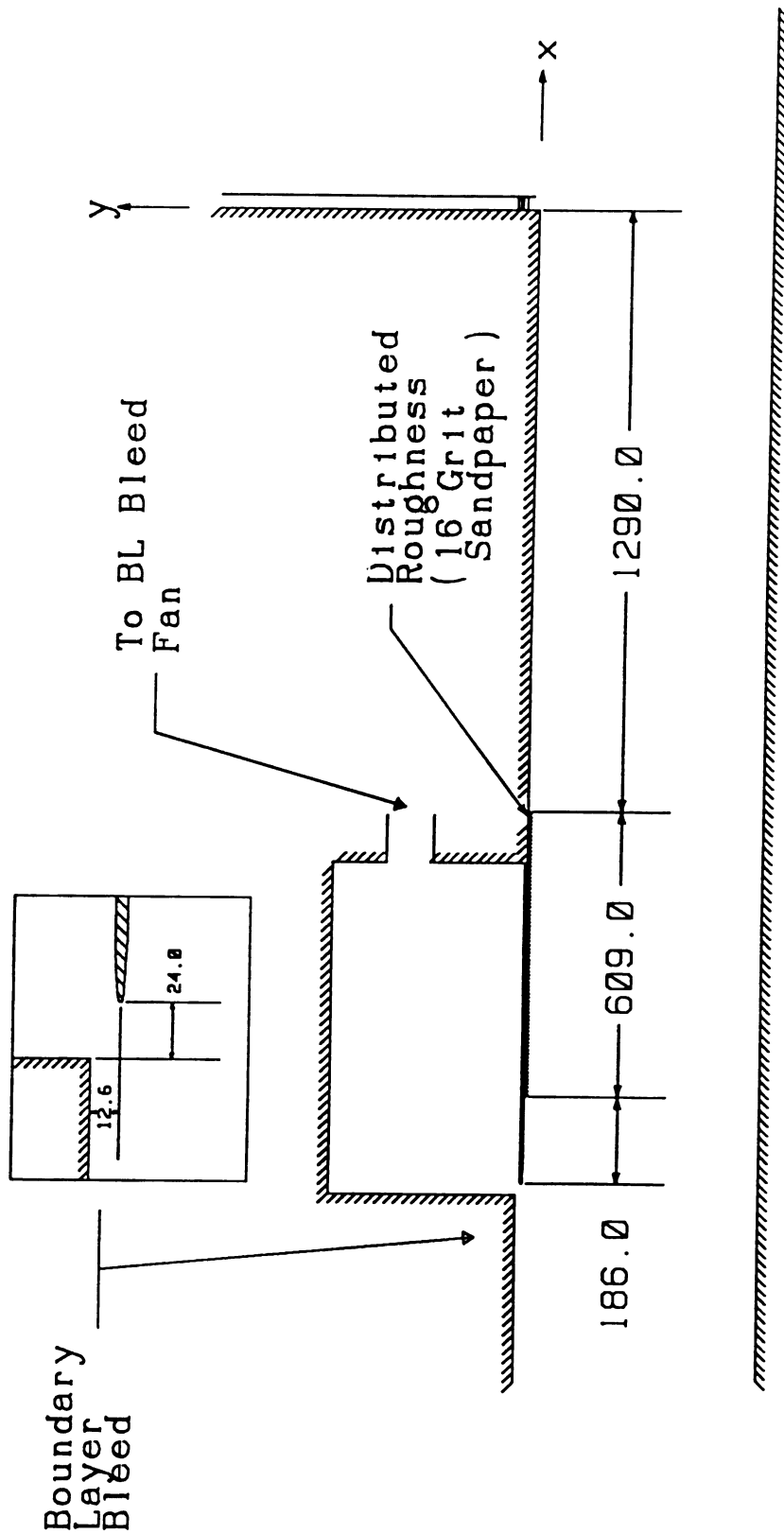
Adapted from Disimile [1984]

Figure 5 - Boundary Layer Development Section

THROTTLE
ADJUSTMENT
SLIDE

VIEW "LOOKING INTO"
ENTRAINMENT MODULE

CAVITY 1

CAVITY 2

SECTION A-A'

A

A'
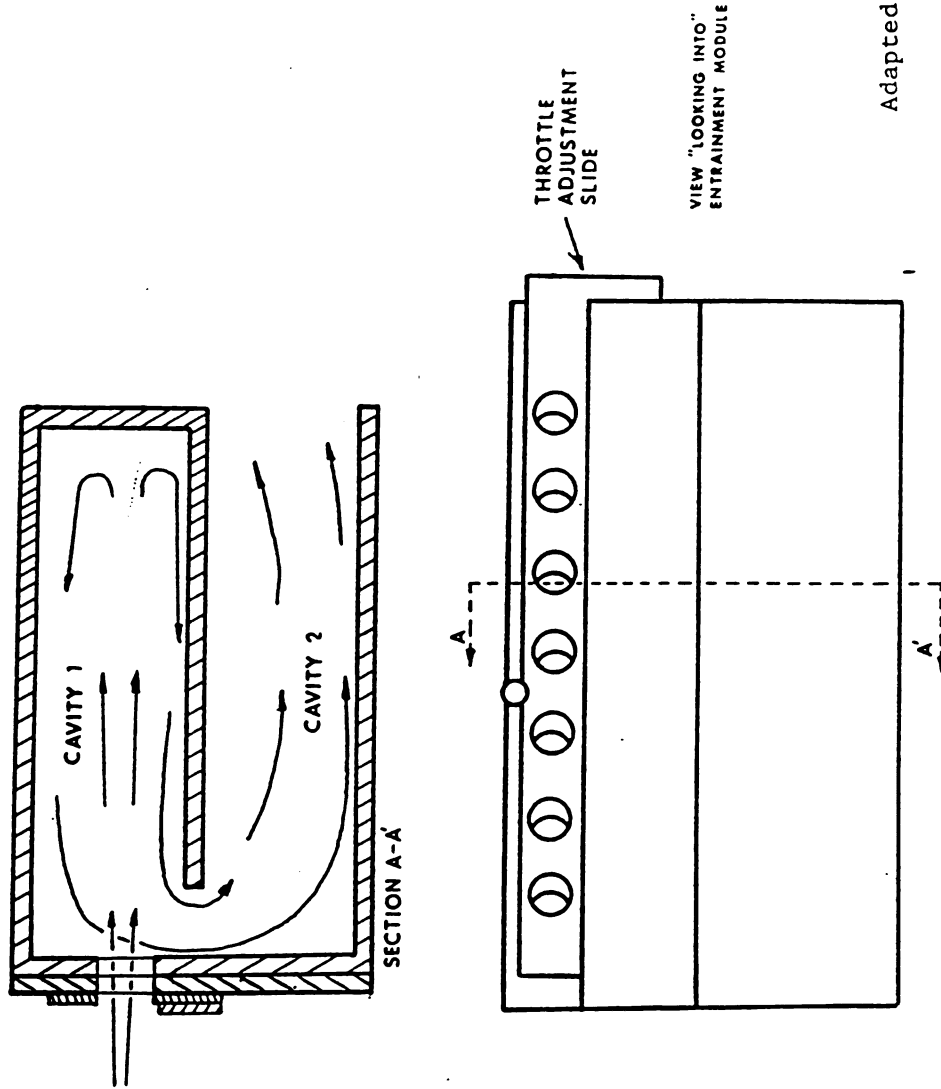
Adapted from Disimile (1984)

Figure 6 - Entrainment Throttling Chamber Detail

COURSE SCREEN

HONEYCOMB

FINE SCREEN
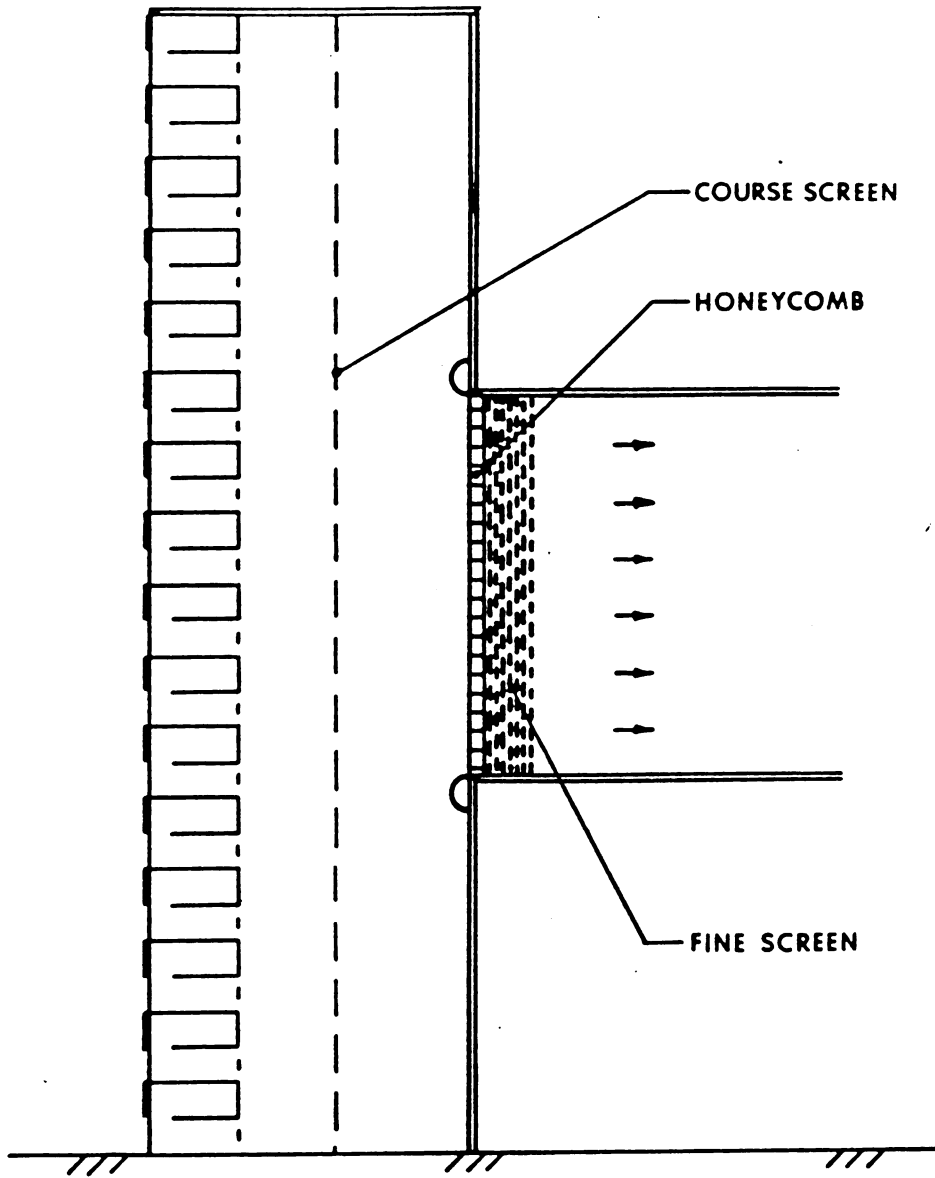
Adapted from Disimile [1984]

Figure 7 - Entrainment Flow Conditioning
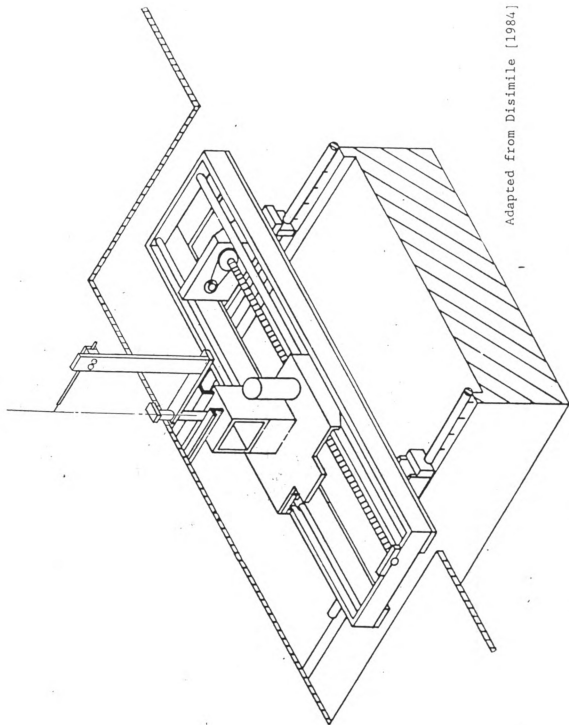
Adapted from Disimile [1984]

Figure 8 - Schematic Representation of the Traversing Mechanism

28.0

12.7

0.76

32.3

21.3

(All Dimensions in mm)

Fully retracted position

Fully extended position
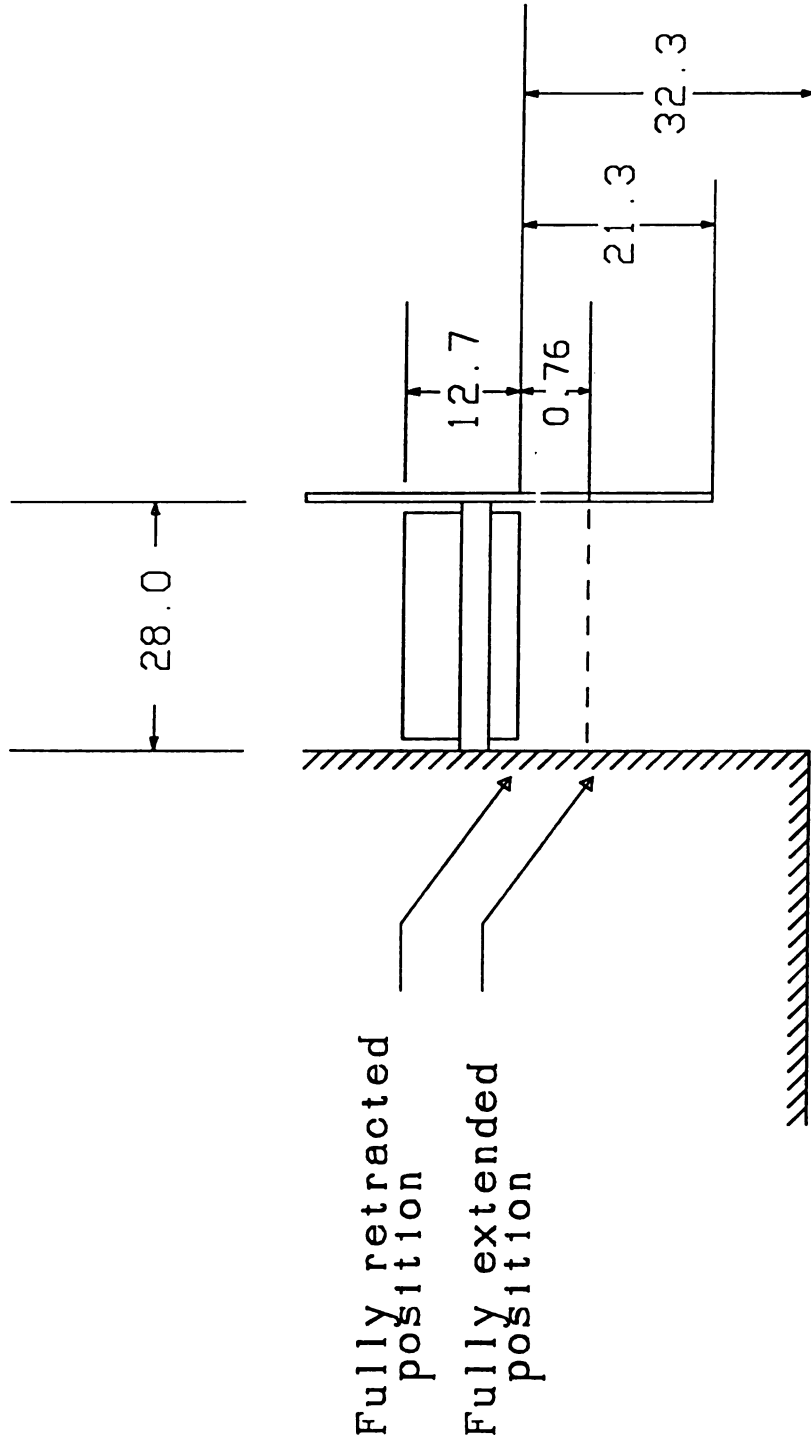
Figure 9 - Forcing Piston Detail

53
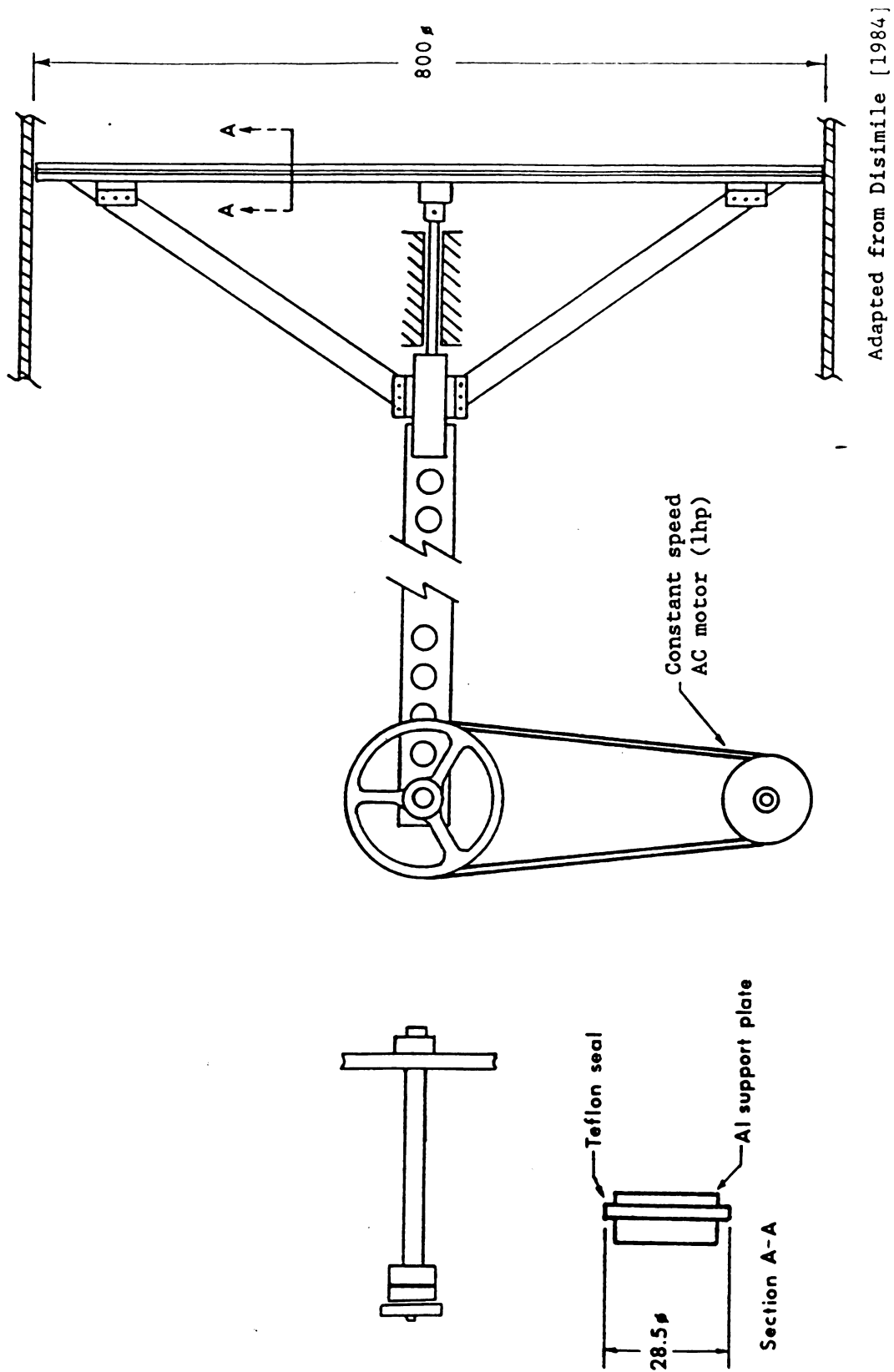
Figure 10 - Forcing Piston Side View

SHOULDER BOLT

Optical pickup

Adapted from Disimile [1984]
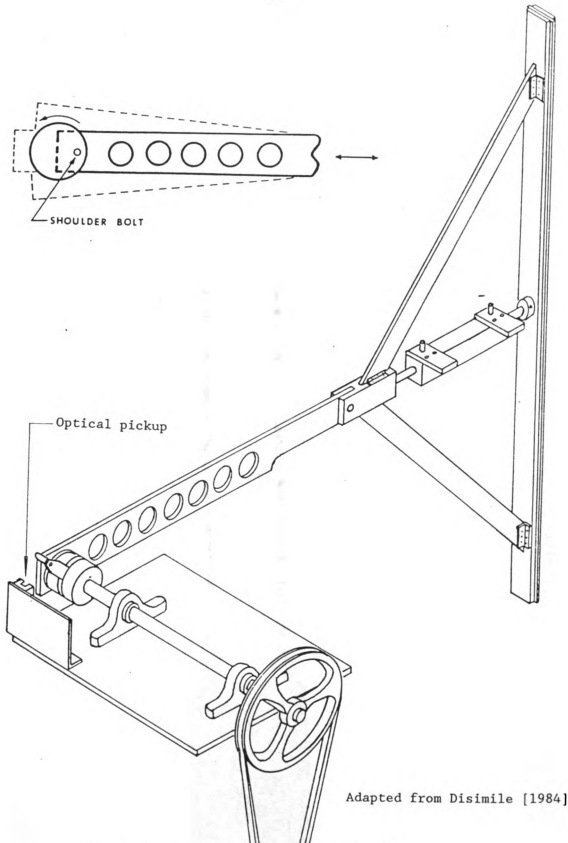
Figure 11 - Forcing Piston Isometric View

Copper Plated
5μ Tungsten
Wire

3.0

1.0

Jewelers Brooch
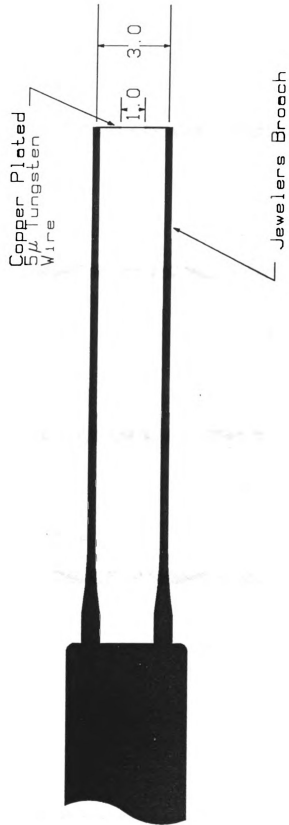
Figure 12 - Typical hot-wire

Hot-wire —

Jewelers Broach —

Normal Wire Mounting

Hot-wire —

Jewelers Broach —
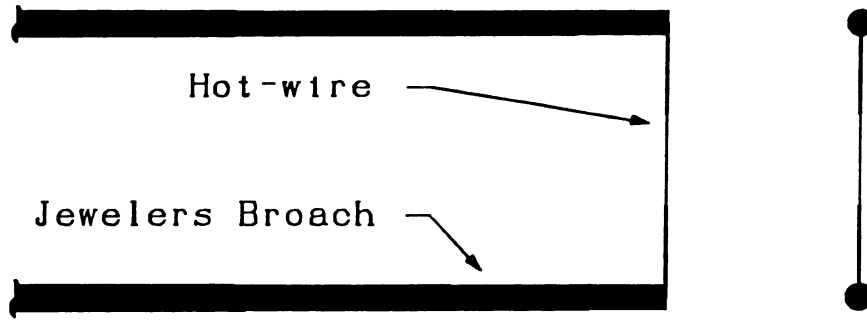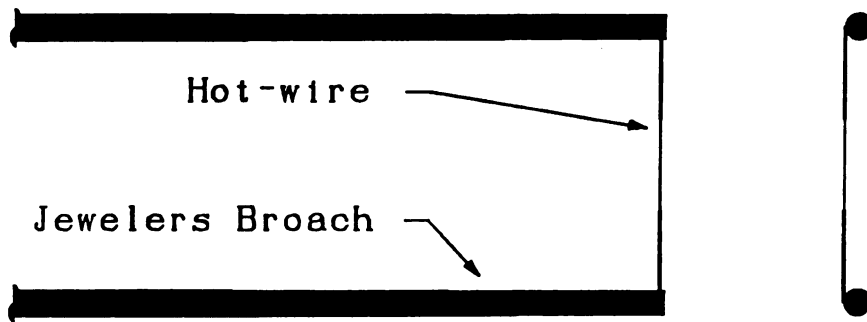
Modified Wire Mounting

Figure 13 - Modified wire mounting for boundary layer surveys

End View

Top View

Side View
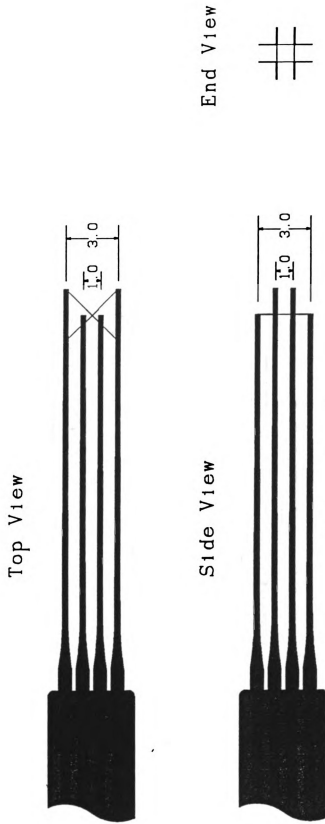
Figure 14 - Schematic presentation of Compact Vorticity Probe
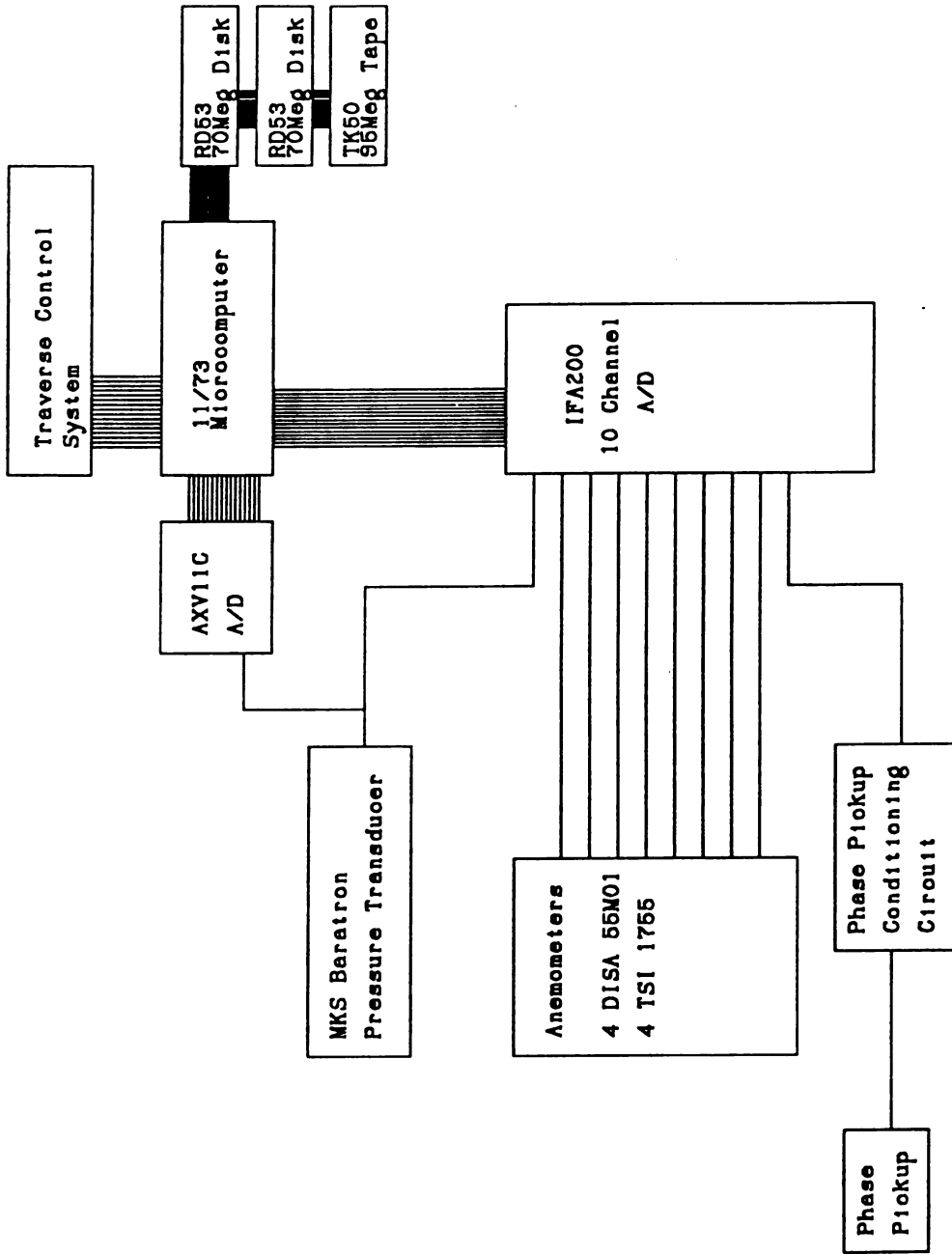
Figure 15 - Data Taking System
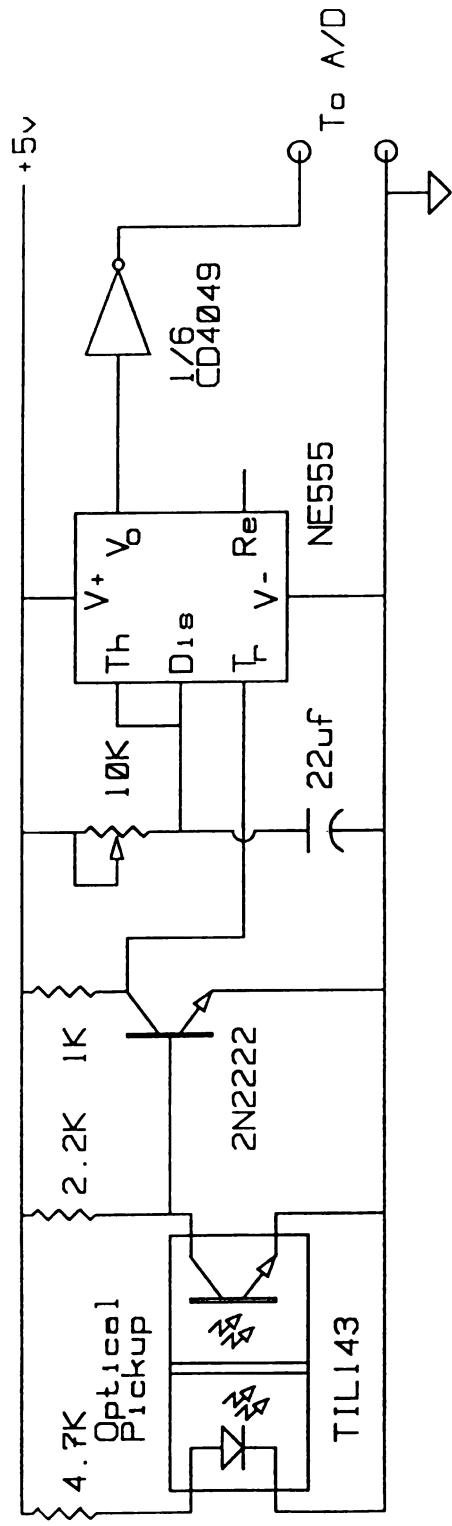
Figure 16 - Optical phase pickup and conditioning circuit
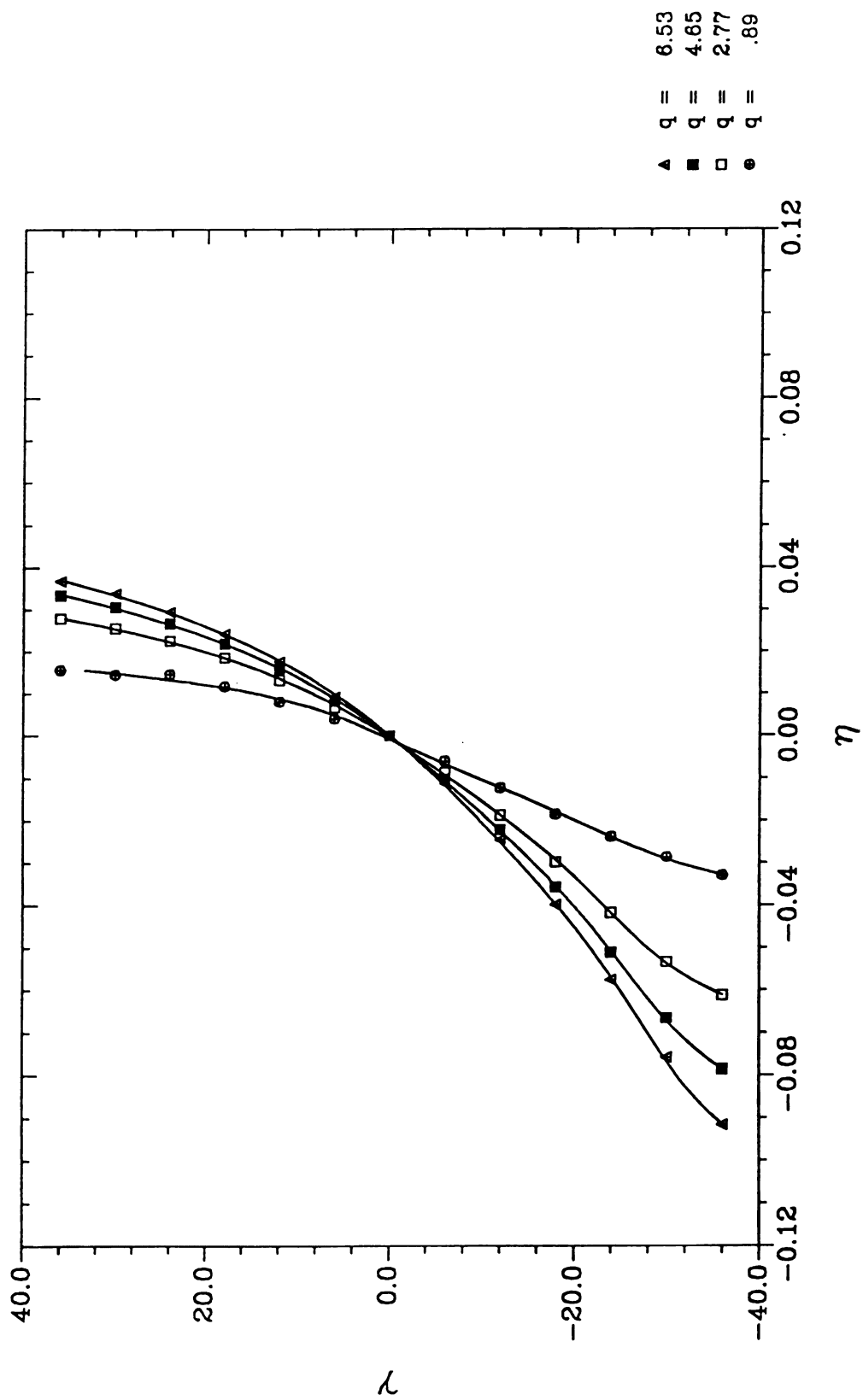
Figure 17 - Raw calibration versus fitted $\gamma = f(\eta)$ curve.

61
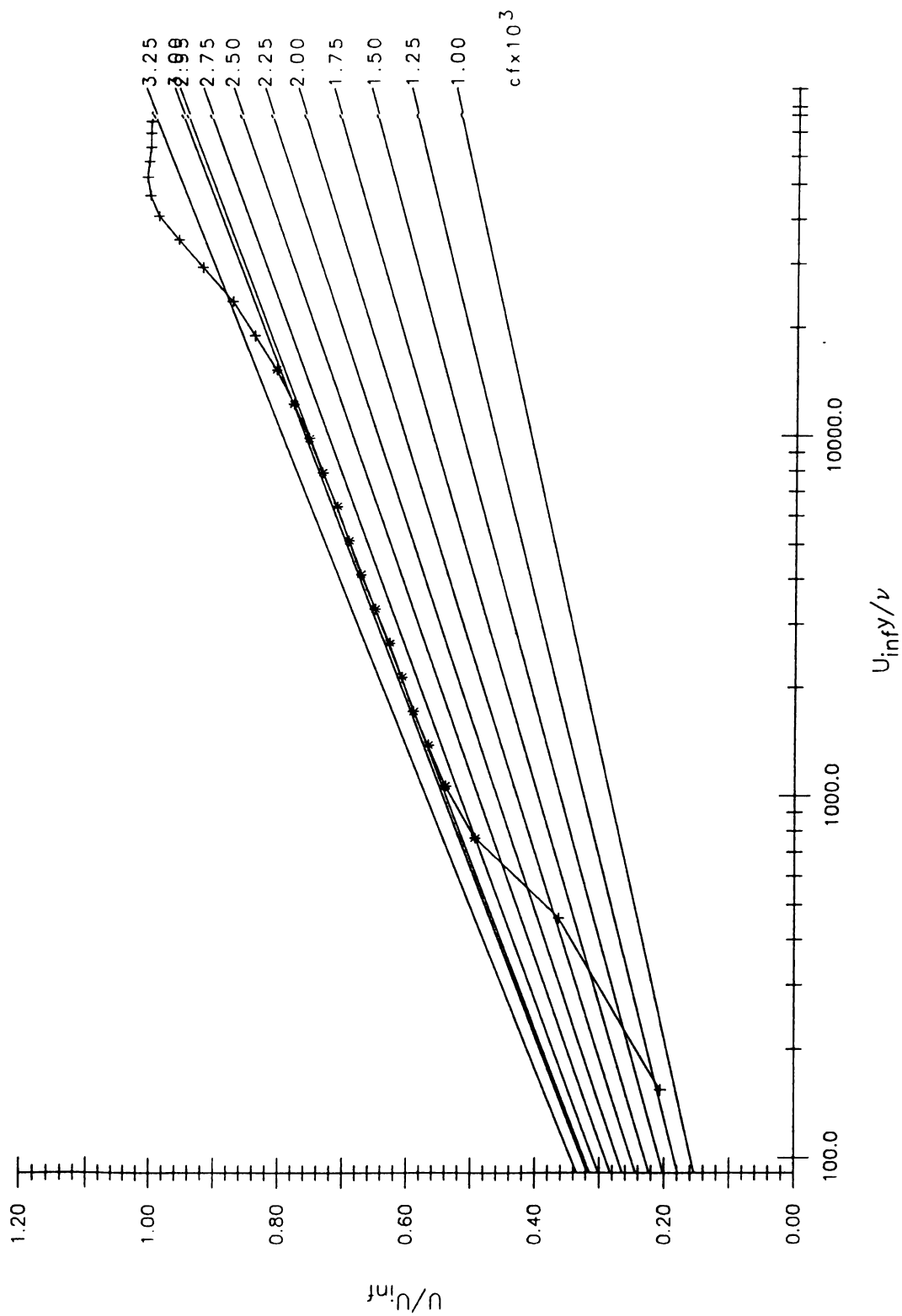
Figure 18 - Clauser Plot of unforced BL at X/θ = 0.0
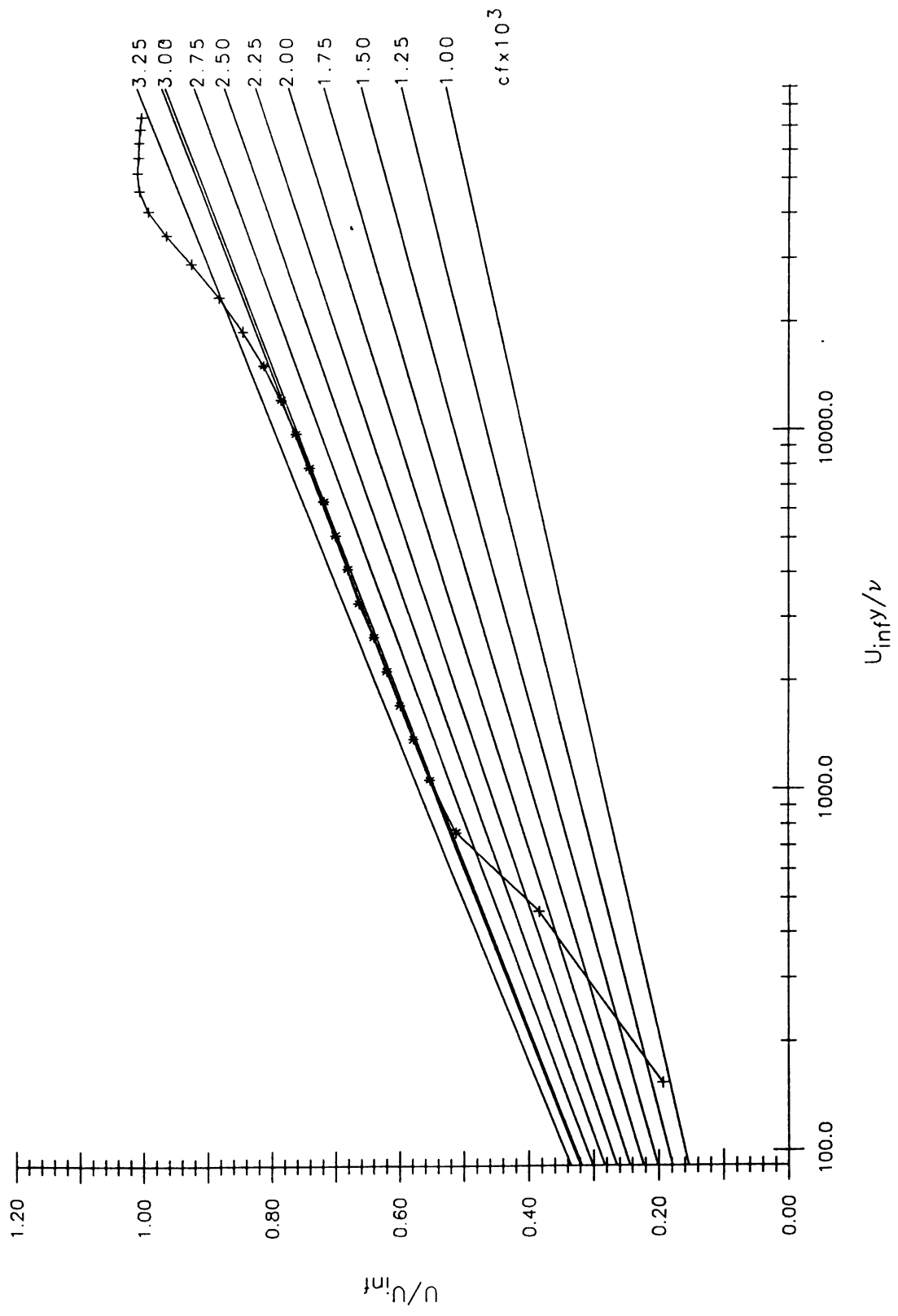
Figure 19 - Clauser Plot of forced BL at $X/\theta = 0.0$
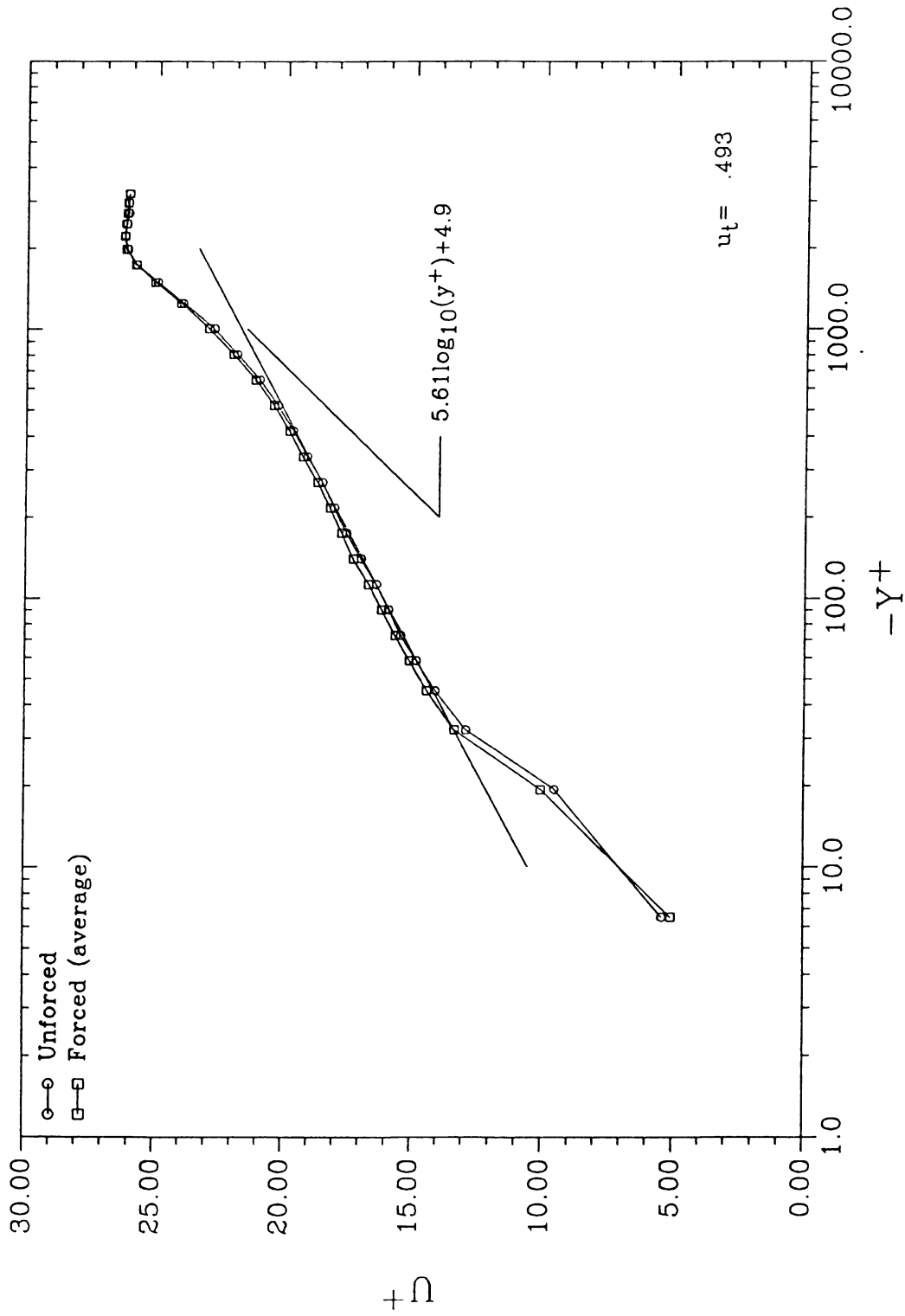
Figure 20 - Boundary layer mean profile at $x/\theta_0 = 0.0$
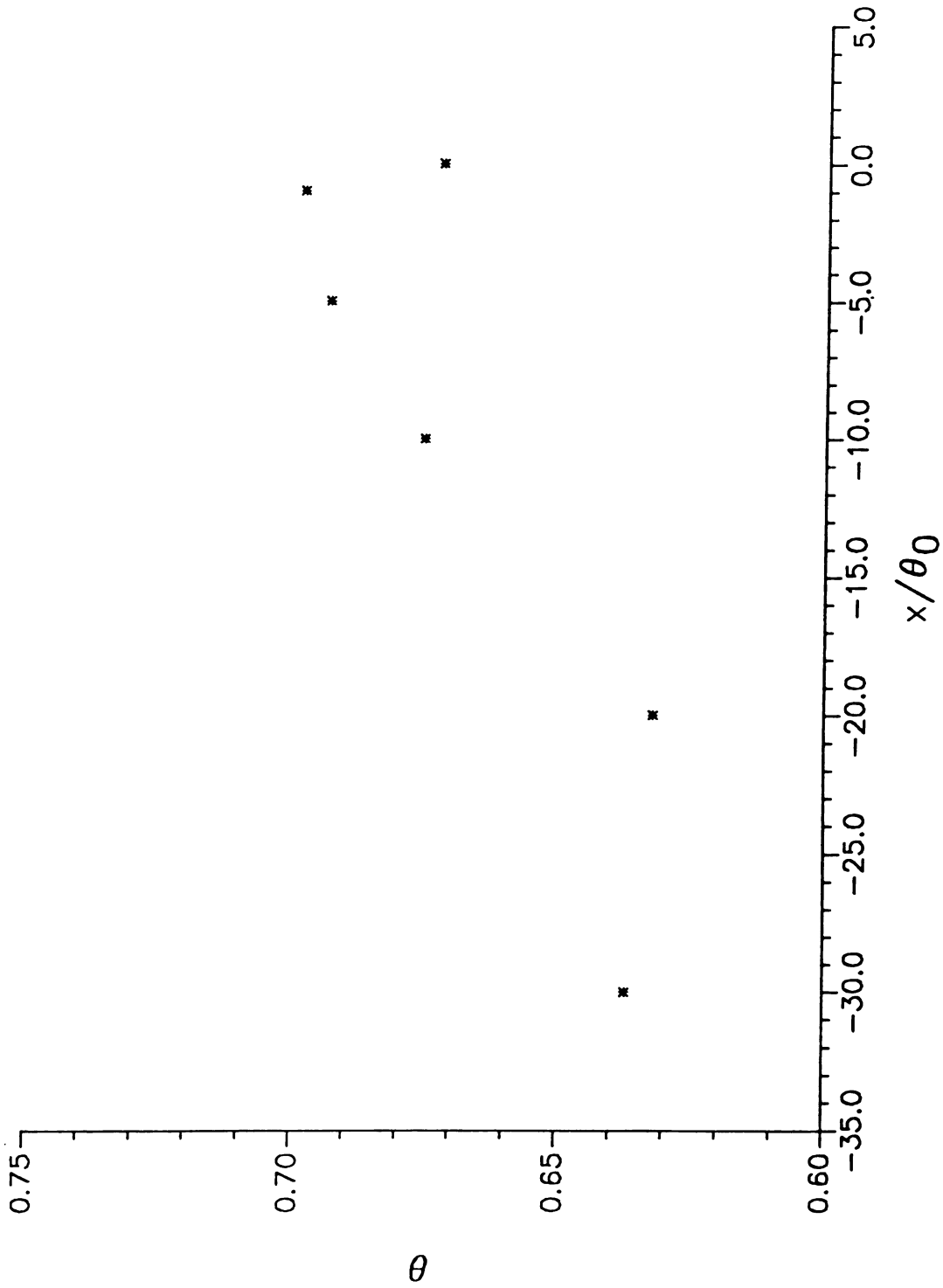
Figure 21 - Boundary layer momentum thickness
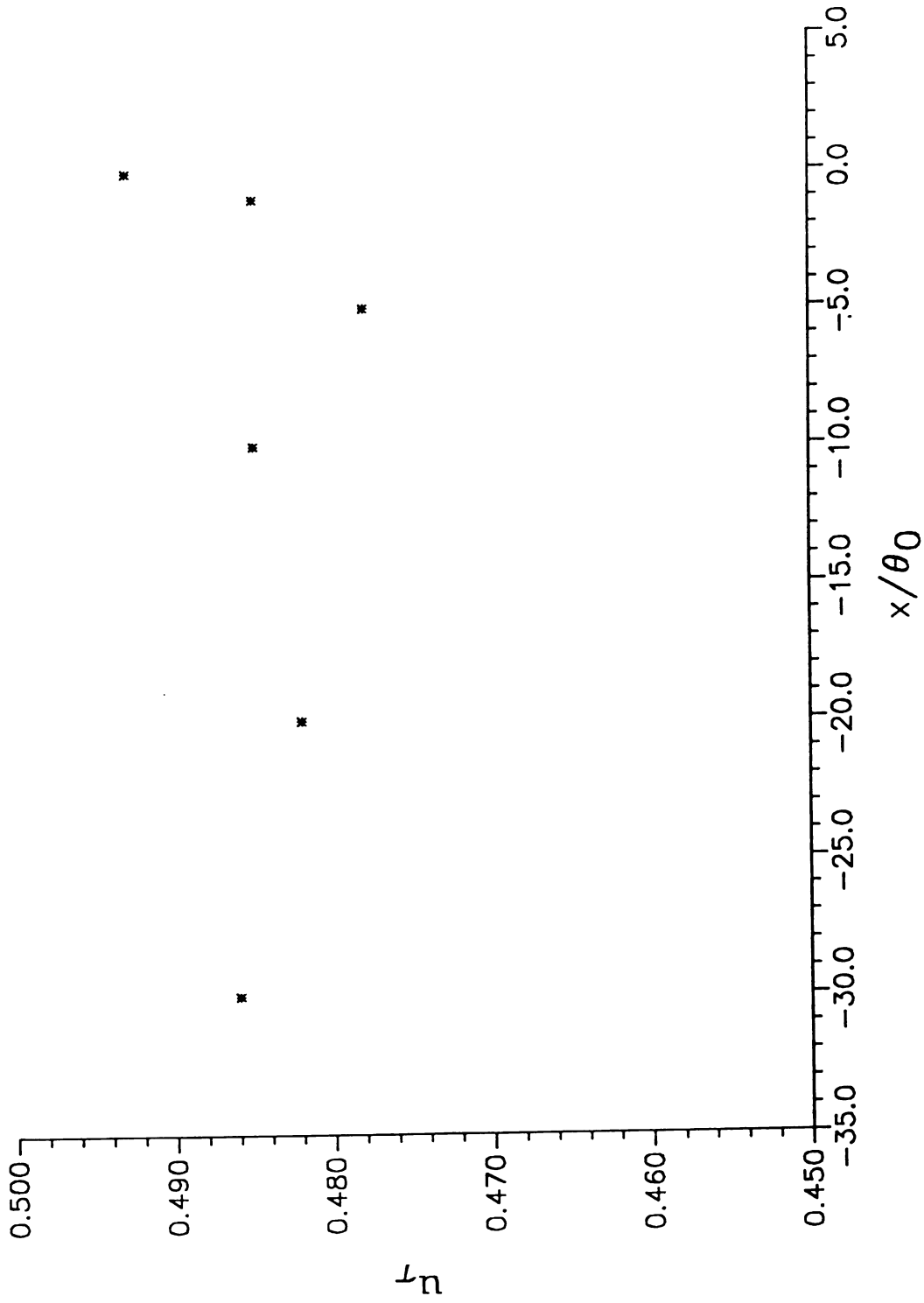
Figure 22 - Boundary layer friction velocity
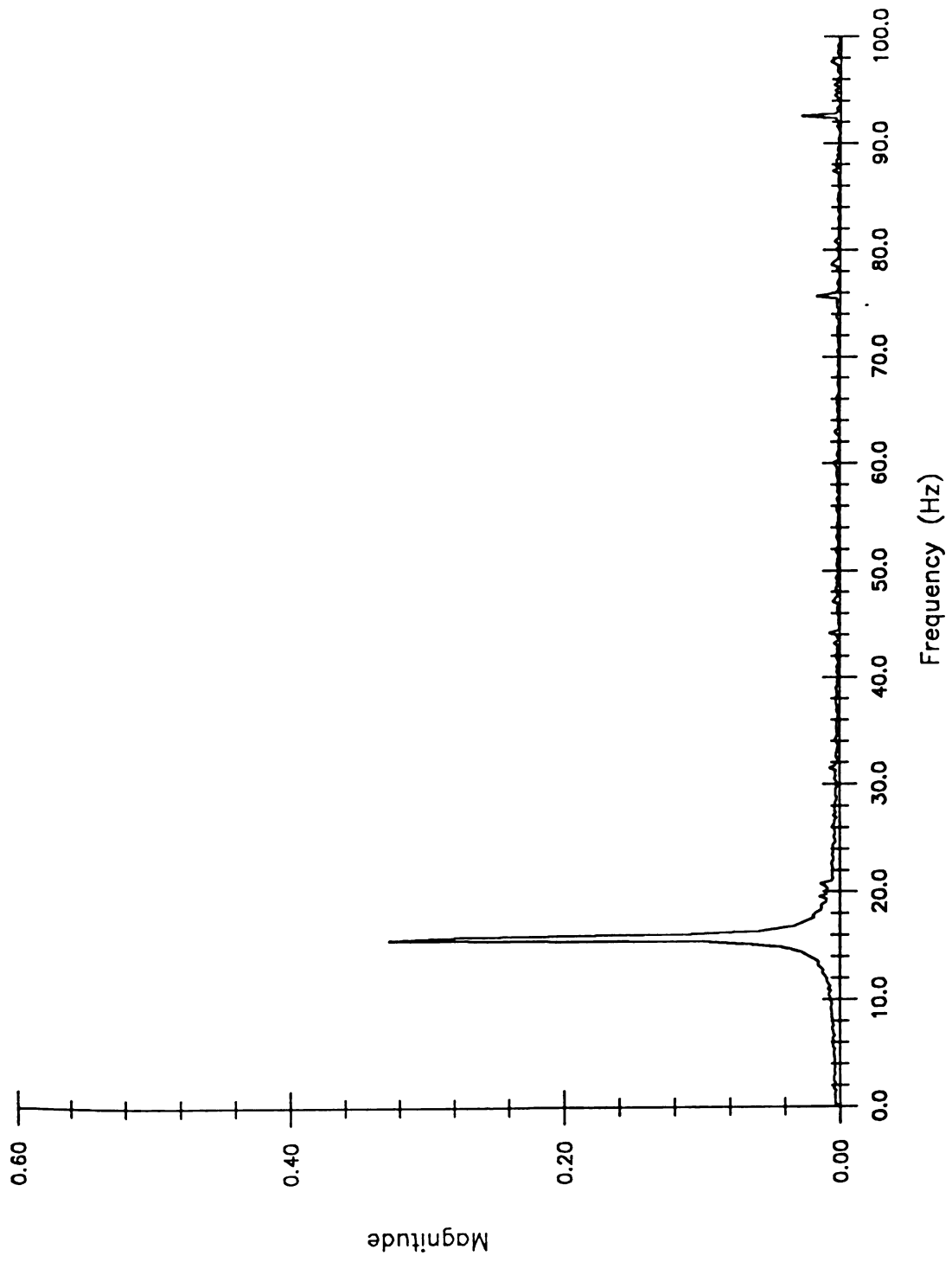
Figure 23 - Power spectrum of piston acceleration (z=0.0)

67
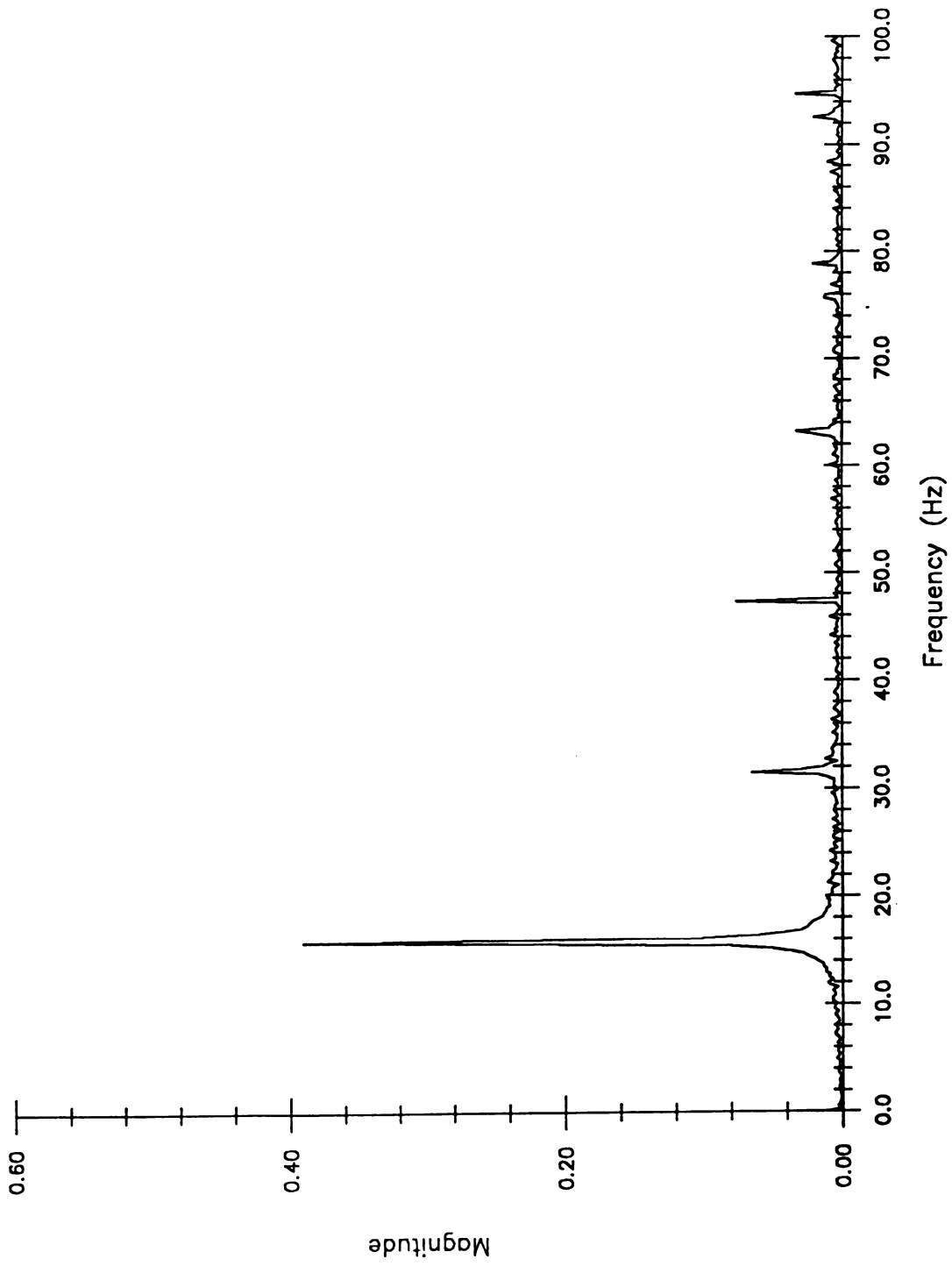
Figure 24 - Power spectrum of piston acceleration (z=-h/2)
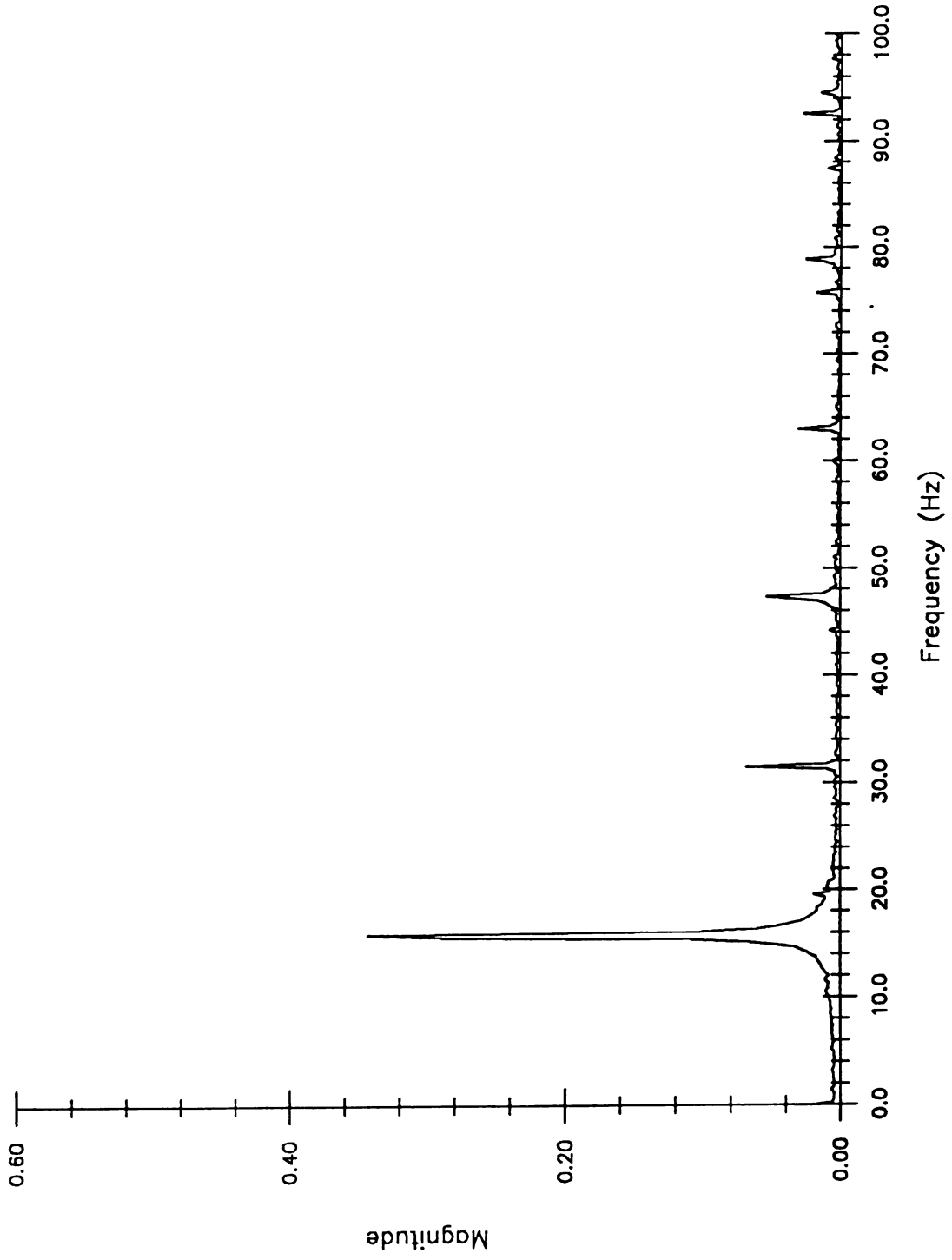
Figure 25 - Power spectrum of piston acceleration (z=+h/2)
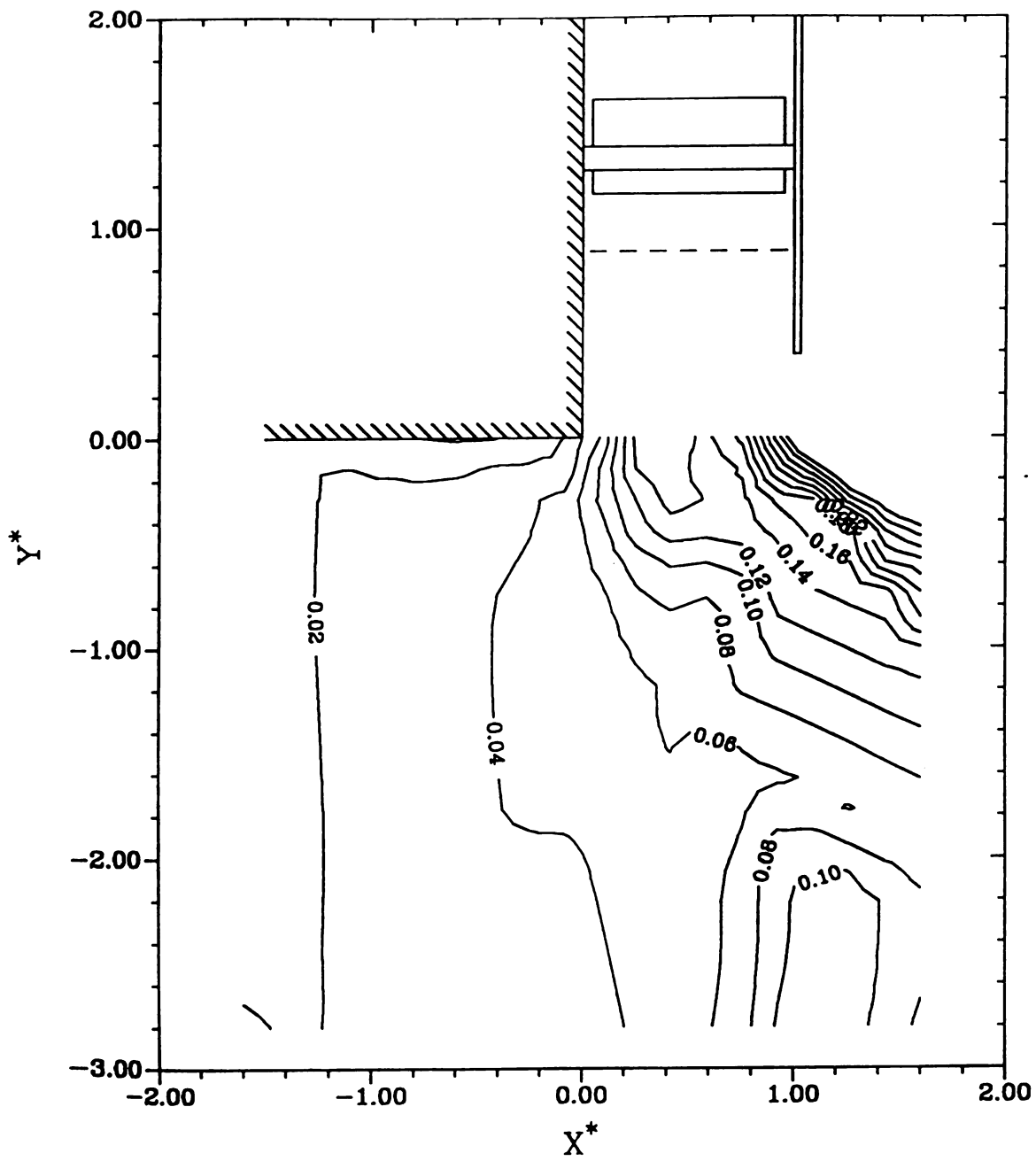
Figure 26 - Hot-wire Response to Forcing with no Flow $\phi = 0$
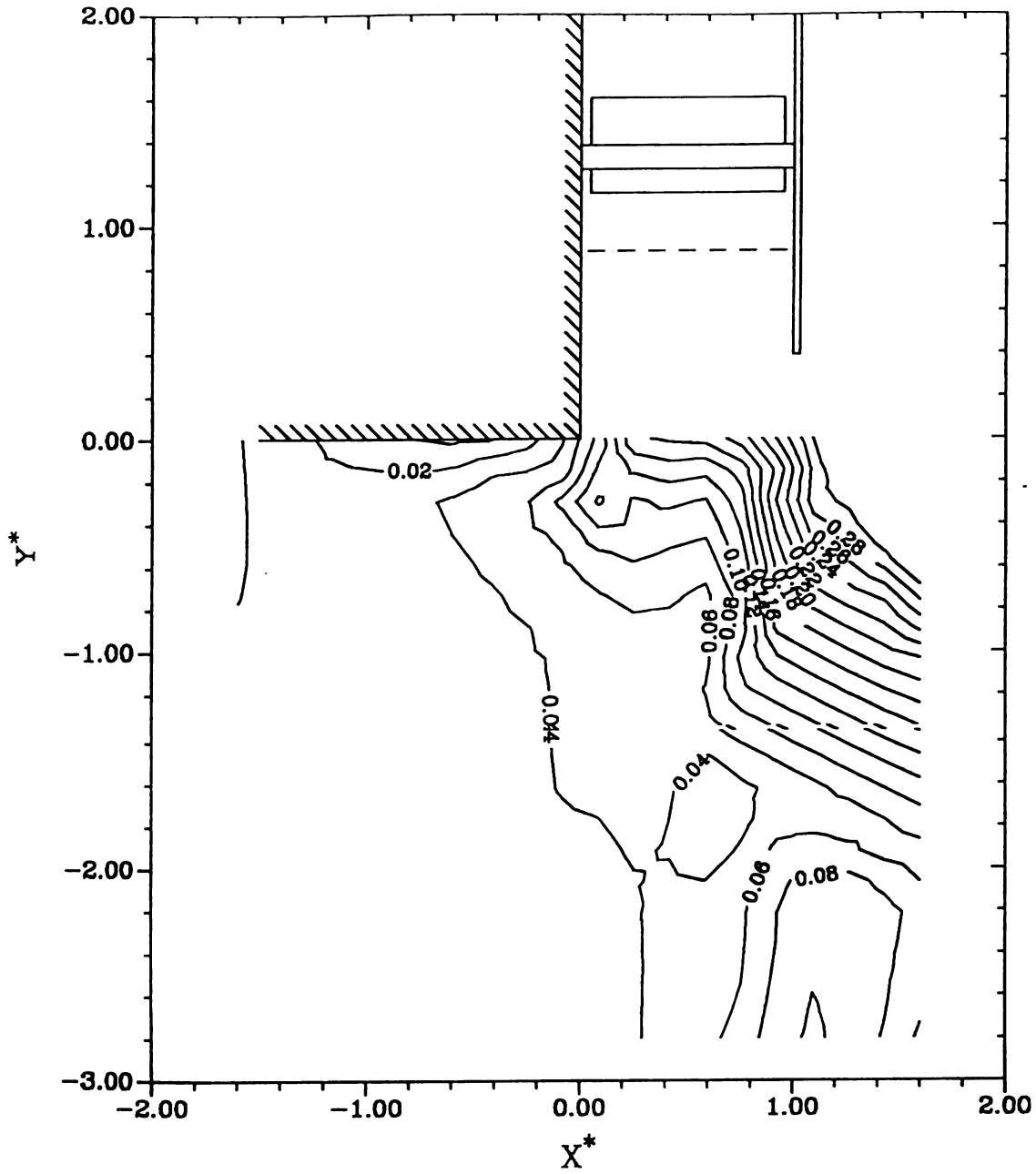
Figure 27 - Hot-wire Response to Forcing with no Flow $\phi = 90$
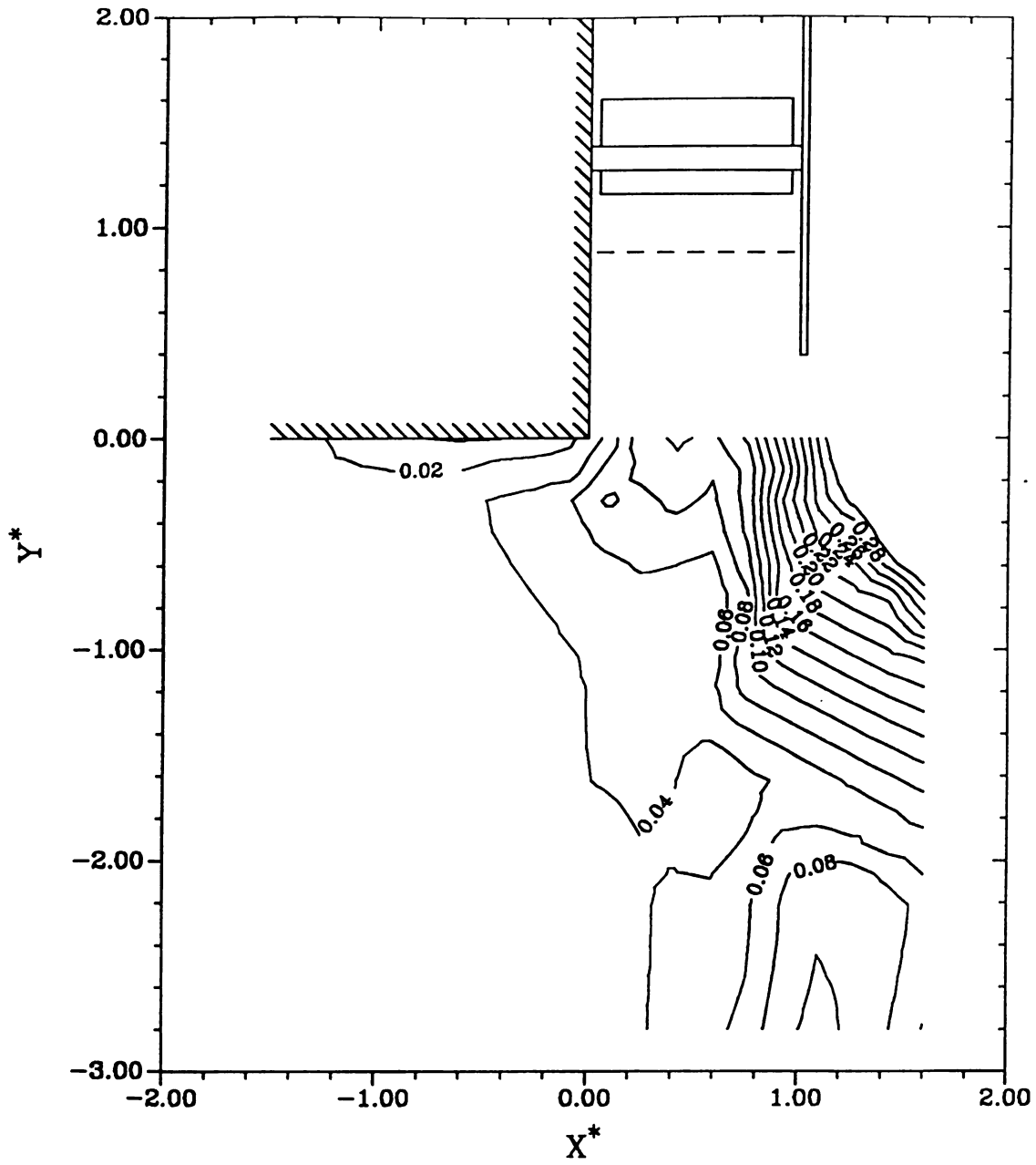
Figure 28 - Hot-wire Response to Forcing with no Flow $\phi = 180$
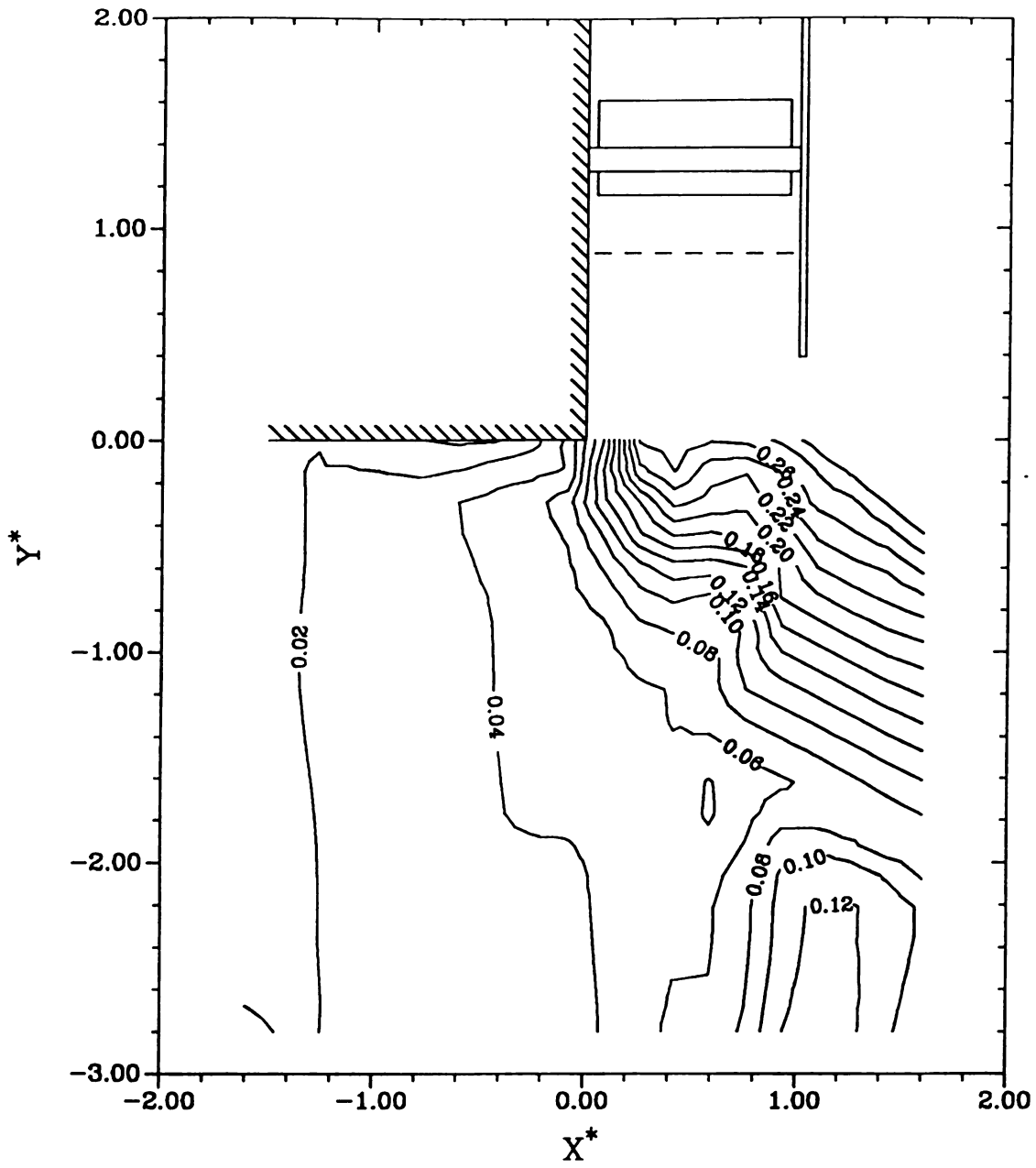
Figure 29 - Hot-wire Response to Forcing with no Flow $\phi = 270$
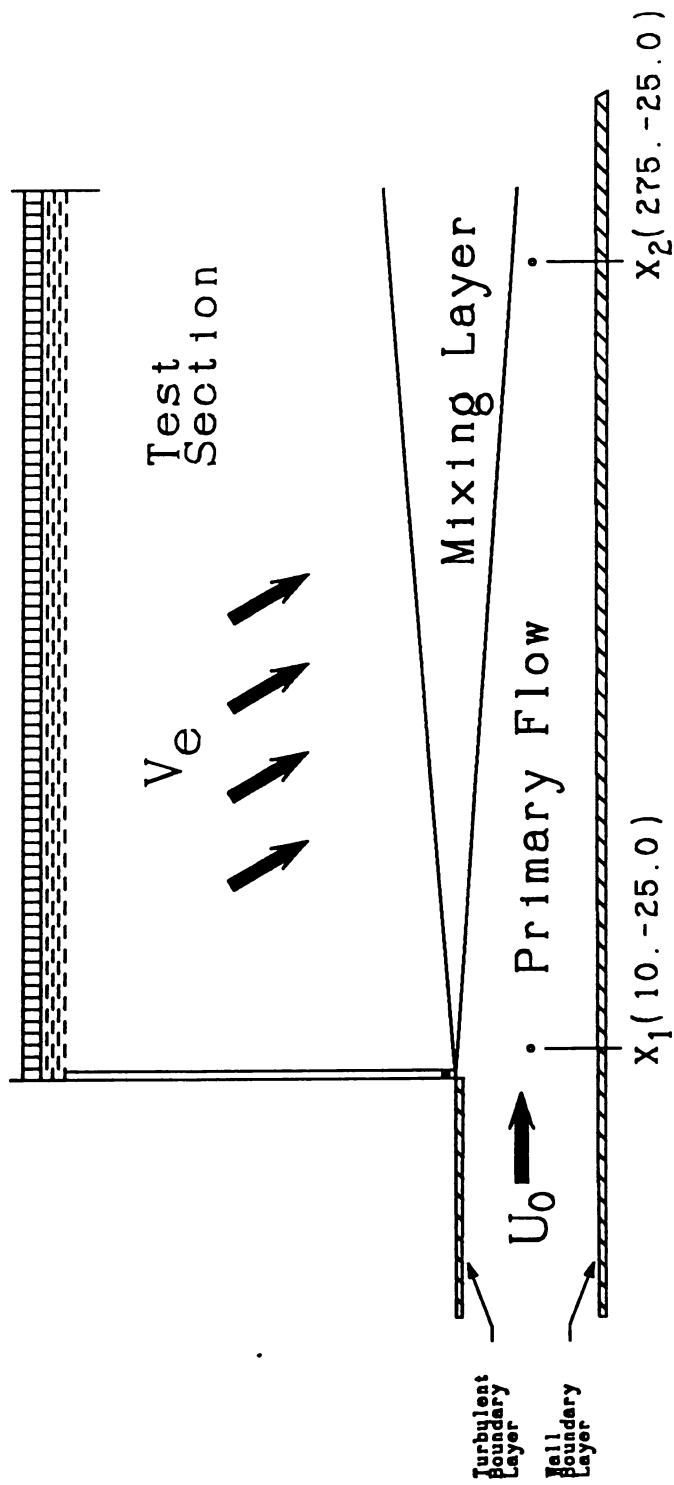
Figure 30 - Entrainment Setting Procedure
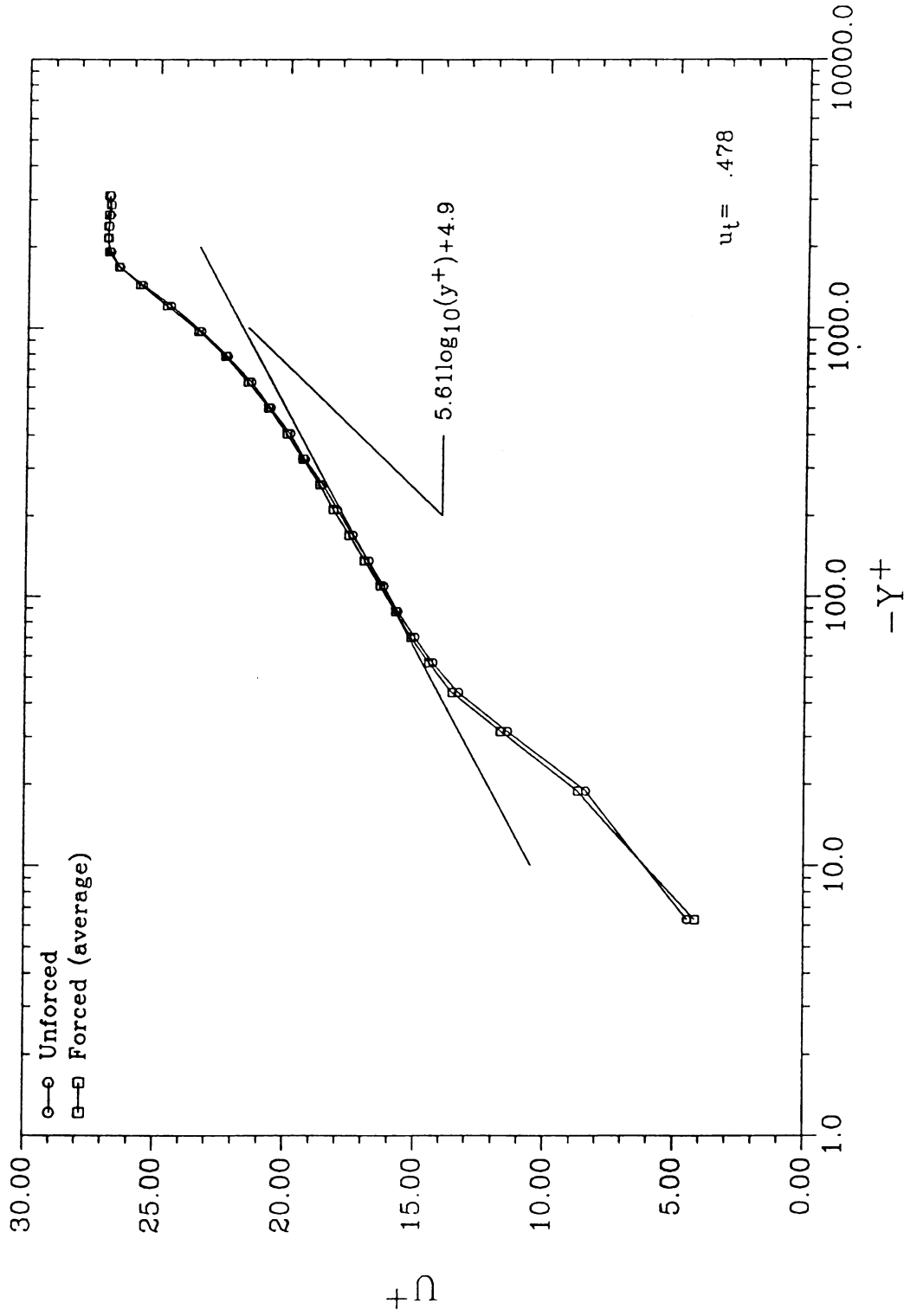
Figure 31 - Boundary layer mean profile at $x/\theta_0 = -5.0$
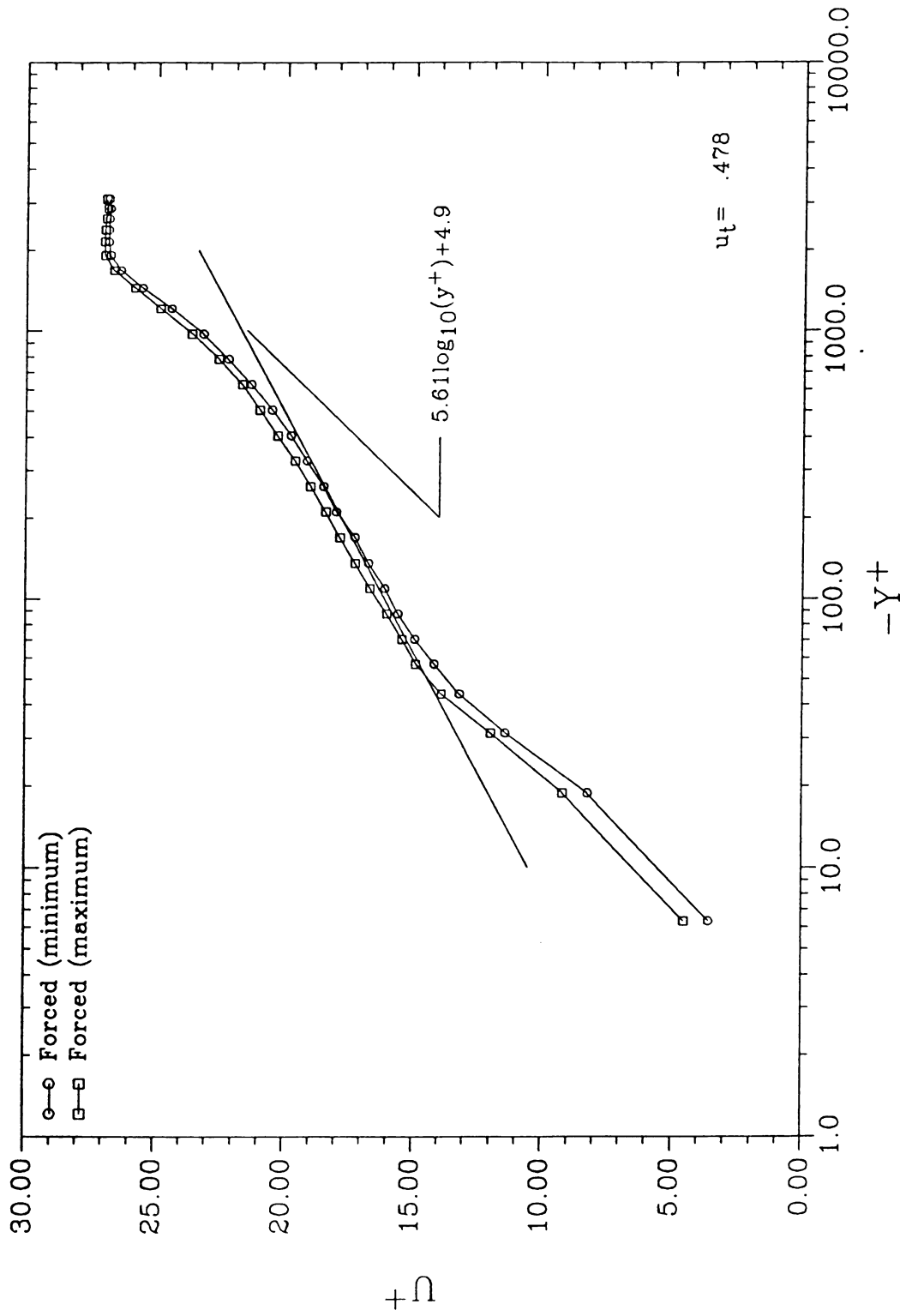
Figure 32 - Comparison of phase averaged min/max U^+ Y^+ at $x/\theta_0 = -5.0$
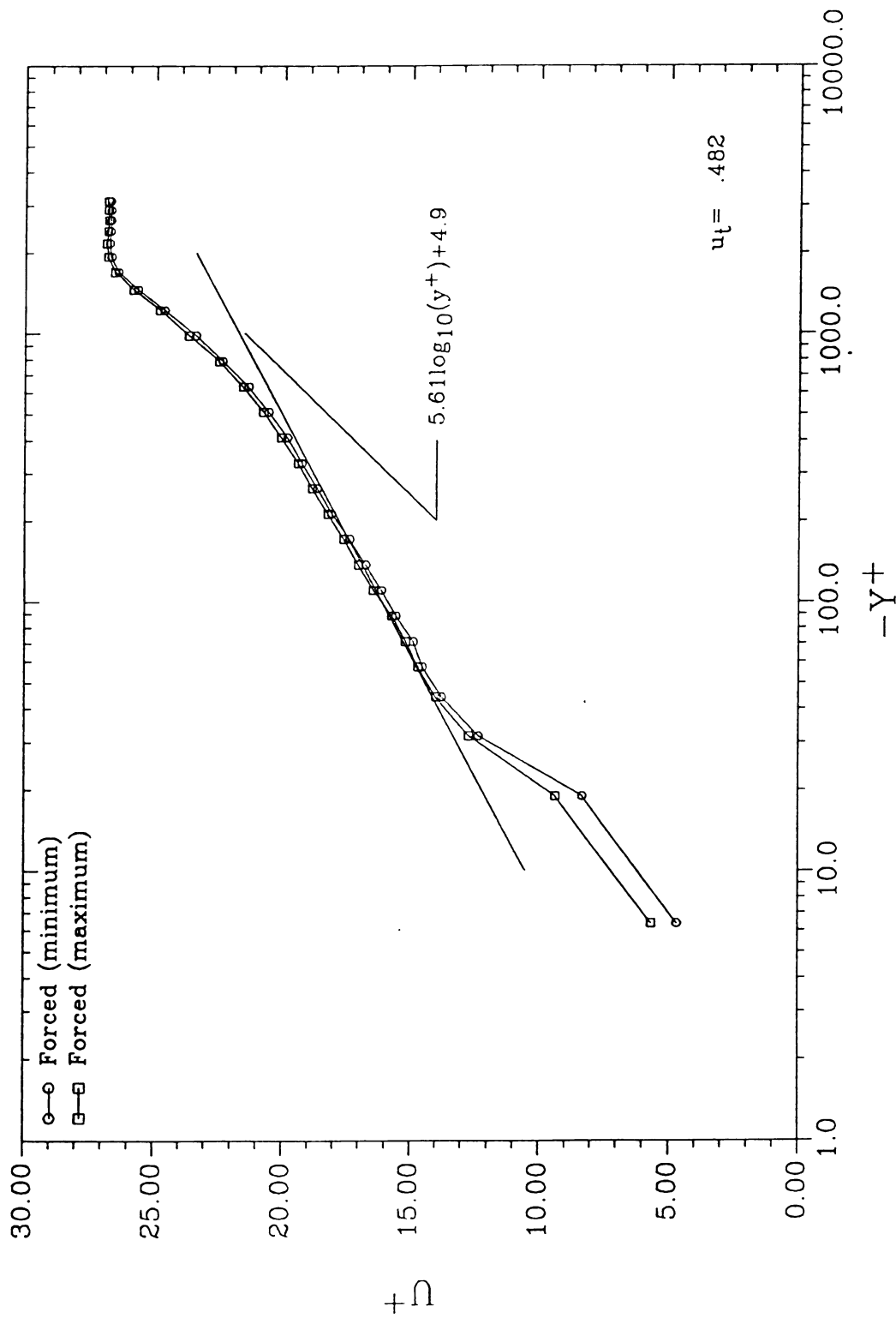
Figure 33 - Comparison of phase averaged min/max U^+ Y^+ at $x/\theta_0 = -20.0$
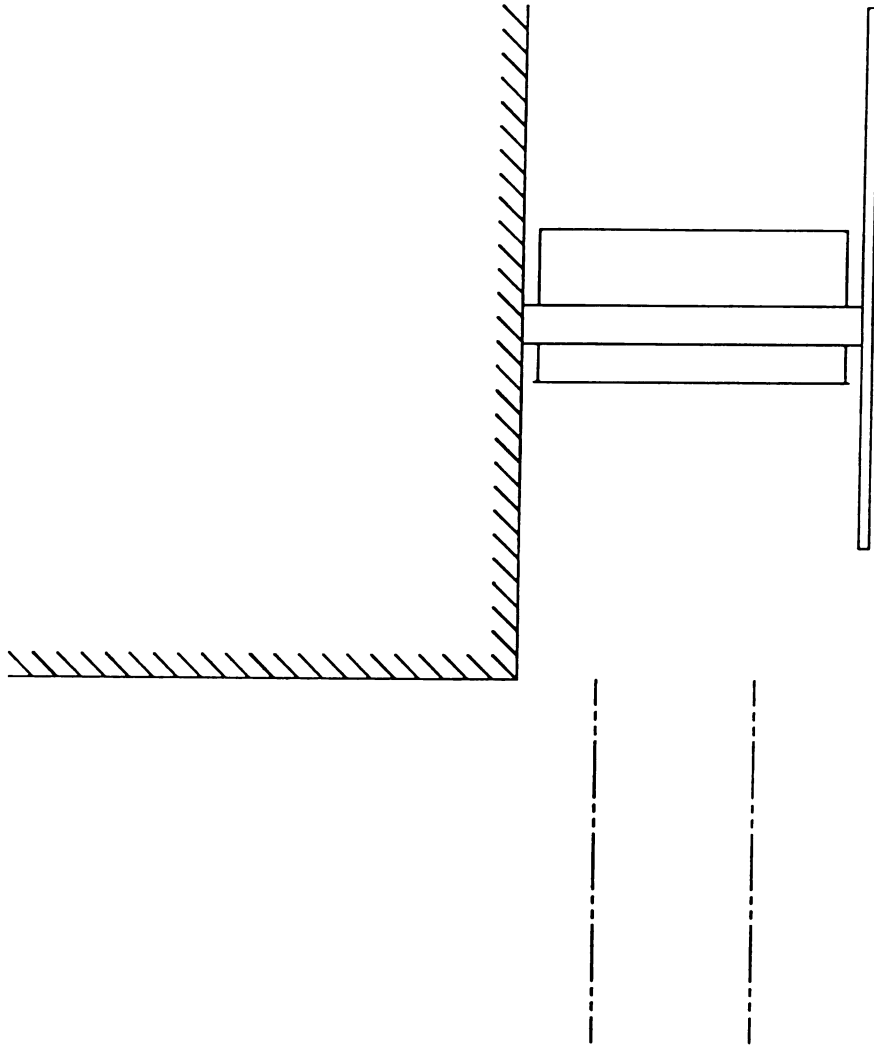
Figure 34 - Streamwise data sampling locations
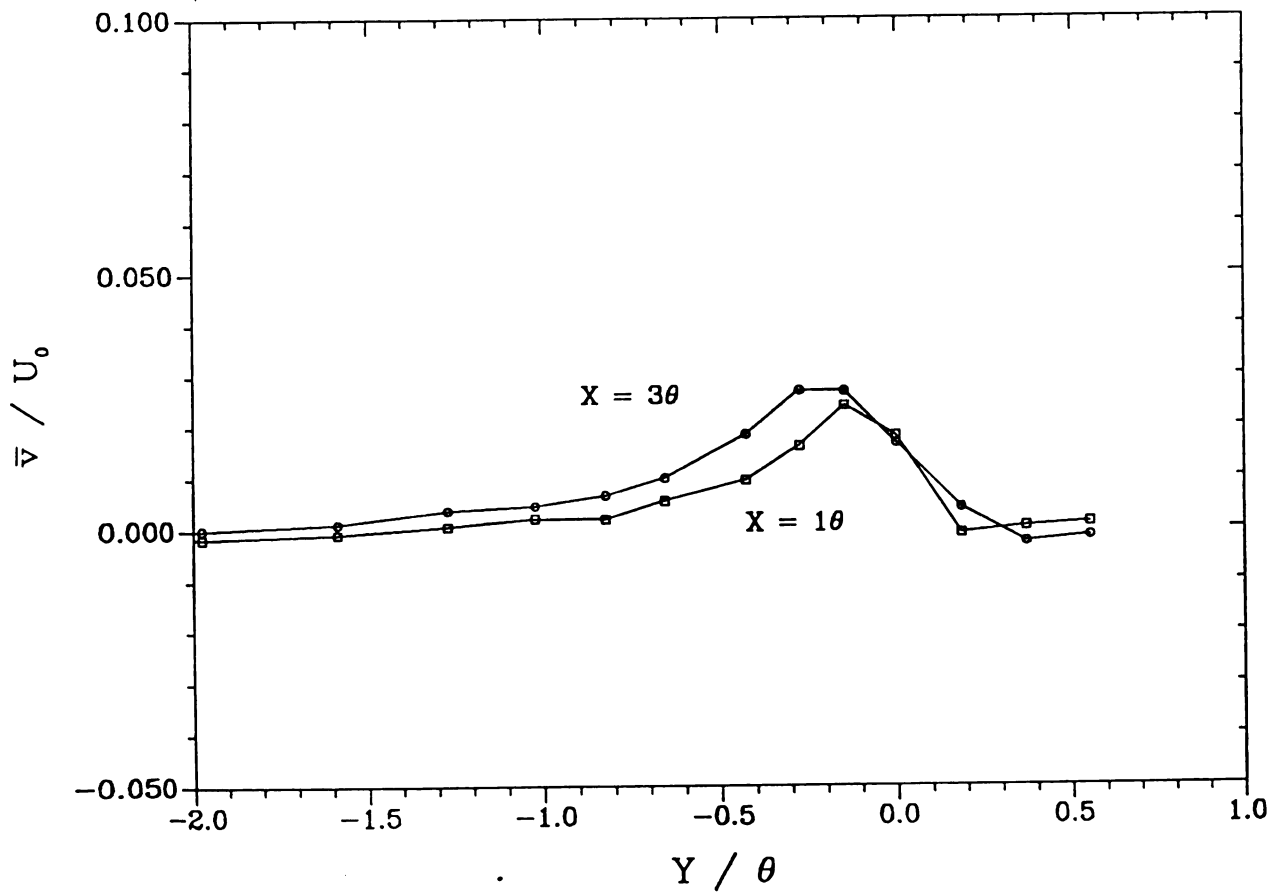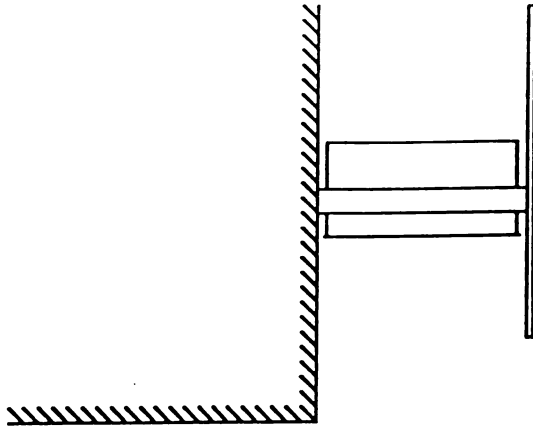
Figure 35 - Unforced $\bar{v}/U_0$ in the separating boundary layer

$\varphi = 0.0$
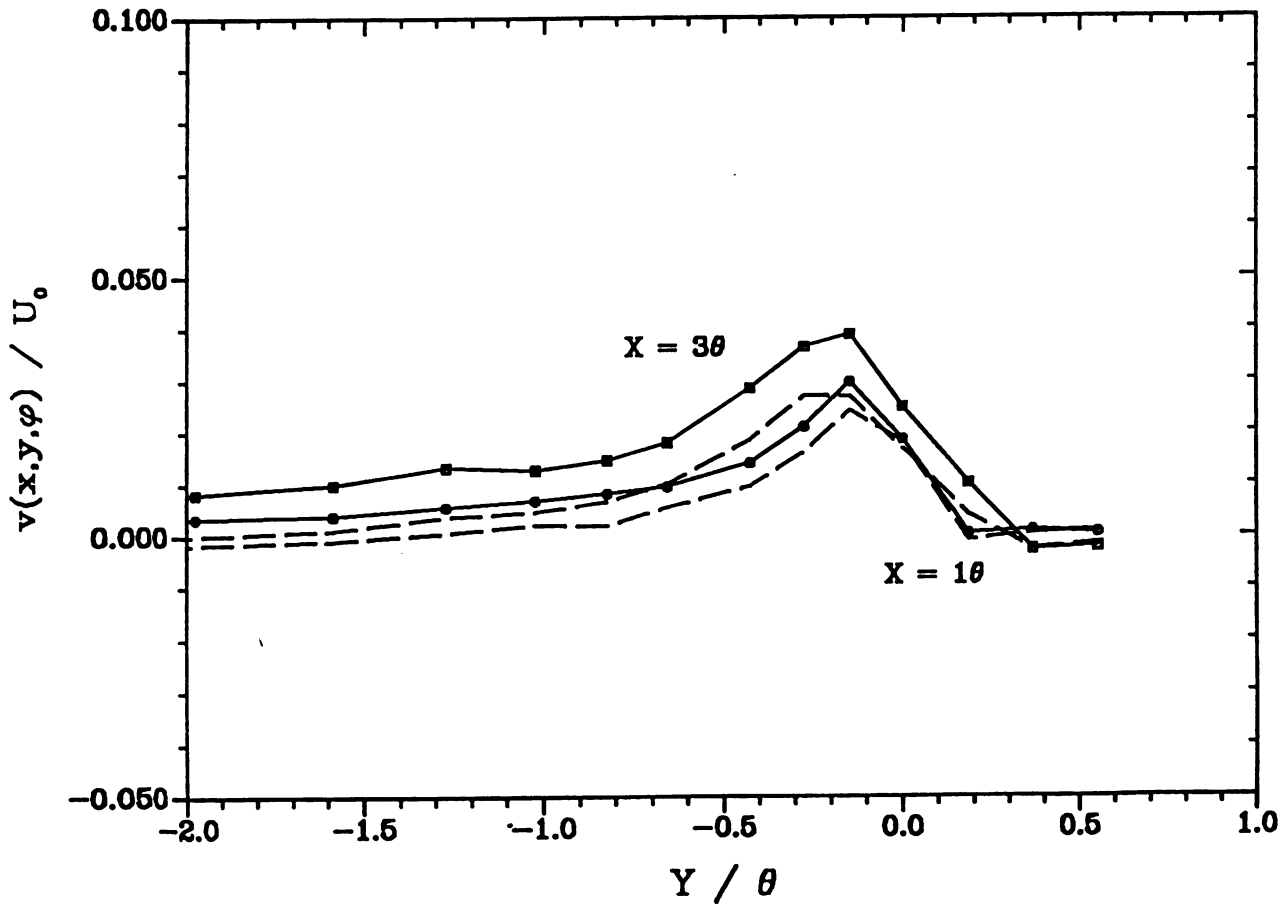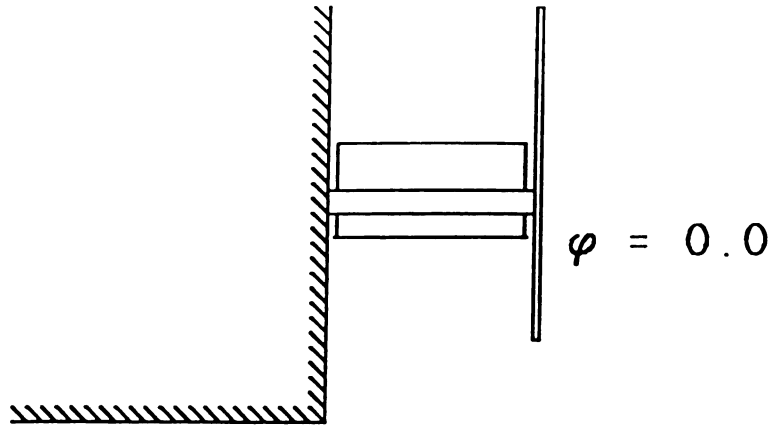
Figure 36 - Phase averaged $\bar{v}/U_0$ at $\phi=0.0$

$\varphi = 90.0$

$\varphi = 0.0$
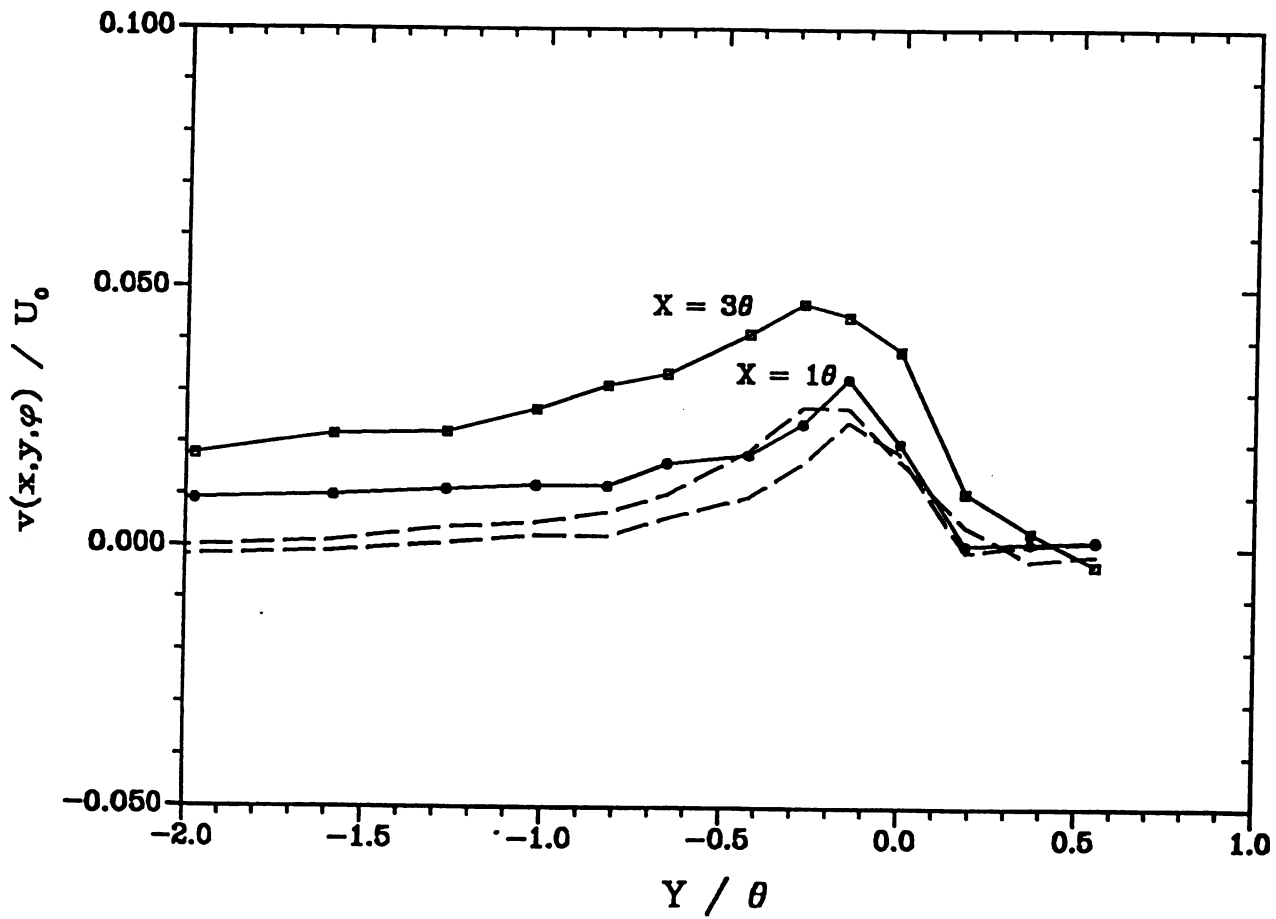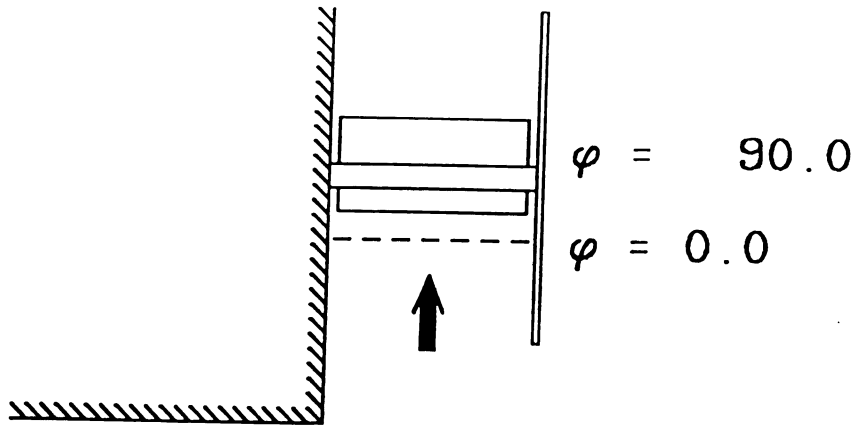
Figure 37 - Phase averaged $\bar{v}/U_0$ at ϕ=90.0

$\varphi = 180.0$

$\varphi = 0.0$
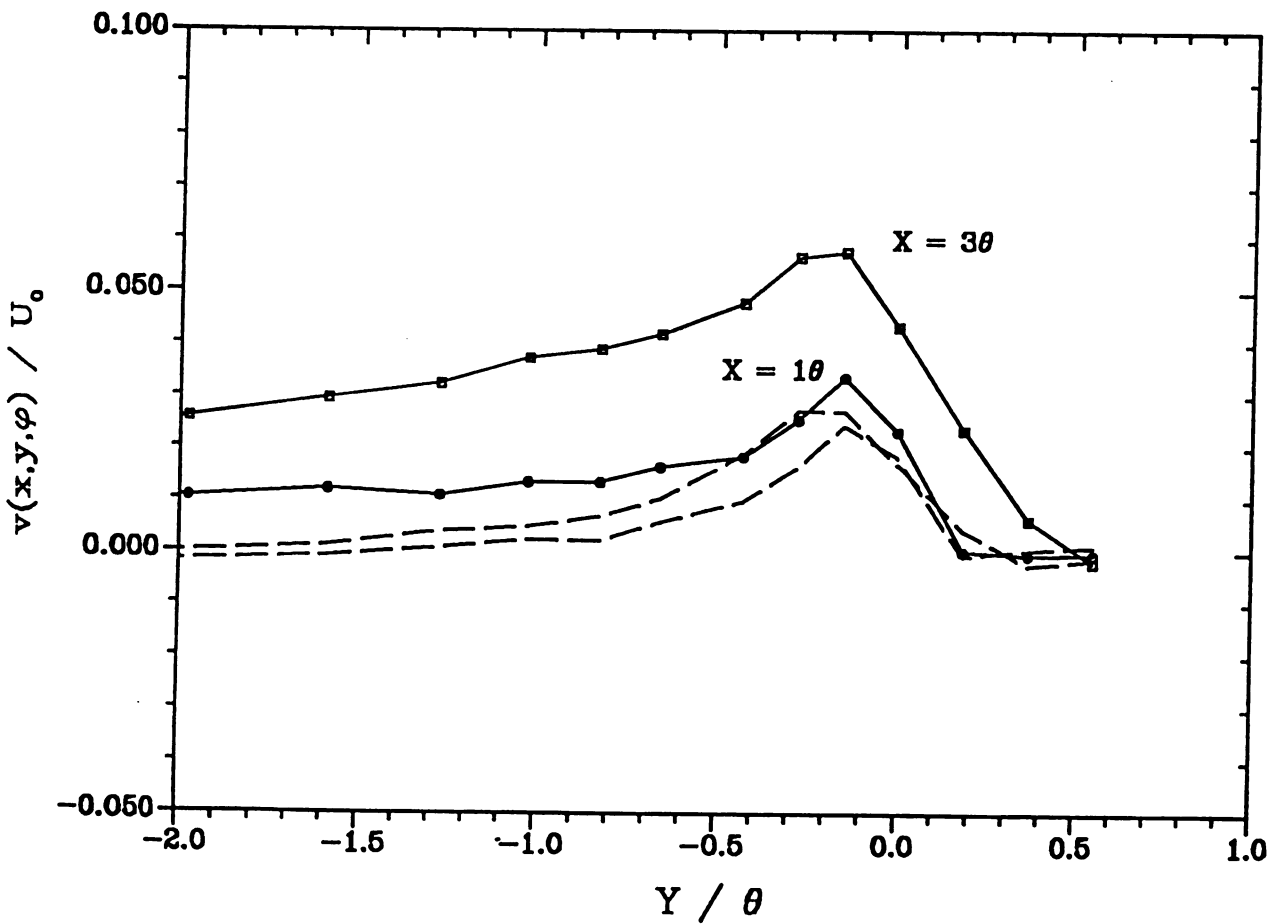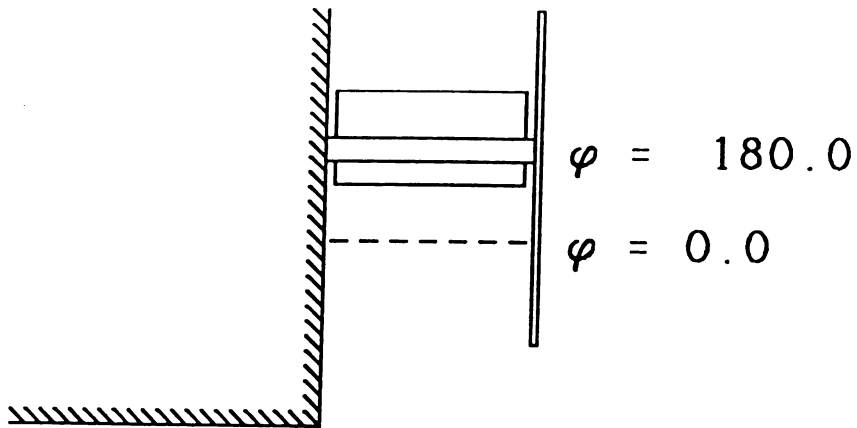
Figure 38 - Phase averaged $\overline{v}/U_0$ at ϕ-180.0

$\varphi = 270.0$

$\varphi = 0.0$
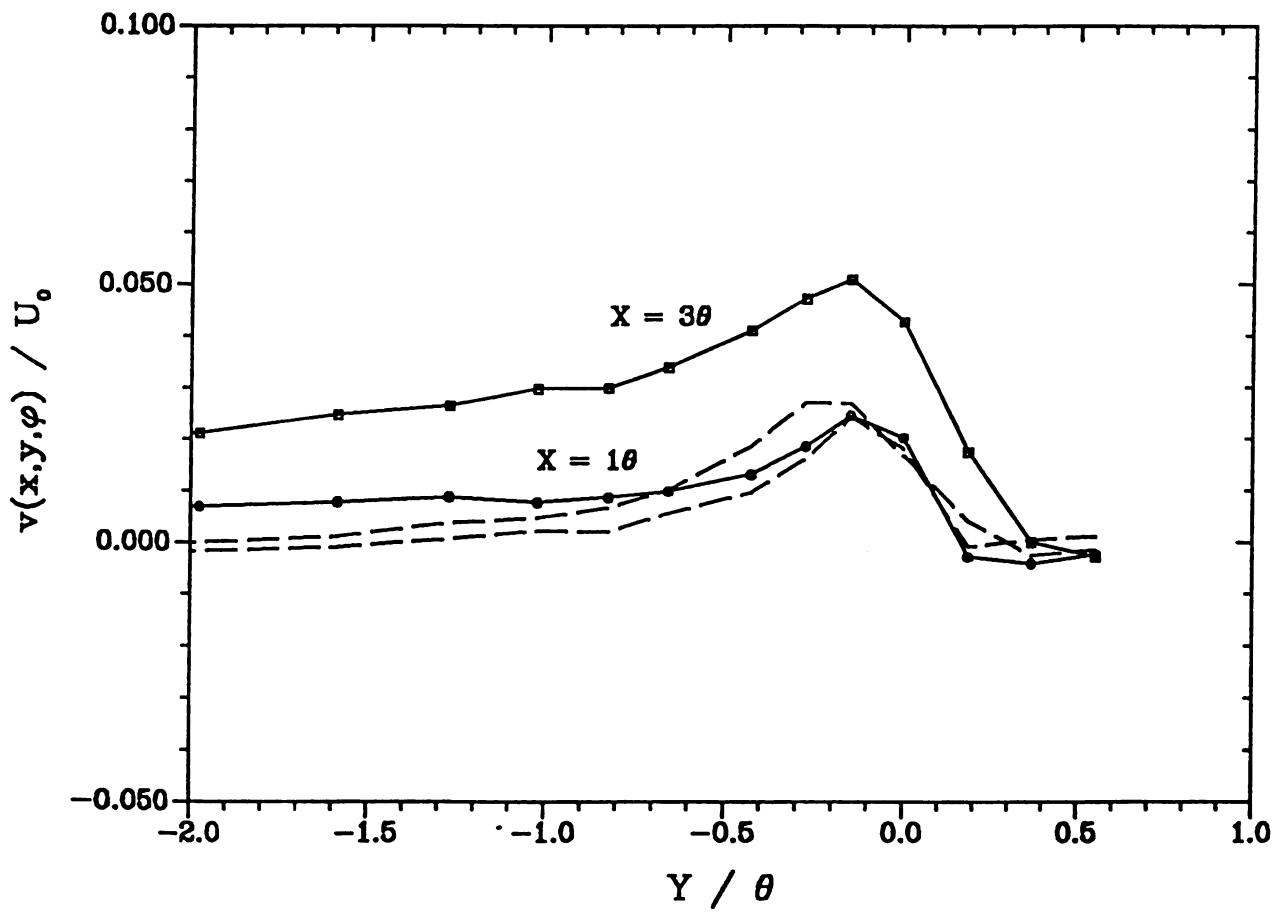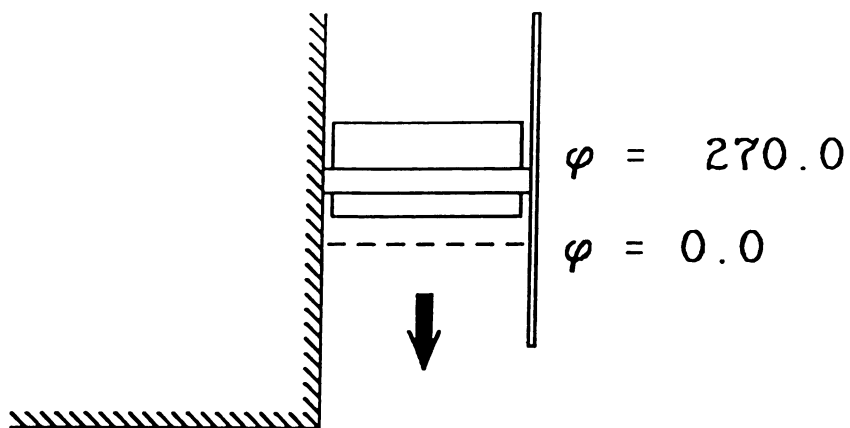
Figure 39 - Phase averaged $\bar{v}/U_0$ at $\phi=270.0$
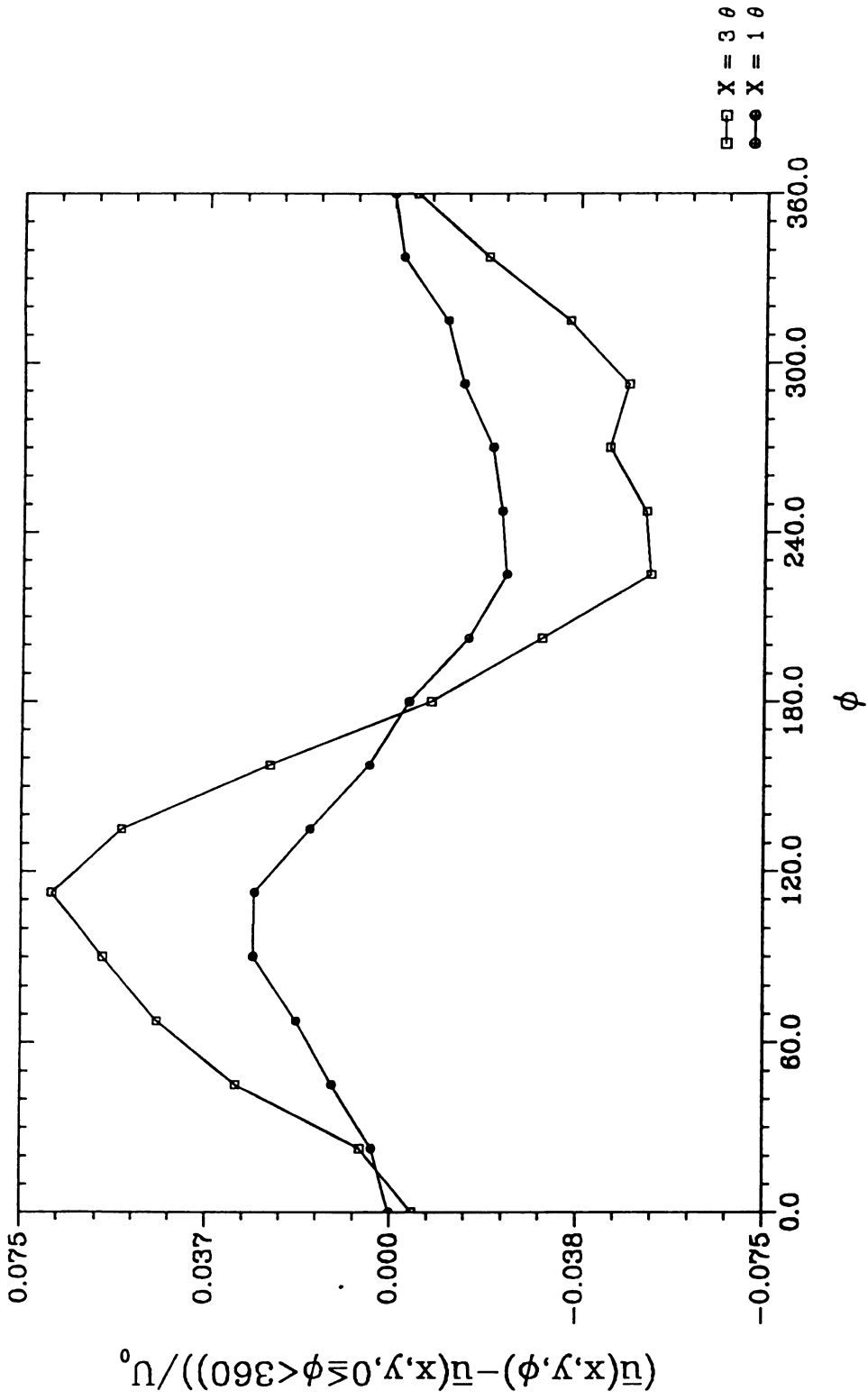
Figure 40 - Phase averaged δu at $y/\theta_0 - 0.0$
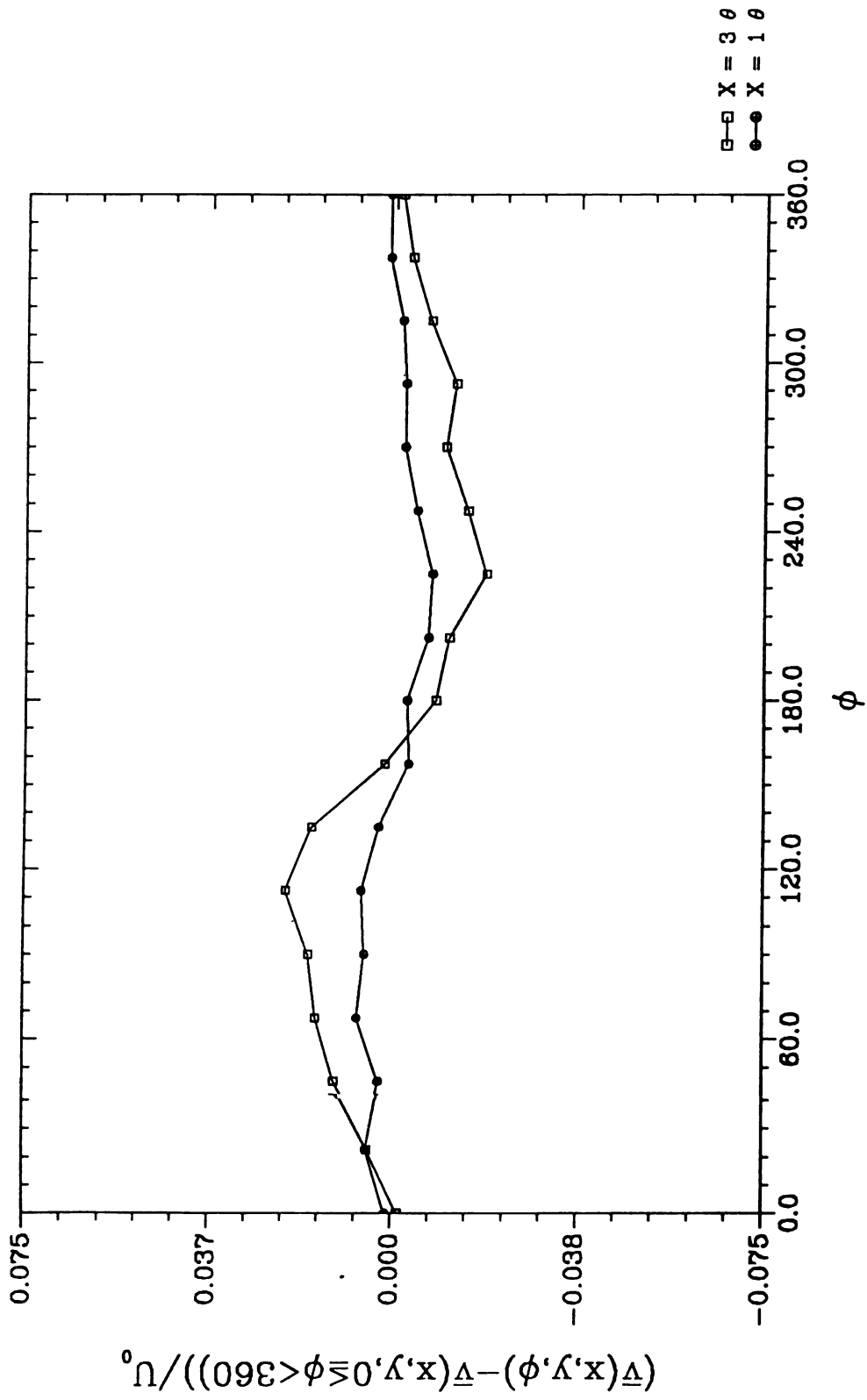
Figure 41 - Phase averaged δv at $y/\theta_0 = 0.0$
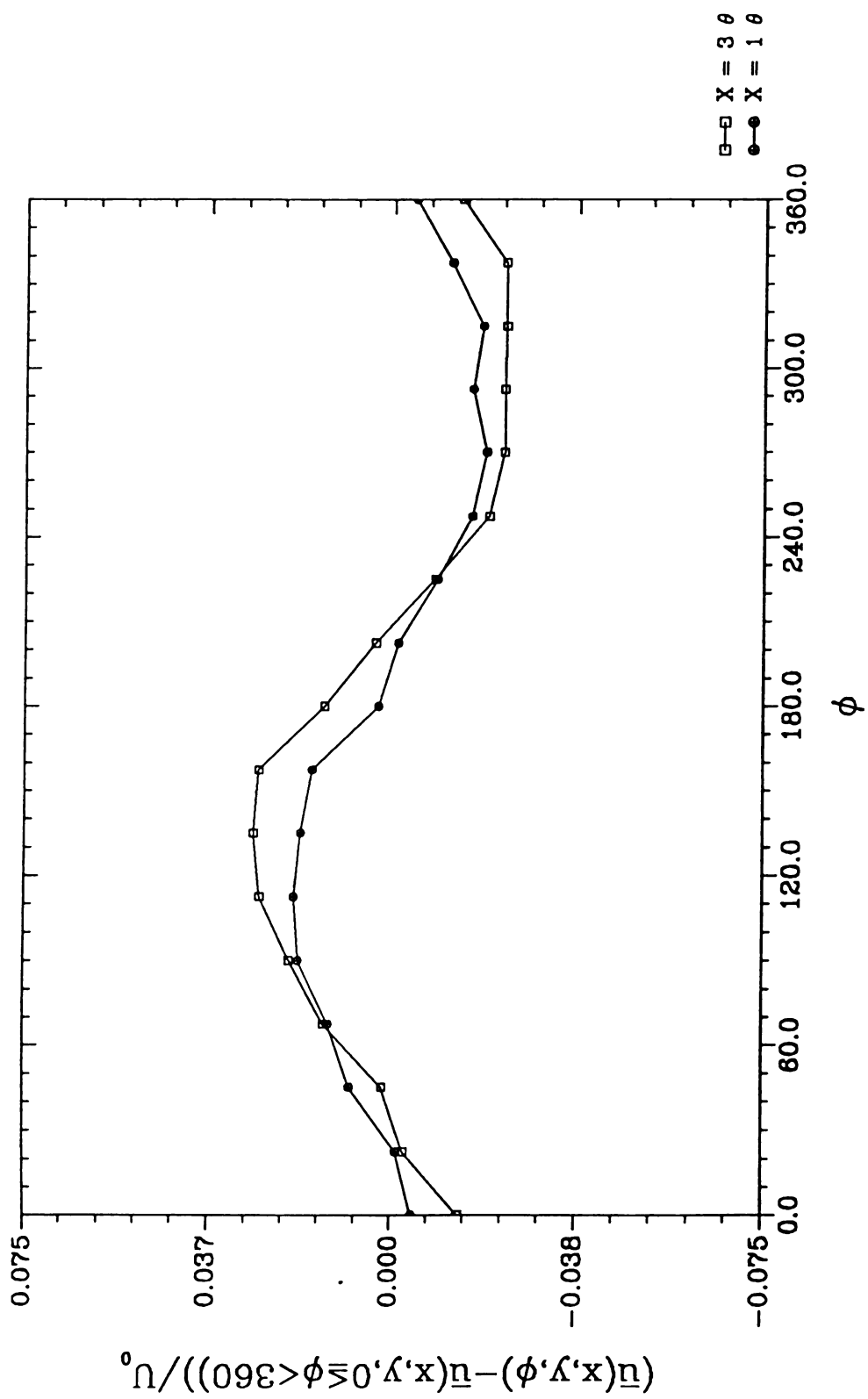
Figure 42 - Phase averaged δu at $y/\theta_0 = -1.02$

86
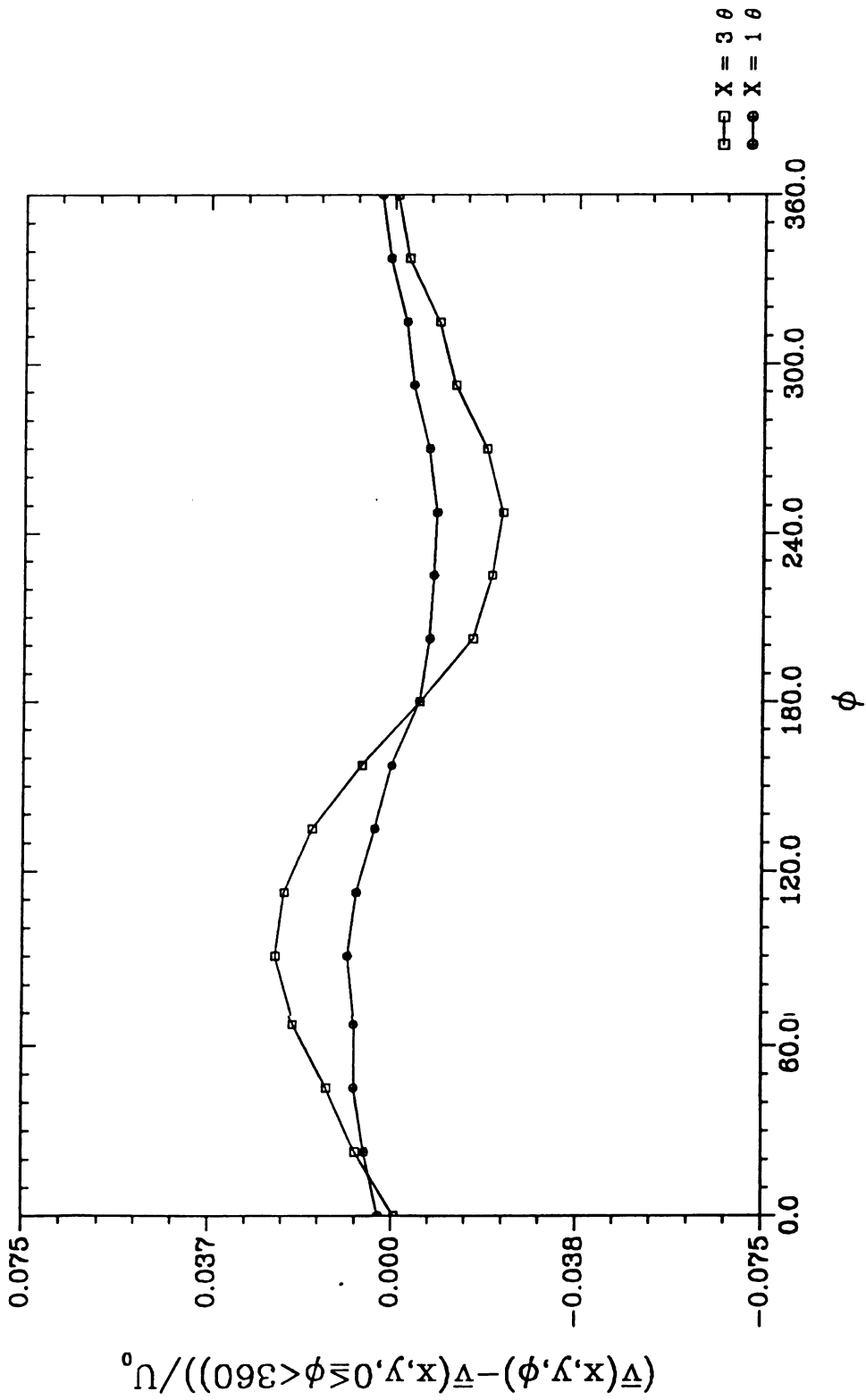
Figure 43 - Phase averaged δv at $y/\theta_0 = -1.02$
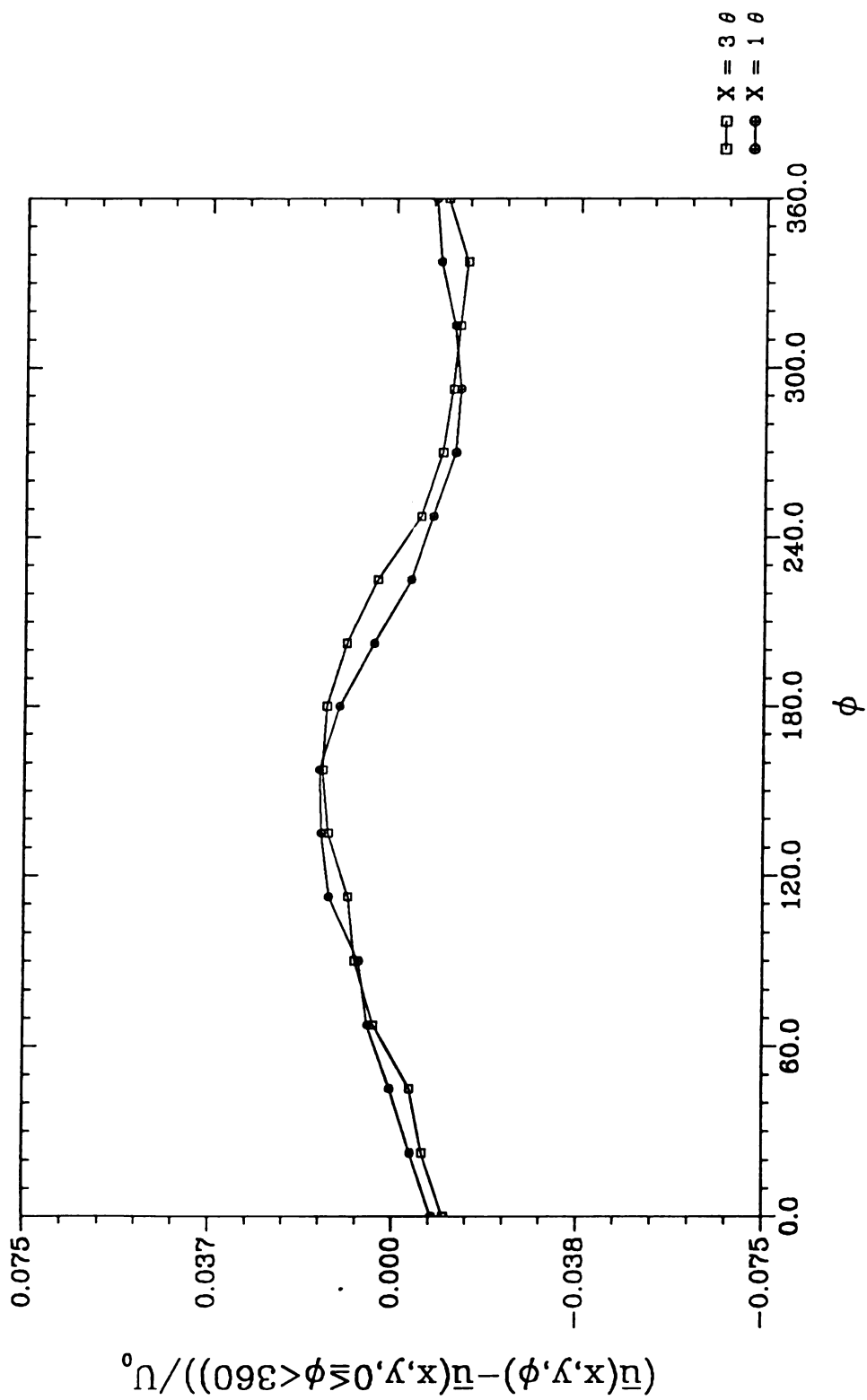
Figure 44 - Phase averaged δu at $y/\theta_0 = -3.06$
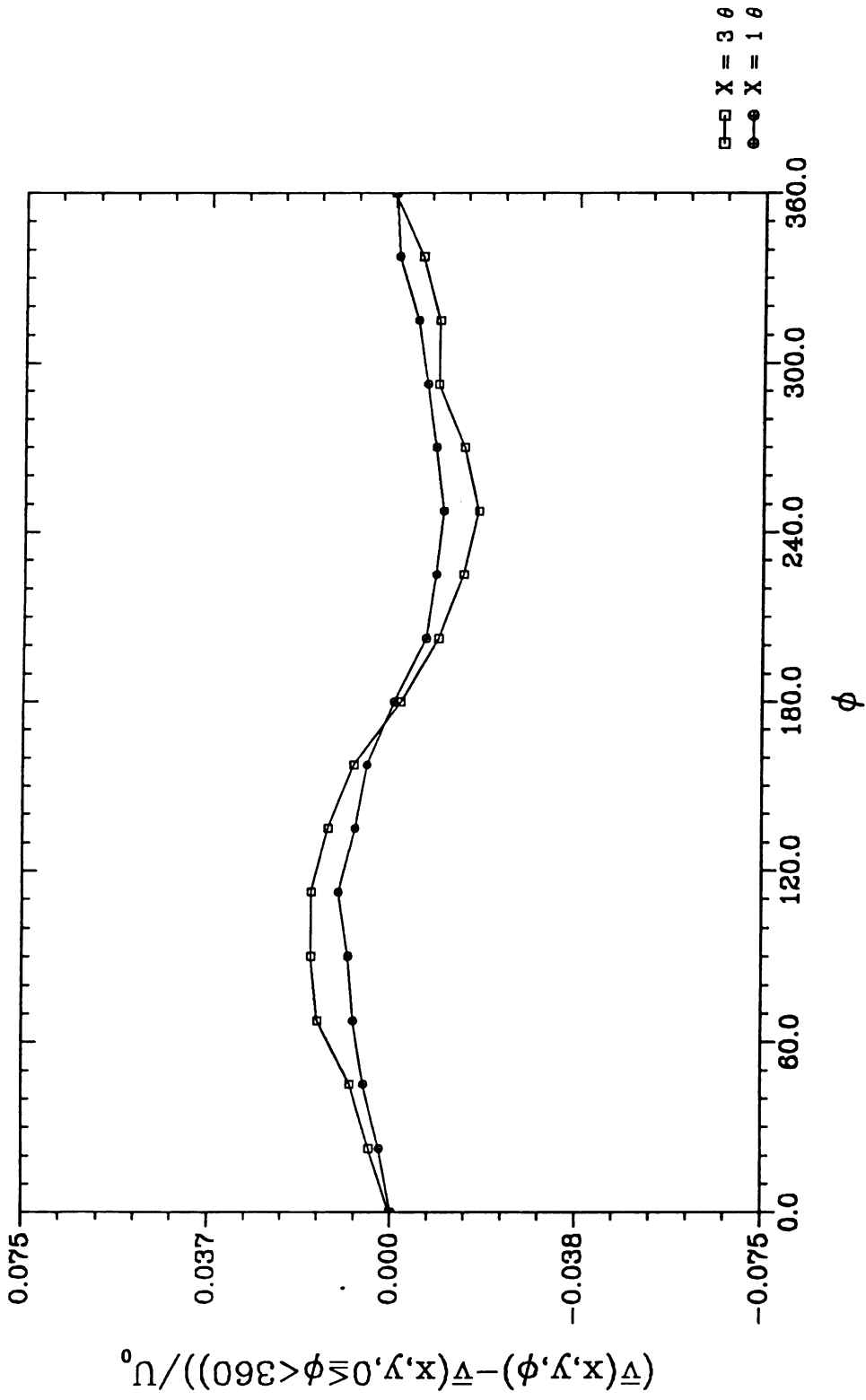
Figure 45 - Phase averaged δv at $y/\theta_0 = -3.06$
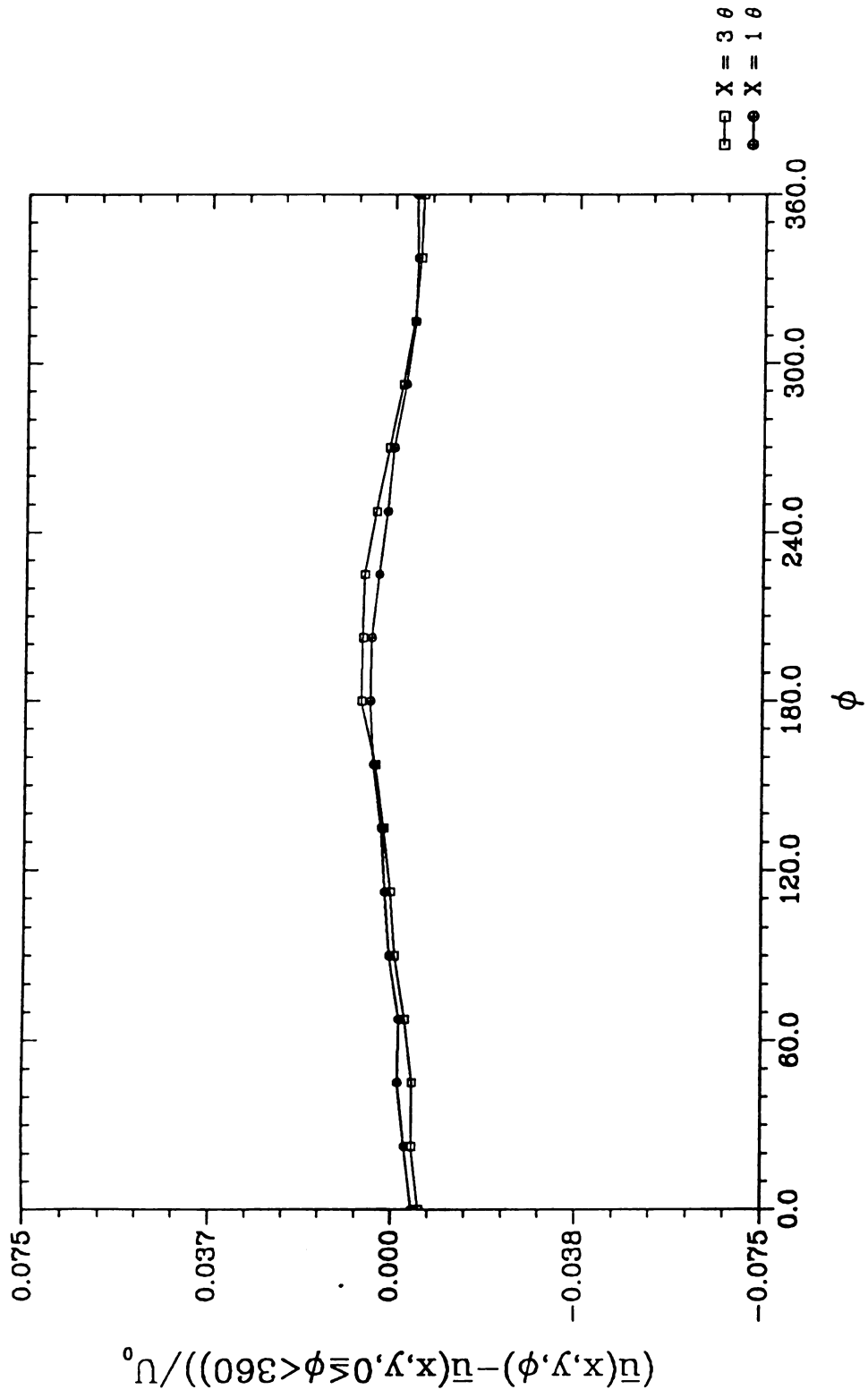
Figure 46 - Phase averaged δu at $y/\theta_0 = -9.36$
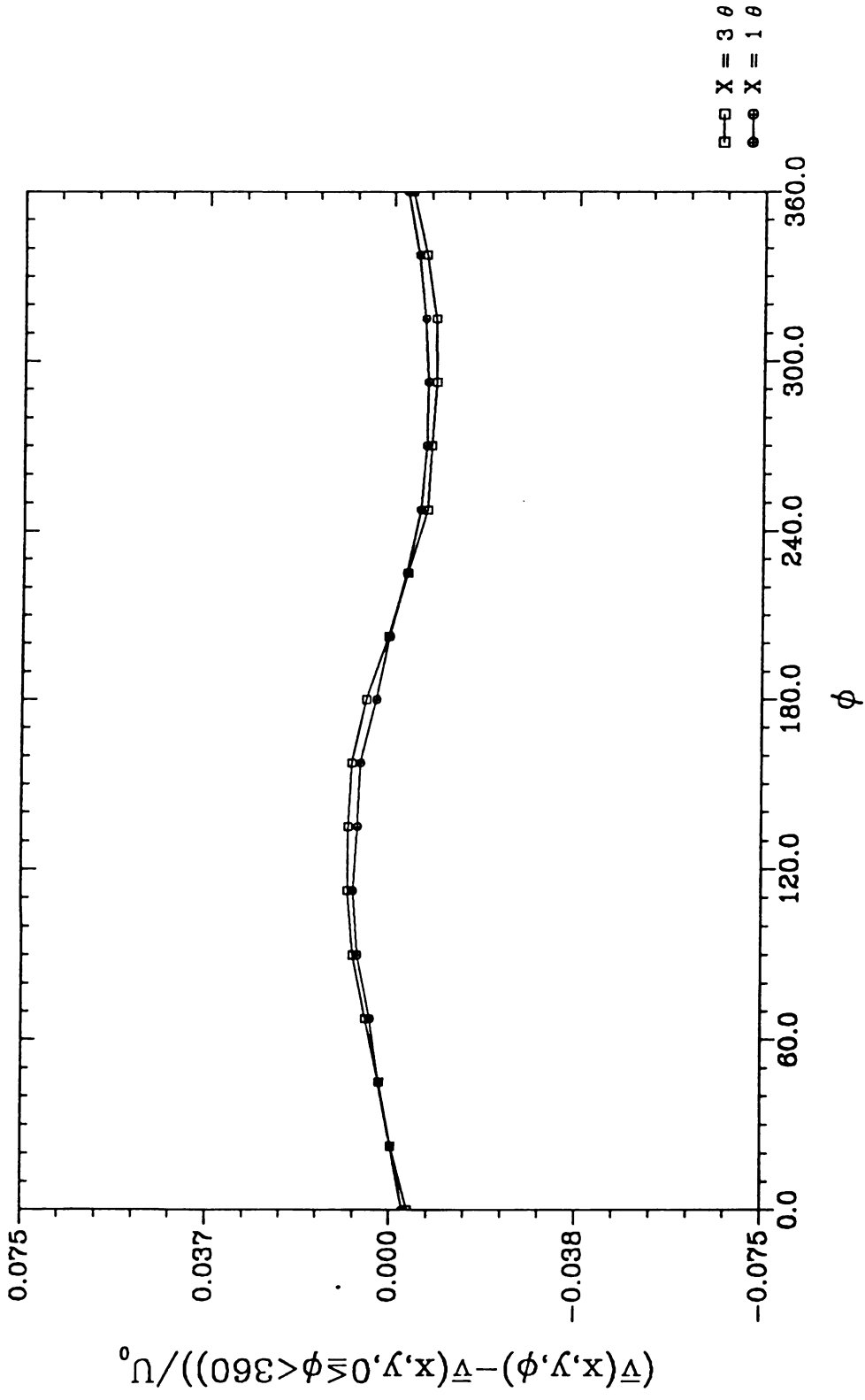
Figure 47 - Phase averaged δv at $y/\theta_0 = -9.36$
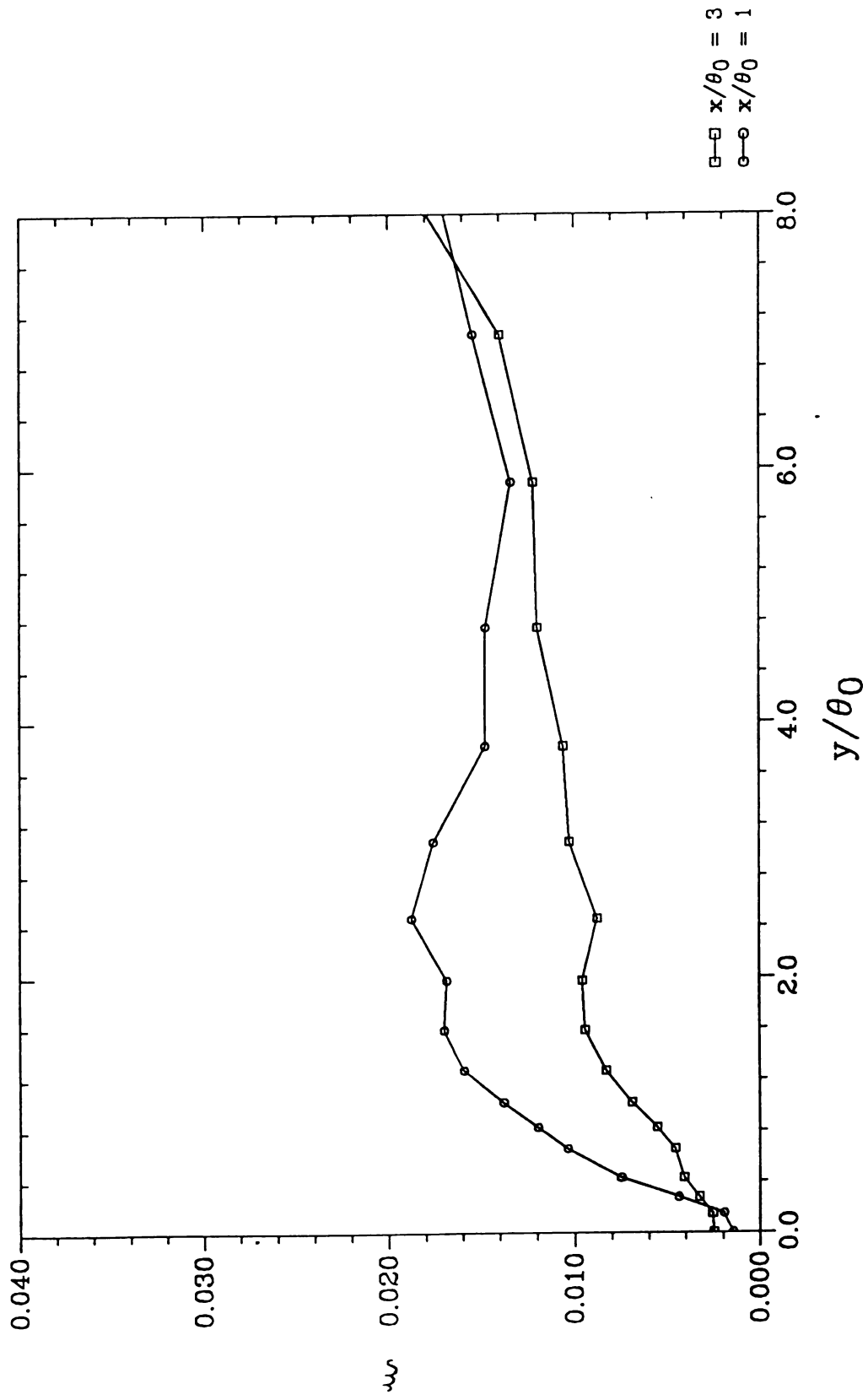
Figure 48 - Forced velocity component intensity relationships
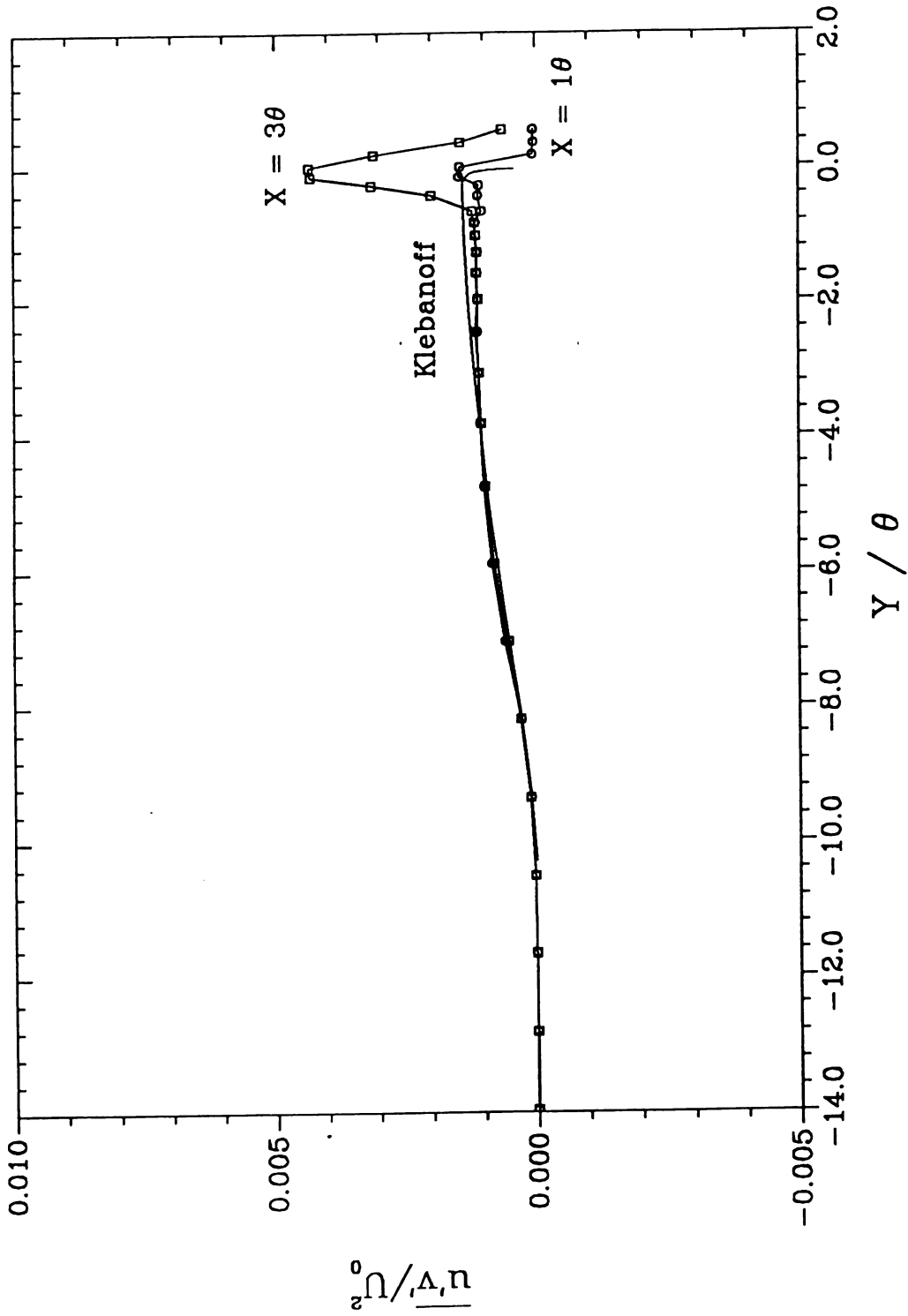
Figure 49 - $\overline{u'v'}$ in the separating boundary layer

$\bar{u}/U_0=0.15$

$\bar{u}/U_0=0.95$

X / θ_o

Y / θ_o
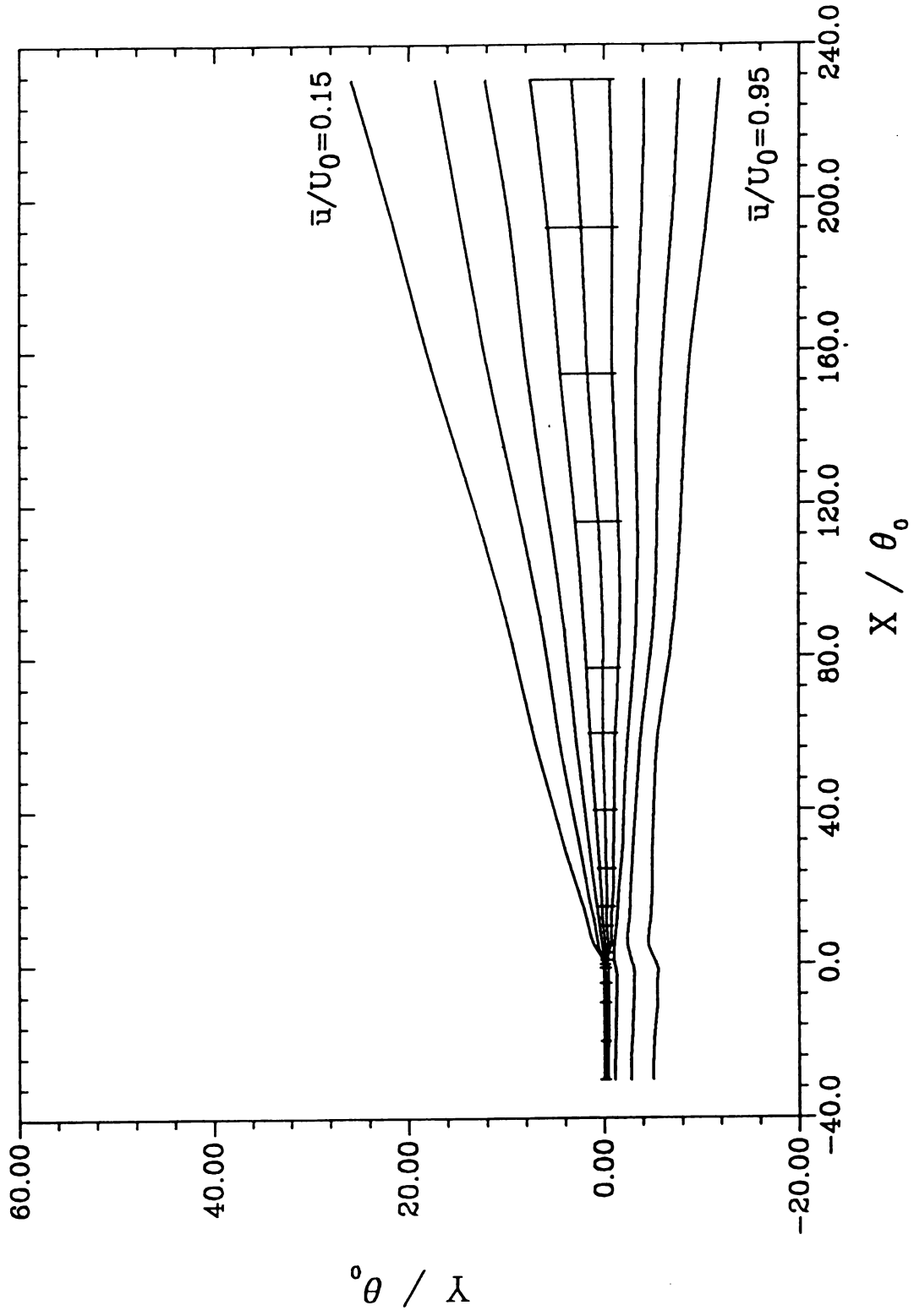
Figure 50 - Unforced Shear Layer Isotachs
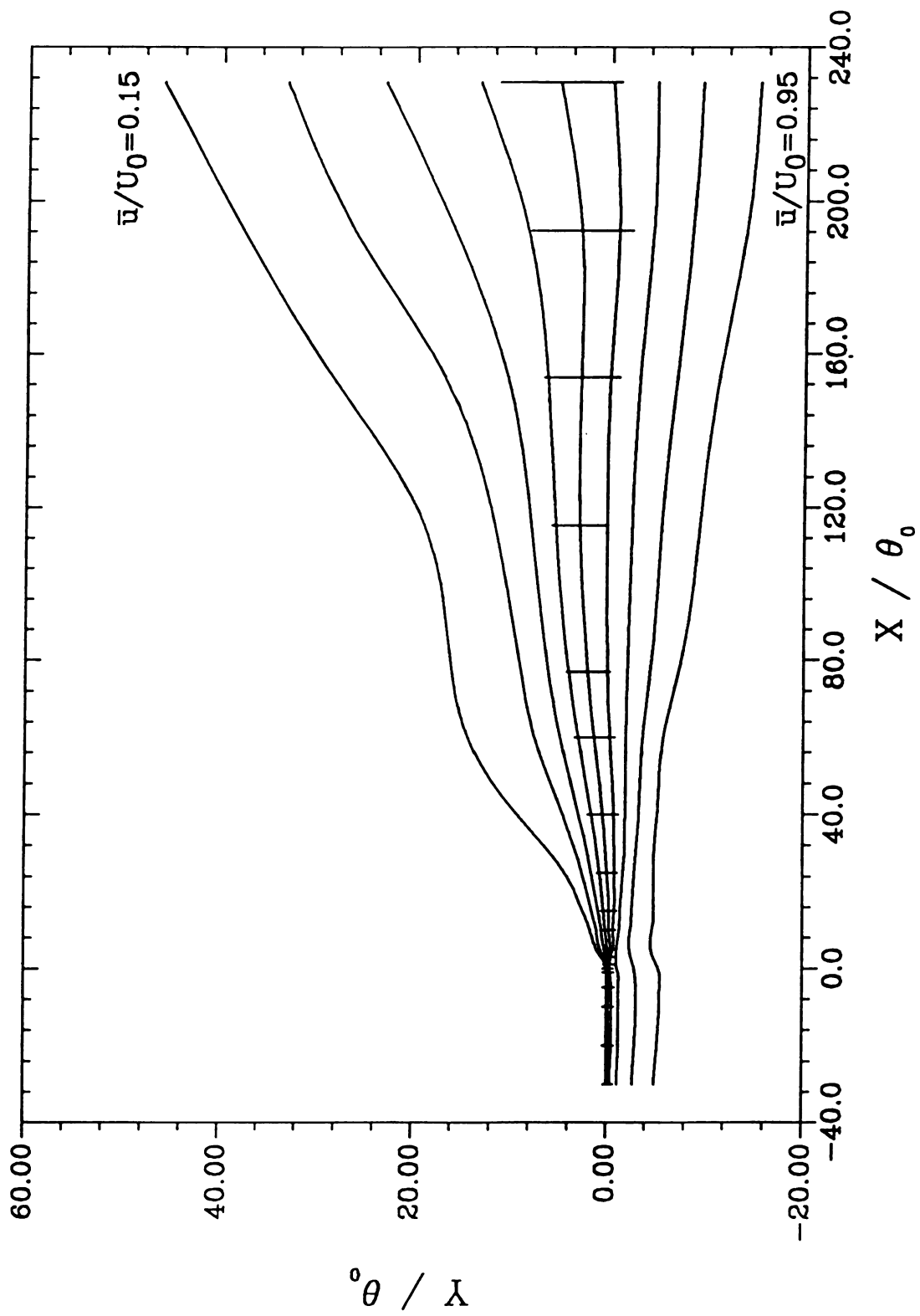
Figure 51 - Forced Shear Layer Isotachs
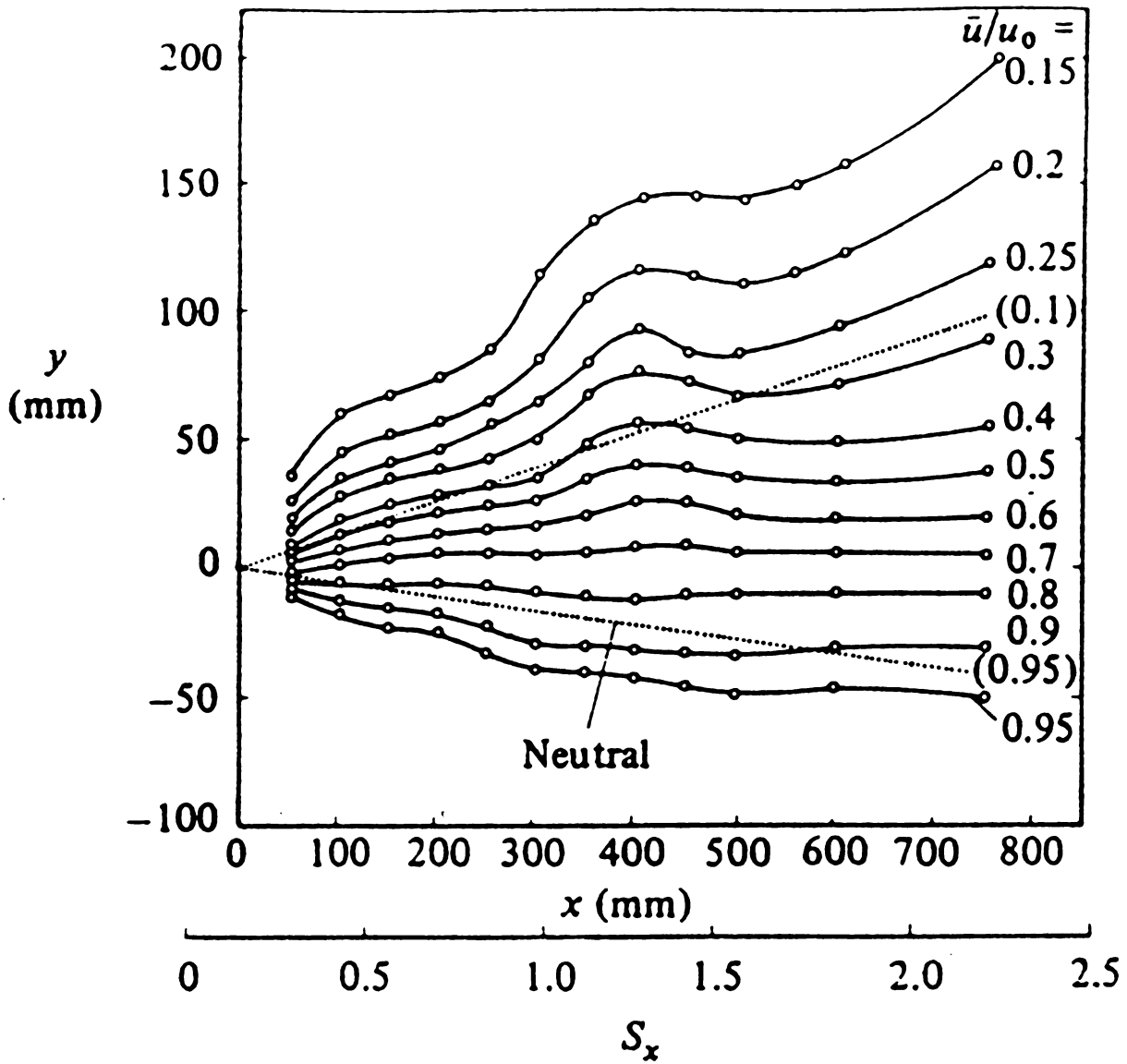
Figure 52 - Forced Shear Layer Isotachs (Fiedler and Mensing [1985])
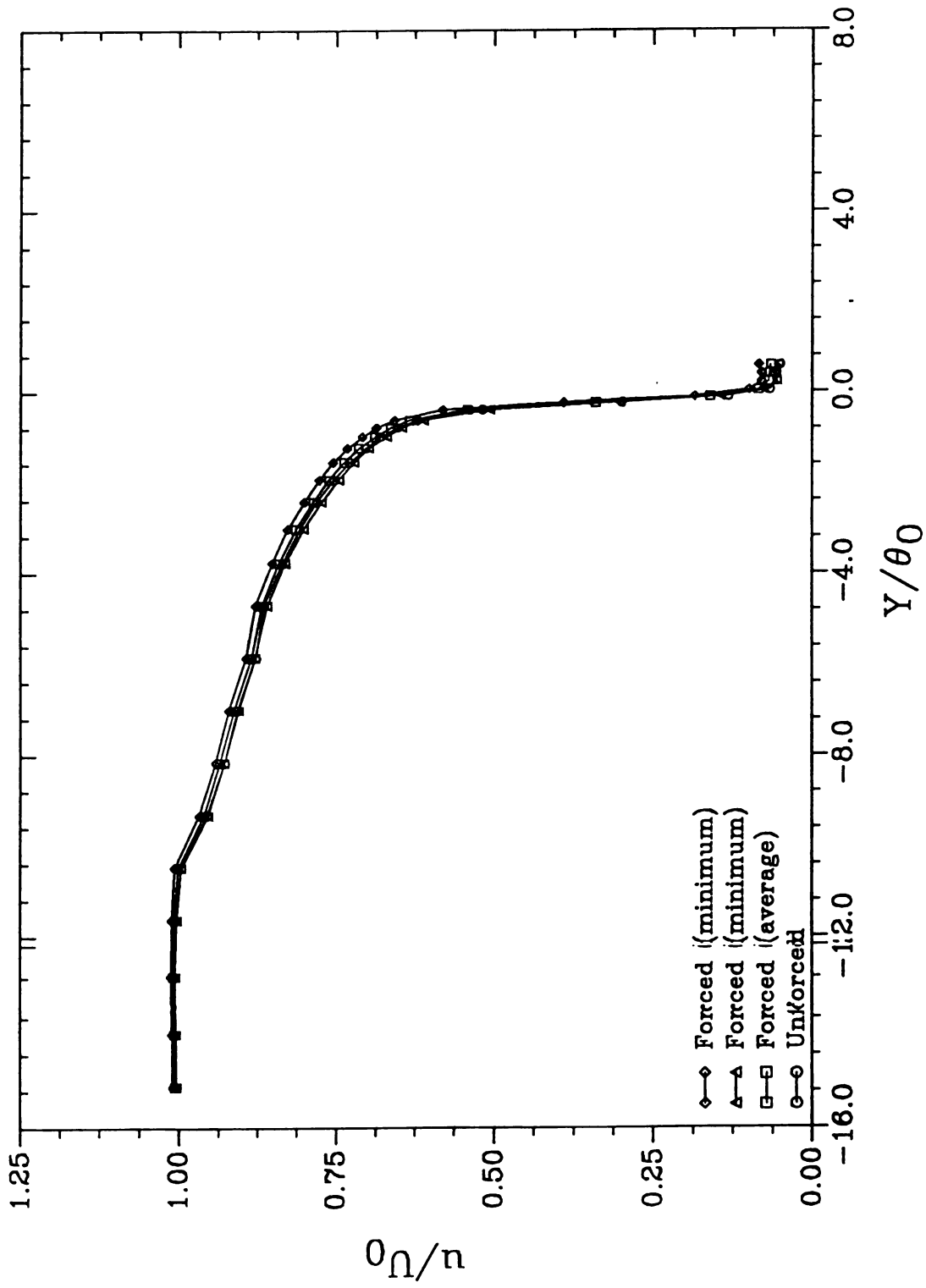
Figure 53 - Mean velocity profiles at $x/\theta_0 = 1$
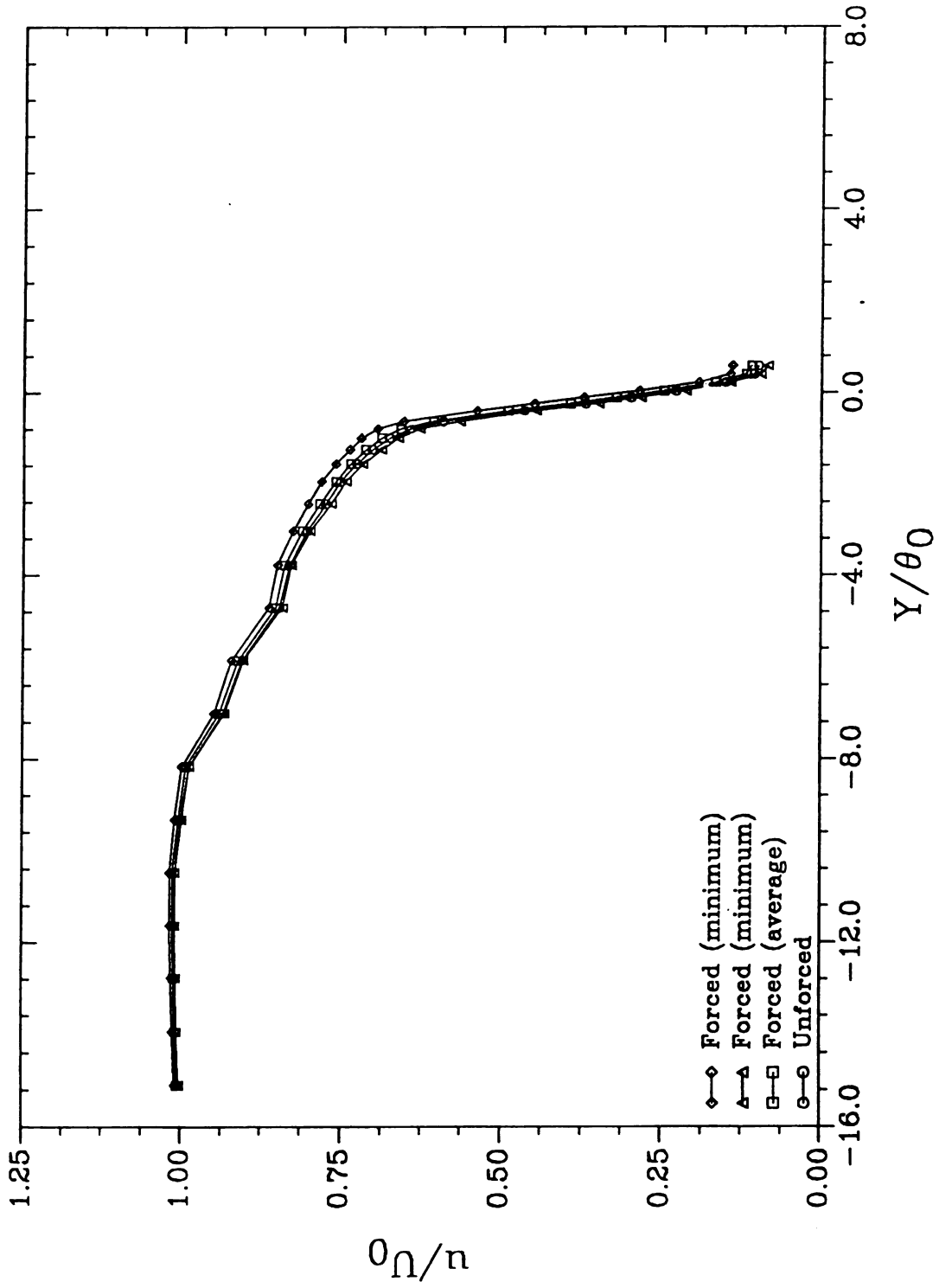
Figure 54 - Mean velocity profiles at $x/\theta_0 = 3$
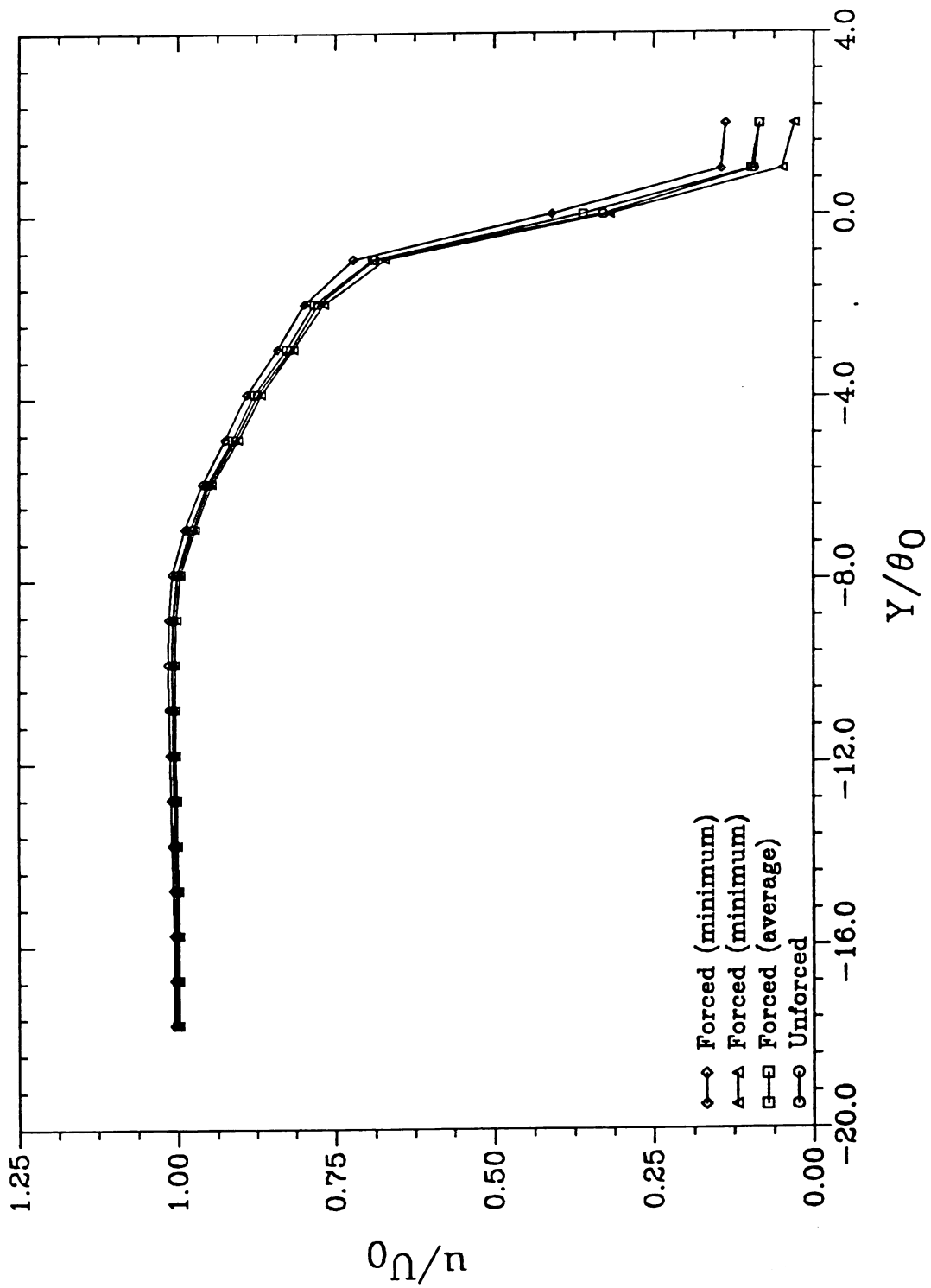
Figure 55 - Mean velocity profiles at $x/\theta_0 = 5$
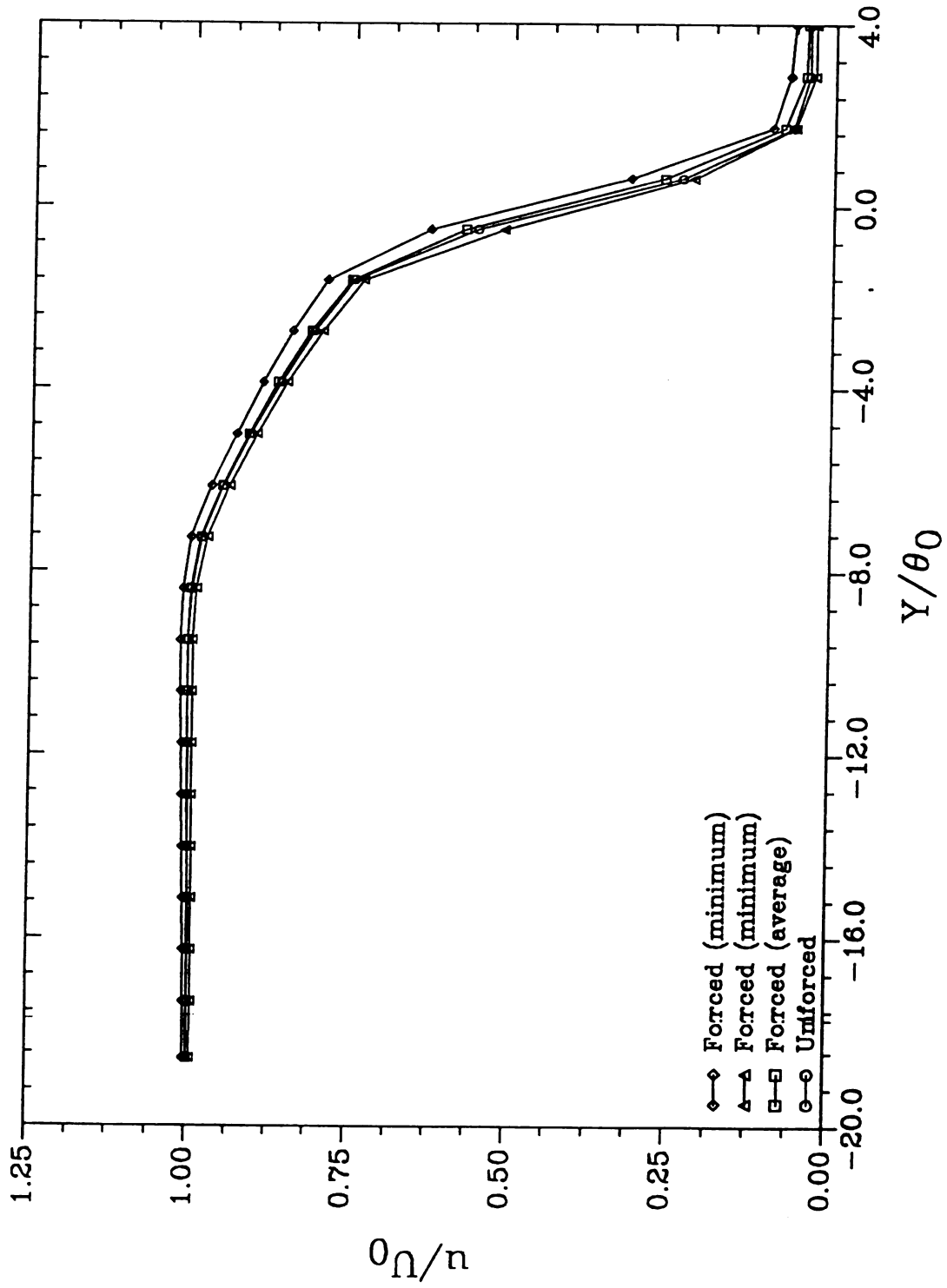
Figure 56 - Mean velocity profiles at $x/\theta_0 = 10$
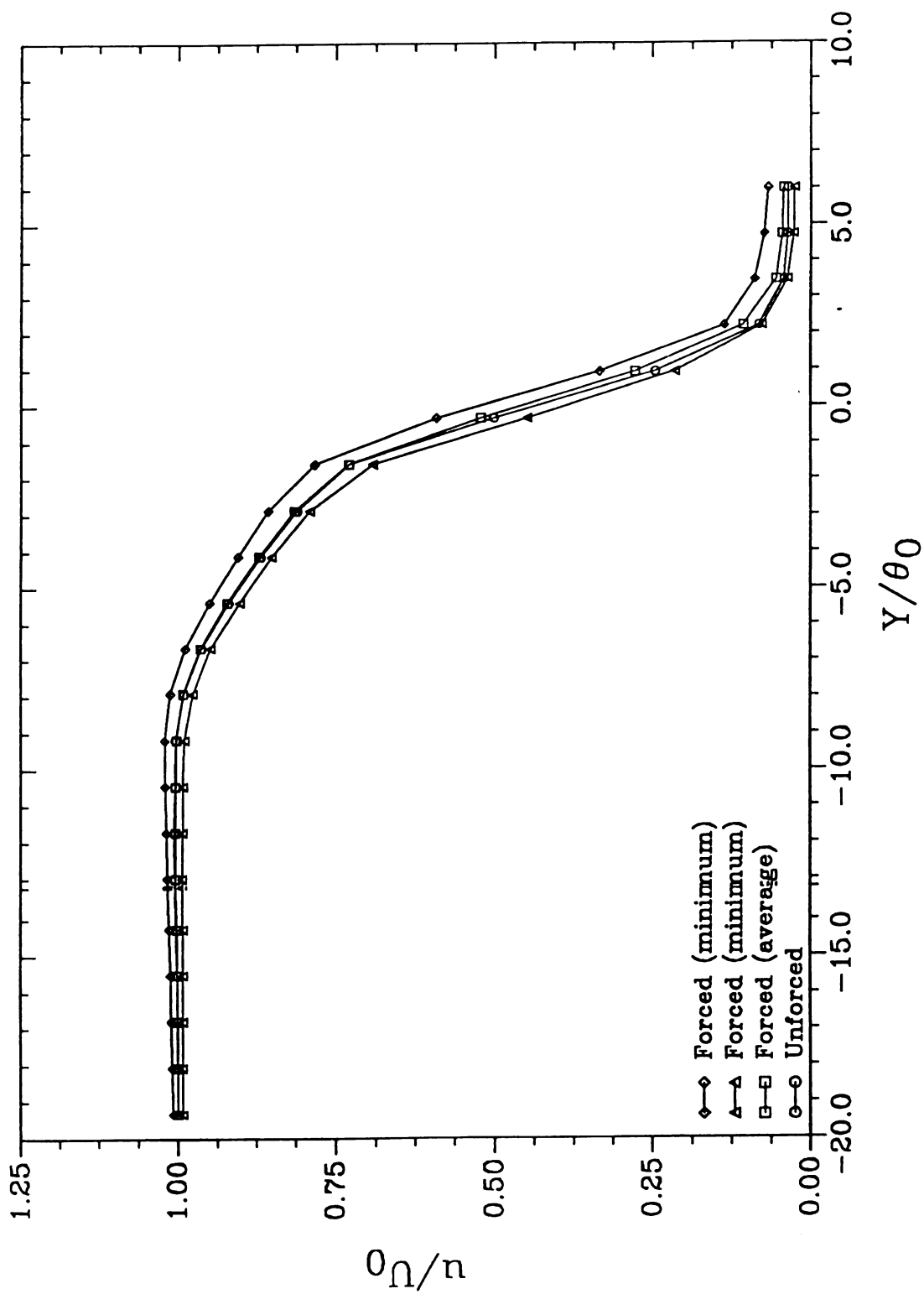
Figure 57 - Mean velocity profiles at $x/\theta_0 = 15$
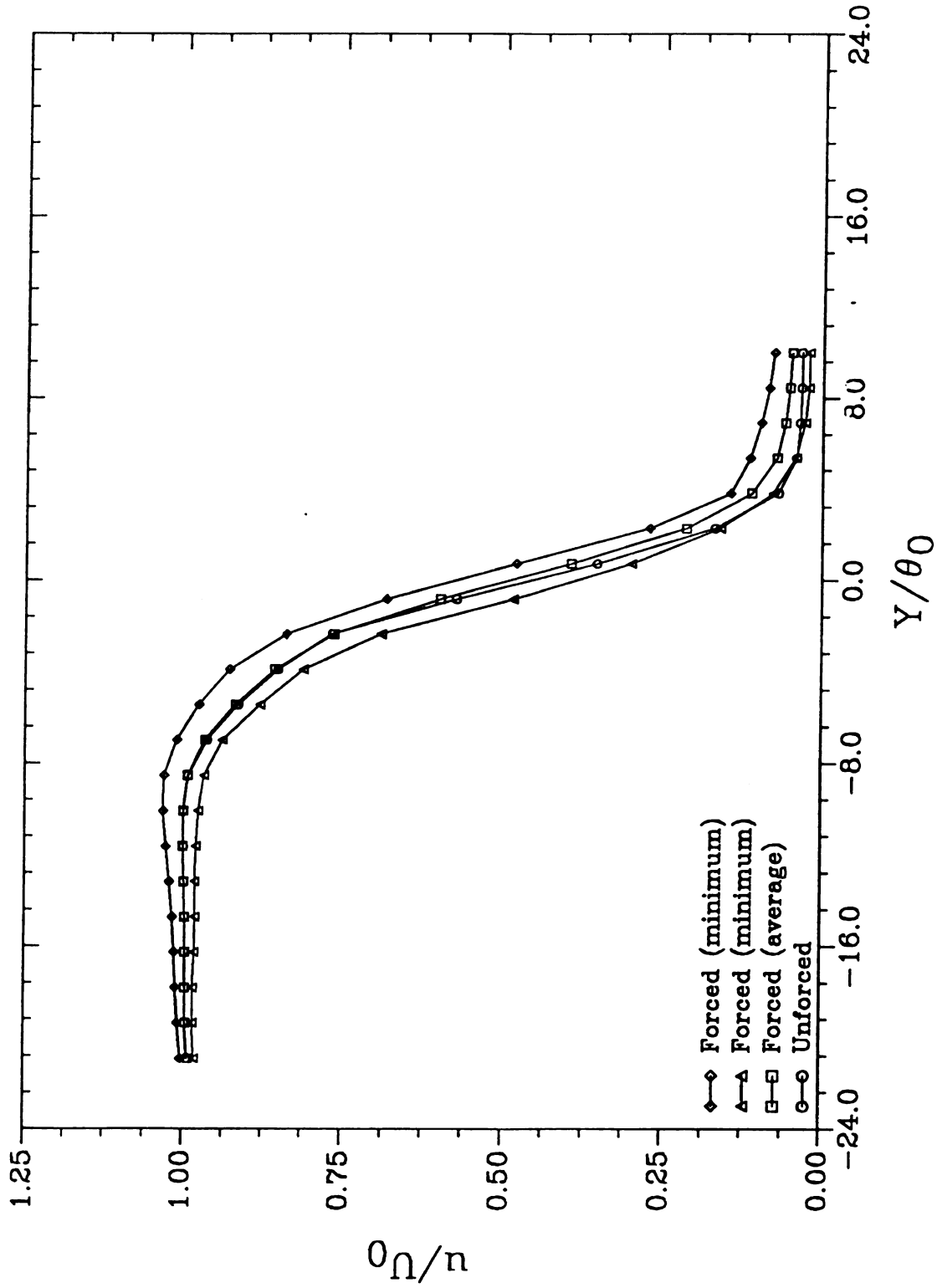
Figure 58 - Mean velocity profiles at $x/\theta_0 = 25$
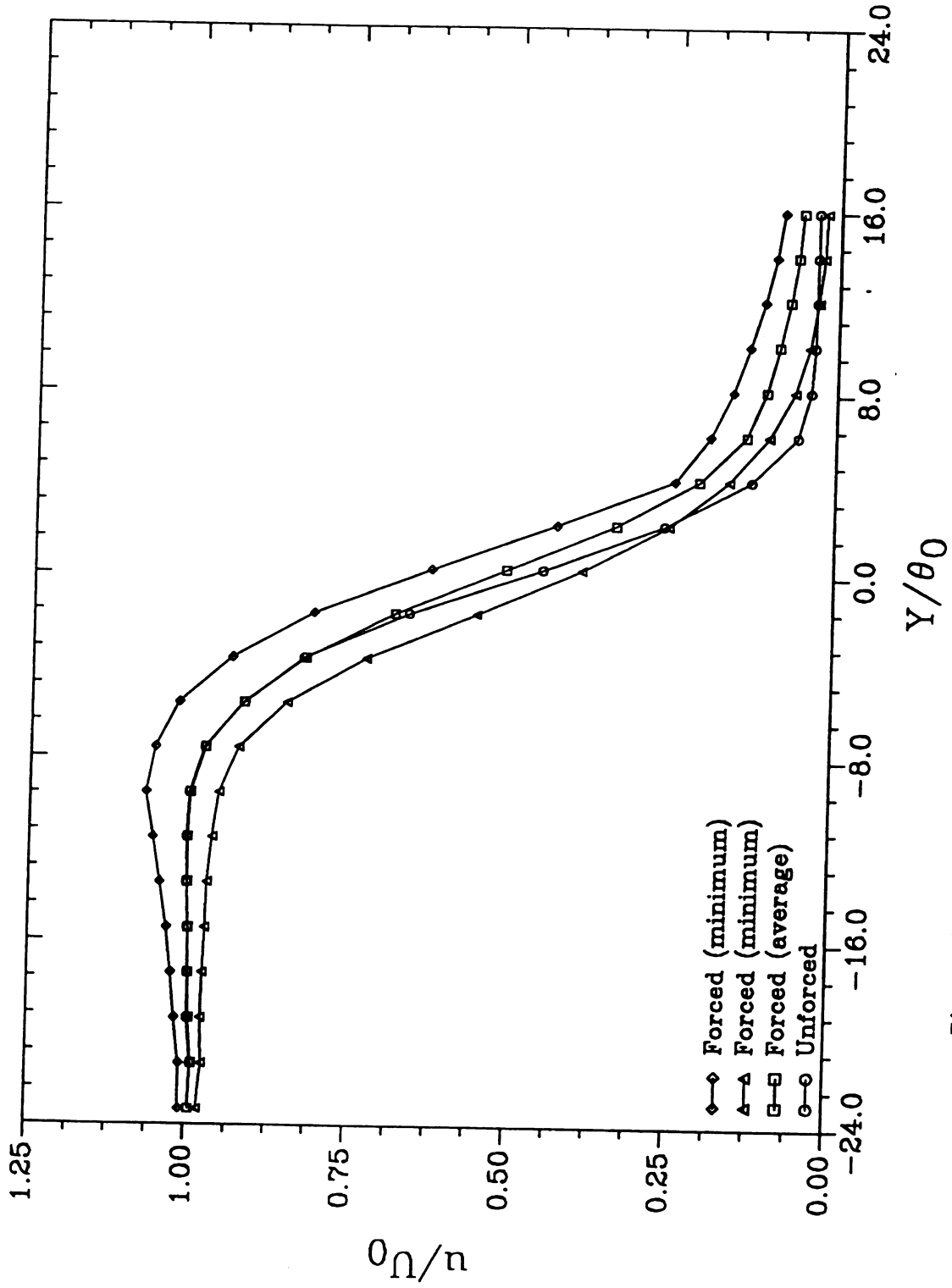
Figure 59 - Mean velocity profiles at $x/\theta_0 = 40$
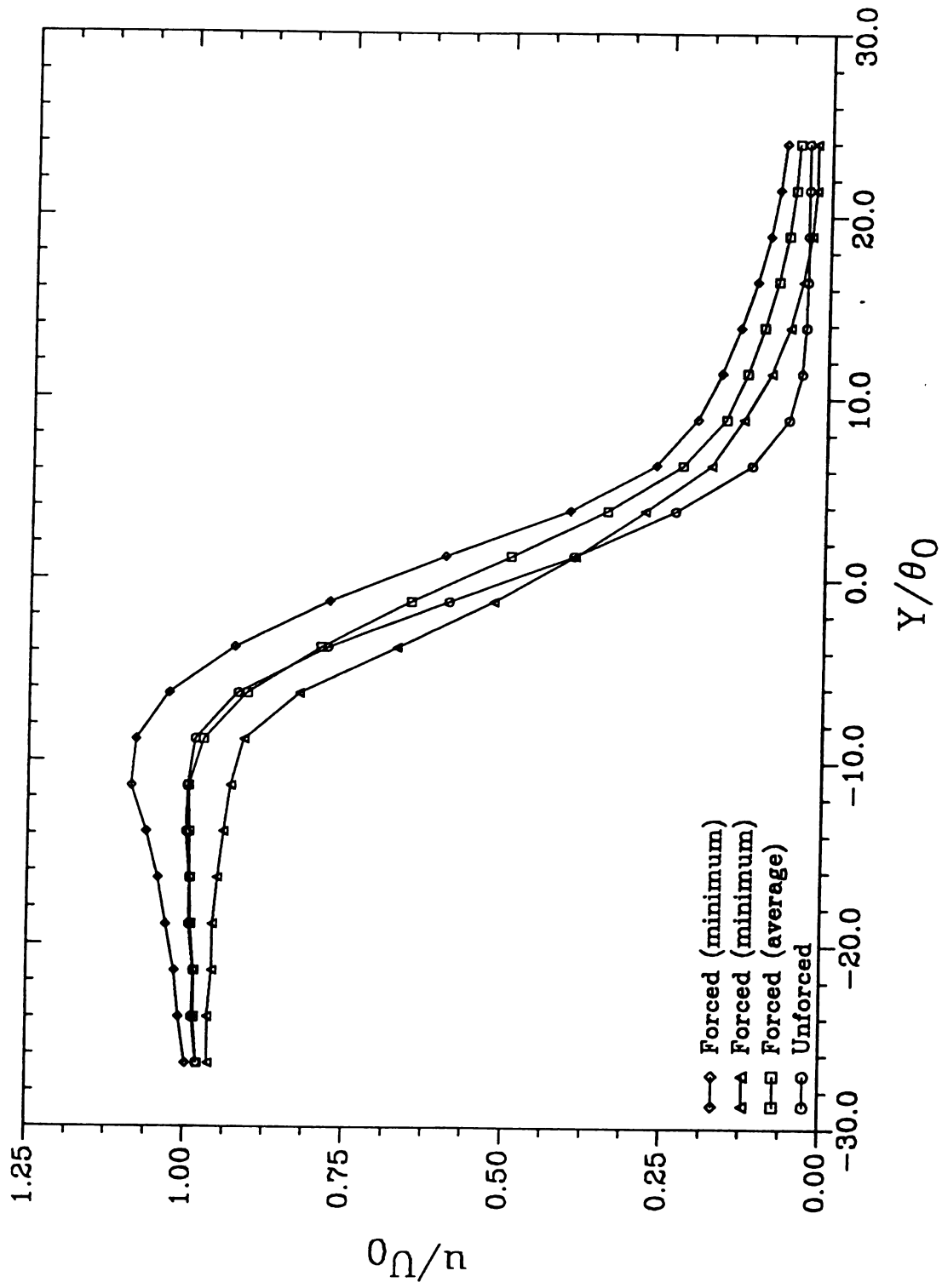
Figure 60 - Mean velocity profiles at $x/\theta_0 = 60$
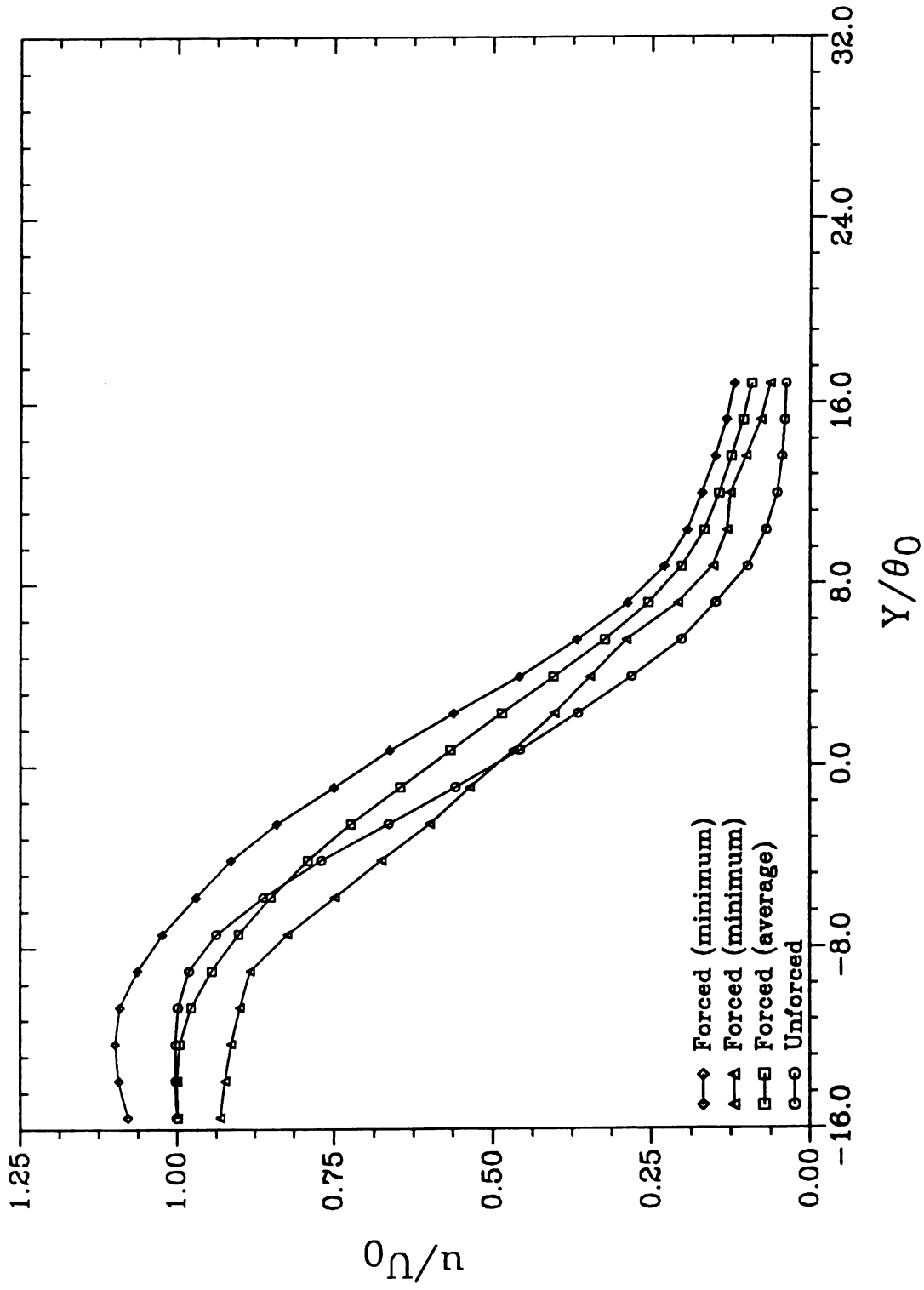
Figure 61 - Mean velocity profiles at $x/\theta_0 = 77$
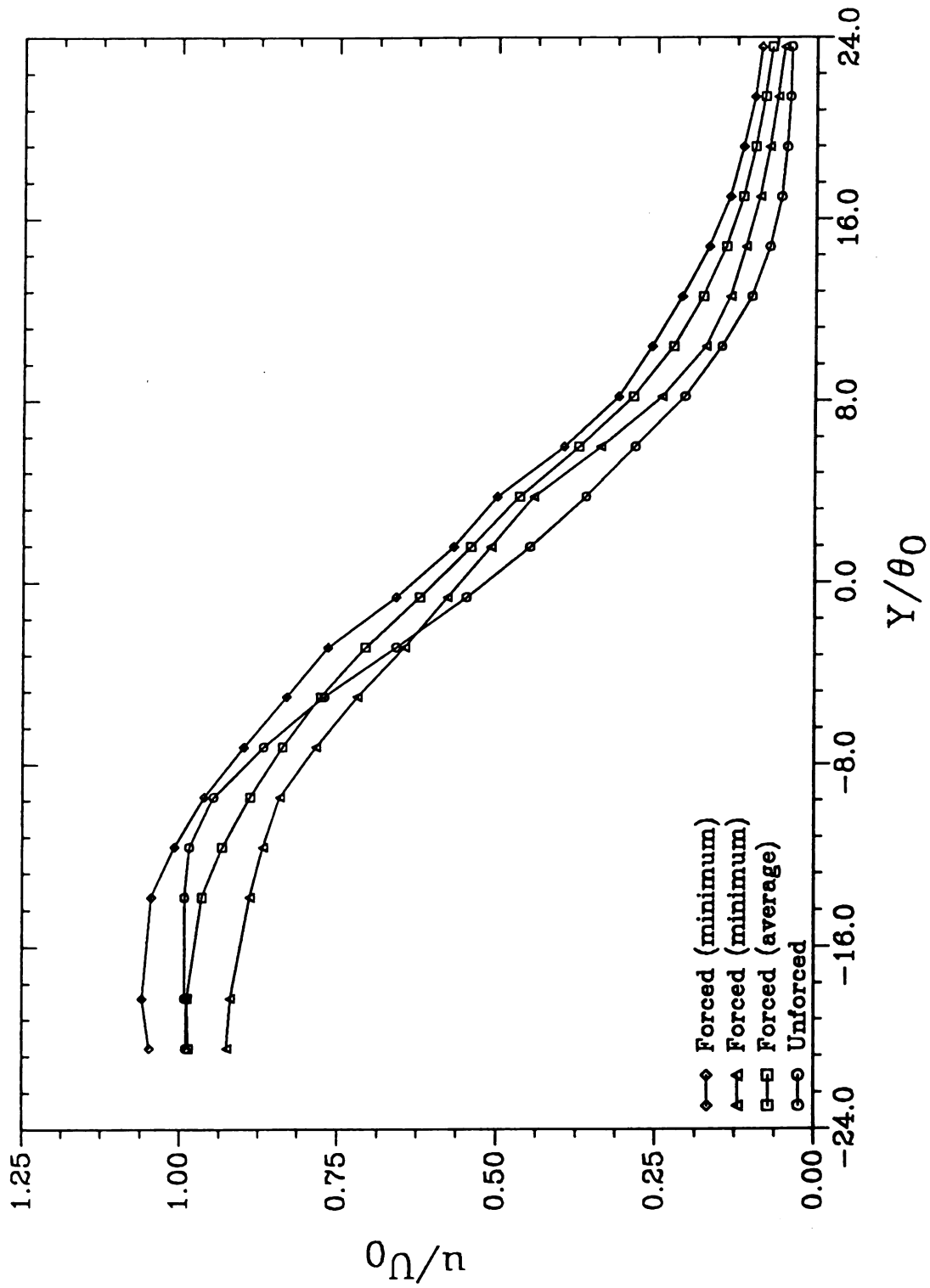
Figure 62 - Mean velocity profiles at $x/\theta_0 = 115$
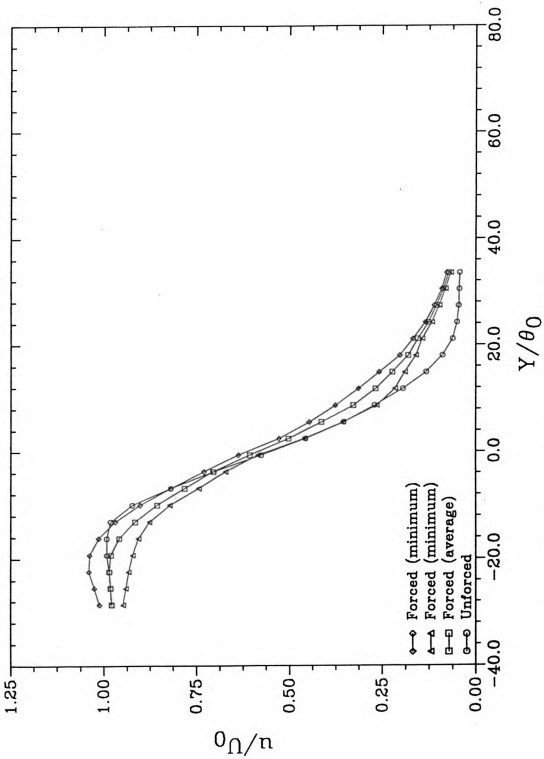
Figure 63 - Mean velocity profiles at x/θ_0 = 153
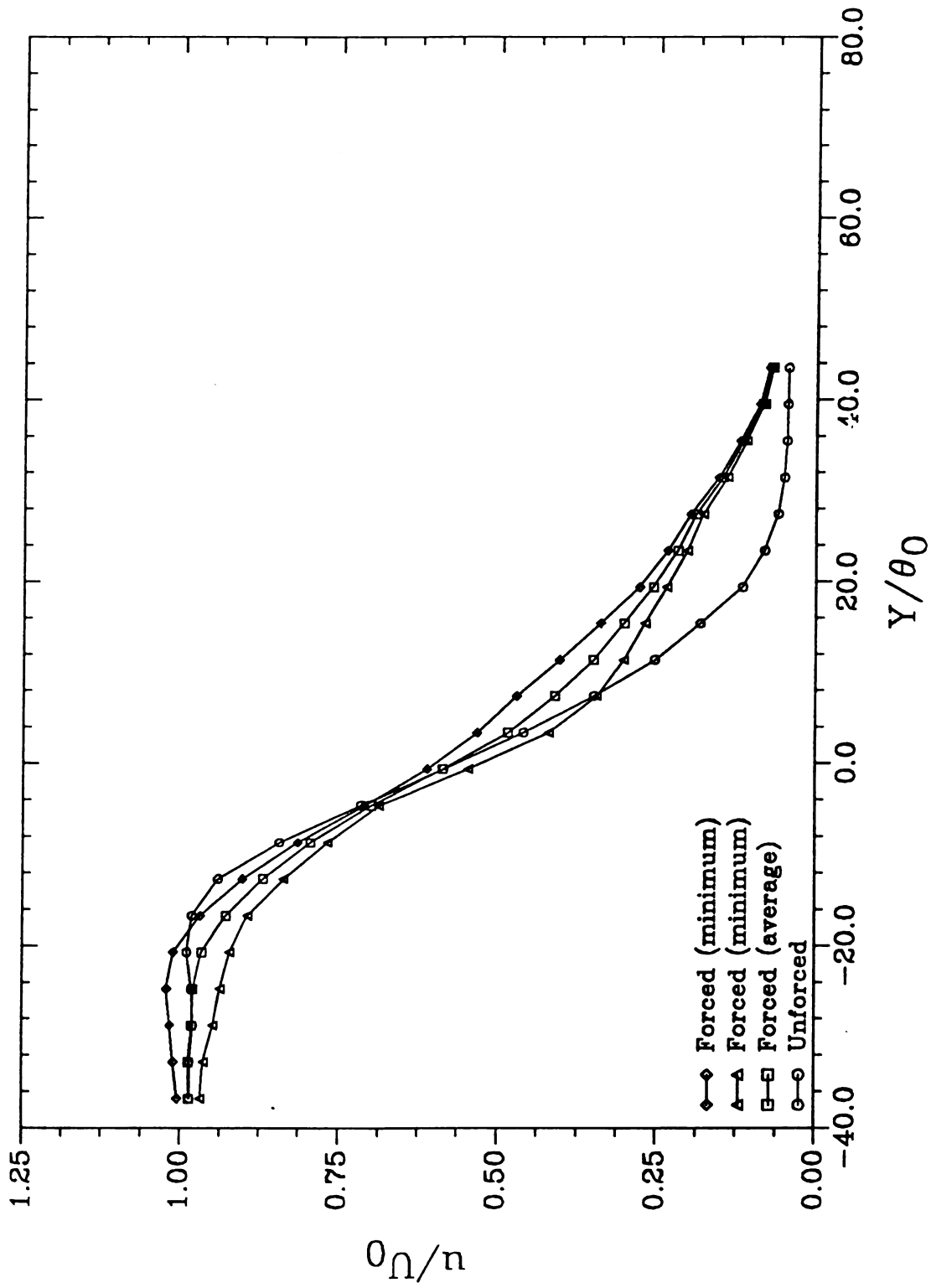
Figure 64 - Mean velocity profiles at $x/\theta_0 = 192$
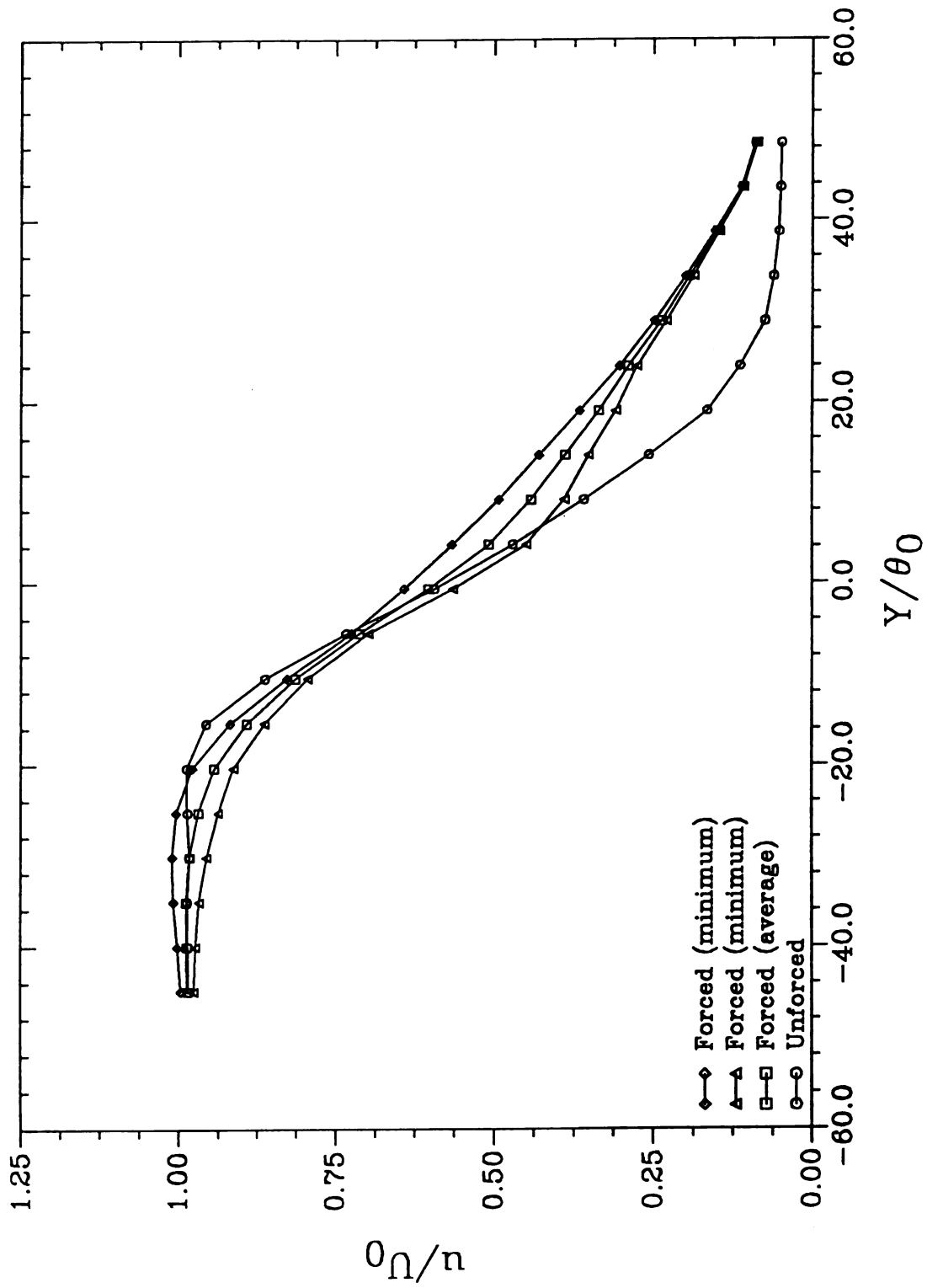
Figure 65 - Mean velocity profiles at x/θ_0 = 230
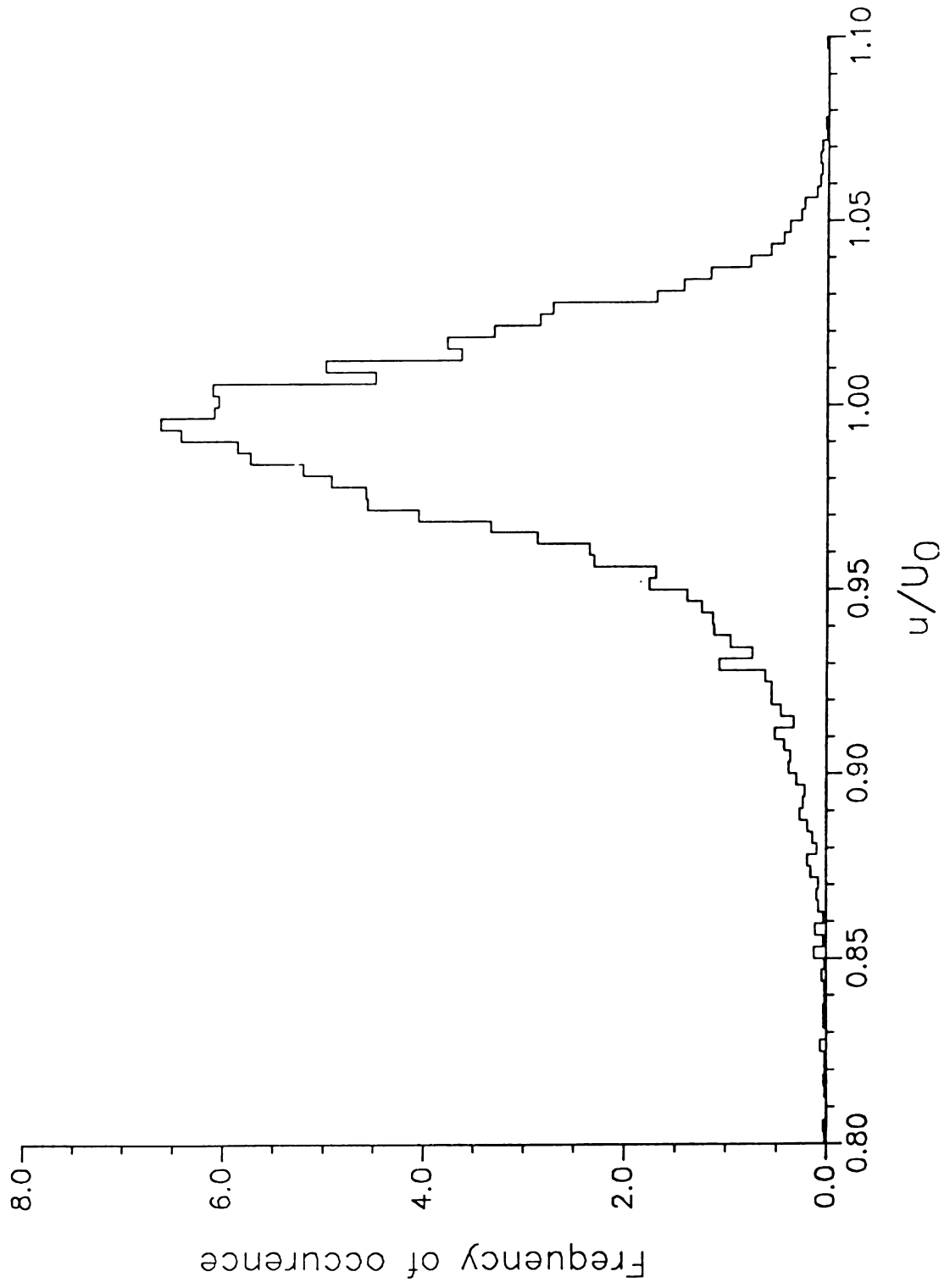
Figure 66 - Unforced condition velocity histogram at $x/\theta_0 = 60$
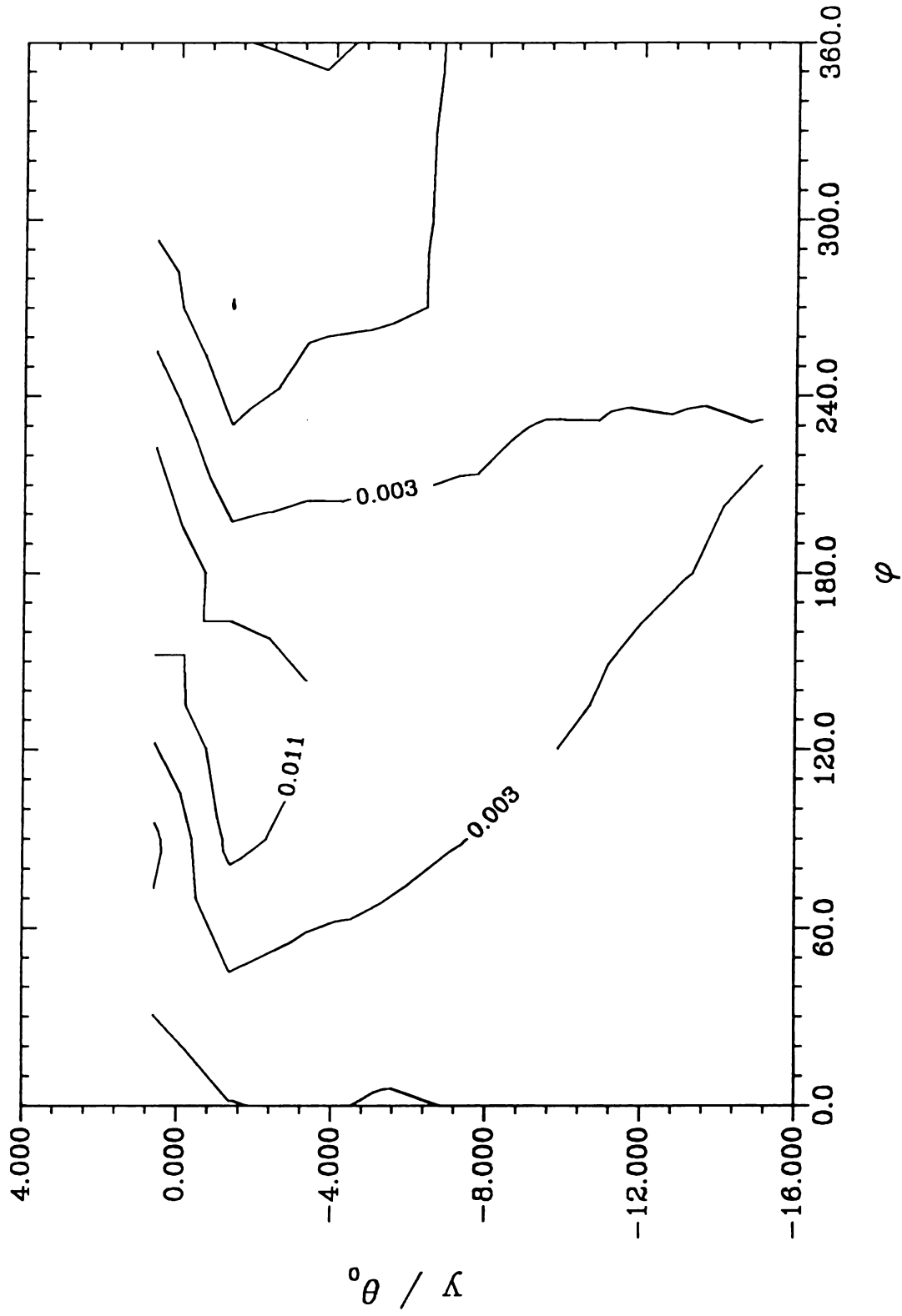
Figure 67 - δu versus phase contours at x/θ₀ = 1
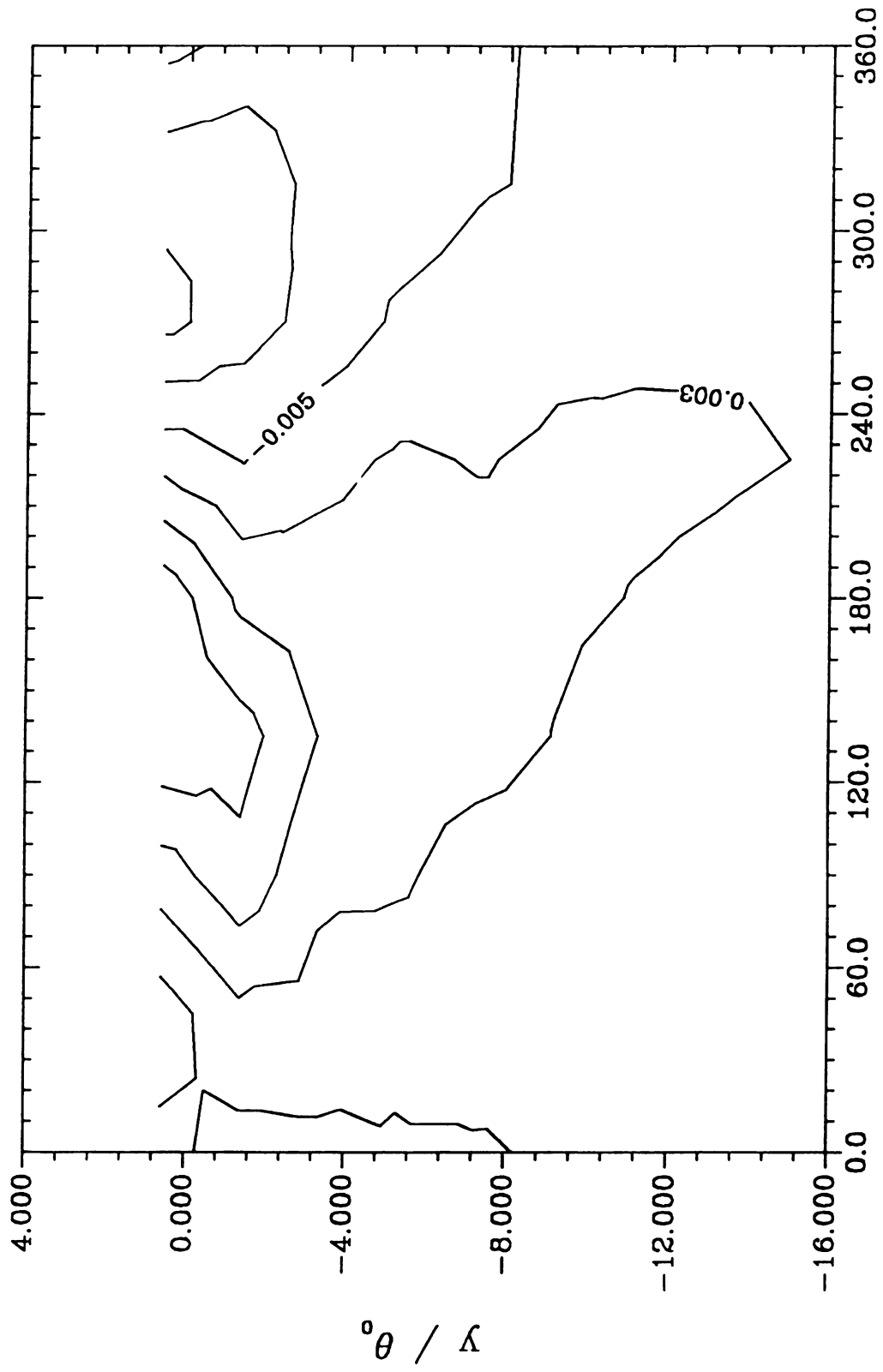
Figure 68 - δu versus phase contours at $x/\theta_0 = 3$

Figure 69 - δu versus phase contours at x/θ₀ = 5
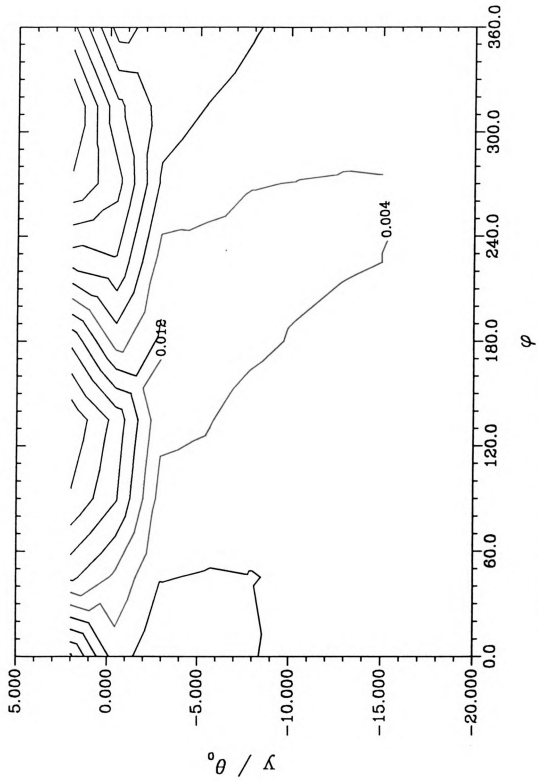
Figure 70 - δu versus phase contours at x/θ₀ = 10
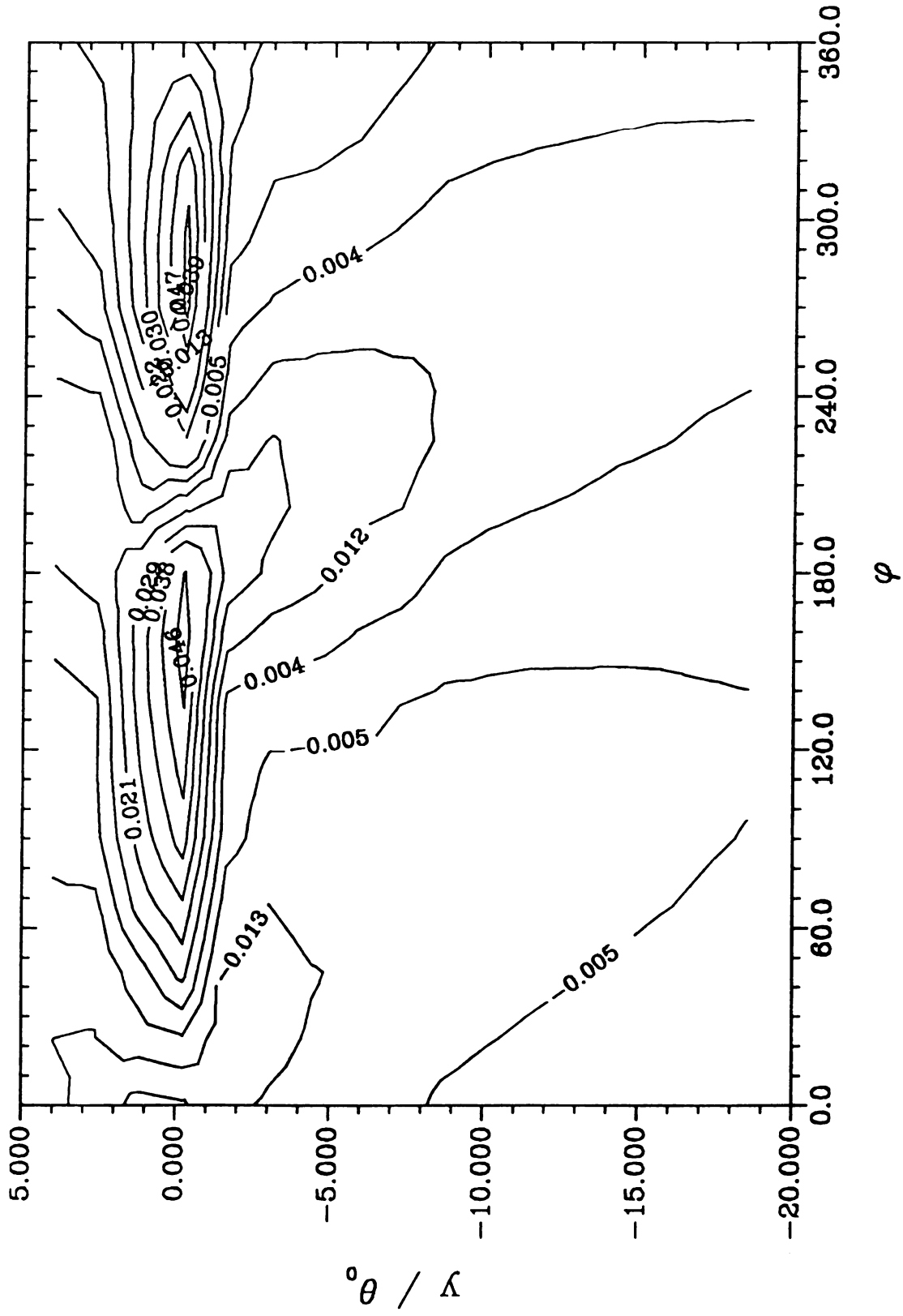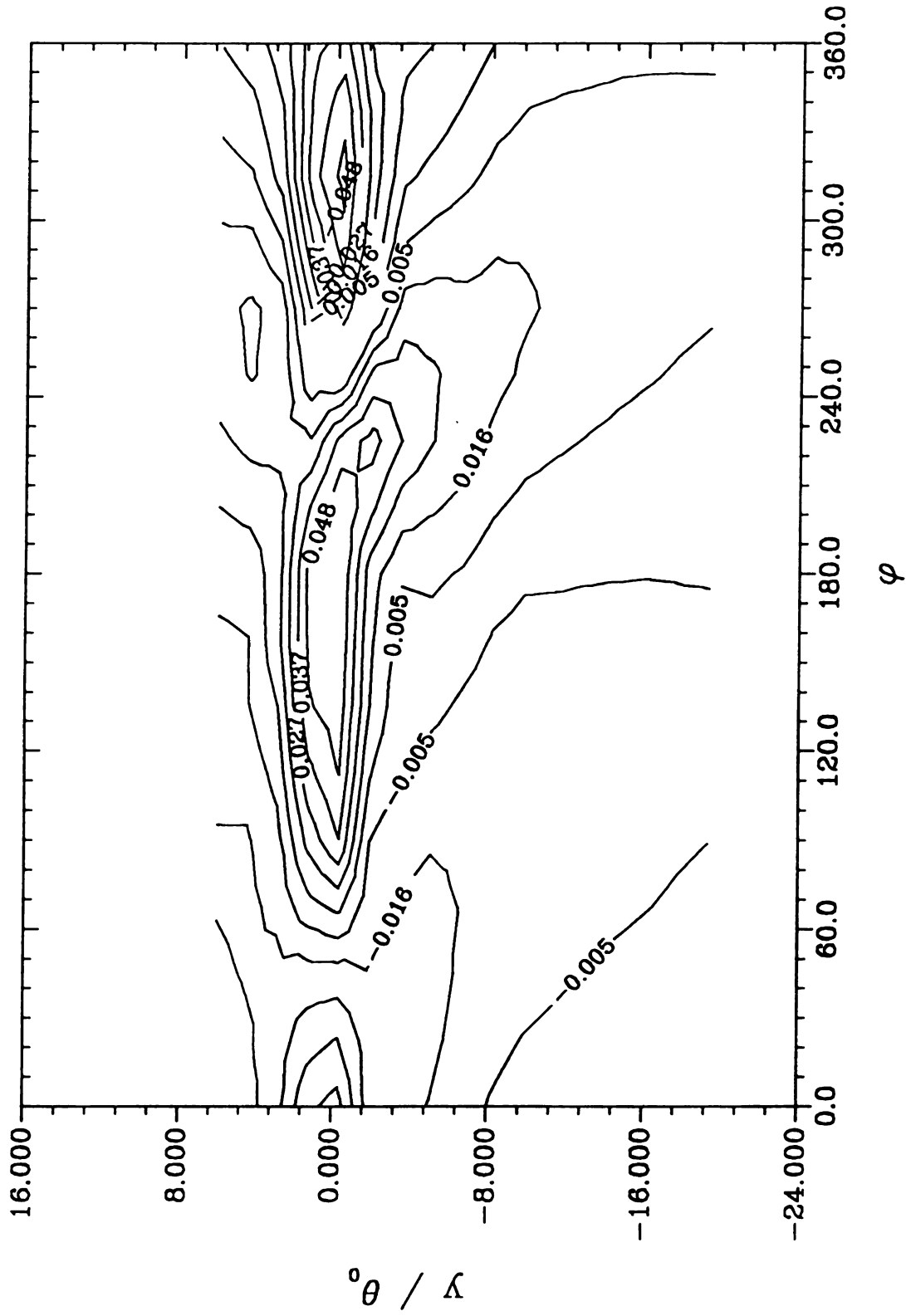
Figure 71 - δu versus phase contours at $x/\theta_0 = 15$
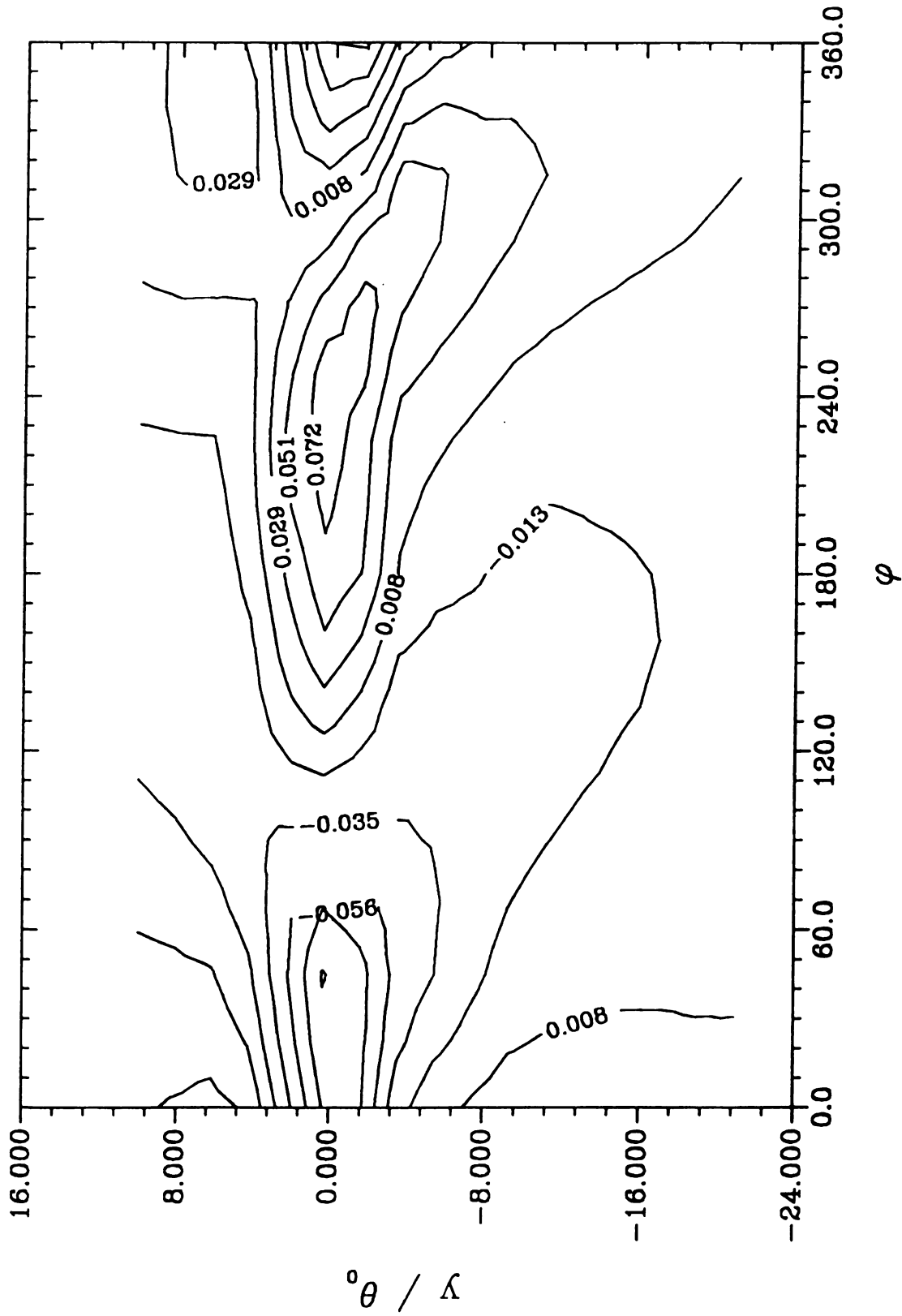
Figure 72 - δu versus phase contours at $x/\theta_0 = 25$
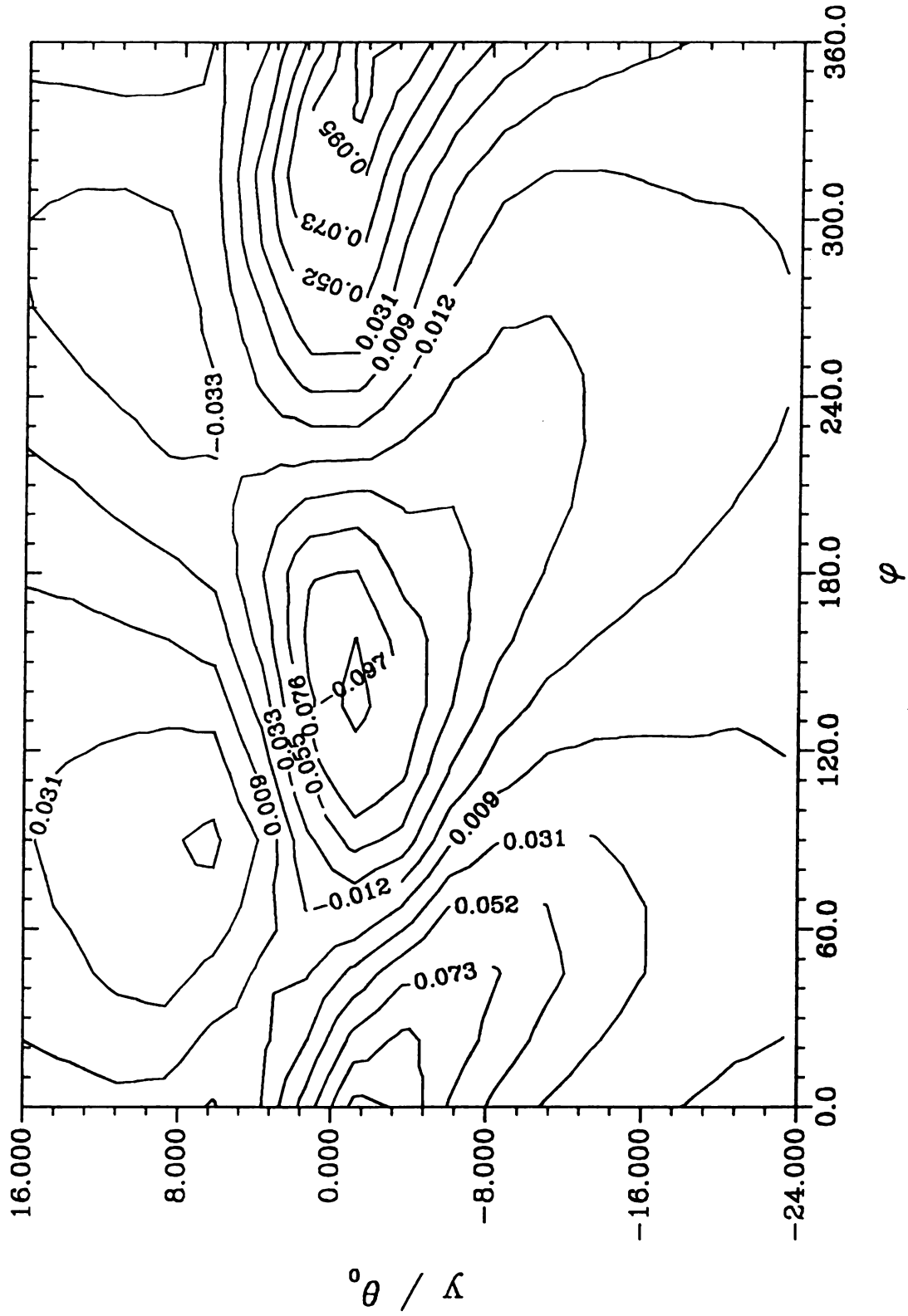
Figure 73 - δu versus phase contours at $x/\theta_0 = 40$

Figure 74 - δu versus phase contours at x/θ₀ = 60

Figure 75 - δu versus phase contours at x/θ₀ = 77

Figure 76 - δu versus phase contours at $x/\theta_0 = 115$
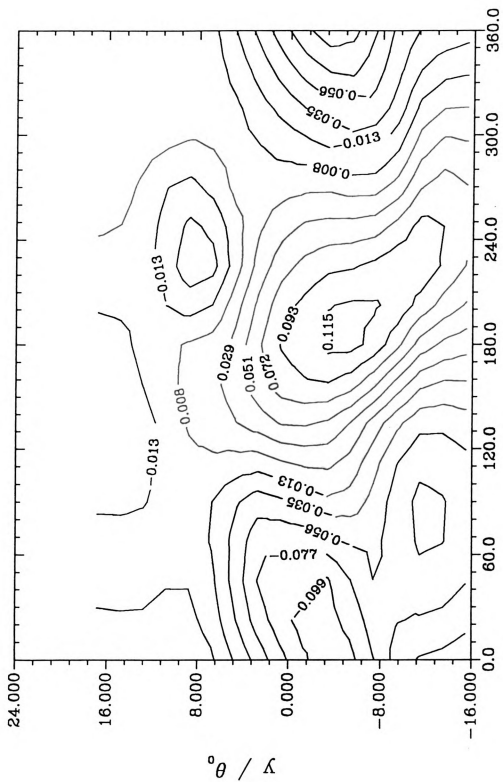
Figure 77 - δu versus phase contours at $x/\theta_0 = 153$
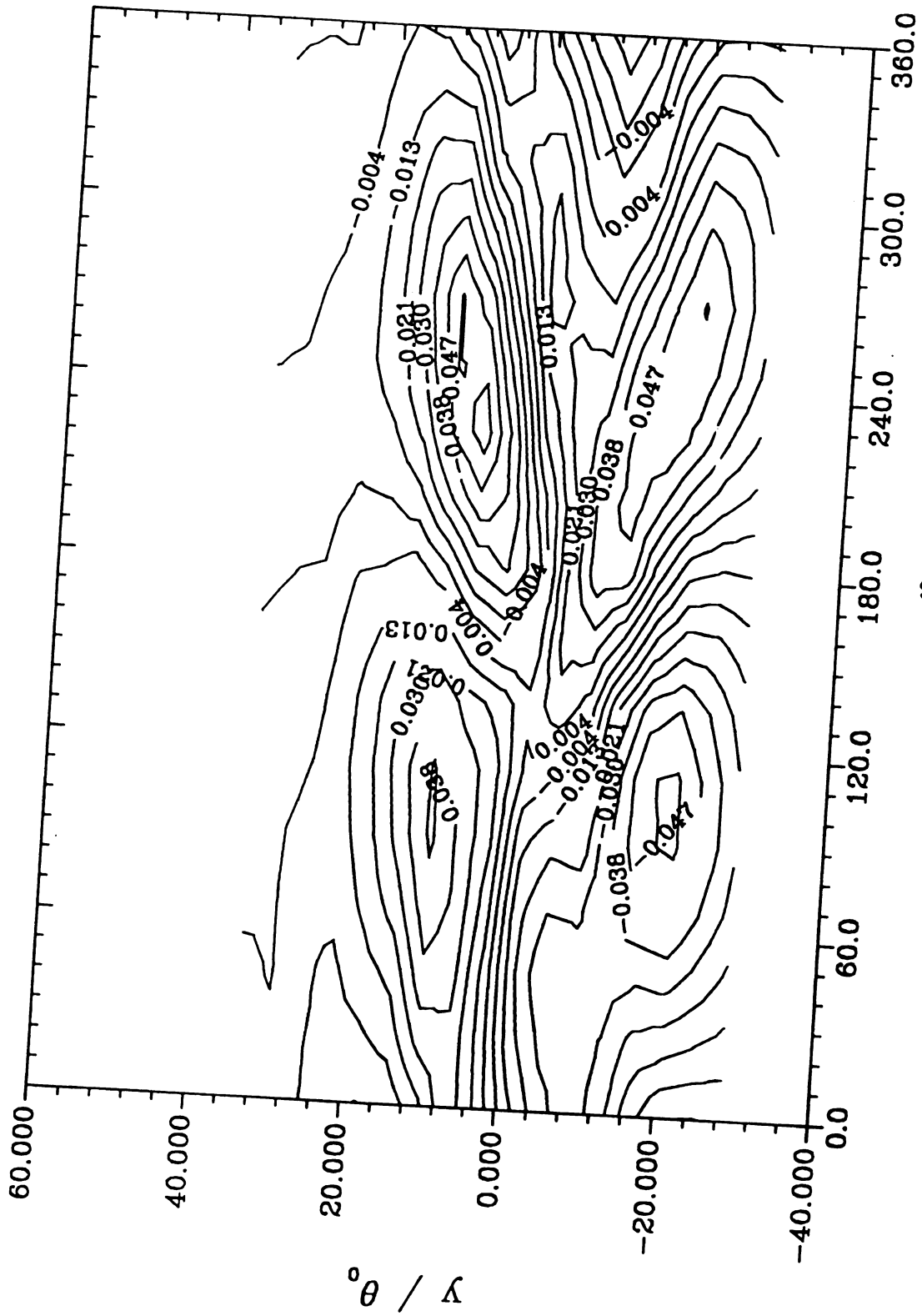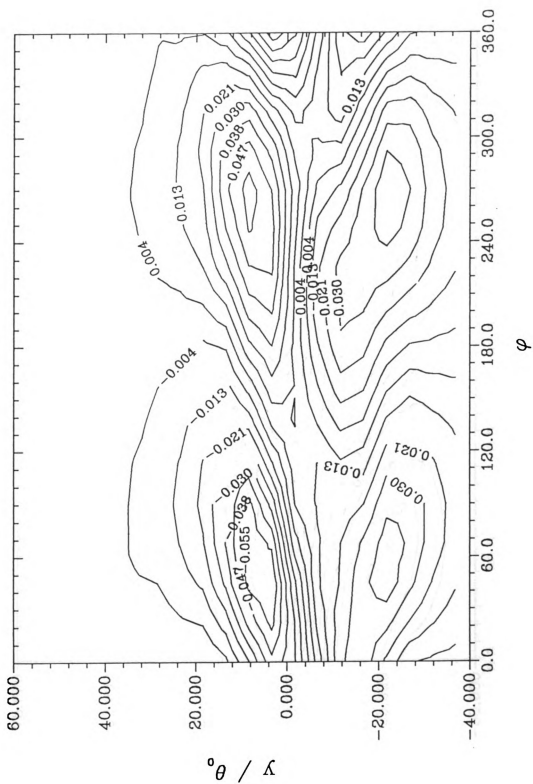
Figure 78 - δu versus phase contours at $x/\theta_0 = 192$

Figure 79 - δu versus phase contours at $x/\theta_0 = 230$

$X_1 = 115.4 \ \theta \quad \varphi_1 = 55.$

$X_2 = 153.8 \ \theta \quad \varphi_2 = 249.$

Figure 80 - Determination of disturbance phase location
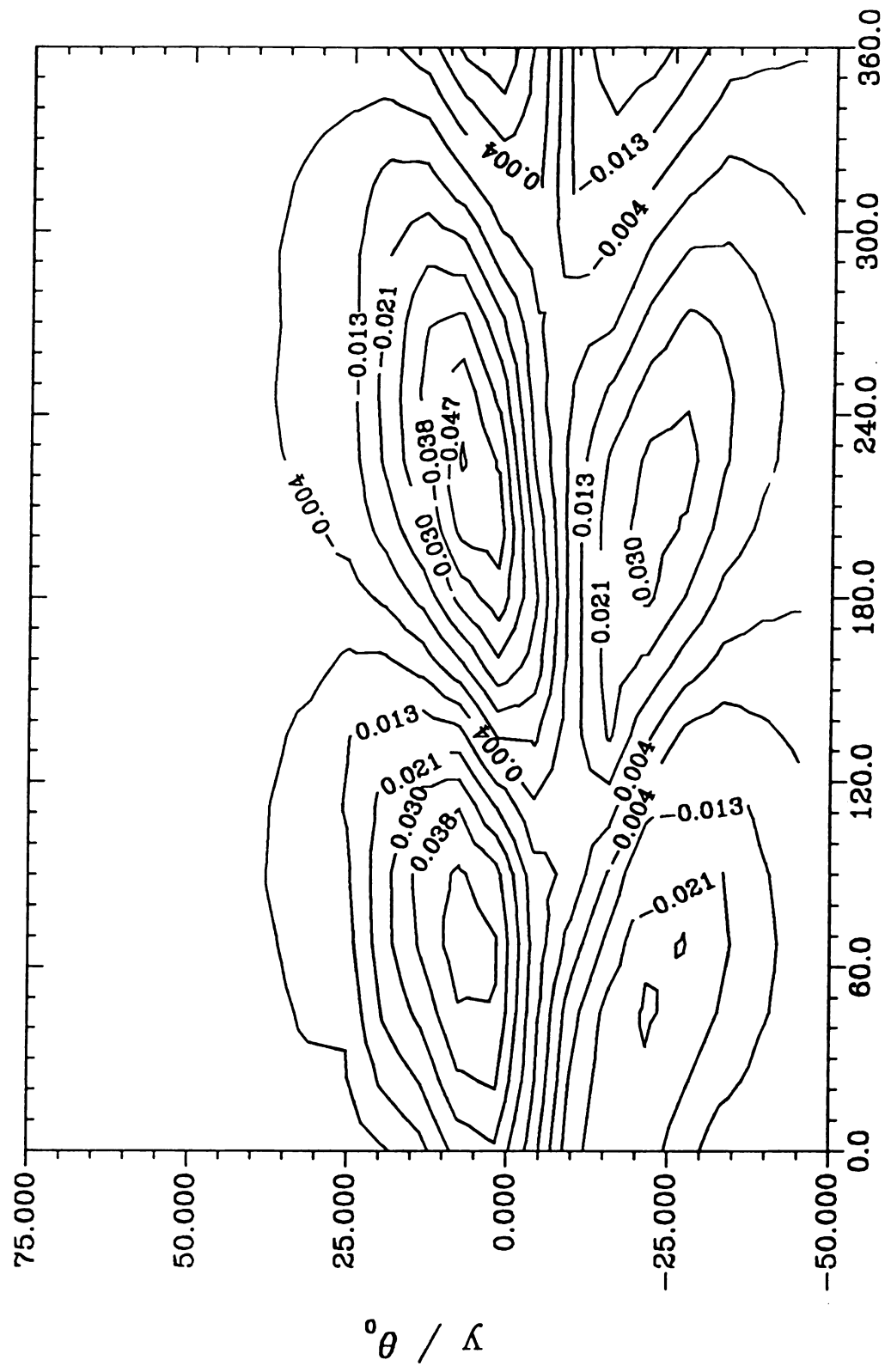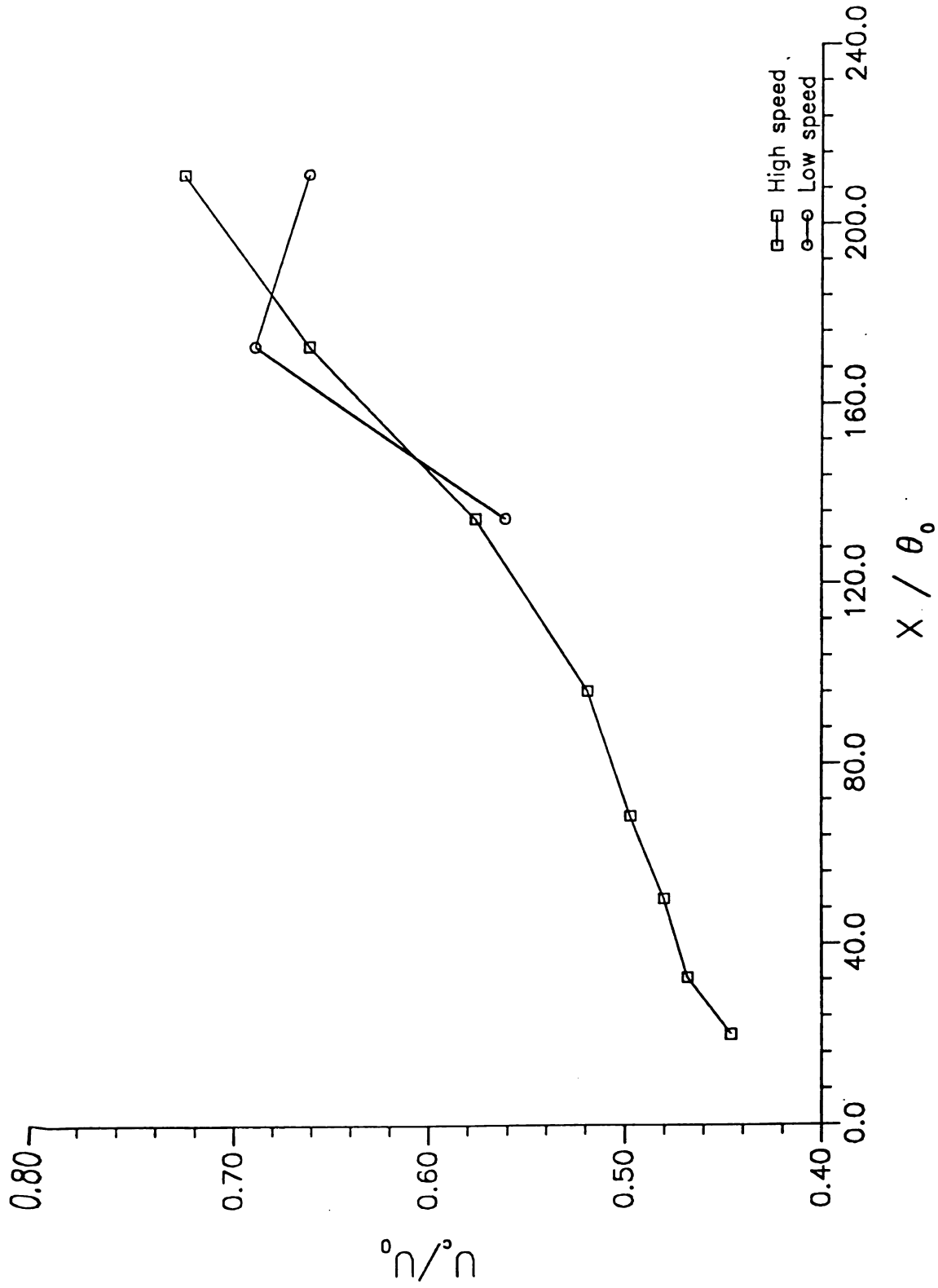
Figure 81 - Convection speed in the developing shear layer
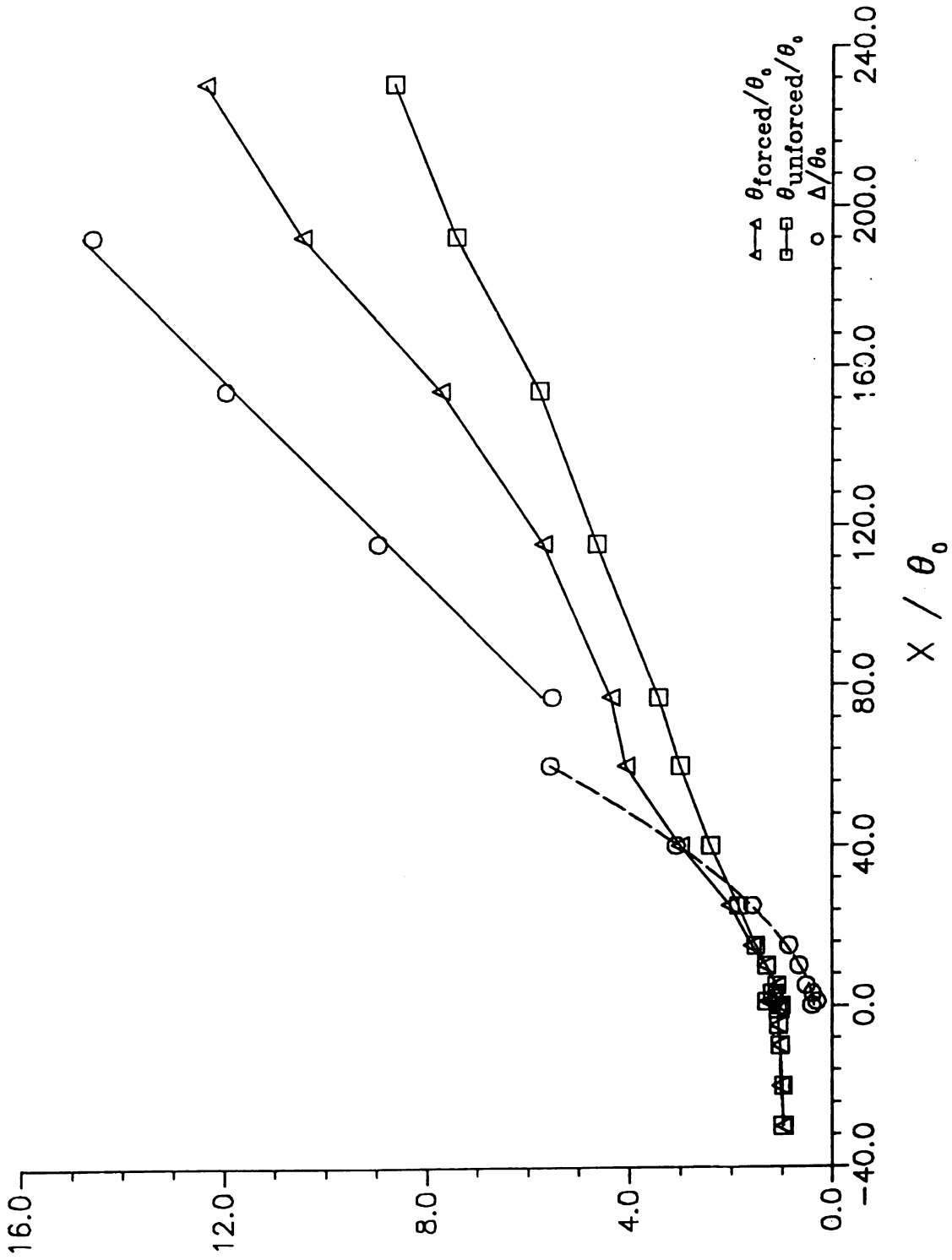
Figure 82 - Width measures in the developing shear layer
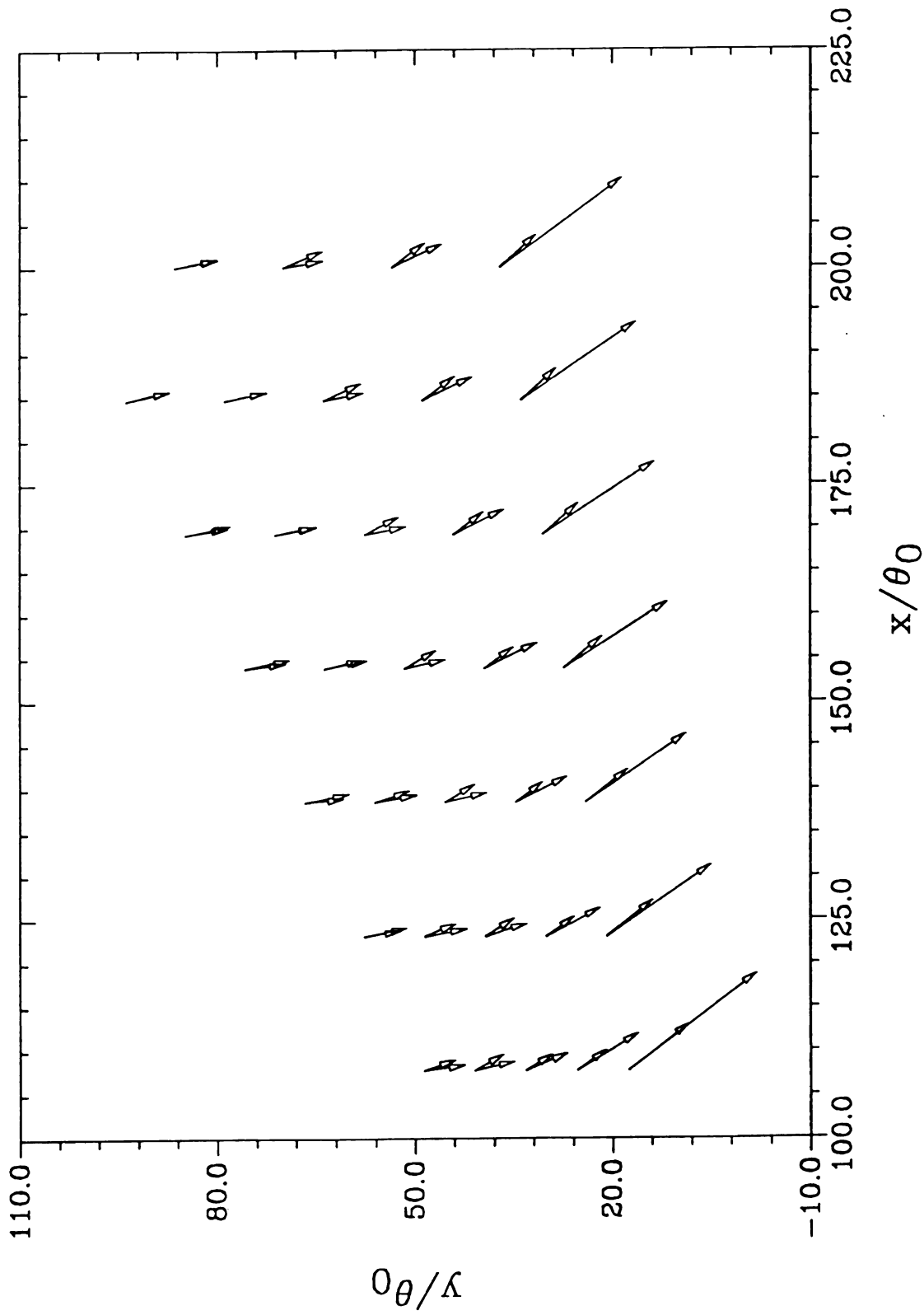
Figure 83 - Entrainment field velocity vectors
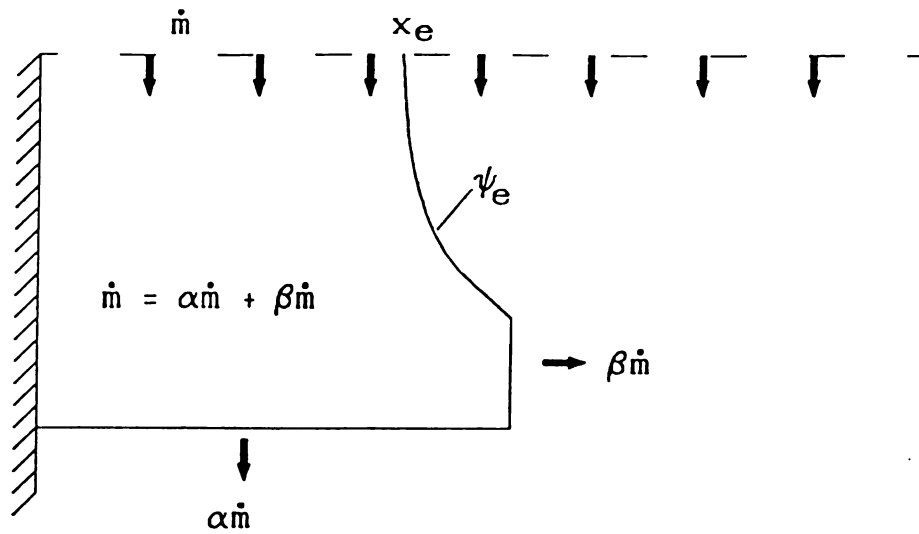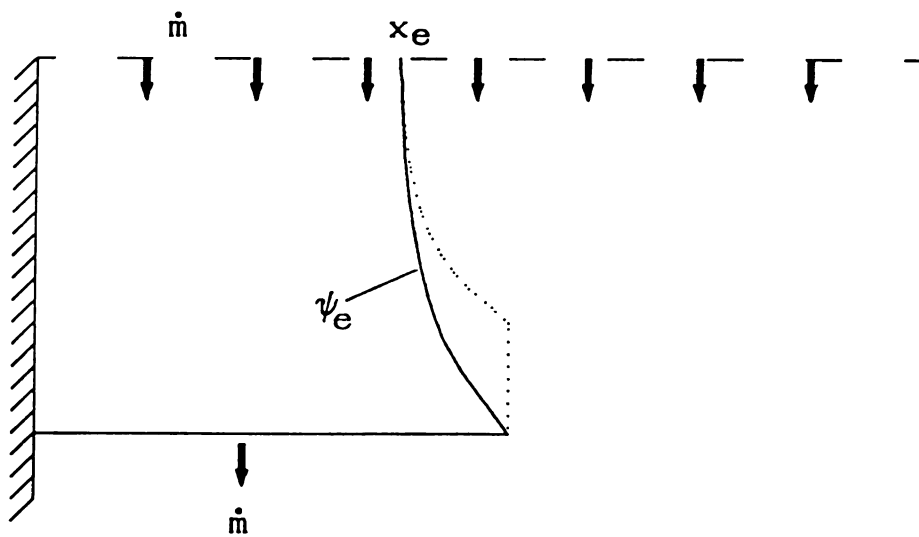
Figure 84 - Schematic representation of entrainment mass flux

APPENDICES

APPENDIX A

EFFECT OF WALL CONTACT ON HOT-WIRE CHARACTERISTICS

A hot-wire anemometer, being a thermal device, is strongly effected by the proximity of a thermally conducting wall. Even when heat loss effects are minimized through use of a poorly conducting wall there is appreciable heat loss to the wall at small wire-to-wall distances. If one of the prongs, which supports the copper plated 5 μ tungsten wire, comes into contact with the wall, the heat loss is strongly intensified. This effect can be used to accurately locate the position of the wire by moving the wire towards the wall until a sharp increase in the anemometer output is noted. This positioning method was evaluated for the current study; it was abandoned after it was discovered that bringing the wire into contact with the wall modified the wires characteristics.

To quantify the variation in wire characteristics, a number of consecutive calibrations were performed with the same wire. All calibrations were executed over a period of 3 hours, during which time

the temperature of the room remained constant to within 1° C. The subject wire had been operated for several days, and it was operated for over two hours in the calibration flow before the first calibration. The wall under consideration was Formica faced, and meticulously cleaned using isopropyl alcohol prior to the study. In each case the wire was calibrated: i) one or more times in the calibration stream, ii) positioned using the wall contact method, and iii) moved back into the calibration stream and recalibrated. The above procedure was executed for a number of cases; see Table A.1 for the resulting data. The calibrations indicated with a "yes" under the heading contact in Table A.1 came into contact with the wall prior to the calibration.

The velocity error in Table A.1 was obtained using the following procedure. The calibration constants for the first calibration were used to compute a reference voltage from an arbitrary reference velocity of 10.0 meters per second. The velocity error for each calibration was then evaluated as the difference between the computed flow speed (using the reference voltage) and the reference velocity of 10.0 meters per second.

Table A.1 - Wall Contact Calibration Results

Run	Contact	A	B	n	Std. Dev.	Computed velocity	Velocity error
A		9.041	3.769	0.41	0.007	10.00	0.00
B	Yes	8.744	3.520	0.42	0.005	11.98	1.98
C		8.852	3.380	0.43	0.012	12.11	2.11
D		8.707	3.519	0.42	0.008	12.09	2.09
E	Yes	8.365	3.621	0.41	0.010	13.00	3.00
F		8.648	3.336	0.43	0.009	13.09	3.09
G	Yes	8.142	3.779	0.40	0.011	13.14	3.14
H		8.475	3.467	0.42	0.006	13.23	3.23
I		8.496	3.453	0.42	0.008	13.28	3.28
J		8.589	3.325	0.43	0.012	13.37	3.37
K	Yes	8.247	3.621	0.41	0.009	13.36	3.36
L		8.414	3.459	0.42	0.009	13.48	3.48

As indicated in Table A.1, the hot-wire characteristics underwent a large change when the wire was brought into contact with the wall. The mechanism behind the change is unknown. For the current study, it was of sufficient interest to ascertain that this type of positioning method was not usable given the experimental configuration.

APPENDIX B

DROP TEST CALIBRATION TECHNIQUE

A novel low speed calibration method was employed for calibration of the hot-wire used in the zero free stream velocity $(U_0=0)$ study. The general details of the calibration technique have been previously detailed, Haw [1987]. The specifics on the method used to obtain the reference velocity for the current study are detailed in the following.

The force balance for an arm in a uniform gravitational field can be written as

$$\alpha = \frac{mg\sin(\theta)\bar{r}}{J} \tag{B.1}$$

where α is the angular acceleration of an arm of mass m and moment of inertia J.

Since the mechanical properties of the arm are constant all of the constant terms can be merged into a single constant A. Adding additional constants to account for aerodynamic drag (B) and for bearing friction (C), the resulting force balance is

$$\alpha = A \sin(\theta) - B\omega^2 - C\omega \qquad \text{(B.2)}$$

This equation of motion can be solved numerically to yield the position and velocity at any time given the appropriate initial conditions. To improve the numerical accuracy, the equation for the angular velocity of the arm can be expanded in terms of a Taylor series and applied at discrete time steps to yield:

$$\theta_{i+1} = \left\{ \left[(\omega_i'' \frac{\Delta t}{4} + \omega_i'') \frac{\Delta t}{3} + \omega_i' \right] \frac{\Delta t}{2} + \omega_i \right\} \Delta t + \theta_i \qquad \text{(B.3)}$$

$$\omega_{i+1} = \left[(\omega_i'' \frac{\Delta t}{3} + \omega_i'') \frac{\Delta t}{2} + \omega_i' \right] \Delta t + \omega_i \qquad \text{(B.4)}$$

where the subcripts i and i+1 denote the current and the subsequent time steps and the deriviatives of the velocity are given as:

$$\omega' = \alpha = A\sin(\theta) - B\omega^2 - C\omega \qquad \text{(B.5)}$$

$$\omega'' = (A\cos(\theta))\omega - 2B\omega\omega' - C\omega' \qquad \text{(B.6)}$$

$$\omega''' = \omega'[Acos(\theta) + 2B\omega'] + \omega[\omega Asin(\theta) - 2B\omega''] - C\omega'' \qquad (B.7)$$

The constants A, B, and C were obtained by minimizing the mean square error in position between the numerical simulation, (from (B.3) and (B.4)), and a series of experimentally measured data points. Although an analytic solution was not possible, numeric results were readily obtained using a steepest descent solution method to minimize the mean squared positional error. The constants obtained in this manner were used in the numerical simulation for the fall, (B.3) and (B.4), to provide the calibration velocities.

APPENDIX C

ZERO MEAN FLOW PRESSURE MEASUREMENTS

Measurements of the pressure field induced by the piston were made for the condition of zero mean flow ($U_0 = 0$). The forcing frequency was sufficiently high, and the pressures sufficiently low to make measurements using a conventional tap and pressure transducer configuration impractical. A microphone, modified with a surrounding cavity and pinhole arrangement, was used as detailed in the following.

A Bruel and Kjaer type 4166 wide response condenser microphone was used with a locally fabricated cavity and pinhole. The microphone had a free air response of 0 to 20 KHz and an open circuit sensitivity of 48.6 mv per Pa. The microphone cavity consisted of a 17 mm diameter cylinder 5 mm long with a 1 mm hole at one end and the microphone face (17 mm diameter) forming the other end. The resulting resonant frequency of the chamber (1900 Hz), was well above the measurement range of interest.

APPENDIX D

NUMERICAL DATA

The following tables contain the primary experimental data for the current study. The data in the tables are non-dimensionalized in the following forms:

a) The velocity measurements of the active shear layer and boundary layer are non-dimensionalized with the free stream velocity (U_0); the corresponding data locations are non-dimensionalized with the separating boundary layer momentum thickness (θ_0).

b) The measurements of the velocity and pressure for the no-flow data are presented in dimensional form. The velocity measurements are given in meters per second; the pressure measurements are given as output voltage from the microphone amplifier. In both cases the corresponding data locations are non-dimensionalized with respect to the forcing piston width (w_p).

Table D.1 - No Flow Hot-wire Mean Velocities

		Unforced	Phase averaged data (at angle ϕ)							
x/w_p	y/w_p	data	0.0	45.0	90.0	135.0	180.0	225.0	270.0	315.0
1.5	.77	.044	.167	.151	.243	.211	.127	.214	.341	.319
1.5	.38	.038	.142	.133	.210	.191	.113	.167	.276	.261
1.5	.00	.036	.147	.120	.178	.162	.104	.172	.274	.261
1.5	-.38	.037	.155	.113	.146	.139	.101	.169	.269	.261
1.5	-.77	.030	.152	.107	.123	.119	.093	.154	.251	.245
1.5	-1.54	.040	.138	.098	.098	.095	.080	.122	.201	.204
1.5	-3.08	.029	.086	.067	.065	.064	.055	.068	.104	.115
1.5	-6.15	.042	.060	.052	.047	.047	.045	.047	.059	.066
1.5	-10.00	.025	.053	.049	.047	.045	.045	.049	.056	.057
1.5	-23.08	.030	.053	.051	.049	.048	.048	.050	.053	.054
-2.9	-.38	.027	.024	.024	.030	.032	.028	.026	.028	.027
-1.0	-.38	.024	.034	.037	.057	.058	.042	.039	.054	.050
.0	-.38	.030	.100	.085	.163	.148	.085	.098	.191	.189
1.0	-.38	.034	.140	.098	.134	.132	.087	.135	.244	.244
2.9	-.38	.036	.086	.098	.149	.137	.084	.101	.158	.141
5.0	-.38	.029	.358	.263	.308	.356	.305	.279	.301	.297
-5.0	-1.00	.042	.022	.023	.025	.027	.025	.024	.024	.023
-1.0	-1.00	.039	.036	.040	.059	.062	.046	.041	.053	.052
.0	-1.00	.041	.062	.067	.112	.109	.072	.068	.105	.102
1.0	-1.00	.041	.116	.081	.098	.100	.072	.102	.180	.183
2.9	-1.00	.033	.087	.082	.115	.107	.073	.096	.147	.135
5.0	-1.00	.046	.190	.252	.309	.268	.285	.290	.281	.243
-15.0	-10.00	.024	.018	.018	.019	.019	.019	.018	.018	.018
-10.0	-10.00	.029	.022	.023	.024	.025	.025	.023	.022	.022
-5.0	-10.00	.032	.021	.022	.023	.024	.023	.022	.021	.021
-1.0	-10.00	.034	.028	.027	.028	.029	.028	.028	.029	.028
.0	-10.00	.025	.036	.034	.032	.032	.032	.034	.038	.039
1.0	-10.00	.037	.045	.041	.037	.035	.036	.041	.048	.049
2.9	-10.00	.032	.067	.061	.055	.052	.054	.063	.074	.074
5.0	-10.00	.021	.110	.103	.095	.091	.097	.111	.126	.123
10.0	-10.00	.018	.047	.044	.042	.040	.040	.044	.051	.051

Table D.2 - No Flow Hot-wire Rms Velocities

x/w_p	y/w_p	Unforced data	Phase averaged data (at angle ϕ)							
			0.0	45.0	90.0	135.0	180.0	225.0	270.0	315.0
1.5	.77	.002	.014	.016	.020	.016	.008	.016	.022	.025
1.5	.38	.001	.016	.013	.019	.014	.007	.017	.023	.028
1.5	.00	.002	.017	.007	.012	.008	.005	.017	.025	.028
1.5	-.38	.004	.012	.004	.008	.007	.004	.012	.019	.019
1.5	-.77	.002	.011	.004	.007	.006	.004	.012	.019	.017
1.5	-1.54	.006	.009	.004	.005	.006	.004	.013	.018	.014
1.5	-3.08	.001	.013	.007	.005	.005	.005	.010	.019	.019
1.5	-6.15	.005	.013	.010	.007	.006	.007	.008	.013	.015
1.5	-10.00	.002	.011	.010	.008	.007	.008	.010	.013	.013
1.5	-23.08	.002	.018	.017	.016	.015	.015	.016	.018	.018
-2.9	-.38	.002	.003	.003	.003	.003	.003	.003	.003	.003
-1.0	-.38	.003	.002	.002	.003	.003	.002	.002	.003	.002
.0	-.38	.005	.004	.003	.005	.005	.003	.003	.005	.007
1.0	-.38	.005	.013	.004	.012	.010	.004	.018	.026	.022
2.9	-.38	.005	.011	.010	.014	.012	.007	.014	.018	.017
5.0	-.38	.003	.070	.095	.153	.110	.054	.029	.021	.033
-5.0	-1.00	.005	.004	.004	.005	.005	.004	.004	.004	.004
-1.0	-1.00	.003	.002	.003	.004	.005	.003	.003	.003	.003
.0	-1.00	.002	.003	.005	.007	.006	.004	.004	.006	.005
1.0	-1.00	.004	.015	.005	.010	.011	.004	.017	.028	.024
2.9	-1.00	.003	.012	.008	.014	.012	.007	.015	.019	.018
5.0	-1.00	.004	.032	.058	.062	.131	.147	.082	.044	.029
-15.0	-10.00	.004	.004	.004	.004	.004	.004	.004	.004	.004
-10.0	-10.00	.005	.005	.005	.005	.005	.005	.005	.005	.005
-5.0	-10.00	.005	.008	.008	.009	.009	.009	.008	.007	.007
-1.0	-10.00	.005	.006	.006	.006	.006	.006	.006	.007	.007
.0	-10.00	.003	.007	.006	.005	.005	.005	.006	.008	.008
1.0	-10.00	.004	.009	.008	.006	.006	.007	.009	.011	.011
2.9	-10.00	.006	.017	.015	.014	.014	.015	.018	.020	.019
5.0	-10.00	.002	.022	.022	.022	.022	.023	.025	.026	.025
10.0	-10.00	.004	.024	.021	.019	.018	.020	.025	.029	.028

Table D.3 - No Flow Microphone Mean Voltages

| x/w_p | y/w_p | Unforced data | Phase averaged data (at angle ϕ) |
			0.0	45.0	90.0	135.0	180.0	225.0	270.0	315.0
1.5	.77	2.326	.945	1.352	2.188	3.299	3.354	3.383	2.524	1.243
1.5	.38	2.327	1.028	1.409	2.193	3.259	3.288	3.333	2.477	1.329
1.5	.00	2.326	1.015	1.442	2.223	3.260	3.295	3.299	2.452	1.320
1.5	-.38	2.327	1.145	1.516	2.246	3.233	3.208	3.211	2.427	1.396
1.5	-.77	2.327	1.206	1.562	2.204	3.165	3.179	3.191	2.427	1.414
1.5	-1.54	2.326	1.274	1.664	2.303	3.178	3.102	3.073	2.349	1.459
1.5	-3.08	2.326	1.312	1.644	2.188	3.050	3.110	3.108	2.452	1.547
1.5	-6.15	2.326	1.488	1.776	2.232	3.019	2.972	2.966	2.401	1.624
1.5	-10.00	2.327	1.489	1.810	2.272	3.018	2.997	2.903	2.357	1.645
1.5	-23.08	2.327	1.667	2.034	2.529	3.063	2.913	2.626	2.044	1.658
-2.9	-.38	2.326	1.417	1.728	2.119	2.982	3.101	3.048	2.493	1.661
-1.0	-.38	2.326	1.371	1.648	2.115	3.063	3.154	3.126	2.462	1.585
.0	-.38	2.326	1.289	1.517	2.092	3.156	3.264	3.227	2.506	1.486
1.0	-.38	2.325	1.257	1.480	2.089	3.210	3.291	3.268	2.498	1.463
2.9	-.38	2.326	1.293	1.487	2.115	3.202	3.240	3.262	2.439	1.462
5.0	-.38	2.326	1.467	1.620	2.104	3.041	3.064	3.113	2.489	1.589
-5.0	-1.00	2.327	1.444	1.738	2.175	2.950	3.098	3.022	2.423	1.684
-1.0	-1.00	2.327	1.385	1.618	2.129	3.061	3.160	3.135	2.426	1.574
.0	-1.00	2.327	1.338	1.553	2.080	3.143	3.218	3.162	2.471	1.527
1.0	-1.00	2.327	1.329	1.502	2.045	3.191	3.243	3.234	2.502	1.489
2.9	-1.00	2.328	1.375	1.488	2.063	3.166	3.233	3.233	2.485	1.511
5.0	-1.00	2.327	1.553	1.621	2.189	3.013	3.028	3.083	2.482	1.587
-15.0	-10.00	2.327	1.584	1.875	2.330	3.012	2.999	2.824	2.306	1.747
-10.0	-10.00	2.328	1.609	1.838	2.268	3.048	2.976	2.827	2.326	1.717
-5.0	-10.00	2.327	1.602	1.786	2.266	3.027	2.985	2.857	2.371	1.689
-1.0	-10.00	2.326	1.577	1.796	2.223	3.060	2.994	2.855	2.407	1.673
.0	-10.00	2.326	1.617	1.741	2.211	3.046	2.988	2.897	2.412	1.665
1.0	-10.00	2.325	1.589	1.769	2.196	3.054	2.993	2.891	2.420	1.679
2.9	-10.00	2.325	1.617	1.759	2.182	3.036	2.986	2.893	2.425	1.684
5.0	-10.00	2.327	1.622	1.760	2.162	3.020	2.976	2.891	2.435	1.692
10.0	-10.00	2.326	1.650	1.789	2.160	2.975	2.934	2.847	2.443	1.735

Table D.4 - No Flow Microphone Rms Voltages

x/w$_p$	y/w$_p$	Unforced data	Phase averaged data (at angle ϕ)							
			0.0	45.0	90.0	135.0	180.0	225.0	270.0	315.0
1.5	.77	.016	.292	.122	.116	.126	.199	.161	.195	.171
1.5	.38	.017	.275	.126	.102	.129	.172	.140	.178	.174
1.5	.00	.018	.254	.112	.111	.128	.155	.132	.170	.140
1.5	-.38	.016	.235	.112	.102	.102	.158	.126	.160	.132
1.5	-.77	.017	.240	.106	.108	.097	.151	.122	.156	.126
1.5	-1.54	.016	.222	.097	.106	.094	.140	.114	.152	.122
1.5	-3.08	.015	.184	.092	.099	.091	.135	.101	.141	.102
1.5	-6.15	.015	.156	.091	.110	.085	.108	.094	.123	.089
1.5	-10.00	.016	.136	.081	.105	.084	.093	.086	.105	.089
1.5	-23.08	.016	.133	.111	.100	.099	.078	.090	.099	.084
-2.9	-.38	.015	.169	.095	.103	.089	.115	.102	.132	.087
-1.0	-.38	.016	.195	.113	.106	.098	.119	.113	.147	.109
.0	-.38	.017	.213	.112	.098	.101	.121	.119	.134	.131
1.0	-.38	.016	.236	.106	.101	.104	.134	.169	.169	.152
2.9	-.38	.016	.228	.100	.097	.107	.135	.164	.168	.137
5.0	-.38	.017	.211	.095	.093	.090	.114	.111	.137	.122
-5.0	-1.00	.015	.165	.106	.107	.090	.117	.099	.136	.095
-1.0	-1.00	.017	.218	.101	.100	.091	.121	.135	.150	.109
.0	-1.00	.017	.235	.106	.101	.097	.133	.153	.154	.128
1.0	-1.00	.017	.216	.109	.093	.098	.134	.165	.166	.134
2.9	-1.00	.016	.232	.097	.091	.098	.127	.137	.167	.133
5.0	-1.00	.016	.194	.089	.099	.110	.126	.126	.136	.126
-15.0	-10.00	.016	.120	.092	.103	.091	.098	.082	.102	.084
-10.0	-10.00	.016	.134	.098	.108	.088	.101	.087	.107	.085
-5.0	-10.00	.016	.135	.090	.092	.086	.096	.080	.108	.084
-1.0	-10.00	.016	.138	.083	.099	.078	.100	.083	.105	.082
.0	-10.00	.016	.135	.083	.093	.085	.093	.082	.101	.083
1.0	-10.00	.017	.134	.073	.094	.075	.091	.080	.098	.084
2.9	-10.00	.016	.131	.073	.089	.074	.093	.076	.102	.075
5.0	-10.00	.017	.137	.081	.089	.073	.097	.076	.101	.078
10.0	-10.00	.016	.138	.089	.095	.076	.097	.083	.096	.082

Table D.5 - Compact Probe $\bar{u}$ (x/θ_0-1.0)

x/θ_0	y/θ_0	Unforced data	0.0	45.0	90.0	135.0	180.0	225.0	270.0	315.0
1.0	.55	.028	.038	.038	.039	.062	.062	.054	.046	.039
1.0	.37	.030	.039	.039	.039	.066	.069	.057	.047	.041
1.0	.18	.048	.055	.054	.059	.081	.090	.078	.066	.060
1.0	-.00	.211	.227	.238	.254	.243	.223	.203	.206	.216
1.0	-.15	.475	.488	.508	.527	.521	.491	.461	.461	.468
1.0	-.28	.569	.576	.595	.611	.610	.590	.560	.553	.559
1.0	-.43	.614	.625	.640	.652	.654	.638	.615	.606	.613
1.0	-.66	.650	.655	.672	.680	.684	.669	.646	.639	.643
1.0	-.82	.669	.673	.686	.697	.702	.690	.669	.660	.663
1.0	-1.02	.685	.693	.706	.717	.716	.700	.688	.678	.679
1.0	-1.27	.706	.709	.724	.732	.737	.725	.709	.699	.701
1.0	-1.59	.724	.727	.739	.749	.752	.744	.728	.721	.720
1.0	-1.98	.746	.752	.763	.768	.771	.764	.749	.742	.743
1.0	-2.46	.772	.773	.782	.789	.792	.788	.773	.764	.769
1.0	-3.06	.796	.794	.802	.809	.817	.813	.799	.790	.790
1.0	-3.81	.830	.827	.837	.844	.846	.843	.833	.824	.825
1.0	-4.74	.865	.865	.869	.879	.883	.880	.872	.862	.860
1.0	-5.89	.909	.906	.912	.917	.922	.920	.915	.909	.905
1.0	-7.05	.948	.945	.951	.957	.960	.959	.953	.947	.944
1.0	-8.20	.980	.978	.980	.985	.986	.990	.985	.979	.977
1.0	-9.36	.996	.995	.998	.999	1.001	1.004	1.002	.999	.995
1.0	-10.51	1.001	1.000	1.002	1.003	1.006	1.008	1.007	1.004	1.001
1.0	-11.66	.999	.999	1.000	1.001	1.004	1.007	1.006	1.004	1.001
1.0	-12.81	1.002	1.000	1.001	1.002	1.004	1.007	1.007	1.004	1.002
1.0	-13.97	1.001	1.000	1.000	1.001	1.003	1.005	1.006	1.004	1.002

Table D.6 - Compact Probe $\tilde{u}$ (x/θ_0=1.0)

x/θ_0	y/θ_0	Unforced data	Phase averaged data (at angle ϕ)							
			0.0	45.0	90.0	135.0	180.0	225.0	270.0	315.0
1.0	.55	.0125	.0161	.0157	.0160	.0246	.0253	.0225	.0197	.0172
1.0	.37	.0125	.0160	.0158	.0167	.0236	.0275	.0235	.0203	.0173
1.0	.18	.0209	.0228	.0239	.0258	.0266	.0285	.0274	.0246	.0250
1.0	-.00	.0737	.0733	.0753	.0777	.0708	.0683	.0693	.0745	.0755
1.0	-.15	.0933	.0900	.0918	.0901	.0891	.0971	.1002	.0946	.0948
1.0	-.28	.0814	.0803	.0802	.0747	.0771	.0816	.0865	.0835	.0832
1.0	-.43	.0754	.0759	.0709	.0734	.0726	.0748	.0757	.0787	.0781
1.0	-.66	.0738	.0726	.0715	.0723	.0717	.0716	.0745	.0788	.0722
1.0	-.82	.0748	.0724	.0733	.0721	.0716	.0724	.0722	.0743	.0748
1.0	-1.02	.0734	.0744	.0731	.0712	.0716	.0710	.0730	.0726	.0720
1.0	-1.27	.0712	.0713	.0700	.0697	.0695	.0712	.0723	.0727	.0727
1.0	-1.59	.0716	.0697	.0706	.0681	.0677	.0685	.0695	.0702	.0713
1.0	-1.98	.0697	.0702	.0689	.0668	.0650	.0669	.0702	.0707	.0692
1.0	-2.46	.0676	.0682	.0671	.0669	.0653	.0663	.0676	.0691	.0683
1.0	-3.06	.0669	.0664	.0648	.0642	.0650	.0651	.0660	.0674	.0653
1.0	-3.81	.0639	.0642	.0649	.0621	.0620	.0616	.0653	.0666	.0651
1.0	-4.74	.0609	.0616	.0606	.0600	.0596	.0611	.0595	.0623	.0601
1.0	-5.89	.0560	.0563	.0545	.0546	.0538	.0547	.0553	.0565	.0542
1.0	-7.05	.0481	.0480	.0480	.0456	.0456	.0480	.0483	.0484	.0496
1.0	-8.20	.0351	.0363	.0350	.0329	.0347	.0338	.0351	.0350	.0361
1.0	-9.36	.0215	.0226	.0211	.0204	.0207	.0209	.0214	.0198	.0223
1.0	-10.51	.0116	.0113	.0116	.0110	.0111	.0118	.0106	.0122	.0125
1.0	-11.66	.0080	.0084	.0079	.0078	.0077	.0077	.0081	.0081	.0082
1.0	-12.81	.0067	.0064	.0063	.0066	.0063	.0064	.0063	.0065	.0069
1.0	-13.97	.0060	.0059	.0061	.0060	.0059	.0059	.0061	.0058	.0060

Table D.7 - Compact Probe $\bar{v}$ (x/θ_0=1.0)

x/θ_0	y/θ_0	Unforced data	Phase averaged data (at angle ϕ)							
			0.0	45.0	90.0	135.0	180.0	225.0	270.0	315.0
1.0	.55	.001	.001	.001	-.000	-.002	-.001	-.000	.001	.001
1.0	.37	.000	.001	.001	-.001	-.004	-.002	-.002	.000	.001
1.0	.18	-.001	.000	.000	.000	-.003	-.006	-.005	-.003	-.000
1.0	-.00	.018	.019	.020	.023	.020	.014	.010	.015	.016
1.0	-.15	.024	.030	.032	.033	.025	.022	.020	.023	.024
1.0	-.28	.016	.021	.024	.025	.018	.014	.012	.013	.014
1.0	-.43	.010	.014	.018	.018	.013	.007	.004	.006	.009
1.0	-.66	.005	.009	.016	.016	.010	.002	-.002	.001	.004
1.0	-.82	.002	.008	.012	.013	.009	.003	-.003	-.001	.002
1.0	-1.02	.002	.007	.012	.013	.008	-.001	-.004	-.003	.002
1.0	-1.27	.001	.006	.011	.011	.009	-.001	-.004	-.003	-.000
1.0	-1.59	-.001	.004	.010	.012	.008	-.002	-.007	-.004	-.002
1.0	-1.98	-.002	.003	.009	.010	.007	-.001	-.006	-.007	-.002
1.0	-2.46	-.001	.003	.007	.012	.008	.001	-.008	-.008	-.002
1.0	-3.06	-.003	.000	.006	.009	.008	.000	-.008	-.008	-.004
1.0	-3.81	-.003	.000	.007	.012	.010	-.001	-.008	-.010	-.005
1.0	-4.74	-.003	.001	.006	.012	.010	.003	-.006	-.009	-.006
1.0	-5.89	-.002	.000	.004	.010	.009	.004	-.004	-.007	-.005
1.0	-7.05	-.001	.001	.005	.011	.010	.004	-.003	-.007	-.006
1.0	-8.20	-.001	.000	.005	.010	.011	.006	-.002	-.005	-.003
1.0	-9.36	-.001	-.000	.005	.009	.009	.006	-.000	-.004	-.004
1.0	-10.51	-.001	-.000	.004	.008	.009	.006	-.000	-.004	-.004
1.0	-11.66	-.001	-.001	.003	.007	.008	.006	.000	-.004	-.004
1.0	-12.81	-.001	-.002	.002	.006	.007	.005	-.000	-.004	-.004
1.0	-13.97	-.000	-.001	.003	.007	.008	.006	.001	-.003	-.003

Table D.8 - Compact Probe $\tilde{v}$ $(x/\theta_0-1.0)$

x/θ_0	y/θ_0	Unforced data	Phase averaged data (at angle ϕ)							
			0.0	45.0	90.0	135.0	180.0	225.0	270.0	315.0
1.0	.55	.0060	.0091	.0096	.0089	.0179	.0209	.0167	.0119	.0092
1.0	.37	.0061	.0090	.0095	.0084	.0162	.0210	.0185	.0126	.0092
1.0	.18	.0126	.0156	.0154	.0156	.0184	.0277	.0242	.0205	.0173
1.0	-.00	.0561	.0581	.0613	.0614	.0583	.0585	.0550	.0571	.0572
1.0	-.15	.0615	.0583	.0600	.0563	.0576	.0611	.0648	.0619	.0621
1.0	-.28	.0457	.0443	.0444	.0430	.0427	.0468	.0480	.0457	.0459
1.0	-.43	.0412	.0409	.0408	.0395	.0402	.0402	.0405	.0429	.0416
1.0	-.66	.0391	.0400	.0390	.0392	.0405	.0401	.0395	.0412	.0411
1.0	-.82	.0402	.0383	.0394	.0385	.0406	.0390	.0406	.0392	.0392
1.0	-1.02	.0395	.0397	.0399	.0387	.0392	.0400	.0391	.0399	.0389
1.0	-1.27	.0396	.0389	.0393	.0384	.0387	.0403	.0387	.0401	.0391
1.0	-1.59	.0401	.0401	.0396	.0383	.0383	.0409	.0397	.0408	.0377
1.0	-1.98	.0393	.0402	.0390	.0386	.0387	.0385	.0386	.0413	.0395
1.0	-2.46	.0398	.0385	.0391	.0396	.0393	.0401	.0400	.0401	.0392
1.0	-3.06	.0393	.0395	.0384	.0388	.0387	.0400	.0402	.0401	.0393
1.0	-3.81	.0381	.0384	.0386	.0381	.0371	.0371	.0384	.0403	.0385
1.0	-4.74	.0373	.0365	.0359	.0364	.0364	.0355	.0367	.0368	.0363
1.0	-5.89	.0335	.0326	.0325	.0330	.0329	.0323	.0326	.0331	.0327
1.0	-7.05	.0286	.0285	.0274	.0274	.0274	.0278	.0287	.0292	.0290
1.0	-8.20	.0221	.0228	.0217	.0210	.0205	.0211	.0226	.0225	.0215
1.0	-9.36	.0157	.0154	.0151	.0160	.0156	.0159	.0156	.0146	.0156
1.0	-10.51	.0100	.0100	.0093	.0098	.0093	.0097	.0104	.0097	.0108
1.0	-11.66	.0063	.0063	.0063	.0063	.0062	.0058	.0063	.0071	.0063
1.0	-12.81	.0050	.0050	.0047	.0048	.0048	.0048	.0052	.0049	.0050
1.0	-13.97	.0041	.0041	.0040	.0040	.0039	.0039	.0040	.0041	.0042

Table D.9 - Compact Probe $\overline{u'v'}$ $(x/\theta_0=1.0)$

x/θ_0	y/θ_0	Unforced data	Phase averaged data (at angle ϕ)							
			0.0	45.0	90.0	135.0	180.0	225.0	270.0	315.0
1.0	.55	.0005	.0006	.0008	.0003	.0011	.0016	.0013	.0009	.0007
1.0	.37	.0003	.0007	.0007	.0003	.0008	.0021	.0012	.0008	.0006
1.0	.18	.0007	.0012	.0013	.0013	.0011	.0026	.0018	.0015	.0014
1.0	-.00	.0186	.0175	.0212	.0211	.0192	.0205	.0181	.0208	.0196
1.0	-.15	.0188	.0141	.0194	.0174	.0172	.0202	.0235	.0196	.0197
1.0	-.28	.0139	.0127	.0134	.0111	.0122	.0167	.0149	.0131	.0167
1.0	-.43	.0142	.0140	.0121	.0118	.0137	.0145	.0127	.0163	.0141
1.0	-.66	.0133	.0130	.0127	.0129	.0134	.0136	.0132	.0151	.0119
1.0	-.82	.0148	.0140	.0136	.0133	.0153	.0143	.0149	.0146	.0140
1.0	-1.02	.0146	.0147	.0145	.0137	.0148	.0154	.0153	.0136	.0129
1.0	-1.27	.0144	.0144	.0139	.0123	.0135	.0158	.0150	.0154	.0135
1.0	-1.59	.0144	.0132	.0130	.0120	.0129	.0147	.0127	.0146	.0136
1.0	-1.98	.0143	.0143	.0132	.0133	.0124	.0139	.0142	.0160	.0138
1.0	-2.46	.0143	.0129	.0124	.0131	.0125	.0134	.0153	.0150	.0146
1.0	-3.06	.0140	.0137	.0130	.0140	.0130	.0146	.0149	.0152	.0136
1.0	-3.81	.0136	.0143	.0143	.0126	.0116	.0121	.0145	.0152	.0137
1.0	-4.74	.0126	.0123	.0108	.0118	.0119	.0122	.0123	.0129	.0128
1.0	-5.89	.0108	.0101	.0094	.0101	.0099	.0099	.0103	.0099	.0100
1.0	-7.05	.0076	.0075	.0074	.0069	.0072	.0073	.0074	.0077	.0082
1.0	-8.20	.0038	.0037	.0035	.0033	.0029	.0034	.0036	.0038	.0034
1.0	-9.36	.0014	.0014	.0013	.0013	.0012	.0015	.0014	.0010	.0016
1.0	-10.51	.0004	.0004	.0003	.0003	.0002	.0005	.0003	.0003	.0004
1.0	-11.66	.0001	.0001	.0001	.0001	.0001	.0001	.0001	.0001	.0000
1.0	-12.81	.0001	.0000	.0001	.0000	.0000	.0001	.0001	.0000	.0001
1.0	-13.97	.0000	.0000	.0000	.0000	.0000	.0000	.0000	.0000	.0000

Table D.10 - Compact Probe $\bar{u}$ (x/θ_0=3.0)

x/θ_0	y/θ_0	Unforced data	Phase averaged data (at angle ϕ)							
			0.0	45.0	90.0	135.0	180.0	225.0	270.0	315.0
3.0	.55	.093	.090	.103	.120	.127	.118	.100	.085	.085
3.0	.37	.120	.125	.151	.159	.158	.144	.124	.112	.117
3.0	.18	.199	.213	.233	.257	.252	.213	.185	.180	.190
3.0	-.00	.307	.327	.363	.390	.386	.324	.280	.288	.296
3.0	-.15	.418	.442	.468	.505	.506	.441	.391	.382	.402
3.0	-.28	.497	.517	.552	.578	.578	.525	.462	.467	.483
3.0	-.43	.579	.594	.612	.644	.649	.597	.556	.548	.566
3.0	-.66	.638	.642	.660	.682	.687	.660	.627	.614	.623
3.0	-.82	.659	.664	.675	.697	.699	.687	.661	.648	.647
3.0	-1.02	.680	.677	.693	.712	.720	.705	.683	.669	.668
3.0	-1.27	.699	.703	.709	.729	.735	.726	.702	.692	.693
3.0	-1.59	.719	.720	.729	.743	.751	.742	.727	.712	.714
3.0	-1.98	.742	.739	.748	.759	.767	.764	.750	.734	.733
3.0	-2.46	.767	.762	.769	.780	.789	.784	.773	.761	.762
3.0	-3.06	.794	.790	.797	.808	.814	.814	.804	.791	.788
3.0	-3.81	.826	.825	.830	.839	.843	.847	.836	.824	.821
3.0	-4.74	.864	.862	.866	.873	.879	.883	.874	.863	.857
3.0	-5.89	.906	.904	.909	.913	.919	.925	.919	.909	.904
3.0	-7.05	.946	.942	.948	.950	.956	.962	.957	.948	.942
3.0	-8.20	.975	.974	.975	.979	.982	.989	.986	.979	.976
3.0	-9.36	.995	.992	.993	.997	.999	1.004	1.003	.998	.993
3.0	-10.51	1.001	.999	1.000	1.001	1.004	1.008	1.009	1.005	1.001
3.0	-11.66	1.001	1.000	1.001	1.001	1.004	1.008	1.009	1.007	1.003
3.0	-12.81	1.002	1.001	1.000	1.001	1.004	1.007	1.009	1.007	1.003
3.0	-13.97	1.002	1.002	1.001	1.002	1.004	1.007	1.009	1.008	1.004

Table D.11 - Compact Probe $\bar{u}$ $(x/\theta_0 = 3.0)$

x/θ_0	y/θ_0	Unforced data	Phase averaged data (at angle ϕ)
			0.0	45.0	90.0	135.0	180.0	225.0	270.0	315.0
3.0	.55	.0440	.0428	.0512	.0546	.0574	.0532	.0488	.0442	.0396
3.0	.37	.0630	.0659	.0773	.0748	.0749	.0737	.0662	.0620	.0651
3.0	.18	.0899	.0975	.0987	.0974	.0981	.0998	.0917	.0905	.0910
3.0	-.00	.1068	.1128	.1150	.1057	.1108	.1162	.1129	.1079	.1114
3.0	-.15	.1150	.1157	.1146	.1055	.1114	.1270	.1221	.1173	.1174
3.0	-.28	.1107	.1076	.1051	.0960	.1029	.1178	.1251	.1181	.1119
3.0	-.43	.0971	.0901	.0846	.0827	.0838	.1027	.1121	.1094	.0984
3.0	-.66	.0804	.0770	.0764	.0734	.0740	.0804	.0897	.0850	.0817
3.0	-.82	.0763	.0742	.0730	.0705	.0709	.0738	.0771	.0770	.0800
3.0	-1.02	.0734	.0719	.0734	.0703	.0689	.0725	.0746	.0748	.0731
3.0	-1.27	.0724	.0696	.0712	.0694	.0698	.0684	.0720	.0725	.0718
3.0	-1.59	.0713	.0697	.0696	.0706	.0686	.0682	.0704	.0717	.0710
3.0	-1.98	.0692	.0704	.0672	.0673	.0654	.0671	.0676	.0712	.0680
3.0	-2.46	.0674	.0679	.0676	.0650	.0657	.0657	.0663	.0663	.0671
3.0	-3.06	.0656	.0642	.0668	.0641	.0629	.0657	.0654	.0659	.0660
3.0	-3.81	.0637	.0629	.0646	.0626	.0608	.0604	.0646	.0638	.0644
3.0	-4.74	.0603	.0602	.0604	.0596	.0612	.0593	.0576	.0606	.0619
3.0	-5.89	.0552	.0552	.0545	.0553	.0553	.0524	.0549	.0552	.0546
3.0	-7.05	.0467	.0466	.0463	.0460	.0451	.0437	.0451	.0476	.0479
3.0	-8.20	.0354	.0342	.0348	.0333	.0344	.0319	.0339	.0354	.0351
3.0	-9.36	.0209	.0217	.0227	.0177	.0189	.0188	.0196	.0208	.0224
3.0	-10.51	.0107	.0119	.0102	.0097	.0103	.0106	.0103	.0109	.0104
3.0	-11.66	.0071	.0072	.0071	.0072	.0075	.0076	.0071	.0075	.0081
3.0	-12.81	.0058	.0060	.0058	.0058	.0059	.0056	.0057	.0063	.0060
3.0	-13.97	.0052	.0053	.0053	.0051	.0052	.0052	.0054	.0054	.0054

Table D.12 - Compact Probe $\bar{v}$ (x/θ_0=3.0)

x/θ_0	y/θ_0	Unforced data	Phase averaged data (at angle ϕ)							
			0.0	45.0	90.0	135.0	180.0	225.0	270.0	315.0
3.0	.55	-.002	-.002	-.003	-.002	-.003	-.005	-.001	.001	-.001
3.0	.37	-.003	-.003	.003	.006	.000	-.001	-.001	-.004	-.001
3.0	.18	.004	.010	.011	.023	.017	.006	.001	.001	.005
3.0	-.00	.017	.025	.038	.043	.043	.017	.007	.016	.019
3.0	-.15	.027	.039	.044	.058	.051	.030	.019	.017	.023
3.0	-.28	.027	.036	.047	.057	.047	.032	.018	.023	.027
3.0	-.43	.018	.029	.041	.048	.041	.023	.010	.012	.020
3.0	-.66	.010	.018	.033	.042	.034	.012	-.001	.000	.010
3.0	-.82	.007	.015	.031	.039	.030	.007	-.003	-.004	.005
3.0	-1.02	.005	.013	.027	.037	.030	.008	-.007	-.006	.004
3.0	-1.27	.004	.013	.022	.032	.026	.006	-.011	-.007	.002
3.0	-1.59	.001	.010	.022	.029	.025	.002	-.009	-.010	.000
3.0	-1.98	.000	.008	.018	.026	.021	.000	-.012	-.012	-.003
3.0	-2.46	-.001	.006	.015	.022	.019	.000	-.012	-.011	-.003
3.0	-3.06	-.003	.003	.011	.019	.016	.001	-.012	-.012	-.007
3.0	-3.81	-.004	.001	.008	.016	.014	.001	-.012	-.013	-.007
3.0	-4.74	-.004	-.000	.006	.015	.012	.002	-.011	-.012	-.007
3.0	-5.89	-.004	-.001	.007	.012	.012	.004	-.007	-.010	-.007
3.0	-7.05	-.003	-.002	.004	.009	.011	.006	-.005	-.010	-.008
3.0	-8.20	-.004	-.002	.003	.008	.010	.005	-.004	-.009	-.008
3.0	-9.36	-.004	-.004	.002	.008	.009	.005	-.003	-.008	-.008
3.0	-10.51	-.004	-.004	.002	.006	.008	.005	-.003	-.008	-.007
3.0	-11.66	-.004	-.004	.000	.005	.007	.004	-.003	-.008	-.008
3.0	-12.81	-.004	-.005	-.000	.004	.006	.004	-.002	-.007	-.007
3.0	-13.97	-.003	-.004	.000	.004	.006	.005	-.001	-.006	-.006

Table D.13 - Compact Probe $\tilde{v}$ $(x/\theta_0\text{-}3.0)$

x/θ_0	y/θ_0	Unforced data	Phase averaged data (at angle ϕ)
			0.0	45.0	90.0	135.0	180.0	225.0	270.0	315.0
3.0	.55	.0390	.0388	.0461	.0504	.0560	.0524	.0430	.0359	.0354
3.0	.37	.0526	.0577	.0647	.0670	.0651	.0674	.0560	.0485	.0521
3.0	.18	.0747	.0807	.0868	.0854	.0833	.0806	.0736	.0702	.0749
3.0	-.00	.0864	.0942	.0973	.0948	.0951	.0907	.0869	.0845	.0882
3.0	-.15	.0875	.0888	.0878	.0862	.0821	.0885	.0902	.0855	.0862
3.0	-.28	.0770	.0749	.0741	.0697	.0727	.0777	.0809	.0757	.0763
3.0	-.43	.0614	.0578	.0539	.0546	.0503	.0644	.0685	.0632	.0590
3.0	-.66	.0468	.0453	.0439	.0427	.0442	.0487	.0528	.0490	.0462
3.0	-.82	.0424	.0430	.0419	.0409	.0397	.0456	.0457	.0452	.0434
3.0	-1.02	.0411	.0402	.0393	.0383	.0387	.0416	.0425	.0423	.0421
3.0	-1.27	.0400	.0395	.0390	.0380	.0385	.0407	.0408	.0409	.0409
3.0	-1.59	.0402	.0396	.0388	.0391	.0397	.0406	.0407	.0403	.0399
3.0	-1.98	.0404	.0402	.0393	.0382	.0386	.0397	.0408	.0407	.0396
3.0	-2.46	.0405	.0388	.0393	.0389	.0398	.0404	.0410	.0392	.0389
3.0	-3.06	.0391	.0387	.0386	.0385	.0393	.0387	.0392	.0397	.0392
3.0	-3.81	.0386	.0377	.0386	.0381	.0369	.0383	.0392	.0379	.0380
3.0	-4.74	.0368	.0364	.0362	.0362	.0367	.0367	.0368	.0364	.0372
3.0	-5.89	.0332	.0326	.0325	.0324	.0317	.0316	.0315	.0324	.0343
3.0	-7.05	.0279	.0284	.0272	.0274	.0264	.0272	.0283	.0284	.0284
3.0	-8.20	.0219	.0221	.0222	.0212	.0212	.0214	.0210	.0228	.0223
3.0	-9.36	.0155	.0153	.0157	.0134	.0148	.0145	.0149	.0145	.0157
3.0	-10.51	.0098	.0103	.0096	.0087	.0093	.0085	.0095	.0096	.0094
3.0	-11.66	.0062	.0060	.0062	.0064	.0061	.0062	.0064	.0062	.0062
3.0	-12.81	.0048	.0048	.0048	.0047	.0048	.0048	.0050	.0057	.0048
3.0	-13.97	.0039	.0038	.0038	.0037	.0037	.0038	.0037	.0040	.0038

Table D.14 - Compact Probe $\overline{u'v'}$ (x/θ_0=3.0)

x/θ_0	y/θ_0	Unforced data	Phase averaged data (at angle ϕ)							
			0.0	45.0	90.0	135.0	180.0	225.0	270.0	315.0
3.0	.55	.0080	.0080	.0111	.0156	.0189	.0156	.0094	.0081	.0056
3.0	.37	.0180	.0194	.0306	.0318	.0299	.0292	.0185	.0128	.0179
3.0	.18	.0390	.0498	.0538	.0539	.0510	.0485	.0351	.0357	.0395
3.0	-.00	.0547	.0659	.0753	.0597	.0606	.0611	.0576	.0518	.0583
3.0	-.15	.0542	.0543	.0565	.0490	.0450	.0611	.0582	.0562	.0543
3.0	-.28	.0395	.0344	.0418	.0311	.0343	.0397	.0515	.0391	.0406
3.0	-.43	.0250	.0216	.0196	.0200	.0141	.0238	.0290	.0258	.0244
3.0	-.66	.0152	.0144	.0130	.0096	.0137	.0167	.0202	.0190	.0154
3.0	-.82	.0146	.0129	.0122	.0118	.0117	.0154	.0145	.0162	.0165
3.0	-1.02	.0144	.0118	.0115	.0119	.0095	.0133	.0165	.0155	.0139
3.0	-1.27	.0141	.0128	.0117	.0118	.0129	.0138	.0137	.0152	.0141
3.0	-1.59	.0143	.0139	.0135	.0118	.0129	.0134	.0147	.0157	.0128
3.0	-1.98	.0139	.0140	.0131	.0115	.0108	.0134	.0136	.0146	.0127
3.0	-2.46	.0144	.0136	.0132	.0116	.0132	.0135	.0145	.0136	.0136
3.0	-3.06	.0136	.0123	.0132	.0114	.0121	.0127	.0149	.0143	.0140
3.0	-3.81	.0132	.0118	.0137	.0134	.0118	.0121	.0154	.0125	.0133
3.0	-4.74	.0122	.0121	.0109	.0120	.0131	.0123	.0122	.0126	.0129
3.0	-5.89	.0101	.0097	.0096	.0087	.0092	.0084	.0096	.0104	.0107
3.0	-7.05	.0068	.0065	.0062	.0063	.0068	.0061	.0062	.0075	.0070
3.0	-8.20	.0038	.0037	.0040	.0033	.0037	.0031	.0036	.0044	.0036
3.0	-9.36	.0014	.0014	.0018	.0009	.0012	.0011	.0012	.0011	.0015
3.0	-10.51	.0003	.0005	.0003	.0002	.0002	.0001	.0002	.0003	.0002
3.0	-11.66	.0001	.0001	.0000	.0001	.0001	.0001	.0000	.0000	.0000
3.0	-12.81	.0000	.0000	.0000	.0000	.0000	.0000	.0000	.0001	.0000
3.0	-13.97	.0000	.0000	.0000	.0000	.0000	.0000	.0000	.0000	.0000

Table D.15 - Mean velocity straight wire results

		Unforced	Phase averaged data (at angle ϕ)							
x/θ_0	y/θ_0	data	0.0	45.0	90.0	135.0	180.0	225.0	270.0	315.0
-30.0	-.03	.175	.151	.144	.149	.148	.169	.168	.168	.168
-30.0	-.09	.377	.379	.372	.374	.377	.398	.399	.389	.394
-30.0	-.15	.470	.473	.468	.472	.476	.482	.484	.485	.479
-30.0	-.21	.515	.515	.514	.516	.522	.523	.522	.522	.517
-30.0	-.28	.552	.552	.551	.554	.554	.557	.557	.557	.555
-30.0	-.34	.574	.577	.578	.579	.581	.579	.583	.581	.577
-30.0	-.43	.595	.596	.595	.600	.601	.603	.600	.601	.599
-30.0	-.53	.617	.617	.621	.618	.621	.624	.623	.622	.619
-30.0	-.66	.644	.644	.644	.645	.646	.646	.646	.646	.646
-30.0	-.82	.661	.663	.668	.665	.667	.668	.669	.667	.666
-30.0	-1.02	.689	.688	.688	.687	.690	.692	.690	.688	.689
-30.0	-1.28	.707	.707	.705	.708	.712	.710	.712	.710	.708
-30.0	-1.59	.728	.724	.728	.730	.728	.733	.730	.731	.729
-30.0	-1.98	.751	.748	.751	.754	.753	.756	.753	.753	.752
-30.0	-2.46	.779	.778	.778	.782	.784	.783	.780	.780	.780
-30.0	-3.06	.805	.804	.807	.809	.811	.815	.810	.811	.809
-30.0	-3.81	.839	.845	.843	.843	.847	.849	.846	.845	.845
-30.0	-4.74	.879	.881	.881	.882	.883	.887	.885	.883	.883
-30.0	-5.89	.925	.926	.927	.928	.928	.929	.927	.928	.928
-30.0	-7.05	.961	.961	.962	.964	.964	.965	.964	.962	.963
-30.0	-8.20	.984	.985	.987	.986	.986	.988	.986	.986	.985
-30.0	-9.36	.990	.991	.992	.993	.993	.993	.991	.992	.991
-30.0	-10.51	.989	.991	.991	.992	.993	.992	.991	.991	.990
-30.0	-11.66	.990	.992	.993	.993	.994	.994	.993	.992	.992
-30.0	-12.82	.991	.991	.992	.993	.993	.993	.992	.992	.991
-30.0	-13.97	.988	.989	.990	.990	.991	.991	.990	.989	.989
-30.0	-15.12	.990	.989	.990	.991	.991	.991	.990	.989	.989
-20.0	-.03	.200	.185	.175	.190	.182	.199	.184	.211	.194
-20.0	-.09	.324	.327	.316	.330	.329	.350	.333	.342	.341
-20.0	-.15	.465	.464	.462	.462	.470	.476	.472	.472	.472
-20.0	-.21	.519	.517	.515	.521	.522	.523	.522	.521	.518
-20.0	-.28	.542	.544	.546	.545	.547	.550	.550	.547	.548
-20.0	-.34	.562	.561	.563	.564	.567	.567	.561	.558	.559
-20.0	-.43	.582	.583	.587	.587	.586	.588	.582	.584	.582
-20.0	-.53	.604	.604	.606	.607	.613	.612	.609	.610	.606
-20.0	-.66	.629	.628	.630	.633	.638	.636	.633	.632	.631
-20.0	-.82	.655	.651	.657	.656	.657	.659	.654	.652	.651
-20.0	-1.02	.678	.679	.681	.681	.680	.682	.679	.679	.677
-20.0	-1.28	.699-	.697	.700	.701	.705	.704	.701	.701	.703
-20.0	-1.59	.719	.721	.725	.723	.723	.723	.725	.723	.722
-20.0	-1.98	.743	.743	.742	.751	.749	.748	.747	.746	.742
-20.0	-2.46	.773	.774	.773	.776	.777	.776	.772	.771	.770
-20.0	-3.06	.800	.802	.803	.805	.807	.806	.802	.802	.799
-20.0	-3.81	.834	.837	.835	.838	.840	.837	.837	.838	.837
-20.0	-4.74	.875	.873	.878	.879	.880	.879	.879	.875	.874

Table D.15 (cont'd).

-20.0	-5.89	.920	.920	.921	.923	.926	.924	.922	.920	.920
-20.0	-7.05	.957	.959	.959	.960	.964	.962	.960	.959	.959
-20.0	-8.20	.986	.986	.988	.988	.990	.989	.988	.987	.985
-20.0	-9.36	.997	.996	.998	.999	1.000	.999	.998	.996	.996
-20.0	-10.51	.998	.998	1.000	1.001	1.001	1.001	.999	.998	.997
-20.0	-11.66	.995	.996	.997	.998	.999	.999	.997	.996	.996
-20.0	-12.82	.995	.995	.996	.998	.998	.998	.997	.996	.995
-20.0	-13.97	.995	.995	.996	.997	.998	.998	.997	.996	.995
-20.0	-15.12	.991	.996	.996	.997	.998	.998	.997	.996	.995
-10.0	-.03	.172	.167	.141	.172	.172	.171	.185	.173	.167
-10.0	-.09	.364	.369	.357	.375	.382	.382	.385	.375	.366
-10.0	-.15	.467	.473	.468	.477	.477	.479	.478	.473	.468
-10.0	-.21	.515	.518	.519	.526	.525	.526	.522	.517	.512
-10.0	-.28	.547	.547	.551	.559	.556	.556	.546	.546	.544
-10.0	-.34	.565	.562	.563	.573	.573	.573	.567	.565	.562
-10.0	-.43	.587	.586	.589	.591	.597	.592	.591	.585	.587
-10.0	-.53	.609	.611	.614	.615	.617	.616	.613	.609	.608
-10.0	-.66	.632	.632	.635	.641	.639	.640	.638	.634	.630
-10.0	-.82	.654	.653	.658	.663	.666	.663	.659	.656	.653
-10.0	-1.02	.677	.677	.678	.683	.684	.685	.679	.678	.672
-10.0	-1.28	.697	.697	.699	.700	.708	.702	.700	.696	.694
-10.0	-1.59	.719	.717	.720	.727	.729	.725	.722	.719	.717
-10.0	-1.98	.742	.744	.746	.750	.751	.751	.744	.743	.740
-10.0	-2.46	.766	.767	.771	.773	.779	.776	.770	.767	.764
-10.0	-3.06	.797	.798	.800	.802	.805	.804	.798	.796	.793
-10.0	-3.81	.832	.831	.834	.839	.839	.836	.833	.827	.828
-10.0	-4.74	.870	.870	.872	.878	.877	.878	.872	.871	.870
-10.0	-5.89	.913	.916	.916	.922	.924	.920	.919	.914	.913
-10.0	-7.05	.953	.955	.954	.957	.961	.960	.956	.954	.955
-10.0	-8.20	.982	.986	.986	.989	.990	.990	.987	.984	.984
-10.0	-9.36	1.000	1.000	1.002	1.004	1.006	1.005	1.003	1.001	.999
-10.0	-10.51	1.003	1.004	1.005	1.007	1.009	1.008	1.006	1.005	1.003
-10.0	-11.66	1.003	1.002	1.004	1.005	1.006	1.006	1.004	1.002	1.002
-10.0	-12.82	.999	1.000	1.001	1.003	1.004	1.004	1.002	1.001	1.000
-10.0	-13.97	.998	.999	.999	1.001	1.002	1.001	1.001	.999	.998
-10.0	-15.12	.997	.998	.999	1.000	1.001	1.001	1.000	.999	.998
-5.0	-.03	.167	.140	.141	.160	.167	.158	.160	.153	.168
-5.0	-.09	.313	.313	.315	.329	.338	.342	.323	.307	.325
-5.0	-.15	.426	.427	.434	.442	.440	.445	.436	.425	.428
-5.0	-.21	.496	.501	.504	.510	.517	.514	.503	.498	.498
-5.0	-.28	.534	.535	.543	.545	.550	.544	.535	.532	.528
-5.0	-.34	.560	.562	.565	.574	.575	.572	.562	.558	.558
-5.0	-.43	.585	.583	.588	.595	.595	.595	.587	.582	.582
-5.0	-.53	.606	.605	.611	.614	.622	.613	.609	.604	.602
-5.0	-.66	.627	.628	.633	.639	.644	.642	.632	.627	.625
-5.0	-.82	.650	.655	.657	.661	.664	.659	.653	.649	.644
-5.0	-1.02	.673	.677	.679	.681	.687	.685	.678	.677	.672
-5.0	-1.28	.694	.693	.699	.706	.706	.704	.698	.691	.692

Table D.15 (cont'd).

-5.0	-1.59	.719	.718	.722	.729	.730	.727	.721	.715	.715
-5.0	-1.98	.741	.739	.746	.750	.757	.751	.746	.744	.741
-5.0	-2.46	.769	.773	.773	.778	.783	.779	.772	.769	.766
-5.0	-3.06	.798	.802	.804	.809	.809	.807	.802	.797	.797
-5.0	-3.81	.832	.830	.837	.838	.842	.842	.834	.833	.830
-5.0	-4.74	.870	.871	.875	.880	.882	.879	.875	.869	.866
-5.0	-5.89	.914	.915	.920	.926	.925	.923	.919	.915	.911
-5.0	-7.05	.953	.955	.957	.961	.962	.963	.959	.953	.952
-5.0	-8.20	.985	.985	.986	.989	.993	.991	.989	.984	.983
-5.0	-9.36	.998	.999	1.000	1.003	1.004	1.005	1.003	.999	.998
-5.0	-10.51	1.002	1.002	1.004	1.006	1.007	1.008	1.006	1.003	1.002
-5.0	-11.66	1.002	1.002	1.003	1.005	1.007	1.007	1.005	1.003	1.002
-5.0	-12.82	.999	1.001	1.002	1.004	1.005	1.005	1.004	1.002	1.001
-5.0	-13.97	.999	.999	1.000	1.002	1.003	1.003	1.003	1.001	.999
-5.0	-15.12	.999	1.001	1.002	1.003	1.004	1.004	1.004	1.003	1.001
-1.0	-.03	.165	.156	.144	.182	.191	.179	.161	.167	.169
-1.0	-.09	.306	.314	.314	.339	.353	.342	.321	.305	.314
-1.0	-.15	.453	.460	.467	.482	.491	.475	.461	.447	.451
-1.0	-.21	.518	.523	.529	.547	.548	.537	.518	.510	.515
-1.0	-.28	.553	.560	.566	.579	.580	.568	.554	.550	.548
-1.0	-.34	.575	.578	.585	.595	.597	.588	.572	.566	.570
-1.0	-.43	.594	.600	.606	.619	.620	.609	.595	.585	.594
-1.0	-.53	.615	.619	.630	.643	.641	.630	.617	.608	.612
-1.0	-.66	.637	.643	.653	.662	.663	.655	.639	.633	.632
-1.0	-.82	.661	.665	.673	.683	.685	.676	.663	.657	.658
-1.0	-1.02	.680	.683	.689	.698	.704	.693	.682	.675	.676
-1.0	-1.28	.700	.704	.710	.718	.719	.710	.702	.695	.697
-1.0	-1.59	.720	.722	.732	.739	.743	.732	.724	.717	.716
-1.0	-1.98	.743	.741	.751	.759	.764	.755	.747	.743	.740
-1.0	-2.46	.768	.771	.779	.785	.788	.779	.771	.766	.765
-1.0	-3.06	.798	.800	.808	.814	.815	.812	.803	.797	.793
-1.0	-3.81	.830	.830	.835	.844	.848	.844	.833	.828	.828
-1.0	-4.74	.870	.872	.871	.881	.883	.881	.873	.866	.865
-1.0	-5.89	.912	.912	.917	.921	.925	.922	.916	.911	.908
-1.0	-7.05	.950	.951	.953	.958	.962	.962	.956	.952	.949
-1.0	-8.20	.981	.982	.985	.988	.991	.991	.987	.983	.980
-1.0	-9.36	.997	.996	.998	1.000	1.003	1.004	1.002	.998	.996
-1.0	-10.51	1.001	1.000	1.002	1.003	1.006	1.006	1.006	1.003	1.000
-1.0	-11.66	1.000	1.000	1.001	1.003	1.005	1.006	1.005	1.003	1.001
-1.0	-12.82	.998	.999	.999	1.001	1.003	1.004	1.004	1.002	1.000
-1.0	-13.97	.999	.998	.998	1.000	1.001	1.003	1.003	1.001	.999
-1.0	-15.12	.999	.997	.997	.998	.999	1.001	1.002	1.000	.998
.0	-.03	.206	.185	.172	.191	.228	.215	.173	.180	.202
.0	-.09	.364	.374	.378	.399	.414	.398	.368	.363	.375
.0	-.15	.494	.508	.524	.535	.538	.521	.495	.486	.495
.0	-.21	.540	.548	.563	.570	.580	.561	.538	.532	.540
.0	-.28	.567	.575	.586	.600	.601	.585	.560	.558	.563
.0	-.34	.591	.595	.608	.619	.621	.603	.584	.582	.583

Table D.15 (cont'd).

.0	-.43	.609	.615	.628	.642	.642	.624	.607	.602	.602
.0	-.53	.628	.637	.650	.656	.659	.642	.628	.626	.625
.0	-.66	.651	.659	.672	.678	.680	.670	.652	.647	.650
.0	-.82	.673	.675	.690	.694	.700	.687	.671	.665	.668
.0	-1.02	.693	.695	.708	.714	.715	.705	.691	.685	.687
.0	-1.28	.711	.712	.725	.732	.734	.726	.709	.707	.707
.0	-1.59	.734	.735	.744	.751	.758	.746	.736	.731	.730
.0	-1.98	.755	.757	.765	.771	.778	.769	.754	.751	.753
.0	-2.46	.779	.782	.791	.796	.799	.795	.783	.777	.775
.0	-3.06	.806	.810	.815	.823	.830	.823	.812	.801	.800
.0	-3.81	.841	.842	.845	.855	.855	.855	.847	.841	.837
.0	-4.74	.876	.879	.883	.891	.895	.893	.885	.875	.875
.0	-5.89	.923	.922	.926	.931	.935	.936	.928	.923	.919
.0	-7.05	.960	.961	.964	.971	.973	.973	.969	.960	.962
.0	-8.20	.992	.990	.992	.995	1.000	1.001	.998	.994	.989
.0	-9.36	1.006	1.005	1.007	1.009	1.012	1.013	1.011	1.008	1.005
.0	-10.51	1.010	1.008	1.009	1.010	1.014	1.016	1.015	1.012	1.009
.0	-11.66	1.008	1.007	1.008	1.009	1.012	1.014	1.013	1.011	1.008
.0	-12.82	1.005	1.006	1.007	1.008	1.010	1.012	1.012	1.010	1.007
.0	-13.97	1.005	1.006	1.006	1.006	1.008	1.010	1.011	1.010	1.007
.0	-15.12	1.005	1.004	1.004	1.004	1.006	1.008	1.009	1.008	1.005
1.0	.58	.051	.053	.063	.058	.072	.084	.077	.064	.056
1.0	.40	.059	.059	.068	.059	.069	.080	.077	.066	.059
1.0	.21	.056	.063	.071	.061	.066	.080	.077	.070	.063
1.0	.03	.067	.076	.081	.079	.086	.100	.097	.085	.079
1.0	-.12	.132	.145	.151	.164	.185	.179	.168	.151	.145
1.0	-.25	.300	.316	.337	.366	.391	.366	.333	.312	.303
1.0	-.40	.518	.522	.547	.566	.580	.560	.533	.506	.514
1.0	-.63	.620	.626	.638	.652	.657	.645	.625	.610	.610
1.0	-.79	.652	.653	.668	.679	.684	.673	.657	.647	.645
1.0	-.99	.680	.681	.690	.705	.708	.698	.683	.671	.669
1.0	-1.24	.703	.707	.717	.729	.732	.721	.708	.698	.701
1.0	-1.56	.728	.731	.739	.749	.754	.746	.734	.725	.724
1.0	-1.95	.753	.753	.764	.774	.774	.769	.759	.748	.747
1.0	-2.43	.781	.782	.789	.796	.800	.793	.781	.772	.775
1.0	-3.03	.808	.810	.814	.824	.827	.823	.812	.805	.802
1.0	-3.78	.835	.834	.840	.848	.850	.846	.838	.834	.831
1.0	-4.71	.864	.860	.866	.873	.877	.875	.867	.859	.860
1.0	-5.86	.877	.878	.884	.890	.890	.889	.884	.879	.878
1.0	-7.02	.906	.905	.909	.914	.919	.919	.912	.906	.906
1.0	-8.17	.926	.929	.932	.938	.941	.941	.937	.930	.928
1.0	-9.32	.955	.955	.957	.960	.964	.966	.963	.956	.956
1.0	-10.48	.996	.997	.997	1.000	1.003	1.006	1.004	.999	.996
1.0	-11.63	1.004	1.003	1.004	1.007	1.009	1.010	1.010	1.007	1.005
1.0	-12.78	1.006	1.006	1.006	1.008	1.010	1.012	1.012	1.010	1.007
1.0	-13.94	1.006	1.005	1.005	1.006	1.008	1.010	1.011	1.009	1.007
1.0	-15.09	1.003	1.005	1.004	1.005	1.006	1.008	1.009	1.008	1.006
3.0	.58	.100	.107	.100	.118	.138	.137	.110	.086	.090

Table D.15 (cont'd).

3.0	.40	.107	.111	.113	.126	.141	.141	.119	.099	.100
3.0	.21	.152	.157	.169	.186	.192	.177	.163	.146	.145
3.0	.03	.228	.241	.262	.285	.281	.255	.233	.214	.218
3.0	-.12	.298	.316	.335	.362	.367	.326	.298	.283	.291
3.0	-.25	.369	.387	.409	.435	.444	.400	.366	.349	.358
3.0	-.40	.464	.483	.511	.535	.534	.493	.460	.447	.454
3.0	-.63	.591	.607	.620	.646	.653	.615	.581	.566	.579
3.0	-.79	.642	.657	.665	.687	.693	.666	.637	.628	.632
3.0	-.99	.675	.683	.687	.714	.719	.700	.678	.661	.662
3.0	-1.24	.702	.703	.714	.732	.737	.723	.704	.692	.689
3.0	-1.56	.726	.729	.736	.751	.759	.744	.733	.720	.717
3.0	-1.95	.752	.749	.757	.771	.781	.769	.758	.745	.743
3.0	-2.43	.774	.777	.783	.798	.802	.795	.784	.771	.767
3.0	-3.03	.803	.805	.812	.817	.824	.818	.811	.800	.801
3.0	-3.78	.830	.830	.838	.844	.849	.847	.840	.828	.827
3.0	-4.71	.846	.847	.850	.858	.862	.858	.855	.846	.841
3.0	-5.86	.904	.904	.906	.914	.917	.920	.916	.908	.902
3.0	-7.02	.934	.933	.938	.939	.947	.946	.942	.938	.933
3.0	-8.17	.987	.987	.989	.991	.994	.998	.996	.991	.988
3.0	-9.32	1.001	.999	1.000	1.003	1.007	1.008	1.008	1.005	1.000
3.0	-10.48	1.009	1.010	1.009	1.011	1.014	1.017	1.017	1.015	1.012
3.0	-11.63	1.010	1.010	1.009	1.010	1.012	1.015	1.017	1.015	1.012
3.0	-12.78	1.008	1.008	1.007	1.008	1.010	1.013	1.015	1.013	1.010
3.0	-13.94	1.007	1.007	1.006	1.006	1.007	1.010	1.012	1.011	1.009
3.0	-15.09	1.004	1.004	1.003	1.003	1.004	1.007	1.009	1.008	1.006
5.0	2.00	.085	.053	.108	.130	.138	.112	.069	.039	.030
5.0	1.01	.093	.059	.107	.137	.144	.118	.089	.066	.055
5.0	.03	.329	.365	.381	.407	.405	.349	.329	.319	.333
5.0	-.96	.688	.679	.689	.703	.715	.707	.687	.671	.670
5.0	-1.94	.777	.768	.778	.784	.795	.799	.791	.780	.772
5.0	-2.93	.821	.816	.823	.828	.834	.841	.835	.824	.818
5.0	-3.92	.874	.867	.872	.878	.884	.891	.885	.877	.871
5.0	-4.90	.909	.904	.907	.915	.920	.925	.921	.912	.906
5.0	-5.89	.950	.946	.949	.952	.956	.960	.960	.956	.950
5.0	-6.88	.976	.973	.974	.978	.983	.988	.989	.982	.976
5.0	-7.86	1.000	.996	.996	.998	1.001	1.007	1.008	1.005	.998
5.0	-8.85	1.007	1.004	1.002	1.004	1.007	1.012	1.014	1.011	1.008
5.0	-9.84	1.008	1.006	1.005	1.006	1.007	1.013	1.015	1.013	1.009
5.0	-10.82	1.007	1.005	1.004	1.004	1.006	1.011	1.014	1.012	1.009
5.0	-11.81	1.006	1.005	1.003	1.003	1.005	1.009	1.012	1.011	1.008
5.0	-12.79	1.004	1.004	1.001	1.001	1.003	1.007	1.010	1.009	1.007
5.0	-13.78	1.003	1.003	1.001	1.000	1.002	1.005	1.009	1.008	1.006
5.0	-14.76	1.001	1.001	.999	.999	1.000	1.003	1.006	1.006	1.004
5.0	-15.75	1.000	1.001	.999	.998	.999	1.002	1.005	1.006	1.004
5.0	-16.74	1.000	1.001	.999	.998	.999	1.001	1.004	1.005	1.004
5.0	-17.72	1.000	1.001	.999	.998	.998	1.001	1.004	1.005	1.004
10.0	4.00	.040	.032	.032	.043	.044	.056	.063	.048	.037
10.0	2.87	.041	.033	.034	.048	.048	.062	.067	.047	.037

Table D.15 (cont'd).

10.0	1.75	.065	.062	.073	.085	.095	.096	.091	.067	.063
10.0	.62	.237	.233	.270	.304	.313	.306	.247	.219	.222
10.0	-.51	.555	.553	.587	.611	.624	.629	.556	.519	.522
10.0	-1.63	.748	.737	.734	.750	.753	.778	.768	.752	.740
10.0	-2.76	.810	.801	.797	.806	.812	.834	.836	.819	.809
10.0	-3.88	.862	.854	.852	.860	.864	.883	.884	.872	.861
10.0	-5.01	.909	.902	.899	.904	.909	.924	.929	.921	.909
10.0	-6.14	.950	.942	.940	.946	.949	.960	.969	.961	.950
10.0	-7.26	.983	.977	.975	.977	.980	.992	1.000	.994	.985
10.0	-8.39	.998	.995	.990	.992	.994	1.003	1.011	1.010	1.003
10.0	-9.51	1.003	1.001	.996	.996	.998	1.005	1.014	1.014	1.008
10.0	-10.64	1.004	1.002	.997	.996	.998	1.004	1.012	1.014	1.009
10.0	-11.77	1.002	1.002	.997	.996	.997	1.003	1.010	1.012	1.008
10.0	-12.89	1.001	1.002	.997	.995	.996	1.002	1.009	1.011	1.007
10.0	-14.02	1.001	1.001	.996	.994	.995	.999	1.006	1.008	1.006
10.0	-15.15	.999	1.001	.996	.994	.994	.998	1.005	1.007	1.005
10.0	-16.27	.998	1.000	.996	.993	.994	.997	1.003	1.006	1.004
10.0	-17.40	.998	1.000	.995	.993	.993	.996	1.001	1.004	1.003
10.0	-18.52	.997	1.001	.997	.994	.994	.997	1.001	1.004	1.004
15.0	6.00	.036	.037	.029	.026	.035	.040	.057	.067	.053
15.0	4.73	.037	.035	.029	.028	.039	.043	.063	.073	.053
15.0	3.47	.042	.038	.037	.040	.052	.055	.077	.085	.056
15.0	2.20	.082	.077	.088	.107	.125	.136	.123	.116	.082
15.0	.93	.246	.229	.257	.302	.331	.334	.297	.252	.215
15.0	-.33	.501	.470	.502	.559	.575	.579	.563	.474	.449
15.0	-1.60	.729	.704	.714	.730	.753	.757	.783	.714	.691
15.0	-2.86	.811	.794	.793	.803	.814	.824	.857	.832	.804
15.0	-4.13	.868	.854	.852	.859	.869	.878	.904	.891	.865
15.0	-5.40	.919	.906	.902	.906	.918	.929	.947	.943	.921
15.0	-6.66	.962	.954	.949	.949	.957	.969	.985	.983	.967
15.0	-7.93	.990	.986	.979	.977	.982	.991	1.007	1.011	.999
15.0	-9.19	1.004	1.001	.993	.989	.992	.999	1.013	1.021	1.013
15.0	-10.46	1.004	1.005	.996	.992	.994	1.000	1.013	1.020	1.015
15.0	-11.73	1.006	1.006	.997	.993	.994	1.000	1.011	1.018	1.015
15.0	-12.99	1.004	1.006	.998	.994	.994	.999	1.009	1.016	1.014
15.0	-14.26	1.002	1.006	.998	.993	.993	.997	1.006	1.013	1.012
15.0	-15.53	1.001	1.005	.998	.993	.992	.996	1.004	1.011	1.011
15.0	-16.79	1.001	1.005	.998	.994	.992	.995	1.003	1.009	1.010
15.0	-18.06	.999	1.005	.999	.994	.993	.995	1.002	1.007	1.009
15.0	-19.32	1.000	1.004	.998	.994	.992	.994	1.000	1.005	1.007
25.0	10.00	.034	.077	.063	.044	.028	.023	.034	.053	.073
25.0	8.45	.034	.083	.066	.044	.027	.024	.038	.058	.081
25.0	6.91	.036	.092	.070	.044	.030	.032	.045	.066	.093
25.0	5.36	.041	.107	.078	.050	.042	.051	.061	.077	.111
25.0	3.81	.070	.132	.095	.079	.092	.111	.125	.121	.139
25.0	2.27	.169	.188	.160	.175	.216	.247	.270	.245	.212
25.0	.72	.353	.325	.299	.350	.415	.455	.479	.447	.384
25.0	-.82	.572	.504	.496	.555	.613	.666	.675	.681	.595

Table D.15 (cont'd).

25.0	-2.37	.766	.705	.698	.734	.751	.791	.803	.834	.792
25.0	-3.92	.851	.843	.811	.818	.828	.857	.871	.903	.919
25.0	-5.46	.914	.918	.883	.884	.890	.910	.929	.956	.971
25.0	-7.01	.963	.975	.944	.938	.941	.956	.970	.996	1.010
25.0	-8.55	.993	1.008	.983	.971	.968	.977	.989	1.014	1.030
25.0	-10.10	1.000	1.019	.997	.983	.976	.981	.993	1.014	1.032
25.0	-11.65	1.000	1.019	1.001	.987	.980	.983	.993	1.011	1.027
25.0	-13.19	.999	1.017	1.002	.989	.981	.983	.991	1.006	1.021
25.0	-14.74	.997	1.014	1.002	.990	.982	.982	.989	1.002	1.015
25.0	-16.29	.997	1.011	1.001	.990	.983	.982	.988	1.000	1.011
25.0	-17.83	.996	1.010	1.002	.992	.985	.984	.989	.998	1.009
25.0	-19.38	.996	1.007	1.000	.992	.985	.984	.988	.996	1.005
25.0	-20.92	.993	1.002	.997	.990	.983	.981	.983	.990	.999
40.0	16.00	.034	.055	.078	.087	.081	.065	.045	.025	.027
40.0	14.03	.034	.063	.089	.098	.089	.070	.047	.026	.033
40.0	12.07	.034	.077	.107	.115	.102	.077	.051	.032	.044
40.0	10.10	.036	.095	.129	.136	.117	.087	.059	.044	.061
40.0	8.13	.041	.108	.148	.161	.135	.101	.072	.066	.084
40.0	6.17	.060	.125	.164	.195	.162	.122	.104	.113	.127
40.0	4.20	.130	.212	.219	.249	.204	.165	.185	.213	.240
40.0	2.24	.264	.374	.343	.334	.271	.261	.317	.379	.432
40.0	.27	.453	.599	.525	.462	.397	.403	.490	.574	.626
40.0	-1.70	.661	.811	.727	.620	.555	.590	.662	.733	.776
40.0	-3.66	.825	.936	.890	.774	.727	.754	.787	.836	.869
40.0	-5.63	.917	.997	1.007	.915	.855	.855	.872	.906	.937
40.0	-7.60	.977	1.033	1.055	.997	.942	.924	.930	.951	.977
40.0	-9.56	1.001	1.036	1.068	1.034	.986	.960	.954	.965	.987
40.0	-11.53	1.003	1.028	1.057	1.037	.998	.972	.964	.970	.989
40.0	-13.49	1.002	1.021	1.044	1.033	1.003	.980	.971	.974	.989
40.0	-15.46	1.000	1.013	1.032	1.026	1.003	.983	.973	.975	.988
40.0	-17.42	.999	1.008	1.024	1.020	1.002	.985	.977	.977	.987
40.0	-19.39	.998	1.003	1.017	1.015	1.001	.987	.978	.978	.986
40.0	-21.36	.992	.994	1.007	1.008	.998	.985	.976	.974	.981
40.0	-23.32	.994	.997	1.007	1.007	.999	.989	.982	.981	.986
60.0	24.00	.036	.043	.028	.028	.048	.065	.072	.069	.058
60.0	21.47	.035	.044	.027	.030	.054	.074	.081	.076	.063
60.0	18.95	.035	.049	.031	.038	.066	.088	.094	.087	.070
60.0	16.42	.035	.058	.042	.055	.084	.108	.113	.102	.081
60.0	13.90	.036	.073	.061	.080	.109	.132	.138	.122	.097
60.0	11.37	.041	.097	.090	.112	.128	.157	.167	.148	.120
60.0	8.84	.061	.132	.139	.156	.134	.172	.205	.186	.154
60.0	6.32	.118	.200	.233	.245	.182	.230	.268	.244	.205
60.0	3.79	.237	.310	.377	.396	.339	.358	.363	.320	.284
60.0	1.26	.396	.452	.548	.597	.551	.518	.482	.414	.394
60.0	-1.26	.590	.630	.709	.779	.747	.675	.604	.531	.529
60.0	-3.79	.781	.774	.825	.899	.906	.822	.734	.671	.702
60.0	-6.31	.922	.872	.904	.978	1.030	.950	.861	.824	.839
60.0	-8.84	.988	.911	.930	1.001	1.081	1.047	.976	.934	.914

Table D.15 (cont'd).

60.0	-11.37	.999	.931	.946	1.003	1.074	1.080	1.028	.975	.940
60.0	-13.89	1.000	.941	.953	.997	1.051	1.061	1.026	.983	.952
60.0	-16.42	.994	.949	.959	.993	1.034	1.043	1.019	.985	.960
60.0	-18.95	.994	.957	.964	.991	1.022	1.030	1.013	.987	.966
60.0	-21.47	.986	.957	.963	.982	1.006	1.016	1.005	.985	.966
60.0	-24.00	.988	.963	.966	.982	1.001	1.009	1.001	.986	.972
60.0	-26.52	.981	.962	.964	.977	.991	.998	.992	.980	.968
76.9	-15.47	1.000	.977	.941	.930	.955	1.015	1.069	1.071	1.029
76.9	-13.86	1.002	.972	.934	.923	.950	1.022	1.086	1.082	1.030
76.9	-12.24	1.003	.964	.924	.913	.944	1.029	1.099	1.076	1.021
76.9	-10.63	.999	.943	.909	.899	.934	1.031	1.091	1.036	.979
76.9	-9.01	.981	.890	.889	.883	.921	1.030	1.052	.978	.913
76.9	-7.40	.938	.823	.846	.860	.901	1.010	1.000	.923	.854
76.9	-5.78	.862	.749	.776	.825	.874	.970	.942	.870	.795
76.9	-4.17	.770	.678	.699	.775	.835	.914	.882	.813	.735
76.9	-2.55	.664	.615	.613	.702	.774	.841	.807	.752	.683
76.9	-.94	.559	.556	.537	.617	.701	.750	.722	.670	.614
76.9	.68	.457	.496	.468	.528	.619	.662	.630	.588	.547
76.9	2.30	.366	.439	.403	.438	.528	.561	.529	.505	.477
76.9	3.91	.281	.377	.346	.367	.438	.451	.422	.424	.410
76.9	5.53	.203	.321	.297	.299	.347	.351	.302	.330	.340
76.9	7.14	.149	.270	.251	.245	.273	.271	.209	.245	.276
76.9	8.76	.099	.225	.209	.198	.213	.214	.154	.183	.227
76.9	10.37	.070	.190	.174	.160	.163	.172	.138	.151	.192
76.9	11.99	.052	.165	.147	.131	.128	.141	.131	.142	.167
76.9	13.60	.045	.143	.126	.110	.102	.114	.123	.132	.149
76.9	15.22	.040	.125	.108	.090	.078	.086	.107	.124	.132
76.9	16.83	.038	.112	.095	.077	.063	.071	.093	.112	.120
115.4	23.58	.040	.054	.051	.063	.077	.086	.086	.079	.066
115.4	21.37	.042	.066	.061	.071	.086	.096	.097	.092	.081
115.4	19.17	.046	.081	.074	.083	.098	.110	.115	.111	.098
115.4	16.97	.055	.104	.089	.094	.112	.128	.135	.134	.124
115.4	14.77	.073	.133	.115	.113	.130	.152	.164	.168	.157
115.4	12.57	.101	.171	.144	.134	.160	.193	.207	.210	.199
115.4	10.37	.148	.222	.183	.173	.208	.241	.252	.257	.250
115.4	8.17	.205	.281	.242	.248	.292	.305	.304	.309	.308
115.4	5.97	.283	.361	.337	.359	.394	.387	.374	.378	.386
115.4	3.77	.360	.451	.464	.485	.499	.472	.444	.442	.454
115.4	1.56	.448	.550	.565	.567	.556	.519	.509	.517	.542
115.4	-.64	.547	.651	.657	.653	.618	.585	.577	.593	.633
115.4	-2.84	.658	.748	.760	.761	.713	.656	.645	.659	.711
115.4	-5.04	.771	.830	.826	.820	.768	.727	.720	.743	.777
115.4	-7.24	.867	.899	.892	.880	.827	.792	.787	.804	.821
115.4	-9.44	.947	.944	.957	.931	.884	.852	.847	.845	.854
115.4	-11.64	.985	.965	1.008	.983	.944	.914	.899	.873	.880
115.4	-13.84	.992	.975	1.044	1.030	.993	.959	.925	.891	.901
115.4	-18.25	.992	.980	1.037	1.059	1.037	.993	.947	.920	.930
115.4	-18.25	.990	.980	1.037	1.059	1.037	.993	.947	.920	.930

Table D.15 (cont'd).

115.4	-20.45	.990	.978	1.026	1.047	1.030	.992	.952	.926	.933
153.8	-28.62	.979	.982	.960	.948	.953	.974	.999	1.011	1.004
153.8	-25.51	.982	.987	.958	.941	.947	.976	1.010	1.025	1.015
153.8	-22.41	.985	.990	.955	.933	.941	.978	1.023	1.040	1.024
153.8	-19.30	.992	.982	.948	.922	.934	.985	1.031	1.036	1.015
153.8	-16.19	.993	.948	.929	.908	.919	.980	1.014	1.002	.976
153.8	-13.09	.982	.890	.883	.877	.894	.959	.966	.947	.911
153.8	-9.98	.924	.822	.824	.837	.860	.903	.893	.870	.843
153.8	-6.87	.820	.749	.744	.768	.802	.817	.808	.799	.772
153.8	-3.76	.703	.688	.671	.684	.719	.710	.724	.727	.715
153.8	-.66	.576	.599	.592	.602	.613	.584	.604	.629	.626
153.8	2.45	.457	.514	.513	.525	.521	.472	.467	.495	.516
153.8	5.56	.353	.442	.443	.446	.436	.388	.355	.378	.420
153.8	8.66	.271	.343	.367	.376	.365	.316	.272	.273	.310
153.8	11.77	.195	.273	.298	.312	.306	.271	.228	.216	.237
153.8	14.88	.133	.219	.236	.254	.254	.231	.203	.190	.200
153.8	17.98	.090	.176	.190	.200	.201	.185	.168	.160	.166
153.8	21.09	.062	.153	.158	.165	.166	.159	.146	.143	.148
153.8	24.20	.050	.130	.132	.135	.131	.124	.117	.119	.125
153.8	27.30	.045	.110	.110	.109	.104	.099	.097	.100	.105
153.8	30.41	.044	.091	.090	.090	.085	.082	.081	.084	.088
153.8	33.52	.043	.077	.077	.074	.070	.067	.067	.071	.075
192.3	43.46	.045	.069	.070	.071	.073	.075	.075	.073	.070
192.3	39.45	.046	.083	.084	.086	.088	.089	.089	.088	.086
192.3	35.43	.047	.114	.113	.112	.113	.117	.118	.118	.117
192.3	31.42	.051	.146	.143	.141	.145	.148	.151	.154	.151
192.3	27.41	.060	.194	.184	.180	.181	.187	.194	.196	.197
192.3	23.40	.082	.221	.209	.203	.208	.215	.226	.232	.230
192.3	19.38	.116	.260	.244	.235	.240	.250	.267	.274	.275
192.3	15.37	.182	.304	.279	.270	.275	.297	.322	.338	.332
192.3	11.36	.253	.341	.308	.302	.323	.351	.386	.403	.383
192.3	7.35	.349	.385	.349	.353	.396	.434	.459	.470	.444
192.3	3.33	.460	.439	.420	.448	.488	.513	.532	.530	.500
192.3	-.68	.585	.550	.554	.586	.599	.601	.605	.610	.589
192.3	-4.69	.715	.686	.701	.707	.710	.698	.689	.696	.701
192.3	-8.70	.843	.806	.811	.812	.792	.772	.767	.787	.810
192.3	-12.72	.941	.902	.894	.886	.863	.841	.837	.852	.886
192.3	-16.73	.982	.963	.964	.949	.925	.904	.894	.897	.925
192.3	-20.74	.990	.989	1.011	1.000	.979	.953	.932	.922	.943
192.3	-24.75	.982	.989	1.017	1.019	1.000	.975	.949	.937	.952
192.3	-28.77	.979	.984	1.009	1.016	1.002	.979	.957	.948	.958
192.3	-32.78	.985	.990	1.006	1.010	1.001	.984	.968	.963	.971
192.3	-36.79	.985	.987	1.000	1.004	.997	.984	.972	.968	.974
230.8	-44.97	.985	.981	.977	.977	.983	.991	.996	.995	.989
230.8	-40.05	.985	.982	.975	.975	.982	.994	1.001	1.001	.992
230.8	-35.13	.987	.982	.970	.969	.980	.996	1.008	1.006	.996
230.8	-30.21	.983	.971	.958	.957	.974	.998	1.010	1.005	.988
230.8	-25.29	.986	.948	.939	.940	.966	.994	1.004	.991	.969

Table D.15 (cont'd).

230.8	-20.37	.987	.916	.913	.923	.952	.975	.973	.957	.936
230.8	-15.46	.956	.864	.868	.888	.914	.917	.914	.895	.876
230.8	-10.54	.862	.794	.803	.824	.825	.826	.824	.815	.797
230.8	-5.62	.733	.715	.722	.725	.710	.698	.708	.710	.715
230.8	-.70	.593	.625	.638	.633	.593	.564	.574	.592	.609
230.8	4.22	.470	.540	.561	.558	.512	.464	.449	.473	.508
230.8	9.14	.359	.462	.484	.488	.461	.414	.389	.401	.432
230.8	14.06	.257	.396	.419	.429	.407	.374	.352	.351	.371
230.8	18.97	.165	.339	.359	.363	.353	.329	.311	.311	.319
230.8	23.89	.114	.289	.297	.303	.303	.288	.278	.277	.279
230.8	28.81	.075	.239	.243	.247	.246	.235	.232	.230	.231
230.8	33.73	.061	.195	.199	.200	.199	.194	.189	.188	.188
230.8	38.65	.053	.150	.151	.154	.151	.149	.146	.147	.148
230.8	43.57	.050	.110	.112	.111	.110	.109	.109	.109	.110
230.8	48.48	.049	.089	.089	.089	.087	.088	.087	.087	.088

Table D.16 - RMS velocity straight wire results

x/θ_0	y/θ_0	Unforced data	Phase averaged data (at angle ϕ)							
			0.0	45.0	90.0	135.0	180.0	225.0	270.0	315.0
-30.0	-.03	.0739	.0576	.0519	.0536	.0545	.0651	.0644	.0677	.0662
-30.0	-.09	.1039	.1031	.1064	.1046	.1042	.1042	.1055	.1056	.1048
-30.0	-.15	.1013	.1052	.1024	.1005	.1002	.0982	.0995	.0998	.1011
-30.0	-.21	.0956	.0946	.0960	.0947	.0967	.0956	.0944	.0924	.0955
-30.0	-.28	.0888	.0874	.0887	.0875	.0886	.0878	.0869	.0896	.0866
-30.0	-.34	.0838	.0828	.0843	.0846	.0829	.0873	.0831	.0835	.0839
-30.0	-.43	.0820	.0822	.0825	.0816	.0830	.0815	.0820	.0817	.0817
-30.0	-.53	.0791	.0794	.0798	.0805	.0788	.0791	.0804	.0798	.0786
-30.0	-.66	.0782	.0793	.0767	.0789	.0774	.0778	.0781	.0778	.0793
-30.0	-.82	.0777	.0771	.0765	.0777	.0764	.0787	.0769	.0786	.0770
-30.0	-1.02	.0770	.0774	.0754	.0780	.0746	.0748	.0762	.0756	.0770
-30.0	-1.28	.0746	.0745	.0753	.0746	.0749	.0767	.0747	.0766	.0748
-30.0	-1.59	.0737	.0731	.0739	.0726	.0735	.0731	.0745	.0732	.0716
-30.0	-1.98	.0725	.0709	.0724	.0710	.0712	.0732	.0711	.0717	.0713
-30.0	-2.46	.0694	.0696	.0707	.0708	.0708	.0680	.0701	.0700	.0709
-30.0	-3.06	.0668	.0662	.0677	.0686	.0675	.0674	.0670	.0680	.0664
-30.0	-3.81	.0649	.0650	.0644	.0645	.0650	.0635	.0628	.0637	.0639
-30.0	-4.74	.0589	.0600	.0599	.0596	.0604	.0589	.0586	.0593	.0594
-30.0	-5.89	.0513	.0505	.0510	.0511	.0515	.0519	.0508	.0488	.0498
-30.0	-7.05	.0376	.0371	.0388	.0375	.0373	.0385	.0367	.0388	.0362
-30.0	-8.20	.0211	.0216	.0202	.0228	.0226	.0226	.0212	.0210	.0207
-30.0	-9.36	.0118	.0103	.0110	.0105	.0116	.0118	.0124	.0103	.0098
-30.0	-10.51	.0070	.0076	.0080	.0078	.0082	.0079	.0078	.0077	.0078
-30.0	-11.66	.0061	.0062	.0061	.0061	.0061	.0060	.0061	.0060	.0061
-30.0	-12.82	.0054	.0058	.0056	.0057	.0058	.0056	.0056	.0056	.0055
-30.0	-13.97	.0054	.0057	.0055	.0056	.0056	.0056	.0055	.0056	.0056
-30.0	-15.12	.0052	.0054	.0054	.0054	.0054	.0055	.0054	.0054	.0054
-20.0	-.03	.0888	.0746	.0689	.0711	.0671	.0733	.0692	.0822	.0790
-20.0	-.09	.0989	.0973	.0984	.0995	.0982	.1006	.1007	.1023	.1004
-20.0	-.15	.1003	.0986	.1015	.1001	.0991	.0986	.0962	.1001	.1003
-20.0	-.21	.0921	.0927	.0924	.0891	.0918	.0912	.0940	.0931	.0897
-20.0	-.28	.0878	.0869	.0889	.0863	.0875	.0889	.0867	.0865	.0882
-20.0	-.34	.0850	.0826	.0849	.0849	.0831	.0860	.0823	.0841	.0872
-20.0	-.43	.0829	.0826	.0831	.0823	.0820	.0822	.0812	.0830	.0818
-20.0	-.53	.0807	.0793	.0812	.0794	.0791	.0811	.0802	.0811	.0799
-20.0	-.66	.0794	.0785	.0782	.0792	.0776	.0793	.0791	.0809	.0769
-20.0	-.82	.0780	.0766	.0760	.0762	.0764	.0770	.0784	.0790	.0755
-20.0	-1.02	.0761	.0781	.0781	.0754	.0747	.0781	.0760	.0751	.0751
-20.0	-1.28	.0755	.0752	.0750	.0737	.0758	.0749	.0760	.0768	.0751
-20.0	-1.59	.0733	.0746	.0733	.0727	.0741	.0739	.0750	.0742	.0728
-20.0	-1.98	.0718	.0721	.0714	.0714	.0712	.0693	.0743	.0710	.0728
-20.0	-2.46	.0694	.0692	.0693	.0684	.0702	.0700	.0701	.0704	.0679
-20.0	-3.06	.0664	.0681	.0672	.0683	.0685	.0672	.0666	.0703	.0677
-20.0	-3.81	.0646	.0624	.0663	.0636	.0633	.0649	.0652	.0652	.0631
-20.0	-4.74	.0607	.0591	.0616	.0610	.0607	.0616	.0597	.0595	.0606

Table D.16 (cont'd).

-20.0	-5.89	.0533	.0522	.0542	.0524	.0513	.0543	.0546	.0529	.0529
-20.0	-7.05	.0429	.0420	.0442	.0420	.0408	.0414	.0421	.0418	.0424
-20.0	-8.20	.0267	.0257	.0265	.0271	.0280	.0280	.0269	.0263	.0274
-20.0	-9.36	.0139	.0150	.0132	.0143	.0142	.0142	.0145	.0147	.0139
-20.0	-10.51	.0085	.0088	.0086	.0083	.0082	.0091	.0087	.0084	.0087
-20.0	-11.66	.0069	.0067	.0066	.0067	.0068	.0067	.0074	.0067	.0068
-20.0	-12.82	.0063	.0058	.0057	.0055	.0057	.0056	.0057	.0057	.0056
-20.0	-13.97	.0056	.0057	.0057	.0057	.0057	.0056	.0057	.0056	.0057
-20.0	-15.12	.0059	.0055	.0054	.0055	.0054	.0054	.0054	.0055	.0054
-10.0	-.03	.0603	.0563	.0441	.0591	.0584	.0576	.0640	.0599	.0576
-10.0	-.09	.1023	.1043	.0998	.1021	.1039	.1045	.1042	.1049	.1032
-10.0	-.15	.0999	.0980	.0987	.0975	.0987	.1012	.0998	.0984	.1014
-10.0	-.21	.0923	.0931	.0913	.0919	.0925	.0931	.0917	.0926	.0911
-10.0	-.28	.0869	.0851	.0876	.0874	.0876	.0863	.0842	.0855	.0882
-10.0	-.34	.0841	.0851	.0854	.0842	.0848	.0833	.0832	.0839	.0844
-10.0	-.43	.0808	.0796	.0813	.0806	.0808	.0815	.0806	.0832	.0816
-10.0	-.53	.0796	.0808	.0790	.0773	.0778	.0792	.0818	.0810	.0801
-10.0	-.66	.0784	.0793	.0783	.0786	.0747	.0788	.0767	.0789	.0808
-10.0	-.82	.0763	.0774	.0797	.0776	.0744	.0761	.0777	.0767	.0764
-10.0	-1.02	.0758	.0751	.0759	.0744	.0766	.0751	.0766	.0772	.0766
-10.0	-1.28	.0745	.0740	.0746	.0730	.0744	.0734	.0761	.0730	.0753
-10.0	-1.59	.0735	.0731	.0730	.0726	.0707	.0715	.0723	.0713	.0733
-10.0	-1.98	.0704	.0715	.0712	.0690	.0700	.0707	.0707	.0712	.0698
-10.0	-2.46	.0694	.0716	.0693	.0677	.0681	.0679	.0689	.0702	.0702
-10.0	-3.06	.0677	.0672	.0680	.0657	.0655	.0664	.0667	.0658	.0677
-10.0	-3.81	.0642	.0632	.0648	.0631	.0633	.0642	.0640	.0639	.0654
-10.0	-4.74	.0610	.0604	.0618	.0604	.0610	.0593	.0609	.0607	.0624
-10.0	-5.89	.0541	.0539	.0559	.0534	.0542	.0528	.0527	.0547	.0543
-10.0	-7.05	.0451	.0438	.0461	.0457	.0439	.0446	.0442	.0453	.0436
-10.0	-8.20	.0313	.0293	.0305	.0304	.0319	.0306	.0322	.0318	.0321
-10.0	-9.36	.0174	.0174	.0177	.0175	.0168	.0173	.0157	.0163	.0173
-10.0	-10.51	.0098	.0097	.0094	.0096	.0103	.0098	.0100	.0091	.0090
-10.0	-11.66	.0070	.0070	.0071	.0069	.0071	.0070	.0068	.0066	.0071
-10.0	-12.82	.0061	.0059	.0056	.0057	.0058	.0057	.0058	.0055	.0056
-10.0	-13.97	.0056	.0055	.0057	.0056	.0057	.0055	.0056	.0055	.0056
-10.0	-15.12	.0052	.0051	.0051	.0052	.0052	.0052	.0051	.0052	.0052
-5.0	-.03	.0648	.0477	.0465	.0557	.0595	.0570	.0587	.0566	.0642
-5.0	-.09	.0967	.0982	.0966	.0979	.1009	.1015	.0971	.0961	.1006
-5.0	-.15	.1020	.1006	.1042	.1022	.1019	.1007	.0999	.1020	.1028
-5.0	-.21	.0938	.0966	.0962	.0956	.0945	.0961	.0948	.0939	.0941
-5.0	-.28	.0875	.0868	.0864	.0881	.0887	.0863	.0884	.0889	.0874
-5.0	-.34	.0840	.0840	.0838	.0823	.0829	.0825	.0842	.0841	.0819
-5.0	-.43	.0806	.0808	.0798	.0797	.0793	.0820	.0799	.0801	.0828
-5.0	-.53	.0797	.0780	.0783	.0783	.0788	.0761	.0777	.0794	.0808
-5.0	-.66	.0786	.0763	.0783	.0756	.0762	.0785	.0779	.0790	.0749
-5.0	-.82	.0763	.0773	.0757	.0754	.0762	.0747	.0748	.0762	.0769
-5.0	-1.02	.0753	.0760	.0763	.0757	.0738	.0743	.0761	.0740	.0756
-5.0	-1.28	.0734	.0738	.0728	.0717	.0727	.0737	.0709	.0742	.0742

Table D.16 (cont'd).

-5.0	-1.59	.0729	.0720	.0711	.0707	.0714	.0721	.0725	.0731	.0728
-5.0	-1.98	.0702	.0700	.0706	.0676	.0717	.0697	.0689	.0714	.0709
-5.0	-2.46	.0685	.0684	.0689	.0679	.0694	.0665	.0681	.0673	.0684
-5.0	-3.06	.0671	.0671	.0674	.0662	.0659	.0671	.0659	.0647	.0649
-5.0	-3.81	.0637	.0663	.0634	.0653	.0658	.0625	.0633	.0633	.0649
-5.0	-4.74	.0600	.0586	.0602	.0602	.0601	.0604	.0597	.0615	.0611
-5.0	-5.89	.0547	.0532	.0525	.0530	.0533	.0545	.0523	.0551	.0541
-5.0	-7.05	.0453	.0442	.0459	.0439	.0447	.0434	.0441	.0459	.0459
-5.0	-8.20	.0312	.0310	.0311	.0318	.0297	.0307	.0299	.0316	.0308
-5.0	-9.36	.0175	.0171	.0187	.0172	.0190	.0156	.0167	.0178	.0173
-5.0	-10.51	.0095	.0084	.0087	.0086	.0090	.0088	.0093	.0089	.0091
-5.0	-11.66	.0068	.0066	.0066	.0066	.0068	.0072	.0066	.0066	.0068
-5.0	-12.82	.0060	.0058	.0058	.0059	.0059	.0059	.0058	.0063	.0059
-5.0	-13.97	.0054	.0057	.0057	.0057	.0058	.0057	.0056	.0058	.0056
-5.0	-15.12	.0055	.0055	.0055	.0054	.0055	.0054	.0055	.0055	.0056
-1.0	-.03	.0512	.0471	.0416	.0553	.0601	.0566	.0527	.0556	.0550
-1.0	-.09	.0921	.0925	.0899	.0949	.0966	.0978	.0975	.0933	.0948
-1.0	-.15	.0999	.1006	.1007	.0997	.0982	.1006	.0986	.1014	.0994
-1.0	-.21	.0916	.0896	.0914	.0914	.0891	.0909	.0913	.0925	.0922
-1.0	-.28	.0851	.0845	.0868	.0835	.0807	.0827	.0857	.0853	.0872
-1.0	-.34	.0820	.0827	.0810	.0795	.0798	.0798	.0807	.0816	.0823
-1.0	-.43	.0779	.0795	.0776	.0790	.0789	.0772	.0787	.0793	.0781
-1.0	-.53	.0784	.0747	.0766	.0765	.0759	.0767	.0791	.0774	.0797
-1.0	-.66	.0762	.0769	.0735	.0758	.0755	.0752	.0744	.0772	.0780
-1.0	-.82	.0752	.0770	.0755	.0735	.0735	.0730	.0741	.0783	.0753
-1.0	-1.02	.0734	.0747	.0722	.0722	.0738	.0730	.0729	.0761	.0739
-1.0	-1.28	.0733	.0727	.0721	.0725	.0700	.0724	.0718	.0750	.0724
-1.0	-1.59	.0704	.0733	.0719	.0703	.0696	.0699	.0714	.0707	.0706
-1.0	-1.98	.0696	.0701	.0697	.0674	.0695	.0695	.0705	.0690	.0714
-1.0	-2.46	.0683	.0660	.0674	.0678	.0664	.0672	.0668	.0660	.0677
-1.0	-3.06	.0661	.0669	.0668	.0651	.0659	.0648	.0661	.0662	.0661
-1.0	-3.81	.0635	.0629	.0646	.0634	.0622	.0644	.0644	.0635	.0641
-1.0	-4.74	.0595	.0604	.0597	.0579	.0603	.0576	.0596	.0601	.0602
-1.0	-5.89	.0538	.0531	.0529	.0525	.0524	.0527	.0542	.0514	.0521
-1.0	-7.05	.0449	.0451	.0454	.0438	.0428	.0439	.0441	.0433	.0442
-1.0	-8.20	.0318	.0304	.0305	.0297	.0298	.0305	.0320	.0324	.0317
-1.0	-9.36	.0179	.0175	.0174	.0163	.0178	.0174	.0175	.0196	.0182
-1.0	-10.51	.0096	.0103	.0090	.0087	.0092	.0098	.0083	.0101	.0094
-1.0	-11.66	.0065	.0070	.0066	.0067	.0064	.0069	.0067	.0067	.0066
-1.0	-12.82	.0060	.0054	.0054	.0053	.0054	.0055	.0055	.0054	.0056
-1.0	-13.97	.0058	.0055	.0055	.0055	.0055	.0057	.0056	.0056	.0055
-1.0	-15.12	.0059	.0051	.0053	.0053	.0053	.0053	.0054	.0052	.0053
.0	-.03	.0731	.0631	.0572	.0640	.0739	.0762	.0679	.0683	.0745
.0	-.09	.1018	.0973	.0972	.1001	.1017	.1063	.1042	.1068	.1033
.0	-.15	.0972	.0979	.0962	.0970	.0961	.0994	.1005	.0993	.0959
.0	-.21	.0927	.0909	.0890	.0898	.0876	.0921	.0935	.0927	.0928
.0	-.28	.0864	.0854	.0855	.0832	.0834	.0896	.0887	.0916	.0883
.0	-.34	.0828	.0830	.0824	.0810	.0805	.0809	.0849	.0839	.0840

Table D.16 (cont'd).

.0	-.43	.0807	.0797	.0775	.0774	.0793	.0803	.0818	.0799	.0808
.0	-.53	.0791	.0792	.0780	.0773	.0785	.0787	.0785	.0808	.0796
.0	-.66	.0779	.0780	.0763	.0780	.0772	.0769	.0786	.0769	.0772
.0	-.82	.0781	.0774	.0762	.0773	.0750	.0763	.0756	.0787	.0754
.0	-1.02	.0755	.0753	.0760	.0752	.0743	.0749	.0764	.0760	.0753
.0	-1.28	.0748	.0749	.0733	.0753	.0717	.0730	.0756	.0751	.0755
.0	-1.59	.0738	.0731	.0742	.0728	.0708	.0715	.0749	.0726	.0745
.0	-1.98	.0715	.0734	.0720	.0725	.0718	.0692	.0731	.0707	.0730
.0	-2.46	.0705	.0679	.0690	.0697	.0692	.0701	.0683	.0700	.0696
.0	-3.06	.0674	.0701	.0679	.0656	.0662	.0668	.0685	.0688	.0687
.0	-3.81	.0646	.0652	.0675	.0655	.0646	.0642	.0667	.0629	.0661
.0	-4.74	.0617	.0611	.0627	.0616	.0606	.0613	.0621	.0611	.0615
.0	-5.89	.0559	.0546	.0568	.0544	.0546	.0546	.0547	.0547	.0566
.0	-7.05	.0464	.0467	.0455	.0442	.0444	.0453	.0433	.0463	.0449
.0	-8.20	.0323	.0338	.0322	.0316	.0299	.0296	.0305	.0309	.0321
.0	-9.36	.0177	.0172	.0180	.0171	.0172	.0161	.0168	.0176	.0188
.0	-10.51	.0102	.0100	.0098	.0101	.0092	.0093	.0096	.0093	.0096
.0	-11.66	.0070	.0065	.0069	.0067	.0067	.0070	.0065	.0078	.0064
.0	-12.82	.0059	.0065	.0062	.0063	.0064	.0062	.0063	.0062	.0065
.0	-13.97	.0057	.0057	.0055	.0056	.0055	.0055	.0056	.0055	.0055
.0	-15.12	.0059	.0053	.0052	.0052	.0053	.0051	.0051	.0052	.0052
1.0	.58	.0197	.0182	.0223	.0192	.0370	.0392	.0317	.0235	.0180
1.0	.40	.0224	.0206	.0240	.0185	.0323	.0365	.0323	.0243	.0201
1.0	.21	.0220	.0234	.0264	.0219	.0245	.0309	.0302	.0258	.0225
1.0	.03	.0324	.0349	.0362	.0376	.0346	.0394	.0404	.0345	.0368
1.0	-.12	.0753	.0795	.0824	.0875	.0871	.0799	.0791	.0758	.0761
1.0	-.25	.1158	.1212	.1223	.1255	.1192	.1252	.1202	.1164	.1178
1.0	-.40	.1107	.1120	.1059	.1049	.0996	.1051	.1098	.1140	.1109
1.0	-.63	.0841	.0826	.0817	.0805	.0805	.0814	.0841	.0844	.0857
1.0	-.79	.0792	.0787	.0787	.0755	.0779	.0792	.0808	.0794	.0800
1.0	-.99	.0776	.0794	.0759	.0773	.0766	.0794	.0770	.0785	.0792
1.0	-1.24	.0772	.0779	.0771	.0730	.0744	.0760	.0766	.0790	.0768
1.0	-1.56	.0750	.0761	.0738	.0745	.0738	.0742	.0776	.0752	.0768
1.0	-1.95	.0727	.0735	.0726	.0715	.0694	.0718	.0731	.0736	.0769
1.0	-2.43	.0706	.0732	.0710	.0717	.0716	.0708	.0705	.0722	.0728
1.0	-3.03	.0691	.0694	.0672	.0692	.0666	.0672	.0696	.0698	.0691
1.0	-3.78	.0660	.0673	.0667	.0649	.0659	.0642	.0649	.0662	.0648
1.0	-4.71	.0632	.0642	.0641	.0625	.0624	.0651	.0633	.0640	.0638
1.0	-5.86	.0625	.0616	.0612	.0600	.0616	.0608	.0603	.0621	.0601
1.0	-7.02	.0580	.0579	.0577	.0581	.0566	.0564	.0592	.0573	.0569
1.0	-8.17	.0556	.0538	.0545	.0527	.0520	.0526	.0530	.0536	.0537
1.0	-9.32	.0477	.0470	.0480	.0461	.0468	.0461	.0461	.0483	.0466
1.0	-10.48	.0264	.0247	.0271	.0265	.0254	.0239	.0251	.0269	.0262
1.0	-11.63	.0176	.0178	.0183	.0170	.0168	.0179	.0162	.0164	.0178
1.0	-12.78	.0082	.0077	.0073	.0077	.0079	.0073	.0076	.0079	.0078
1.0	-13.94	.0067	.0064	.0065	.0065	.0064	.0063	.0063	.0064	.0064
1.0	-15.09	.0058	.0059	.0060	.0059	.0059	.0059	.0059	.0059	.0060
3.0	.58	.0403	.0385	.0375	.0572	.0655	.0604	.0452	.0334	.0325

Table D.16 (cont'd).

3.0	.40	.0489	.0482	.0543	.0614	.0626	.0623	.0564	.0506	.0452
3.0	.21	.0772	.0789	.0876	.0872	.0872	.0845	.0882	.0788	.0776
3.0	.03	.1010	.1045	.1078	.1095	.1087	.1156	.1104	.1053	.1020
3.0	-.12	.1167	.1160	.1202	.1209	.1238	.1235	.1217	.1167	.1147
3.0	-.25	.1238	.1223	.1296	.1237	.1278	.1343	.1359	.1256	.1259
3.0	-.40	.1267	.1232	.1253	.1207	.1230	.1379	.1361	.1311	.1237
3.0	-.63	.1083	.1017	.1017	.0972	.0985	.1113	.1178	.1126	.1084
3.0	-.79	.0895	.0862	.0844	.0835	.0832	.0917	.0978	.0977	.0932
3.0	-.99	.0816	.0798	.0809	.0797	.0756	.0817	.0814	.0841	.0802
3.0	-1.24	.0787	.0799	.0761	.0755	.0765	.0748	.0771	.0780	.0808
3.0	-1.56	.0762	.0770	.0760	.0752	.0726	.0739	.0762	.0751	.0773
3.0	-1.95	.0738	.0734	.0720	.0732	.0740	.0705	.0736	.0746	.0746
3.0	-2.43	.0702	.0708	.0721	.0696	.0690	.0706	.0715	.0706	.0714
3.0	-3.03	.0693	.0698	.0689	.0690	.0684	.0670	.0679	.0702	.0698
3.0	-3.78	.0667	.0669	.0660	.0665	.0654	.0651	.0686	.0672	.0671
3.0	-4.71	.0652	.0644	.0666	.0627	.0640	.0655	.0652	.0643	.0656
3.0	-5.86	.0587	.0588	.0585	.0571	.0569	.0586	.0580	.0582	.0583
3.0	-7.02	.0537	.0541	.0515	.0523	.0520	.0535	.0536	.0534	.0534
3.0	-8.17	.0355	.0336	.0331	.0336	.0336	.0337	.0339	.0358	.0341
3.0	-9.32	.0252	.0248	.0249	.0235	.0223	.0251	.0254	.0225	.0273
3.0	-10.48	.0113	.0105	.0111	.0115	.0103	.0098	.0098	.0104	.0095
3.0	-11.63	.0084	.0085	.0080	.0077	.0085	.0083	.0087	.0090	.0087
3.0	-12.78	.0064	.0061	.0061	.0063	.0061	.0061	.0060	.0061	.0064
3.0	-13.94	.0056	.0057	.0056	.0055	.0056	.0056	.0056	.0056	.0054
3.0	-15.09	.0062	.0059	.0059	.0060	.0059	.0061	.0057	.0058	.0059
5.0	2.00	.0102	.0135	.0108	.0114	.0129	.0134	.0143	.0109	.0096
5.0	1.01	.0306	.0269	.0342	.0410	.0427	.0365	.0351	.0311	.0264
5.0	.03	.1274	.1224	.1334	.1363	.1408	.1419	.1349	.1253	.1183
5.0	-.96	.0873	.0844	.0836	.0808	.0772	.0859	.0976	.0972	.0924
5.0	-1.94	.0713	.0720	.0712	.0711	.0693	.0706	.0717	.0720	.0698
5.0	-2.93	.0676	.0679	.0673	.0669	.0665	.0667	.0678	.0664	.0674
5.0	-3.92	.0625	.0632	.0615	.0616	.0591	.0603	.0607	.0609	.0620
5.0	-4.90	.0575	.0570	.0581	.0562	.0548	.0566	.0562	.0571	.0592
5.0	-5.89	.0498	.0492	.0489	.0492	.0488	.0503	.0483	.0484	.0486
5.0	-6.88	.0399	.0411	.0385	.0379	.0369	.0364	.0382	.0398	.0398
5.0	-7.86	.0249	.0251	.0238	.0232	.0231	.0228	.0240	.0250	.0266
5.0	-8.85	.0152	.0151	.0162	.0147	.0136	.0134	.0147	.0152	.0147
5.0	-9.84	.0088	.0094	.0087	.0084	.0086	.0089	.0088	.0088	.0096
5.0	-10.82	.0073	.0067	.0073	.0068	.0066	.0064	.0067	.0070	.0066
5.0	-11.81	.0061	.0062	.0063	.0064	.0063	.0062	.0063	.0062	.0063
5.0	-12.79	.0060	.0058	.0057	.0057	.0057	.0056	.0057	.0058	.0057
5.0	-13.78	.0062	.0057	.0057	.0057	.0057	.0058	.0056	.0057	.0057
5.0	-14.76	.0062	.0057	.0057	.0057	.0056	.0059	.0059	.0058	.0058
5.0	-15.75	.0058	.0053	.0053	.0052	.0053	.0055	.0054	.0054	.0055
5.0	-16.74	.0055	.0052	.0050	.0051	.0051	.0051	.0053	.0052	.0052
5.0	-17.72	.0054	.0051	.0051	.0051	.0051	.0051	.0051	.0052	.0052
10.0	4.00	.0067	.0062	.0064	.0081	.0091	.0103	.0094	.0079	.0064
10.0	2.87	.0108	.0097	.0107	.0142	.0159	.0187	.0157	.0109	.0101

Table D.16 (cont'd).

10.0	1.75	.0369	.0385	.0501	.0507	.0579	.0497	.0387	.0332	.0360
10.0	.62	.1062	.1055	.1162	.1172	.1218	.1240	.1004	.1053	.1038
10.0	-.51	.1271	.1220	.1172	.1150	.1151	.1245	.1355	.1361	.1271
10.0	-1.63	.0766	.0765	.0769	.0751	.0729	.0742	.0832	.0851	.0807
10.0	-2.76	.0680	.0686	.0695	.0679	.0657	.0653	.0657	.0670	.0680
10.0	-3.88	.0621	.0630	.0621	.0617	.0620	.0595	.0620	.0627	.0632
10.0	-5.01	.0560	.0558	.0552	.0544	.0552	.0533	.0547	.0549	.0576
10.0	-6.14	.0473	.0487	.0476	.0462	.0448	.0457	.0462	.0464	.0491
10.0	-7.26	.0334	.0338	.0328	.0319	.0312	.0288	.0304	.0322	.0333
10.0	-8.39	.0208	.0198	.0189	.0180	.0182	.0176	.0179	.0187	.0204
10.0	-9.51	.0112	.0107	.0100	.0100	.0103	.0096	.0108	.0099	.0113
10.0	-10.64	.0073	.0073	.0070	.0069	.0071	.0071	.0068	.0072	.0076
10.0	-11.77	.0063	.0061	.0061	.0062	.0060	.0063	.0062	.0062	.0064
10.0	-12.89	.0060	.0057	.0056	.0057	.0058	.0059	.0058	.0057	.0057
10.0	-14.02	.0057	.0058	.0058	.0058	.0058	.0058	.0058	.0058	.0059
10.0	-15.15	.0063	.0057	.0057	.0058	.0058	.0057	.0059	.0059	.0057
10.0	-16.27	.0053	.0052	.0051	.0053	.0052	.0051	.0053	.0052	.0052
10.0	-17.40	.0052	.0052	.0051	.0052	.0053	.0052	.0053	.0053	.0053
10.0	-18.52	.0053	.0050	.0052	.0052	.0053	.0052	.0052	.0054	.0053
15.0	6.00	.0061	.0056	.0053	.0055	.0072	.0087	.0088	.0079	.0067
15.0	4.73	.0089	.0076	.0075	.0086	.0121	.0137	.0144	.0120	.0097
15.0	3.47	.0164	.0153	.0163	.0211	.0240	.0266	.0297	.0215	.0159
15.0	2.20	.0503	.0505	.0563	.0698	.0724	.0832	.0650	.0412	.0433
15.0	.93	.1091	.1092	.1129	.1232	.1202	.1241	.1158	.0999	.1054
15.0	-.33	.1326	.1334	.1330	.1266	.1276	.1258	.1312	.1305	.1383
15.0	-1.60	.0922	.0976	.0906	.0817	.0800	.0774	.0919	.1127	.1095
15.0	-2.86	.0687	.0709	.0691	.0705	.0664	.0674	.0683	.0716	.0713
15.0	-4.13	.0619	.0626	.0622	.0621	.0586	.0610	.0597	.0598	.0635
15.0	-5.40	.0550	.0558	.0547	.0531	.0511	.0513	.0516	.0541	.0543
15.0	-6.66	.0430	.0448	.0432	.0421	.0398	.0384	.0403	.0429	.0436
15.0	-7.93	.0273	.0294	.0285	.0255	.0259	.0233	.0247	.0265	.0281
15.0	-9.19	.0142	.0147	.0147	.0139	.0117	.0125	.0130	.0133	.0136
15.0	-10.46	.0087	.0081	.0082	.0079	.0077	.0076	.0080	.0084	.0094
15.0	-11.73	.0070	.0067	.0068	.0067	.0067	.0068	.0065	.0068	.0068
15.0	-12.99	.0062	.0057	.0056	.0057	.0059	.0059	.0057	.0058	.0059
15.0	-14.26	.0059	.0057	.0059	.0057	.0059	.0059	.0058	.0060	.0061
15.0	-15.53	.0065	.0057	.0058	.0056	.0056	.0057	.0058	.0058	.0058
15.0	-16.79	.0057	.0055	.0056	.0054	.0056	.0055	.0056	.0056	.0055
15.0	-18.06	.0059	.0053	.0053	.0052	.0055	.0055	.0055	.0053	.0052
15.0	-19.32	.0054	.0054	.0054	.0053	.0054	.0053	.0054	.0054	.0053
25.0	10.00	.0053	.0071	.0067	.0058	.0047	.0056	.0084	.0091	.0076
25.0	8.45	.0071	.0076	.0069	.0068	.0052	.0064	.0103	.0124	.0102
25.0	6.91	.0103	.0112	.0097	.0087	.0076	.0120	.0163	.0188	.0156
25.0	5.36	.0164	.0162	.0133	.0138	.0217	.0305	.0314	.0317	.0264
25.0	3.81	.0421	.0278	.0253	.0463	.0665	.0741	.0746	.0688	.0454
25.0	2.27	.0888	.0551	.0724	.0983	.1130	.1148	.1150	.1094	.0736
25.0	.72	.1253	.0987	.1204	.1303	.1350	.1305	.1337	.1343	.1175
25.0	-.82	.1318	.1258	.1440	.1318	.1189	.1136	.1143	.1181	.1320

Table D.16 (cont'd).

25.0	-2.37	.0911	.1189	.1059	.0882	.0800	.0748	.0740	.0779	.1128
25.0	-3.92	.0658	.0766	.0712	.0659	.0657	.0617	.0603	.0629	.0703
25.0	-5.46	.0554	.0563	.0588	.0558	.0550	.0527	.0504	.0519	.0544
25.0	-7.01	.0420	.0432	.0451	.0413	.0382	.0352	.0342	.0379	.0417
25.0	-8.55	.0230	.0276	.0252	.0231	.0202	.0180	.0171	.0171	.0237
25.0	-10.10	.0108	.0117	.0123	.0106	.0101	.0095	.0096	.0093	.0100
25.0	-11.65	.0073	.0077	.0078	.0076	.0073	.0076	.0072	.0071	.0070
25.0	-13.19	.0063	.0066	.0065	.0061	.0061	.0062	.0062	.0062	.0062
25.0	-14.74	.0062	.0059	.0061	.0060	.0059	.0063	.0062	.0063	.0060
25.0	-16.29	.0054	.0054	.0055	.0055	.0057	.0056	.0057	.0057	.0055
25.0	-17.83	.0054	.0052	.0053	.0051	.0053	.0055	.0055	.0055	.0052
25.0	-19.38	.0054	.0056	.0056	.0054	.0055	.0056	.0055	.0055	.0057
25.0	-20.92	.0050	.0053	.0052	.0051	.0052	.0055	.0055	.0055	.0055
40.0	16.00	.0043	.0085	.0081	.0069	.0062	.0058	.0054	.0046	.0067
40.0	14.03	.0056	.0113	.0110	.0090	.0077	.0069	.0064	.0057	.0100
40.0	12.07	.0076	.0160	.0148	.0116	.0088	.0078	.0078	.0084	.0144
40.0	10.10	.0100	.0230	.0216	.0158	.0112	.0099	.0105	.0160	.0236
40.0	8.13	.0150	.0385	.0368	.0248	.0149	.0131	.0163	.0365	.0446
40.0	6.17	.0325	.0610	.0539	.0362	.0203	.0199	.0498	.0754	.0800
40.0	4.20	.0746	.0994	.0730	.0527	.0325	.0506	.1006	.1176	.1207
40.0	2.24	.1146	.1254	.1020	.0680	.0559	.1010	.1360	.1393	.1366
40.0	.27	.1360	.1304	.1181	.0901	.1021	.1344	.1401	.1312	.1268
40.0	-1.70	.1274	.1069	.1304	.1128	.1269	.1298	.1157	.0940	.0845
40.0	-3.66	.0858	.0714	.1109	.1191	.1133	.0888	.0754	.0666	.0628
40.0	-5.63	.0581	.0520	.0688	.0814	.0728	.0615	.0548	.0480	.0455
40.0	-7.60	.0387	.0313	.0436	.0487	.0471	.0429	.0333	.0275	.0262
40.0	-9.56	.0172	.0153	.0194	.0243	.0233	.0188	.0147	.0138	.0118
40.0	-11.53	.0097	.0092	.0095	.0113	.0115	.0102	.0094	.0091	.0084
40.0	-13.49	.0072	.0081	.0075	.0078	.0083	.0080	.0078	.0079	.0079
40.0	-15.46	.0067	.0071	.0066	.0070	.0071	.0070	.0068	.0071	.0069
40.0	-17.42	.0059	.0061	.0058	.0061	.0061	.0061	.0061	.0064	.0062
40.0	-19.39	.0055	.0059	.0058	.0059	.0056	.0055	.0057	.0061	.0061
40.0	-21.36	.0060	.0065	.0061	.0059	.0058	.0057	.0060	.0063	.0064
40.0	-23.32	.0054	.0058	.0054	.0053	.0054	.0053	.0054	.0056	.0057
60.0	24.00	.0038	.0056	.0058	.0062	.0059	.0051	.0046	.0047	.0051
60.0	21.47	.0048	.0062	.0058	.0078	.0074	.0066	.0057	.0058	.0059
60.0	18.95	.0061	.0070	.0078	.0123	.0106	.0095	.0083	.0079	.0074
60.0	16.42	.0081	.0085	.0120	.0185	.0166	.0145	.0120	.0100	.0088
60.0	13.90	.0104	.0118	.0205	.0319	.0275	.0259	.0191	.0137	.0112
60.0	11.37	.0159	.0173	.0397	.0516	.0427	.0430	.0312	.0210	.0160
60.0	8.84	.0333	.0364	.0789	.0819	.0565	.0586	.0449	.0309	.0234
60.0	6.32	.0689	.0855	.1220	.1158	.0870	.0776	.0599	.0456	.0377
60.0	3.79	.1078	.1248	.1434	.1277	.1216	.0935	.0721	.0578	.0753
60.0	1.26	.1314	.1387	.1261	.1146	.1228	.1025	.0873	.0751	.1111
60.0	-1.26	.1379	.1115	.0847	.0877	.1213	.1115	.0937	.0968	.1253
60.0	-3.79	.1097	.0728	.0580	.0643	.1091	.1136	.1024	.1120	.1099
60.0	-6.31	.0618	.0445	.0328	.0423	.0762	.0986	.1047	.0963	.0641
60.0	-8.84	.0326	.0220	.0188	.0215	.0369	.0632	.0661	.0504	.0319

Table D.16 (cont'd).

60.0	-11.37	.0153	.0157	.0150	.0147	.0183	.0228	.0238	.0202	.0155
60.0	-13.89	.0108	.0135	.0134	.0120	.0118	.0123	.0133	.0128	.0120
60.0	-16.42	.0084	.0092	.0093	.0096	.0090	.0079	.0088	.0094	.0091
60.0	-18.95	.0069	.0077	.0077	.0079	.0075	.0064	.0069	.0074	.0075
60.0	-21.47	.0065	.0081	.0085	.0078	.0074	.0069	.0068	.0068	.0070
60.0	-24.00	.0061	.0068	.0069	.0069	.0067	.0060	.0057	.0060	.0063
60.0	-26.52	.0056	.0062	.0064	.0064	.0062	.0058	.0057	.0056	.0058
76.9	-15.47	.0125	.0147	.0145	.0145	.0139	.0150	.0144	.0146	.0149
76.9	-13.86	.0150	.0172	.0170	.0169	.0158	.0171	.0175	.0231	.0198
76.9	-12.24	.0184	.0252	.0201	.0199	.0189	.0198	.0255	.0436	.0392
76.9	-10.63	.0254	.0416	.0240	.0194	.0175	.0233	.0461	.0726	.0737
76.9	-9.01	.0407	.0786	.0345	.0267	.0228	.0318	.0724	.0923	.0937
76.9	-7.40	.0628	.0955	.0607	.0308	.0255	.0457	.0888	.0965	.1001
76.9	-5.78	.0894	.1042	.0886	.0424	.0322	.0593	.0995	.1028	.0984
76.9	-4.17	.1150	.1029	.1052	.0607	.0440	.0766	.1072	.1008	.0960
76.9	-2.55	.1317	.0968	.1159	.0858	.0566	.0910	.1107	.1052	.0946
76.9	-.94	.1367	.0940	.1148	.1106	.0740	.0968	.1148	.1080	.0980
76.9	.68	.1351	.0896	.1043	.1200	.0874	.1065	.1179	.1048	.0936
76.9	2.30	.1281	.0853	.0900	.1248	.1102	.1097	.1200	.1073	.0920
76.9	3.91	.1180	.0749	.0767	.1181	.1221	.1130	.1254	.1052	.0842
76.9	5.53	.0983	.0729	.0708	.1027	.1246	.1112	.1203	.1016	.0810
76.9	7.14	.0831	.0620	.0583	.0855	.1229	.1061	.0986	.0912	.0715
76.9	8.76	.0576	.0533	.0501	.0578	.1059	.0973	.0756	.0743	.0626
76.9	10.37	.0392	.0445	.0416	.0445	.0834	.0890	.0570	.0603	.0541
76.9	11.99	.0244	.0389	.0325	.0340	.0611	.0812	.0521	.0533	.0470
76.9	13.60	.0187	.0319	.0282	.0286	.0428	.0632	.0471	.0431	.0382
76.9	15.22	.0131	.0225	.0202	.0214	.0303	.0430	.0360	.0315	.0286
76.9	16.83	.0112	.0188	.0159	.0169	.0223	.0296	.0267	.0240	.0227
115.4	23.58	.0124	.0264	.0283	.0283	.0281	.0280	.0264	.0267	.0250
115.4	21.37	.0140	.0376	.0362	.0344	.0340	.0339	.0347	.0348	.0358
115.4	19.17	.0183	.0471	.0473	.0459	.0430	.0425	.0442	.0456	.0455
115.4	16.97	.0251	.0613	.0583	.0525	.0519	.0534	.0537	.0543	.0608
115.4	14.77	.0414	.0772	.0725	.0600	.0586	.0619	.0655	.0693	.0728
115.4	12.57	.0597	.0904	.0855	.0756	.0826	.0868	.0852	.0844	.0867
115.4	10.37	.0834	.1082	.0984	.0976	.1057	.1021	.0990	.0985	.1044
115.4	8.17	.0994	.1140	.1131	.1339	.1328	.1183	.1075	.1074	.1156
115.4	5.97	.1204	.1171	.1297	.1471	.1458	.1332	.1194	.1174	.1238
115.4	3.77	.1308	.1113	.1365	.1515	.1462	.1314	.1206	.1224	.1271
115.4	1.56	.1422	.1012	.1216	.1395	.1357	.1291	.1265	.1270	.1205
115.4	-.64	.1447	.0911	.1210	.1375	.1348	.1280	.1282	.1290	.1007
115.4	-2.84	.1405	.0804	.1151	.1291	.1320	.1297	.1266	.1252	.0750
115.4	-5.04	.1278	.0696	.1059	.1218	.1288	.1268	.1245	.1064	.0508
115.4	-7.24	.1042	.0574	.0960	.1091	.1189	.1174	.1159	.0821	.0388
115.4	-9.44	.0687	.0436	.0860	.1036	.1080	.1130	.1005	.0528	.0322
115.4	-11.64	.0428	.0350	.0686	.0961	.0996	.0981	.0743	.0368	.0291
115.4	-13.84	.0258	.0312	.0442	.0746	.0831	.0728	.0433	.0273	.0248
115.4	-18.25	.0206	.0231	.0270	.0280	.0275	.0230	.0193	.0187	.0199
115.4	-18.25	.0174	.0231	.0270	.0280	.0275	.0230	.0193	.0187	.0199

Table D.16 (cont'd).

115.4	-20.45	.0148	.0216	.0225	.0204	.0168	.0140	.0154	.0161	.0175
153.8	-28.62	.0131	.0119	.0115	.0141	.0177	.0214	.0237	.0217	.0167
153.8	-25.51	.0162	.0178	.0138	.0161	.0203	.0258	.0283	.0269	.0226
153.8	-22.41	.0199	.0287	.0187	.0187	.0224	.0292	.0335	.0335	.0333
153.8	-19.30	.0240	.0555	.0373	.0261	.0289	.0344	.0402	.0556	.0634
153.8	-16.19	.0339	.0932	.0647	.0350	.0323	.0398	.0639	.0875	.0989
153.8	-13.09	.0532	.1263	.1068	.0612	.0396	.0507	.0881	.1115	.1246
153.8	-9.98	.0929	.1431	.1302	.0908	.0516	.0699	.1077	.1305	.1392
153.8	-6.87	.1290	.1524	.1535	.1294	.0785	.0887	.1210	.1445	.1474
153.8	-3.76	.1423	.1592	.1545	.1534	.1089	.1028	.1269	.1541	.1522
153.8	-.66	.1495	.1608	.1579	.1591	.1366	.1213	.1433	.1681	.1669
153.8	2.45	.1443	.1627	.1605	.1609	.1445	.1302	.1506	.1680	.1671
153.8	5.56	.1334	.1640	.1558	.1517	.1432	.1257	.1380	.1663	.1702
153.8	8.66	.1209	.1480	.1482	.1446	.1404	.1208	.1128	.1276	.1429
153.8	11.77	.1028	.1250	.1342	.1367	.1307	.1137	.1001	.1016	.1131
153.8	14.88	.0773	.1063	.1153	.1199	.1214	.1102	.0983	.0912	.1001
153.8	17.98	.0523	.0877	.0976	.1058	.1101	.1011	.0892	.0831	.0859
153.8	21.09	.0321	.0789	.0807	.0897	.0929	.0949	.0838	.0783	.0791
153.8	24.20	.0201	.0682	.0694	.0725	.0759	.0738	.0647	.0660	.0660
153.8	27.30	.0152	.0575	.0566	.0594	.0594	.0576	.0583	.0551	.0545
153.8	30.41	.0126	.0456	.0448	.0487	.0489	.0486	.0485	.0463	.0454
153.8	33.52	.0113	.0368	.0362	.0363	.0374	.0365	.0363	.0371	.0376
192.3	43.46	.0109	.0433	.0433	.0431	.0456	.0456	.0455	.0445	.0444
192.3	39.45	.0127	.0540	.0537	.0553	.0561	.0544	.0557	.0552	.0577
192.3	35.43	.0155	.0737	.0729	.0701	.0703	.0701	.0722	.0736	.0740
192.3	31.42	.0197	.0885	.0896	.0849	.0814	.0852	.0860	.0889	.0895
192.3	27.41	.0297	.1114	.1028	.0963	.0966	.0982	.1044	.1047	.1081
192.3	23.40	.0505	.1169	.1072	.0990	.0990	.1039	.1095	.1150	.1179
192.3	19.38	.0688	.1203	.1105	.1085	.1078	.1113	.1218	.1280	.1280
192.3	15.37	.0952	.1261	.1155	.1112	.1150	.1280	.1425	.1455	.1405
192.3	11.36	.1198	.1272	.1136	.1190	.1309	.1427	.1539	.1562	.1426
192.3	7.35	.1395	.1240	.1252	.1430	.1561	.1633	.1626	.1608	.1466
192.3	3.33	.1536	.1329	.1497	.1708	.1745	.1726	.1681	.1623	.1457
192.3	-.68	.1532	.1424	.1686	.1839	.1804	.1701	.1641	.1604	.1441
192.3	-4.69	.1496	.1370	.1575	.1704	.1673	.1643	.1647	.1542	.1289
192.3	-8.70	.1298	.1111	.1346	.1493	.1532	.1574	.1563	.1326	.0969
192.3	-12.72	.0910	.0913	.1229	.1366	.1404	.1465	.1361	.0971	.0682
192.3	-16.73	.0541	.0637	.0968	.1145	.1224	.1232	.1030	.0627	.0479
192.3	-20.74	.0345	.0453	.0642	.0823	.0887	.0857	.0618	.0352	.0365
192.3	-24.75	.0245	.0364	.0447	.0518	.0542	.0455	.0339	.0219	.0281
192.3	-28.77	.0184	.0283	.0312	.0305	.0280	.0241	.0172	.0176	.0223
192.3	-32.78	.0138	.0237	.0242	.0218	.0186	.0148	.0124	.0150	.0198
192.3	-36.79	.0126	.0205	.0214	.0192	.0153	.0114	.0100	.0126	.0168
230.8	-44.97	.0125	.0109	.0105	.0137	.0176	.0200	.0200	.0177	.0141
230.8	-40.05	.0147	.0151	.0131	.0163	.0206	.0237	.0238	.0215	.0170
230.8	-35.13	.0177	.0174	.0170	.0181	.0233	.0276	.0279	.0263	.0236
230.8	-30.21	.0227	.0405	.0252	.0232	.0289	.0351	.0386	.0454	.0498
230.8	-25.29	.0320	.0762	.0523	.0355	.0377	.0491	.0620	.0760	.0811

Table D.16 (cont'd).

230.8	-20.37	.0485	.1086	.0825	.0546	.0497	.0746	.0931	.1084	.1135
230.8	-15.46	.0848	.1377	.1170	.0810	.0723	.1023	.1223	.1356	.1394
230.8	-10.54	.1277	.1578	.1454	.1128	.1097	.1290	.1467	.1546	.1608
230.8	-5.62	.1570	.1646	.1589	.1440	.1359	.1531	.1703	.1712	.1639
230.8	-.70	.1610	.1691	.1636	.1528	.1406	.1545	.1741	.1776	.1751
230.8	4.22	.1582	.1659	.1627	.1591	.1435	.1395	.1506	.1616	.1652
230.8	9.14	.1418	.1601	.1633	.1585	.1466	.1327	.1296	.1430	.1552
230.8	14.06	.1221	.1454	.1516	.1551	.1437	.1266	.1249	.1284	.1376
230.8	18.97	.0940	.1305	.1427	.1423	.1345	.1292	.1227	.1201	.1237
230.8	23.89	.0661	.1252	.1280	.1338	.1363	.1288	.1180	.1182	.1204
230.8	28.81	.0390	.1162	.1157	.1186	.1202	.1173	.1144	.1137	.1100
230.8	33.73	.0237	.1027	.1056	.1054	.1068	.1051	.1035	.1014	.0993
230.8	38.65	.0179	.0890	.0910	.0926	.0931	.0889	.0874	.0859	.0868
230.8	43.57	.0150	.0683	.0718	.0708	.0716	.0727	.0722	.0693	.0697
230.8	48.48	.0131	.0581	.0578	.0576	.0571	.0580	.0568	.0572	.0576

Table D.17 - Entrainment Field $\bar{u}$ ($\theta=-60°$)

		Unforced	Phase averaged data (at angle ϕ)							
x/θ_0	y/θ_0	data	0.0	45.0	90.0	135.0	180.0	225.0	270.0	315.0
107.7	17.54	.027	.033	.035	.038	.052	.079	.095	.078	.046
107.7	25.31	.012	.015	.017	.015	.016	.026	.035	.031	.019
107.7	33.07	.010	.008	.008	.007	.007	.011	.015	.015	.010
107.7	40.83	.010	.005	.004	.004	.005	.006	.007	.008	.006
107.7	48.59	.006	.003	.003	.004	.003	.004	.003	.003	.003
123.1	20.79	.021	.052	.033	.027	.027	.032	.042	.058	.064
123.1	30.00	.011	.021	.015	.013	.013	.012	.015	.021	.024
123.1	39.21	.011	.010	.008	.006	.005	.006	.007	.009	.010
123.1	48.42	.008	.004	.004	.004	.003	.004	.005	.005	.005
123.1	57.63	.003	.006	.005	.005	.005	.005	.005	.005	.006
138.5	24.04	.019	.052	.052	.045	.034	.029	.029	.034	.044
138.5	34.70	.012	.018	.019	.017	.014	.013	.012	.013	.015
138.5	45.36	.011	.006	.007	.007	.006	.005	.005	.005	.006
138.5	56.01	.007	.005	.005	.004	.004	.004	.004	.005	.005
138.5	66.67	.002	.005	.005	.005	.005	.005	.005	.005	.005
153.8	27.29	.019	.037	.042	.044	.046	.040	.036	.032	.034
153.8	39.40	.013	.014	.015	.017	.017	.016	.015	.014	.014
153.8	51.50	.011	.005	.005	.006	.006	.006	.005	.005	.004
153.8	63.61	.005	.005	.005	.004	.005	.004	.005	.004	.004
153.8	75.71	.003	.005	.006	.005	.005	.005	.005	.005	.005
169.2	30.54	.018	.036	.041	.043	.047	.047	.045	.044	.040
169.2	44.09	.013	.014	.014	.015	.015	.016	.016	.015	.015
169.2	57.65	.010	.004	.004	.004	.005	.005	.005	.005	.004
169.2	71.20	.005	.005	.004	.004	.005	.005	.005	.005	.005
169.2	84.75	.004	.006	.006	.006	.005	.005	.005	.006	.006
184.6	33.79	.019	.045	.042	.040	.045	.048	.051	.051	.048
184.6	48.79	.014	.014	.013	.013	.013	.013	.014	.015	.014
184.6	63.79	.010	.004	.004	.004	.004	.004	.004	.005	.005
184.6	78.80	.005	.005	.005	.005	.005	.005	.006	.005	.005
184.6	93.80	.006	.006	.005	.005	.005	.006	.005	.005	.005
200.0	37.04	.019	.055	.053	.049	.049	.050	.053	.055	.056
200.0	53.49	.014	.014	.014	.014	.013	.013	.013	.014	.014
200.0	69.94	.010	.004	.004	.004	.004	.004	.004	.004	.004
200.0	86.39	.004	.005	.005	.005	.005	.005	.005	.005	.006

Table D.18 - Entrainment Field $\tilde{u}$ ($\theta=-60°$)

		Unforced	Phase averaged data (at angle ϕ)						
x/θ_0	y/θ_0	data	0.0	45.0	90.0	135.0	180.0	225.0	270.0	315.0
107.7	17.54	.0243	.0351	.0356	.0427	.0538	.0569	.0546	.0511	.0433
107.7	25.31	.0081	.0143	.0161	.0166	.0162	.0180	.0194	.0195	.0160
107.7	33.07	.0038	.0079	.0102	.0109	.0105	.0101	.0107	.0100	.0071
107.7	40.83	.0029	.0059	.0076	.0082	.0078	.0074	.0068	.0063	.0055
107.7	48.59	.0023	.0054	.0065	.0081	.0072	.0062	.0059	.0049	.0045
123.1	20.79	.0176	.0434	.0362	.0316	.0337	.0379	.0408	.0471	.0478
123.1	30.00	.0070	.0169	.0148	.0129	.0144	.0159	.0156	.0167	.0178
123.1	39.21	.0037	.0080	.0071	.0082	.0090	.0092	.0086	.0083	.0085
123.1	48.42	.0030	.0062	.0064	.0068	.0080	.0086	.0079	.0071	.0065
123.1	57.63	.0031	.0060	.0061	.0068	.0075	.0073	.0070	.0061	.0060
138.5	24.04	.0162	.0446	.0464	.0425	.0381	.0356	.0360	.0377	.0435
138.5	34.70	.0064	.0156	.0156	.0154	.0142	.0140	.0149	.0149	.0154
138.5	45.36	.0036	.0081	.0076	.0076	.0077	.0082	.0088	.0089	.0085
138.5	56.01	.0034	.0078	.0075	.0071	.0073	.0077	.0084	.0089	.0084
138.5	66.67	.0034	.0075	.0076	.0074	.0077	.0077	.0079	.0083	.0081
153.8	27.29	.0136	.0435	.0459	.0459	.0466	.0439	.0422	.0399	.0402
153.8	39.40	.0058	.0154	.0163	.0166	.0158	.0156	.0152	.0154	.0161
153.8	51.50	.0040	.0093	.0091	.0087	.0082	.0079	.0082	.0085	.0090
153.8	63.61	.0040	.0096	.0091	.0084	.0080	.0077	.0083	.0087	.0090
153.8	75.71	.0044	.0093	.0094	.0089	.0083	.0078	.0083	.0087	.0089
169.2	30.54	.0129	.0466	.0495	.0500	.0524	.0510	.0507	.0508	.0485
169.2	44.09	.0061	.0162	.0172	.0171	.0166	.0159	.0164	.0156	.0166
169.2	57.65	.0047	.0092	.0100	.0100	.0094	.0087	.0083	.0086	.0089
169.2	71.20	.0044	.0090	.0092	.0092	.0088	.0081	.0077	.0076	.0083
169.2	84.75	.0054	.0099	.0106	.0106	.0099	.0093	.0089	.0089	.0090
184.6	33.79	.0132	.0492	.0504	.0486	.0512	.0533	.0539	.0535	.0529
184.6	48.79	.0068	.0162	.0155	.0164	.0162	.0163	.0164	.0160	.0163
184.6	63.79	.0051	.0092	.0096	.0093	.0095	.0096	.0086	.0085	.0087
184.6	78.80	.0047	.0086	.0091	.0092	.0091	.0086	.0084	.0081	.0083
184.6	93.80	.0065	.0096	.0101	.0102	.0100	.0097	.0093	.0090	.0091
200.0	37.04	.0132	.0571	.0563	.0557	.0548	.0532	.0538	.0557	.0566
200.0	53.49	.0070	.0164	.0155	.0164	.0170	.0167	.0163	.0165	.0161
200.0	69.94	.0057	.0085	.0089	.0087	.0089	.0089	.0089	.0086	.0084
200.0	86.39	.0046	.0087	.0091	.0092	.0095	.0090	.0088	.0087	.0087

Table D.19 - Entrainment Field $\bar{v}$ ($\theta=-60°$)

x/θ_0	y/θ_0	Unforced data	Phase averaged data (at angle ϕ)							
			0.0	45.0	90.0	135.0	180.0	225.0	270.0	315.0
107.7	17.54	-.047	-.094	-.088	-.099	-.120	-.120	-.099	-.085	-.094
107.7	25.31	-.023	-.032	-.038	-.054	-.066	-.065	-.053	-.037	-.031
107.7	33.07	-.020	-.021	-.027	-.035	-.042	-.043	-.037	-.028	-.022
107.7	40.83	-.022	-.024	-.028	-.033	-.036	-.036	-.033	-.028	-.024
107.7	48.59	-.024	-.028	-.030	-.032	-.035	-.035	-.033	-.030	-.028
123.1	20.79	-.036	-.076	-.072	-.068	-.073	-.085	-.095	-.095	-.085
123.1	30.00	-.021	-.036	-.031	-.033	-.039	-.047	-.052	-.051	-.043
123.1	39.21	-.022	-.028	-.026	-.027	-.031	-.035	-.037	-.037	-.033
123.1	48.42	-.024	-.031	-.029	-.029	-.031	-.034	-.035	-.035	-.033
123.1	57.63	-.028	-.033	-.032	-.031	-.032	-.033	-.034	-.035	-.034
138.5	24.04	-.033	-.083	-.081	-.076	-.074	-.072	-.076	-.082	-.084
138.5	34.70	-.021	-.044	-.040	-.035	-.033	-.036	-.040	-.045	-.046
138.5	45.36	-.023	-.035	-.033	-.030	-.028	-.029	-.032	-.035	-.036
138.5	56.01	-.027	-.034	-.033	-.031	-.030	-.030	-.031	-.033	-.034
138.5	66.67	-.030	-.035	-.035	-.034	-.033	-.033	-.033	-.034	-.035
153.8	27.29	-.030	-.084	-.084	-.083	-.080	-.079	-.077	-.078	-.081
153.8	39.40	-.023	-.045	-.045	-.043	-.039	-.036	-.037	-.039	-.042
153.8	51.50	-.025	-.034	-.034	-.033	-.031	-.029	-.029	-.031	-.032
153.8	63.61	-.029	-.034	-.034	-.034	-.033	-.032	-.031	-.032	-.033
153.8	75.71	-.032	-.035	-.035	-.035	-.035	-.034	-.034	-.034	-.035
169.2	30.54	-.028	-.088	-.087	-.088	-.087	-.086	-.087	-.087	-.087
169.2	44.09	-.023	-.039	-.041	-.042	-.041	-.039	-.037	-.037	-.038
169.2	57.65	-.027	-.032	-.033	-.034	-.033	-.032	-.031	-.030	-.031
169.2	71.20	-.031	-.032	-.033	-.033	-.033	-.032	-.032	-.032	-.032
169.2	84.75	-.033	-.035	-.035	-.035	-.035	-.034	-.034	-.034	-.035
184.6	33.79	-.027	-.089	-.089	-.089	-.090	-.092	-.091	-.089	-.089
184.6	48.79	-.025	-.037	-.038	-.039	-.040	-.040	-.039	-.038	-.037
184.6	63.79	-.029	-.030	-.030	-.031	-.031	-.031	-.031	-.030	-.030
184.6	78.80	-.032	-.032	-.032	-.032	-.032	-.032	-.032	-.032	-.032
184.6	93.80	-.034	-.034	-.034	-.034	-.034	-.034	-.034	-.034	-.034
200.0	37.04	-.028	-.095	-.093	-.094	-.095	-.097	-.095	-.096	-.096
200.0	53.49	-.026	-.038	-.038	-.038	-.039	-.040	-.040	-.040	-.039
200.0	69.94	-.030	-.030	-.030	-.030	-.030	-.030	-.030	-.030	-.030
200.0	86.39	-.033	-.033	-.033	-.033	-.032	-.032	-.032	-.032	-.033

Table D.20 - Entrainment Field $\tilde{v}$ ($\theta=-60°$)

x/θ_0	y/θ_0	Unforced data	Phase averaged data (at angle ϕ)						
			0.0	45.0	90.0	135.0	180.0	225.0	270.0	315.0
107.7	17.54	.0308	.0648	.0535	.0545	.0554	.0500	.0461	.0448	.0601
107.7	25.31	.0113	.0203	.0214	.0235	.0222	.0199	.0184	.0188	.0202
107.7	33.07	.0064	.0121	.0144	.0151	.0149	.0134	.0122	.0113	.0106
107.7	40.83	.0044	.0091	.0100	.0105	.0105	.0098	.0089	.0082	.0081
107.7	48.59	.0030	.0062	.0067	.0073	.0073	.0069	.0063	.0058	.0056
123.1	20.79	.0232	.0452	.0490	.0448	.0432	.0432	.0435	.0465	.0452
123.1	30.00	.0097	.0207	.0202	.0213	.0226	.0226	.0215	.0198	.0190
123.1	39.21	.0059	.0110	.0110	.0122	.0133	.0139	.0136	.0127	.0118
123.1	48.42	.0039	.0079	.0078	.0083	.0090	.0095	.0094	.0091	.0085
123.1	57.63	.0032	.0049	.0048	.0052	.0056	.0060	.0061	.0058	.0052
138.5	24.04	.0222	.0404	.0477	.0496	.0501	.0447	.0421	.0401	.0385
138.5	34.70	.0091	.0197	.0194	.0188	.0188	.0209	.0219	.0223	.0213
138.5	45.36	.0053	.0126	.0119	.0112	.0112	.0118	.0125	.0131	.0131
138.5	56.01	.0039	.0081	.0078	.0072	.0070	.0073	.0079	.0083	.0083
138.5	66.67	.0028	.0054	.0054	.0050	.0050	.0050	.0052	.0056	.0056
153.8	27.29	.0183	.0435	.0444	.0476	.0488	.0521	.0491	.0469	.0439
153.8	39.40	.0080	.0238	.0225	.0228	.0220	.0211	.0223	.0227	.0233
153.8	51.50	.0050	.0124	.0124	.0120	.0113	.0108	.0108	.0113	.0120
153.8	63.61	.0038	.0076	.0076	.0075	.0071	.0069	.0069	.0071	.0075
153.8	75.71	.0029	.0057	.0059	.0057	.0054	.0051	.0052	.0052	.0054
169.2	30.54	.0167	.0531	.0506	.0509	.0493	.0513	.0554	.0587	.0577
169.2	44.09	.0079	.0219	.0228	.0224	.0233	.0236	.0219	.0226	.0226
169.2	57.65	.0052	.0123	.0126	.0127	.0127	.0122	.0118	.0115	.0123
169.2	71.20	.0040	.0068	.0070	.0070	.0070	.0069	.0066	.0064	.0065
169.2	84.75	.0029	.0056	.0059	.0057	.0057	.0056	.0054	.0053	.0053
184.6	33.79	.0168	.0612	.0611	.0567	.0550	.0561	.0564	.0578	.0595
184.6	48.79	.0083	.0242	.0238	.0242	.0244	.0242	.0228	.0235	.0235
184.6	63.79	.0055	.0110	.0111	.0113	.0115	.0116	.0115	.0113	.0111
184.6	78.80	.0042	.0064	.0065	.0066	.0067	.0067	.0066	.0066	.0065
184.6	93.80	.0029	.0054	.0055	.0055	.0057	.0056	.0054	.0053	.0053
200.0	37.04	.0160	.0605	.0606	.0636	.0618	.0624	.0586	.0572	.0585
200.0	53.49	.0080	.0241	.0241	.0249	.0250	.0256	.0250	.0256	.0259
200.0	69.94	.0057	.0108	.0106	.0105	.0105	.0106	.0108	.0109	.0108
200.0	86.39	.0038	.0065	.0065	.0065	.0067	.0066	.0065	.0066	.0065

Table D.21 - Entrainment Field $\overline{u'v'}$ ($\theta=-60°$)

x/θ_0	y/θ_0	Unforced data	Phase averaged data (at angle ϕ)							
			0.0	45.0	90.0	135.0	180.0	225.0	270.0	315.0
107.7	17.54	-.0034	-.0088	-.0063	-.0085	-.0086	-.0083	-.0080	-.0087	-.0131
107.7	25.31	-.0000	-.0001	.0013	.0012	.0003	-.0003	-.0002	-.0001	-.0003
107.7	33.07	-.0001	.0005	.0009	.0011	.0006	.0001	.0000	.0002	.0001
107.7	40.83	.0000	.0003	.0004	.0004	.0002	.0001	.0001	.0001	.0001
107.7	48.59	.0000	.0001	.0001	.0002	.0001	-.0001	-.0001	-.0000	.0000
123.1	20.79	-.0014	-.0060	-.0060	-.0051	-.0042	-.0054	-.0050	-.0082	-.0063
123.1	30.00	-.0001	-.0005	-.0003	.0000	.0007	.0004	-.0002	-.0007	-.0008
123.1	39.21	-.0000	.0001	.0002	.0006	.0007	.0006	.0004	.0000	.0000
123.1	48.42	.0000	.0000	.0001	.0002	.0003	.0003	.0001	-.0001	-.0001
123.1	57.63	.0000	.0000	.0001	.0002	.0002	.0002	.0002	.0001	.0000
138.5	24.04	-.0010	-.0045	-.0058	-.0066	-.0059	-.0040	-.0035	-.0045	-.0052
138.5	34.70	-.0001	-.0009	-.0008	-.0007	-.0003	-.0003	.0001	.0001	-.0004
138.5	45.36	-.0000	.0002	.0001	.0002	.0004	.0005	.0005	.0005	.0003
138.5	56.01	.0000	.0001	.0001	.0001	.0002	.0002	.0003	.0003	.0001
138.5	66.67	.0000	.0002	.0002	.0002	.0002	.0003	.0003	.0003	.0002
153.8	27.29	-.0003	-.0067	-.0064	-.0063	-.0078	-.0086	-.0082	-.0049	-.0052
153.8	39.40	-.0001	-.0004	-.0006	-.0010	-.0009	-.0008	-.0008	-.0002	-.0001
153.8	51.50	.0000	.0004	.0003	.0003	.0002	.0003	.0004	.0005	.0005
153.8	63.61	.0000	.0004	.0003	.0003	.0002	.0002	.0003	.0003	.0003
153.8	75.71	-.0000	.0004	.0004	.0003	.0003	.0002	.0003	.0003	.0003
169.2	30.54	-.0001	-.0059	-.0075	-.0073	-.0083	-.0091	-.0087	-.0124	-.0113
169.2	44.09	-.0001	-.0005	-.0002	-.0007	-.0010	-.0012	-.0009	-.0009	-.0009
169.2	57.65	.0000	.0005	.0005	.0004	.0004	.0003	.0004	.0004	.0004
169.2	71.20	.0000	.0004	.0004	.0004	.0003	.0003	.0002	.0002	.0003
169.2	84.75	-.0001	.0005	.0005	.0005	.0004	.0004	.0004	.0004	.0004
184.6	33.79	-.0002	-.0124	-.0122	-.0103	-.0101	-.0124	-.0130	-.0129	-.0147
184.6	48.79	-.0000	-.0010	-.0005	-.0009	-.0006	-.0006	-.0008	-.0006	-.0009
184.6	63.79	.0001	.0005	.0006	.0006	.0006	.0005	.0005	.0004	.0005
184.6	78.80	.0000	.0003	.0004	.0004	.0004	.0003	.0003	.0003	.0003
184.6	93.80	-.0001	.0004	.0005	.0005	.0005	.0004	.0004	.0004	.0004
200.0	37.04	-.0000	-.0150	-.0165	-.0137	-.0143	-.0127	-.0122	-.0133	-.0145
200.0	53.49	-.0000	-.0010	-.0004	-.0011	-.0005	-.0007	-.0007	-.0010	-.0010
200.0	69.94	.0001	.0005	.0005	.0005	.0005	.0005	.0005	.0005	.0004
200.0	86.39	.0000	.0003	.0004	.0004	.0005	.0004	.0004	.0003	.0003

Table D.22 - Entrainment Field $\bar{u}$ ($\theta=-45°$)

x/θ_0	y/θ_0	Unforced data	Phase averaged data (at angle ϕ)							
			0.0	45.0	90.0	135.0	180.0	225.0	270.0	315.0
107.7	17.54	.028	.050	.053	.058	.062	.076	.092	.088	.060
107.7	33.07	.012	.015	.018	.016	.014	.015	.017	.016	.013
107.7	48.59	.013	.012	.012	.010	.008	.007	.007	.009	.010
138.5	24.04	.020	.059	.061	.055	.047	.045	.047	.049	.054
138.5	45.36	.015	.011	.012	.012	.013	.013	.013	.012	.011
138.5	66.67	.010	.007	.007	.007	.007	.008	.007	.007	.007
169.2	30.54	.019	.058	.060	.064	.067	.068	.064	.061	.058
169.2	57.65	.015	.013	.012	.012	.012	.012	.012	.012	.013
169.2	84.75	.009	.007	.007	.007	.007	.007	.007	.007	.007
200.0	37.04	.020	.073	.070	.067	.068	.068	.071	.073	.074
200.0	69.94	.014	.012	.012	.013	.012	.012	.012	.012	.012

Table D.23 - Entrainment Field $\tilde{u}$ ($\theta=-45°$)

x/θ_0	y/θ_0	Unforced data	Phase averaged data (at angle ϕ)							
			0.0	45.0	90.0	135.0	180.0	225.0	270.0	315.0
107.7	17.54	.0208	.0380	.0325	.0348	.0379	.0432	.0441	.0451	.0443
107.7	33.07	.0048	.0069	.0084	.0091	.0085	.0090	.0090	.0078	.0057
107.7	48.59	.0039	.0056	.0060	.0059	.0051	.0043	.0041	.0048	.0053
138.5	24.04	.0114	.0421	.0435	.0439	.0400	.0379	.0348	.0364	.0383
138.5	45.36	.0062	.0071	.0071	.0067	.0070	.0074	.0077	.0072	.0072
138.5	66.67	.0041	.0038	.0040	.0043	.0045	.0045	.0044	.0041	.0039
169.2	30.54	.0111	.0490	.0497	.0525	.0548	.0559	.0524	.0506	.0488
169.2	57.65	.0070	.0077	.0074	.0073	.0070	.0071	.0071	.0074	.0077
169.2	84.75	.0039	.0042	.0043	.0043	.0043	.0044	.0044	.0043	.0042
200.0	37.04	.0104	.0627	.0614	.0609	.0600	.0612	.0620	.0629	.0628
200.0	69.94	.0078	.0070	.0072	.0073	.0073	.0070	.0069	.0070	.0070

Table D.24 - Entrainment Field $\bar{v}$ ($\theta=-45°$)

x/θ_0	y/θ_0	Unforced data	0.0	45.0	90.0	135.0	180.0	225.0	270.0	315.0
					Phase averaged data (at angle ϕ)					
107.7	17.54	-.029	-.053	-.056	-.067	-.086	-.091	-.071	-.046	-.047
107.7	33.07	-.018	-.013	-.017	-.027	-.035	-.038	-.033	-.024	-.016
107.7	48.59	-.024	-.021	-.022	-.025	-.029	-.031	-.030	-.027	-.023
138.5	24.04	-.023	-.062	-.054	-.048	-.045	-.047	-.053	-.060	-.065
138.5	45.36	-.024	-.031	-.028	-.024	-.022	-.023	-.026	-.030	-.032
138.5	66.67	-.028	-.031	-.031	-.030	-.029	-.029	-.030	-.030	-.031
169.2	30.54	-.024	-.061	-.064	-.064	-.063	-.061	-.058	-.058	-.059
169.2	57.65	-.027	-.025	-.026	-.027	-.027	-.026	-.025	-.024	-.024
169.2	84.75	-.030	-.030	-.030	-.029	-.030	-.030	-.029	-.030	-.030
200.0	37.04	-.026	-.061	-.059	-.061	-.062	-.064	-.065	-.064	-.063
200.0	69.94	-.030	-.023	-.022	-.022	-.023	-.024	-.024	-.024	-.024

Table D.25 - Entrainment Field $\tilde{v}$ ($\theta=-45°$)

x/θ_0	y/θ_0	Unforced data	0.0	45.0	90.0	135.0	180.0	225.0	270.0	315.0
					Phase averaged data (at angle ϕ)					
107.7	17.54	.0218	.0421	.0377	.0397	.0404	.0373	.0339	.0327	.0349
107.7	33.07	.0083	.0117	.0148	.0163	.0163	.0149	.0130	.0112	.0098
107.7	48.59	.0048	.0084	.0093	.0093	.0083	.0074	.0068	.0066	.0071
138.5	24.04	.0164	.0351	.0348	.0359	.0352	.0343	.0369	.0375	.0364
138.5	45.36	.0073	.0136	.0128	.0122	.0120	.0128	.0137	.0141	.0141
138.5	66.67	.0038	.0059	.0058	.0057	.0058	.0060	.0062	.0062	.0061
169.2	30.54	.0168	.0441	.0446	.0435	.0407	.0413	.0413	.0428	.0425
169.2	57.65	.0073	.0127	.0130	.0131	.0130	.0126	.0123	.0122	.0124
169.2	84.75	.0036	.0052	.0053	.0055	.0055	.0055	.0054	.0052	.0052
200.0	37.04	.0162	.0459	.0435	.0446	.0456	.0458	.0452	.0435	.0449
200.0	69.94	.0074	.0119	.0118	.0118	.0119	.0121	.0123	.0123	.0121

Table D.26 - Entrainment Field $\overline{u'v'}$ ($\theta=-45°$)

x/θ_0	y/θ_0	Unforced data	Phase averaged data (at angle ϕ)							
			0.0	45.0	90.0	135.0	180.0	225.0	270.0	315.0
107.7	17.54	-.0019	-.0096	-.0046	-.0028	-.0006	.0005	.0013	-.0007	-.0054
107.7	33.07	.0001	.0004	.0008	.0010	.0007	.0001	-.0001	.0001	.0002
107.7	48.59	.0002	.0005	.0006	.0006	.0004	.0003	.0003	.0003	.0004
138.5	24.04	-.0004	-.0022	-.0031	-.0050	-.0050	-.0048	-.0038	-.0025	-.0033
138.5	45.36	.0002	.0004	.0004	.0005	.0006	.0007	.0007	.0007	.0006
138.5	66.67	.0001	.0002	.0002	.0003	.0003	.0003	.0003	.0003	.0002
169.2	30.54	-.0004	-.0052	-.0052	-.0034	-.0040	-.0058	-.0058	-.0070	-.0065
169.2	57.65	.0003	.0007	.0007	.0007	.0007	.0007	.0007	.0007	.0007
169.2	84.75	.0001	.0002	.0002	.0003	.0003	.0003	.0003	.0002	.0002
200.0	37.04	-.0001	-.0073	-.0068	-.0107	-.0069	-.0069	-.0069	-.0067	-.0086
200.0	69.94	.0004	.0007	.0007	.0007	.0007	.0007	.0007	.0007	.0007

Table D.27 - Entrainment Field $\bar{u}$ (θ--90°)

		Unforced	Phase averaged data (at angle ϕ)							
x/θ_0	y/θ_0	data	0.0	45.0	90.0	135.0	180.0	225.0	270.0	315.0
107.7	17.54	-.005	-.027	-.024	-.027	-.002	.035	.038	.002	-.031
107.7	33.07	.012	.007	.006	.005	.005	.006	.010	.012	.010
107.7	48.59	.007	-.001	-.002	-.002	-.001	.001	.003	.003	.001
138.5	24.04	.004	.006	.004	-.005	-.011	-.010	-.006	-.004	.003
138.5	45.36	.011	.006	.006	.005	.002	.001	.001	.002	.004
138.5	66.67	.007	-.006	-.005	-.006	-.006	-.007	-.008	-.007	-.006
169.2	30.54	.008	-.011	-.011	-.006	-.007	-.009	-.011	-.012	-.010
169.2	57.65	.009	-.006	-.006	-.006	-.004	-.004	-.004	-.005	-.006
169.2	84.75	.007	-.009	-.010	-.009	-.009	-.009	-.009	-.009	-.009
200.0	37.04	.011	-.014	-.015	-.015	-.013	-.011	-.010	-.010	-.013
200.0	69.94	.009	-.005	-.006	-.006	-.006	-.006	-.006	-.005	-.005

Table D.28 - Entrainment Field $\tilde{u}$ (θ--90°)

		Unforced	Phase averaged data (at angle ϕ)							
x/θ_0	y/θ_0	data	0.0	45.0	90.0	135.0	180.0	225.0	270.0	315.0
107.7	17.54	.0391	.0452	.0496	.0584	.0729	.0763	.0704	.0579	.0499
107.7	33.07	.0093	.0139	.0127	.0127	.0135	.0157	.0174	.0172	.0156
107.7	48.59	.0012	.0037	.0039	.0039	.0044	.0051	.0053	.0050	.0044
138.5	24.04	.0264	.0509	.0502	.0483	.0448	.0429	.0407	.0434	.0478
138.5	45.36	.0050	.0123	.0121	.0113	.0114	.0108	.0106	.0114	.0116
138.5	66.67	.0014	.0049	.0050	.0052	.0052	.0052	.0050	.0049	.0048
169.2	30.54	.0208	.0475	.0491	.0486	.0493	.0501	.0512	.0494	.0471
169.2	57.65	.0028	.0099	.0097	.0095	.0093	.0098	.0096	.0096	.0104
169.2	84.75	.0018	.0050	.0051	.0050	.0050	.0051	.0052	.0052	.0051
200.0	37.04	.0164	.0516	.0509	.0491	.0497	.0498	.0500	.0508	.0519
200.0	69.94	.0029	.0087	.0088	.0088	.0089	.0086	.0087	.0087	.0088

Table D.29 - Entrainment Field $\bar{v}$ (θ—-90°)

x/θ_0	y/θ_0	Unforced data	Phase averaged data (at angle ϕ)						
			0.0	45.0	90.0	135.0	180.0	225.0	270.0	315.0
107.7	17.54	-.097	-.135	-.131	-.150	-.177	-.186	-.171	-.156	-.150
107.7	33.07	-.024	-.037	-.034	-.036	-.041	-.047	-.050	-.047	-.042
107.7	48.59	-.023	-.025	-.026	-.029	-.031	-.031	-.029	-.027	-.025
138.5	24.04	-.061	-.116	-.117	-.112	-.103	-.095	-.093	-.099	-.109
138.5	45.36	-.024	-.039	-.036	-.034	-.034	-.036	-.039	-.041	-.042
138.5	66.67	-.027	-.033	-.032	-.031	-.031	-.032	-.032	-.033	-.033
169.2	30.54	-.045	-.113	-.115	-.116	-.119	-.120	-.120	-.118	-.114
169.2	57.65	-.029	-.033	-.034	-.034	-.033	-.032	-.032	-.032	-.032
169.2	84.75	-.029	-.032	-.032	-.032	-.032	-.032	-.032	-.032	-.032
200.0	37.04	-.036	-.127	-.124	-.122	-.120	-.119	-.122	-.125	-.127
200.0	69.94	-.031	-.027	-.027	-.027	-.028	-.028	-.029	-.029	-.028

Table D.30 - Entrainment Field $\tilde{v}$ (θ—-90°)

x/θ_0	y/θ_0	Unforced data	Phase averaged data (at angle ϕ)						
			0.0	45.0	90.0	135.0	180.0	225.0	270.0	315.0
107.7	17.54	.0596	.0786	.0812	.0941	.0925	.0832	.0771	.0713	.0750
107.7	33.07	.0094	.0190	.0203	.0200	.0196	.0182	.0181	.0179	.0181
107.7	48.59	.0028	.0063	.0068	.0068	.0064	.0057	.0053	.0053	.0058
138.5	24.04	.0413	.0667	.0707	.0738	.0682	.0628	.0579	.0579	.0610
138.5	45.36	.0061	.0142	.0142	.0138	.0143	.0144	.0148	.0148	.0144
138.5	66.67	.0027	.0044	.0041	.0039	.0040	.0043	.0046	.0047	.0046
169.2	30.54	.0275	.0683	.0693	.0674	.0709	.0749	.0797	.0780	.0728
169.2	57.65	.0053	.0118	.0122	.0124	.0118	.0118	.0120	.0123	.0119
169.2	84.75	.0027	.0043	.0043	.0043	.0043	.0042	.0041	.0041	.0042
200.0	37.04	.0186	.0798	.0808	.0783	.0753	.0742	.0763	.0761	.0783
200.0	69.94	.0050	.0100	.0097	.0098	.0102	.0109	.0111	.0102	.0103

Table D.31 - Entrainment Field $\overline{u'v'}$ ($\theta=-90°$)

x/θ_0	y/θ_0	Unforced data	Phase averaged data (at angle ϕ)							
			0.0	45.0	90.0	135.0	180.0	225.0	270.0	315.0
107.7	17.54	.0105	.0202	.0189	.0265	.0257	.0181	.0125	.0151	.0226
107.7	33.07	-.0002	.0002	-.0001	.0001	-.0003	-.0003	-.0001	.0004	.0002
107.7	48.59	-.0000	.0001	.0001	.0001	.0000	-.0001	-.0001	.0000	.0001
138.5	24.04	.0036	.0100	.0133	.0157	.0132	.0073	.0020	.0013	.0034
138.5	45.36	.0000	.0000	.0001	.0001	.0002	.0002	.0002	.0000	-.0000
138.5	66.67	-.0000	-.0000	-.0000	.0000	.0000	.0001	.0001	.0000	-.0000
169.2	30.54	.0012	.0081	.0093	.0073	.0109	.0167	.0176	.0149	.0118
169.2	57.65	-.0001	.0005	.0004	.0004	.0002	.0003	.0002	.0003	.0004
169.2	84.75	.0000	.0000	.0000	.0000	-.0000	-.0000	-.0000	.0000	.0000
200.0	37.04	-.0004	.0209	.0219	.0191	.0145	.0156	.0147	.0159	.0200
200.0	69.94	-.0001	.0003	.0003	.0004	.0004	.0004	.0003	.0003	.0003

List of References

Ali, S.K., Klewicki, C.L., Disimile, P.J., Lawson, I. and Foss, J.F. "Entrainment Region Phenomena for a Large Plane Shear Layer", Turbulent Shear flows V, 1985, pp. 3.7-3.12.

Clauser, G.H. [1954] "Turbulent Boundary Layers in Adverse Pressure Gradients", Journal of Aeronautical Science, vol 21, pp 91-108.

Coles, D. [1962] "The Turbulent Boundary in a compressible fluid", Rand Corp., Rep. R-403-PR.

Disimile, P.J. [1984] "Phase Averaged Transverse Vorticity Measurements in an Excited, Two-dimensional Mixing Layer", Phd Thesis, Michigan State University.

Disimile, P.J. [1986] "Phase Averaged Transverse Vorticity Measurements in an Excited, Two-dimensional Mixing Layer", AIAA Journal, vol. 24 No. 10, pp. 231-269.

Fiedler, H.E. and Mensing [1985] "The Plane Turbulent Shear Layer with Periodic Excitation", Journal of Fluid Mechanics, vol 15, pp281-309.

Fiedler, H.E. [1988] "Coherent Structures in Turbulent Flows", Prog. in Aerospace Sciences, vol. 25, pp. 231-269.

Foss J.F., Davis, E.D. Haw, R.C. and Ali S.K. [1987] "Coherent Motion Induced Fluctuations in the Primary Transition Region of Plane Shear Layer", Forum on Turbulent Flows, ADME FED - vol. 51, pp. 1-13.

Haw R.C., Ali S.K., and Foss J.F. [1987] "Gravitationally Defined Velocities for a Low Speed Hot-wire Calibration", Symposium on Thermal Anemometry, ADME FED - vol. 53, pp. 7-13.

Hussain, A.K.M.F. [1983] "Coherent Structures - Reality and Myth", Phys. Fluids, vol. 26, pp.2816-2850.

Hussain, A.K.M.F. [1986] "Coherent Structures and Turbulence", Journal of Fluid Mechanics,vol. 173, pp. 303-356.

Klebanoff, P.S. and Diehl, Z.W. [1951] "Some Features of Artificially Thickened Fully Developed Turbulent Boundary Layers with Zero Pressure Gradient", NACA Technical note 2475.